NOTE TO USERS

This reproduction is the best copy available.

UMI®

University of Alberta

Application of Ichnology in the Paleoenvironmental Reconstruction and Reservoir Characterization of the Avalon and Ben Nevis Formations, Hibernia Field, Jeanne d'Arc Basin, Grand Banks of Newfoundland

by

Michelle Victoria Spila

©

A thesis submitted to the Faculty of Graduate Studies and Research in partial fulfillment of the requirements for the degree of Doctor of Philosophy

Department of Earth and Atmospheric Sciences

Edmonton, Alberta
Fall 2005

Library and
Archives Canada

Published Heritage
Branch

395 Wellington Street
Ottawa ON K1A 0N4
Canada

Bibliothèque et
Archives Canada

Direction du
Patrimoine de l'édition

395, rue Wellington
Ottawa ON K1A 0N4
Canada

0-494-08735-8

Your file Votre référence
ISBN:
Our file Notre reterence
ISBN:

NOTICE:
The author has granted a non-exclusive license allowing Library and Archives Canada to reproduce, publish, archive, preserve, conserve, communicate to the public by telecommunication or on the Internet, loan, distribute and sell theses worldwide, for commercial or non-commercial purposes, in microform, paper, electronic and/or any other formats.

The author retains copyright ownership and moral rights in this thesis. Neither the thesis nor substantial extracts from it may be printed or otherwise reproduced without the author's permission.

AVIS:
L'auteur a accordé une licence non exclusive permettant à la Bibliothèque et Archives Canada de reproduire, publier, archiver, sauvegarder, conserver, transmettre au public par télécommunication ou par l'Internet, prêter, distribuer et vendre des thèses partout dans le monde, à des fins commerciales ou autres, sur support microforme, papier, électronique et/ou autres formats.

L'auteur conserve la propriété du droit d'auteur et des droits moraux qui protège cette thèse. Ni la thèse ni des extraits substantiels de celle-ci ne doivent être imprimés ou autrement reproduits sans son autorisation.

In compliance with the Canadian Privacy Act some supporting forms may have been removed from this thesis.

While these forms may be included in the document page count, their removal does not represent any loss of content from the thesis.

Conformément à la loi canadienne sur la protection de la vie privée, quelques formulaires secondaires ont été enlevés de cette thèse.

Bien que ces formulaires aient inclus dans la pagination, il n'y aura aucun contenu manquant.

Canada

"Not all those who wonder are lost."
~ J.R.R. Tolkien ~

"The best way out is always through."
~ Robert Frost ~

Dedication

To Dad, Mom, Quentin, Gwen, Jason and Baba

"The family - that dear octopus from whose tentacles we never quite escape,
nor, in our inmost hearts, ever quite wish to."
~ Dodie Smith ~

Abstract

Ichnology, the study of fossilized tracks, trails and burrows, greatly refines sedimentological and stratigraphic analysis within hydrocarbon-bearing strata. Because trace fossils represent the behavioral response of organisms to their physical and chemical surroundings, they provide unique insight toward the characterization of paleoenvironmental settings. Additionally, in highly bioturbated reservoirs, trace fossils represent heterogeneities that drastically alter production properties such as effective permeability, fluid flow paths, and petroleum saturation in comparison with non-bioturbated media.

The mid-Cretaceous Avalon/Ben Nevis interval comprises a variety of marginal marine and marine settings, making it a good candidate for illustrating the strength of high-resolution, integrated lithofacies and ichnofacies analysis. Trace fossil assemblages characteristic of brackish versus open marine depositional settings are easily recognized. As such, a paleoenvironmental framework within the Hibernia area is attainable, despite limited core and wireline log coverage. A range of sedimentary environments including arid coastal plain/marsh, barrier-island or micro- to mesotidal estuary, delta and offshore have been delineated. Ichnology also aides in the identification of an unconformity and a transgressive surface of erosion within this interval.

Although two sandstone bodies constitute the main producing units, substantial petroleum reserves are found within bioturbated muddy sandstones of the Ben Nevis Formation. Biogenic textural heterogeneity, manifested as mud-filled, mud-lined or meniscate-filled burrows within a sandy framework, is a major concern for enhanced recovery strategies. Probe permeameter analysis confirms that permeability is significantly lower in muddy burrows (herein interpreted as *Pelosichnus mumorpha* n. ichnogen., n. ichnosp.) than in the hosting sediment. Flow is therefore focused in the more permeable sandy framework with the burrows acting as baffles to flow, creating dispersivity and non-uniform saturation. New modeling software utilizing a modified invasion-percolation technique (MPath) can incorporate burrow morphology, connectivity, density, and burrow-framework permeability contrast to accurately predict fluid trajectories through bioturbated

media. Using this method, flow properties at the burrow scale can ultimately be incorporated at the reservoir production scale.

This study represents the first sedimentological/stratigraphic analysis of the Avalon and Ben Nevis formations approached from an ichnological perspective. As a result of this integrated methodology, understanding of the facies architecture and reservoir properties of this interval is greatly improved.

Acknowledgements

First and foremost, I would like to thank Dr. S. George Pemberton. I first encountered George in my second year of university; he was my instructor for clastic sedimentology. I was still a general sciences student at the time, having not yet decided what direction I would like to take. I had really enjoyed the introductory geology course I took the previous year so thought I would try a few more courses. After experiencing George's easy-going attitude and enthusiasm for petroleum geology, I realized that I had chosen the right path. In my fourth year, George was my instructor for basin analysis. After the term projects were presented, he asked me if I was considering graduate studies, and if I was, if I would like to work with him. I was both greatly honored and stunned. At the time, I barely even knew what being a graduate student was about, let alone envision myself as one! George has given me his full support and encouragement on everything I have done since that day. He opened the door to a world of endless possibilities for me, a leap of faith for which I am very grateful. George has not only been a gracious and accommodating supervisor, but a truly exceptional mentor in both geology and life.

Over the last six years, I have had the pleasure of being a part of the Ichnology Research Group (IRG) and interacting with many of its past and present members. I would like to thank Susan Fleming for her friendship, benevolence and tenacity in her role as the glue that held us all together. I am grateful to Tom Saunders and Murray Gingras for their insights in ichnology, sedimentology and surviving the IRG. Although I've see many IRG students come and go, I consider all of them colleagues and friends for life, especially Gladys Fong, Corinne Bagdan, Dwayne Giggs, Curtis Lettley, Cynthia Hagstrom, Scott Reid, Michael Hearn, Demian Robbins and Arjun Keswani.

The Hibernia Management and Development Company (HMDC) of St. John's, Newfoundland kindly provided funding and logistical support for my Ph.D. thesis. Iain Sinclair (now at Husky Energy) played an integral role in the conception and initiation of this project; I am indebted to him for his guidance and willingness to full-heartedly share data, information and ideas. I would also like to thank Robert Stokes of HMDC for his kind hospitality during my last trip to Newfoundland.

Over the course of this project, I was also fortunate to work with several individuals from the Canada-Newfoundland/Labrador Offshore Petroleum Board (C-NLOPB). Graham Dillabough and Neil DeSilva were extraordinarily accommodating and Winston Howell was a pleasure to work with at the C-NLOPB core lab. I am grateful to the Natural Sciences and Engineering Research Council (NSERC) for also provided financial support for this project.

As a student of both the University of Alberta and Memorial University, I would like to thank all the graduate students, staff and faculty members who contributed to the success of this project, either through kind and patient assistance or knowledgeable and forthcoming instruction. In the past year, I was fortunate to be able to work with Ben Rostron and Dan Khan of the Hydrogeology Group at the U of A. I am very appreciative of their cooperation and indulgence, and I look forward to future collaborations. I must send out a great big thank you to Alex MacNeil and the Carbonate Research Group at the U of A for considerately allowed me to use their microscope equipment when I was in a pinch. I would also like to thank Rick Hiscott, Andy Pulham and Elliot Burden for making me feel welcome at Memorial and ensuring that my experience there was truly an unforgettable one. In addition to Drs. George Pemberton and Murray Gingras, I would like to thank the members of my candidacy and defense committees, Dr. Charlie Stelck, Dr. Brian Jones, Dr. George Evans, Dr. Heather Proctor and Dr. Gerry Reinson, for their kind comments and very constructive feedback.

Last, but certainly not least, I must send out deep and heartfelt thanks to my friends and family who tolerated my lifestyle and antics over the past six years. I would like to extend sincere gratitude and appreciation to my Dad and Mom, John and Vicky. Even though they could never quite understand what I was doing or why I was doing it, they always expressed interest in my work and heart-felt congratulations for each of my successes, no matter how big or little. They took time to help me out with the small stuff, like rides to school or to the airport and surprise visits or trips to the store for groceries and other delights. I will never forget the sacrifices they made in order to put a roof over my head, food in my belly and money in my pocket when times were tough and thesis deadlines were perpetually delayed. No matter what I do or where I go, I hope that they know that

I will always love them and that I'll never forget where home is. I am also greatly indebted to my brothers (Quentin and Jason), sister (Gwen), grandma (Katie) and friends (Joanna, Hang and Mark) for putting up with me through thick and thin these past few years. Despite the quips about being an "over-educated bum", their support and encouragement meant the world to me.

It's been a long and often hectic journey, but George was right, the ride was definitely worth it!

Table of Contents

Page

Chapter 1 – Introduction and Background Information 1
- 1.1 Introductory remarks 1
- 1.2 Objectives 3
- 1.3 Methodology 3
- 1.4 Outline 4
- 1.5 Background information 6
- 1.6 Rationale 22

Chapter 2 – Facies Descriptions and Interpretations 23
- 2.1 Introduction 23
- 2.2 Facies descriptions and interpretations 23
- 2.3 Burrow-demarcated surfaces 66
- 2.4 Summary 68

Chapter 3 – Facies Associations, Stratigraphy, Paleogeography and Depositional History 69
- 3.1 Introduction 69
- 3.2 Facies associations 69
- 3.3 Stratigraphy 86
- 3.4 Paleogeography and depositional history 92
- 3.5 Summary 102

Chapter 4 – Bioturbate Textures 103
- 4.1 Introduction 103
- 4.2 Bioturbate texture: definition and usage 103
- 4.3 Bioturbate textures in trace fossil and facies analyses 106
- 4.4 Textural elements 107
- 4.5 Fabric 109
- 4.6 Summary 112

Chapter 5 – Biogenic Textural Heterogeneity, Fluid Flow and Hydrocarbon Production 113

5.1 Introduction 113

5.2 Petrographic characteristics 113

5.3 Trace fossil characteristics 118

5.4 Plug and probe permeametry 119

5.5 Modeling fluid flow through a bioturbate reservoir 124

5.6 Discussion 129

5.7 Summary 135

Chapter 6 – Conclusion 137

References 141

Appendix 1 – *Pelosichnus mumorpha* n. ichnogen., n. ichnosp.: Inclined to Branching, Mud-filled Burrows 156

Appendix 2 – Lithologs 167

List of Tables

Table **Page**

1.1 List of cored intervals utilized in this study ______ 4

2.1a Summary of facies characteristics ______ 24

2.1b Continuation of summary of facies characteristics ______ 25

5.1 Summary of plug and probe permeability values ______ 120

List of Figures

Figure **Page**

1.1 Grand Banks of Newfoundland, offshore eastern Canada 7

1.2 Mesozoic rift basins of the Grand Banks 8

1.3 Jeanne d'Arc Basin 9

1.4 Migrated time seismic section oriented SW-NE across Jeanne d'Arc Basin 10

1.5 Structure of the Hibernia Field 11

1.6 Simplified structure of the Hibernia Field 12

1.7 Seismic reflection profile illustrating the prograding wedge 13

1.8 Seismic reflection profile showing the lens-shaped sedimentary package 13

1.9 Lithostratigraphy of the Jeanne d'Arc Basin 15

2.1 Facies 1 – Dark, organic rich mudstone 26

2.2 Facies 2 – Multicoloured mudstone and siltstone 28

3.3 Subfacies 3A – *Teichichnus*, *Asterosoma* and *Scolicia*-dominated silty to sandy mudstone 31

2.4 Subfacies 3B – *Chondrites* and *Planolites*-dominated silty to sandy mudstone 32

2.5 Facies 4 – Wavy to lenticular bedded mudstone 34

2.6 Oyster accumulation 36

2.7 Subfacies 5A – Bioclastic mudstone 37

2.8 Subfacies 5B – Bioclastic silty sandstone 38

9.9 Subfacies 6A – *Asterosoma*, *Scolicia* and *Teichichnus*-dominated muddy to silty sandstone 41

9.10 Subfacies 6B – *Phycosiphon* and *Pelosichnus*-dominated muddy to silty sandstone 42

2.11 Subfacies 6C – *Ophiomorpha* and *Thalassinoides*-dominated muddy to silty sandstone 44

2.12 Facies 7 – Ripple cross-laminated sandstone with mudstone 47

2.13 Facies 8 – Massive to mottled sandstone 49

2.14 Facies 9 – Massive, planar to low-angle laminated sandstone 51

2.15 Facies 10 – Wavy to low-angle laminated sandstone 53
2.16 Facies 11 – Trough to high-angle cross-laminated sandstone 55
2.17 Facies 12 – Bioturbated sandstone 58
2.18 Facies 13 – Coaly to muddy sandstone 60
2.19 Facies 14 – Conglomerate 62
2.20 Facies 15 – Pebbly, carbonaceous sandstone 64
2.21 Burrow-demarcated surfaces 67
3.1 Representative litholog for FA0 – fan delta 70
3.2 Representative litholog for FA1 – coastal plain 72
3.3 Representative litholog for FA2 – brackish bay 73
3.4 Representative litholog for FA3 – bay mouth complex 75
3.5 Isopach map of the FA3 interval 77
3.6 Representative litholog for FA4 – upper shoreface/distributary mouth bar 79
3.7 Representative litholog for FA5 – deltaically influenced lower shoreface/shallow embayment (delta front) 80
3.8 Representative litholog for FA6 – deltaically influenced offshore/deep embayment (prodelta) 83
3.9 Representative litholog for FA7 – shallow marine 85
3.10 Location map showing lines of cross section 86
3.11 Cross section A-A’ 88
3.12 Cross section B-B’ 89
3.13 Cross section C-C’ 91
3.14 Paleogeographic map for Stage 1 – shallow marine 93
3.15 Paleogeographic map for Stage 2 – unconformity and coastal plain 95
3.16 Paleogeographic map for Stage 3 – prograding wedge and estuary 97
3.17 Paleogeographic map for Stage 4 – transgressive surface of erosion 99
3.18 Paleogeographic map for Stage 5 – delta within an embayment 101
4.1 Review of terminology pertaining to the bioturbate texture concept 105
4.2 Characteristic appearance of the three-bioturbate textures of Facies 6 108
4.3 Relative abundance for each ichnogenus in Facies 6 110

4.4 Tier diagram for the trace fossils appearing in Facies 6 ______ 111
5.1 Core 4, boxes 11, 10 and 9 within uncemented Facies 6B ______ 114
5.2 Core 3, boxes 18 and 17 within cemented Facies 6B ______ 115
5.3 Petrographic characteristics of Facies 6B ______ 116
5.4 Porosity characteristics of Facies 6B ______ 117
5.5 Characteristic trace fossils of Facies 6B ______ 119
5.6 Comparison of horizontal and vertical sections through Facies 6B ______ 120
5.7 Core slab utilized in probe permeametry and MPath simulation ______ 122
5.8 Scatter plot of probe-derived permeabilities ______ 123
5.9 Histogram of capillary pressure data ______ 126
5.10 Scatter plot of capillary pressure versus permeability ______ 127
5.11a Key increments or steps of MPath simulation ______ 130
5.11b Continuation of key increments or steps of MPath simulation ______ 131
5.12 Interpreted fluid flow paths as traced from MPath simulation ______ 133
A1.1 Gross morphology of *Pelosichnus mumorpha* n. ichnogen., n. ichnosp. ______ 158
A1.2 Characteristic features of *Pelosichnus* n. ichnogen. in core ______ 159
A1.3 Characteristic features of *Pelosichnus* n. ichnogen. in core ______ 160
A1.4 Comparison of *Pelosichnus* n. ichnogen., n. ichnosp. with other ichnogenera ______ 161
A1.5 Comparison of bow-form burrows and *Pelosichnus* n. ichnogen. ______ 162
A1.6 *Nereis diversicolor* ______ 163
A1.7 Traced radiographic images of U- and Y-shaped burrows ______ 164
A1.8 Progressive development of a nereid burrow over time ______ 165

Chapter 1

Introduction and Background Information

1.1 Introductory Remarks

Ichnology has become an indispensable tool in paleoenvironmental studies thanks to Seilacher (1964; 1967) and his revelations regarding the relationship of trace fossils to bathymetry. Trace fossil analysis is especially useful when the environment of the deposit under consideration may not be readily identified on the basis of physical sedimentology alone. Fluctuations in ecological parameters, such as salinity, oxygenation, water turbidity, temperature or substrate consistency, can occur in such a way that only the biological community will register a response. In the rock record, this response is typically manifested as a change in ichnological signature.

In the past half century, ichnology has been credited for significant advances in the paleoenvironmental modeling of terrestrial settings (Frey *et al.*, 1984; Smith *et al.*, 1993; Buatois and Mangano, 1995), the shallow marine realm (MacEachern and Pemberton, 1992; Pemberton *et al.*, 1992; Pemberton and MacEachern, 1995), and brackish water environments (Ekdale *et al.*, 1984; Wightman *et al.*, 1987; Pemberton and Wightman, 1992). A survey of these studies and others reveals that a high degree of infaunal activity, which commonly results in a bioturbate texture, can be found anywhere environmental conditions are conducive to the establishment of a healthy benthic population or community. Where an organism lives is based on its daily living requirements (e.g. an ample supply of food, appropriate levels of oxygen, a safe place to build a home). Each species is genetically adapted to exploit these resources in their own way; i.e. their behavior is linked to the environment. Thus, it is only through ichnological analysis of the bioturbate texture that an accurate environmental interpretation can be made.

The Avalon and Ben Nevis formations are composed a number of highly to intensely bioturbated intervals in which little or no physical sedimentary structures remain. As a direct result of this discrepancy, previous paleoenvironmental interpretations based largely on physical sedimentologic data are likely to be inaccurate due to the bias of the investigators in favour of physical sedimentary structures over biogenic sedimentary structures. (e.g. Tankard and Welsink, 1987; Sinclair, 1988; 1993; Soliman, 1995). To date, no studies have attempted an ichnological based facies analysis of the Avalon/Ben Nevis interval in the Hibernia Field. Since the ichnological signatures of the Avalon/Ben Nevis are so well developed, a better understanding of their occurrence and significance could potentially enhance the capability to predict the distribution of hydrocarbon reservoir facies.

More recently, ichnology has also proven to be an invaluable tool in the characterization of bioturbated petroleum reservoirs. Bioturbation, particularly the introduction of mud and organic material by infaunal or burrowing organisms, is typically regarded as one of the main causes of reduced reservoir quality. As a consequence, enhanced oil recovery is often difficult and commonly fails in bioturbated reservoirs because burrows represent baffles to flow and induce permeability heterogeneity, two aspects typically not considered in residual oil calculations (Weber, 1986). To combat the ideology that all bioturbation is "bad", recent ichnological studies examined reservoirs in which bioturbation enhances reservoir quality, either pervasively, as in the case of Paleozoic carbonates within the Western Canada Sedimentary Basin (Pak *et al.*, 2001; Gingras *et al.*, 2002a, 2004), or within "special" bioturbated horizons such as *Glossifungites* surfaces (Gingras *et al.*, 1999a; Pemberton *et al.*, 2001a). Very few studies address the negative effects of bioturbation on fluid flow and petroleum migration (Weber, 1982, 1986; Carruthers, 2003).

Biogenically produced textural heterogeneity can directly control reservoir properties such as porosity, permeability, tortuosity and dispersivity. In addition to reducing porosity, the introduction of mud and organics by infaunal organisms, especially as burrow linings and fills, produces permeability heterogeneity. This is invariably linked to tortuosity in fluid flow pathways; burrow linings and fills of lower permeability act as baffles to fluid migration, creating much longer, more sinuous flow paths. Burrows also induce eddies, mixing, recirculation, backfilling, dead-end pores and adsorption. The presence of burrows in a reservoir can therefore result in reduced reservoir volume, high remaining oil saturation, reduced production rates and increased reservoir drainage time. These effects may remain unrealized during primary production, but with the initiation of water flooding and other secondary production strategies, complications can quickly arise if biogenic textural heterogeneity is ignored.

Although the principal targets for production in the Avalon/Ben Nevis reservoir interval are relatively clean, well sorted sandstones, substantial reserves are hosted in highly bioturbated muddy to silty sandstones. Integrating ichnological elements such as burrow morphology, connectivity and density with permeability measurements clearly illustrates the relationship between effective permeability and biogenic textural heterogeneity. In combination with modified percolation-invasion modeling techniques, this approach can lead to a better understanding of hydrocarbon recovery and migration in burrowed portions of the Avalon/Ben Nevis reservoir.

1.2 Objectives

This study is divided into two parts. The first part aims to incorporate ichnology into a detailed sedimentary facies analysis of the Avalon and Ben Nevis formations in an attempt to refine the depositional/stratigraphic model currently in use by industry geologists. Depositional systems and the tectono-sedimentary history of the Avalon/Ben Nevis interval will be investigated. The second part of this study focuses on the effect that bioturbation has on fluid flow and hydrocarbon production in the Avalon/Ben Nevis reservoir. The role that biogenic textural heterogeneity plays in determining flow properties and reservoir quality is specifically addressed. These two objectives are bridged by a re-examination of the bioturbate texture concept.

1.3 Methodology

Objectives of part one were achieved via in-depth examination of 820 m of core at a scale of 1:25 (Table 1.1; see Appendix 2 for representative lithologs). Two cores (J-34 and K-14) were shipped to the Ichnology Research Group (IRG) laboratory in Edmonton, Alberta; however, all other cores were logged at the Canada-Newfoundland/Labrador Offshore Petroleum Board (C-NLOPB) Core Research Facility in St. John's, Newfoundland. Lithologies, grain size variations, accessory components, physical and chemical sedimentary structures, degree of bioturbation, trace fossil types/diversity/relative abundance, facies and facies boundaries were documented. Fifteen facies were delineated and grouped into eight facies associations, which were correlated laterally between wells using gamma ray logs in conjunction with the cored intervals. An isopach map illustrating sand distribution and geometry within the lowermost hydrocarbon zone was constructed. Finally, the depositional and tectonic history was contemplated using paleogeographic maps representing the successively younger packages of sediment and hiatuses of the Avalon/Ben Nevis interval.

In order to achieve the objectives of part two, the nature of porosity and permeability over a bioturbated portion of core (i.e. Facies 6B in the Hibernia J-34 well) was examined on three levels: at the core scale, in thin section and through pressure-decay profile permeametry. Slices of core

Table 1.1: List of the cored intervals utilized in this study. Indicated depths are measured from the Kelly Bushing.

Well Name	Cored Interval (Depth from K.B.)	Core Length
Hibernia B-16 3	Cores 1-2: 2561.25 - 2589 m	27.75 m
Hibernia B-16 19Z	Cores 1-2: 4080 - 4141.5 m	61.5 m
Hibernia B-16 20Y	Core 1: 5830 - 5851 m	21 m
Hibernia B-16 23	Core 1: 4123 - 4155.1 m Cores 2-3: 4237 - 4290.6 m	85.7 m
Hibernia B-16 25	Cores 1-2: 4199 - 4296 m	97 m
Hibernia B-27	Cores 1-4: 2545.4 - 2610 m	64.6 m
Hibernia B-44	Cores 1-3: 2865 - 2949 m Core 4: 3145 - 3166 m	105 m
Hibernia C-96	Cores 2-4: 2302.5 - 2334.8 m	32.3 m
Hibernia G-55	Core 1: 2443.2 - 2453.9 m Core 2: 3352.8 - 3371 m	28.9 m
Hibernia J-34	Cores 1-13: 2455.4 - 2621.6 m	166.2 m
Hibernia K-14	Cores 1-6: 2345.1 - 2440 m	94.9 m
Hibernia K-18	Core 1: 2286 - 2304.2 m	18.2 m
Hibernia O-35	Core 1: 2184 - 2200.3 m	16.3 m

Total: 819.35 m

strategically cut through an interval of high burrow density were used to discern the morphology of the burrows. Eighteen thin sections were microscopically examined in order to determine porosity, textural differences between the framework and burrows, the structure of the burrow fill, sorting, grain size, cement types and cement distribution. Probe permeability measurements (specifically adapted to illustrate permeability contrasts between the framework and muddy burrows) were collected to ascertain the range and distribution of permeability values over the bioturbated interval (see Chapter 5 for details). Probe measurements were then compared to plug permeability measurements. MPath, computer software supplied by the Permedia Group of Ottawa, Ontario, was used for modeling fluid flow through the bioturbated medium. Details of the program, its operation and output are supplied in Chapter 5.

1.4 Outline

This study is presented in 6 chapters and 2 appendices as summarized below.

Chapter 1: Introduction and Background Information

In addition to the introductory material already discussed, this chapter goes on to provide a synopsis of all background information pertaining to the Avalon and Ben Nevis formations. Topics discussed include exploration history, geologic setting, basin evolution and lithostratigraphy, hydrocarbon migration and trapping, reservoir properties, biostratigraphy and previous work. A rationale for the initiation and implementation of this study is also provided.

Chapter 2: Facies Descriptions and Interpretations

Chapter 2 presents descriptions and interpretations of fifteen sedimentary facies. Particular consideration is given to the ichnological characteristics of the facies, especially those exhibiting high to intense degrees of bioturbation. Interpretations focus on the physical and biological processes that were responsible for the deposition of each facies. The characteristics of burrow-demarcated surfaces are also discussed.

Chapter 3: Facies Associations, Stratigraphy, Paleogeography and Tectonic Configuration

This chapter begins with the assignment of facies to eight facies associations. Stratal relationships between the facies associations are illustrated using stratigraphic cross sections. The latter part of Chapter 3 provides the tectonic and depositional history of the Avalon/Ben Nevis interval as illustrated by paleogeography.

Chapter 4: Bioturbate Textures

Bioturbate textures can play an integral role in both paleoenvironmental analysis and reservoir characterization. Chapter 4 is a transitional chapter that takes a closer look at the bioturbate texture concept and its history. Guidelines for the basic description of a bioturbate texture are also included.

Chapter 5: Biogenic Textural Heterogeneity, Fluid Flow and Hydrocarbon Production

The relationship between biogenically produced textural heterogeneity and fluid flow is examined in Chapter 5. The effect that this interaction has on hydrocarbon production in bioturbated reservoirs is also addressed.

Chapter 6: Conclusion

Chapter 6 presents the key conclusions from each of the previous chapters.

Appendix 1: **Pelosichnus mumorpha n. ichnogen., n. ichnosp.**: ***Inclined to Branching, Mud-filled Burrows***

High densities of inclined to branching, mud-filled burrows produce a conspicuous bioturbate texture within the Ben Nevis Formation. Appendix 1 provides a taxonomic classification, morphological description and ethological diagnosis of this trace fossil, herein referred to as *Pelosichnus mumorpha* n. ichnogen., n. ichnosp.

Appendix 2: Lithologs

Appendix 2 contains detailed illustrations representative of the cored sedimentary columns examined in this study. A gamma ray log accompanies most of the lithologs.

1.5 Background Information

Exploration History

Offshore eastern Canada has been one of the most intensely studied regions in frontier exploration for the last fifty years (Figure 1.1). Early exploration began in the 1950s when seismic refraction surveys, conducted offshore Newfoundland, concluded that the northeast portion of the Grand Banks was underlain by a thick succession of sedimentary deposits. In the 1960s, the Grand Banks and Flemish Cap/Pass areas were involved in a flurry of activity that included sea and air magnetometer surveys, shipborne gravity studies, refraction seismic surveys, bottom dredging and coring. The first industrial interest in the Jeanne d'Arc Basin was initiated through land acquisition in the southern portion by Pan American Petroleum (Amoco and Imperial, 1973). Shortly after in 1965, Mobil picked up the northeast portion. Gulf acquired a share in Mobil's acreage in 1970. Between 1966 and 1975, a total of 32 dry holes were drilled on the Grand Banks of Newfoundland, resulting in Amoco surrendering all of its land. Interest was renewed in the basin however, upon the drilling of the Mobil-Gulf Adolphus 2K-41 well located on a piercement saltdome in late 1971 into 1972. It tested oil flow at a rate of 43 m^3/day (Sinclair *et al.*, 1992). Despite this oil flow test and the penetration of both high quality source and reservoir rocks at the Egret K-36 well (drilled by

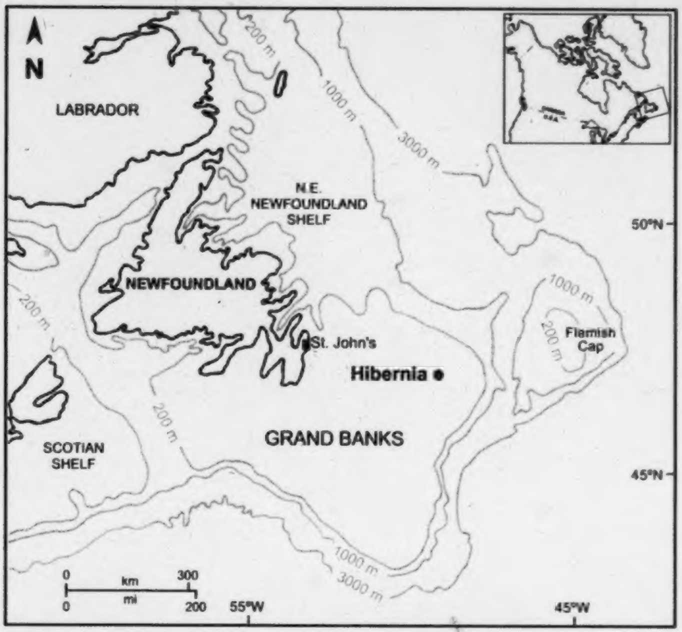
N
LABRADOR
N.E. NEWFOUNDLAND SHELF
NEWFOUNDLAND
St. John's
Hibernia
GRAND BANKS
SCOTIAN SHELF
Flemish Cap
200 m
1000 m
3000 m
50°N
45°N
55°W
45°W
0 km 300
0 mi 200

Figure 1.1: The Grand Banks of Newfoundland, offshore eastern Canada. The Hibernia Field is located approximately 315 km east of St. John's, Newfoundland. (Modified from Mackay and Tankard, 1990)

Amoco and partners in 1973), there was a lull in exploration activity in the Jeanne d'Arc Basin. It was not until 1978/79, when Petro-Canada exercised its buy-in option and Chevron and Columbia Gas farmed in on the Mobil/Gulf acreage, that the Hibernia P-15 well finally spudded. The P-15 well flowed 32° API at a flow rate of 3180 m^3/day, the most productive well in Canada at the time (Sinclair *et al.*, 1992). This discovery, now the giant class Hibernia Field, ushered in a whole new phase of oil exploration on the East Coast. Seventeen additional discoveries were made, with hopes that there are several more to be found.

Geologic Setting

The Grand Banks is a broad continental shelf located off the eastern coast of Newfoundland. It is partially underlain by a number of Mesozoic, fault-bounded rift basins that were developed upon the opening of the North Atlantic Ocean (Figure 1.2). Geologic boundaries of the Grand Banks include the Charlie Gibbs Transform Fault Zone to the north, the Newfoundland Transform Fault Zone to the south and the continent-ocean boundary to the east (Welsink *et al.*, 1989). The Jeanne

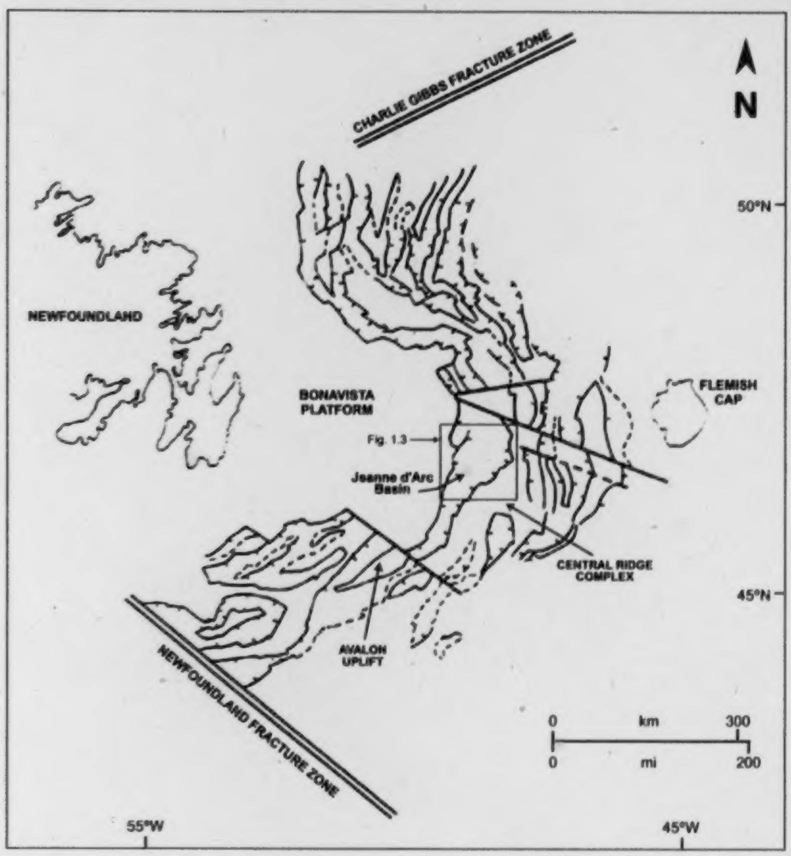
CHARLIE GIBBS FRACTURE ZONE
N
50°N
NEWFOUNDLAND
BONAVISTA PLATFORM
FLEMISH CAP
Fig. 1.3
Jeanne d'Arc Basin
CENTRAL RIDGE COMPLEX
45°N
AVALON UPLIFT
NEWFOUNDLAND FRACTURE ZONE
0
km
300
0
mi
200
55°W
45°W

Figure 1.2: Mesozoic rift basins of the Grand Banks. The location of Figure 1.3 is indicated. (Modified from Mackay and Tankard, 1990)

d'Arc Basin, which is located 315 km offshore eastern Newfoundland, has proven to be the most suitable for hydrocarbon accumulation (Figure 1.3). It is the deepest basin (up to 20 km of upper Triassic to Cenozoic sedimentary fill in the northerly located depo-center) with the most complete stratigraphic record (Keen *et al.*, 1987). This sedimentary section overlies a basement consisting of Precambrian metamorphic rocks and Paleozoic sedimentary, meta-sedimentary and igneous rocks (Enachescu, 1987; Grant and McAlpine, 1990). Major tectonic elements active during its creation include the Bonavista Platform to the west, the Avalon Uplift to the south and the Central Ridge Complex to the east. These highlands defined a narrow and elongate basin, which was enclosed to the south and connected to the newly forming North Atlantic Ocean to the north. The Murre Fault,

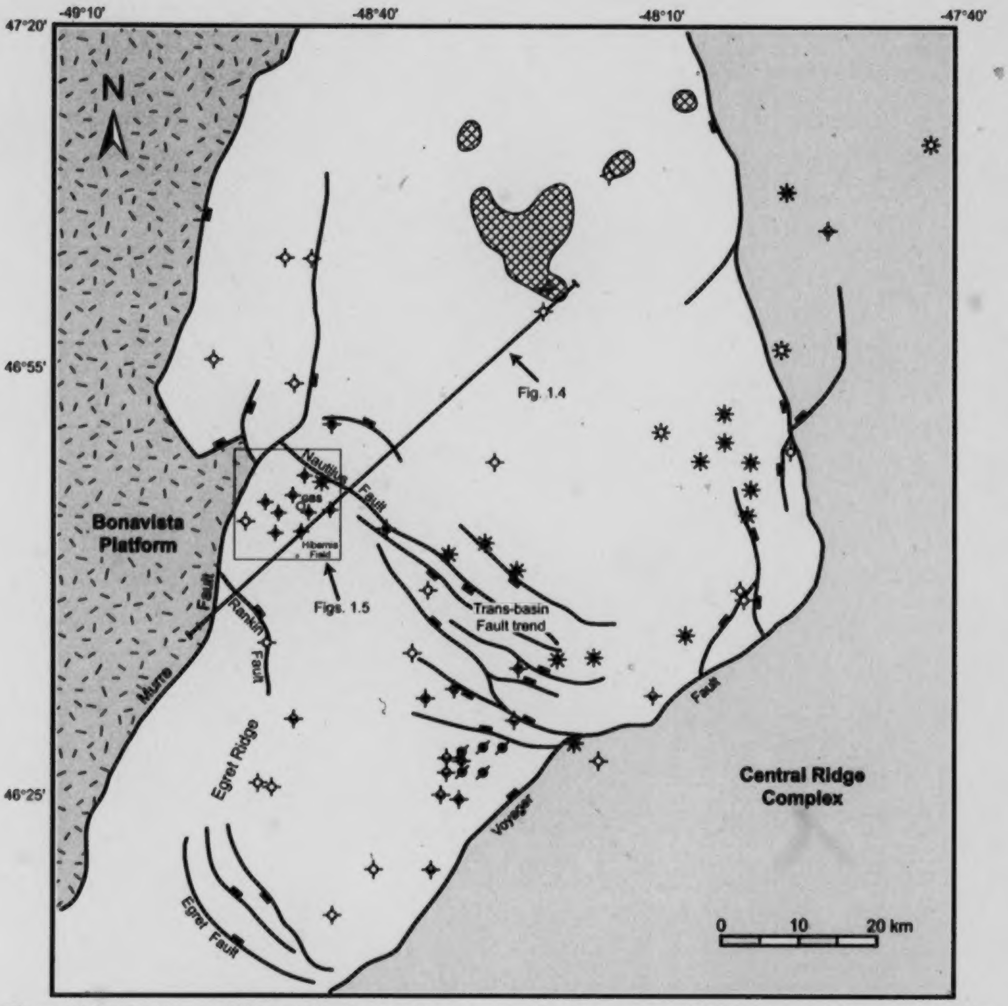
47°20'
-49°10'
-48°40'
-48°10'
-47°40'
46°55'
46°25'
N
Fig. 1.4
Nautilus Fault
gas
Hibernia Field
Bonavista Platform
Figs. 1.5
Trans-basin Fault trend
Murre Fault
Rankin Fault
Egret Ridge
Egret Fault
Voyager Fault
Central Ridge Complex
0
10
20 km

Figure 1.3: The Jeanne d'Arc Basin. Faults shown are as they occur in the Mid-Aptian to Upper Albian syn-rift sequence. The locations of Figures 1.4 and 1.5 are indicated. (Modified from Sinclair, 1995a)

a listric fault that penetrates the crust and soles out about 26 km to the east, forms the western boundary of the Jeanne d'Arc Basin (Figure 1.4); the eastern margin is terraced by a number of antithetic listric and planar faults (Tankard and Welsink, 1987). A major NW-SE trending fault trend known as the Trans-basin Fault Trend, dissects the basin; all hydrocarbon discoveries in the Avalon/Ben Nevis to date are located along or adjacent to this fault trend.

Located at the intersections of the Murre, Nautilus and Rankin faults, the Hibernia structure is a highly faulted, south-plunging rollover anticline (Figure 1.5). Numerous N-S and NW-SE oriented

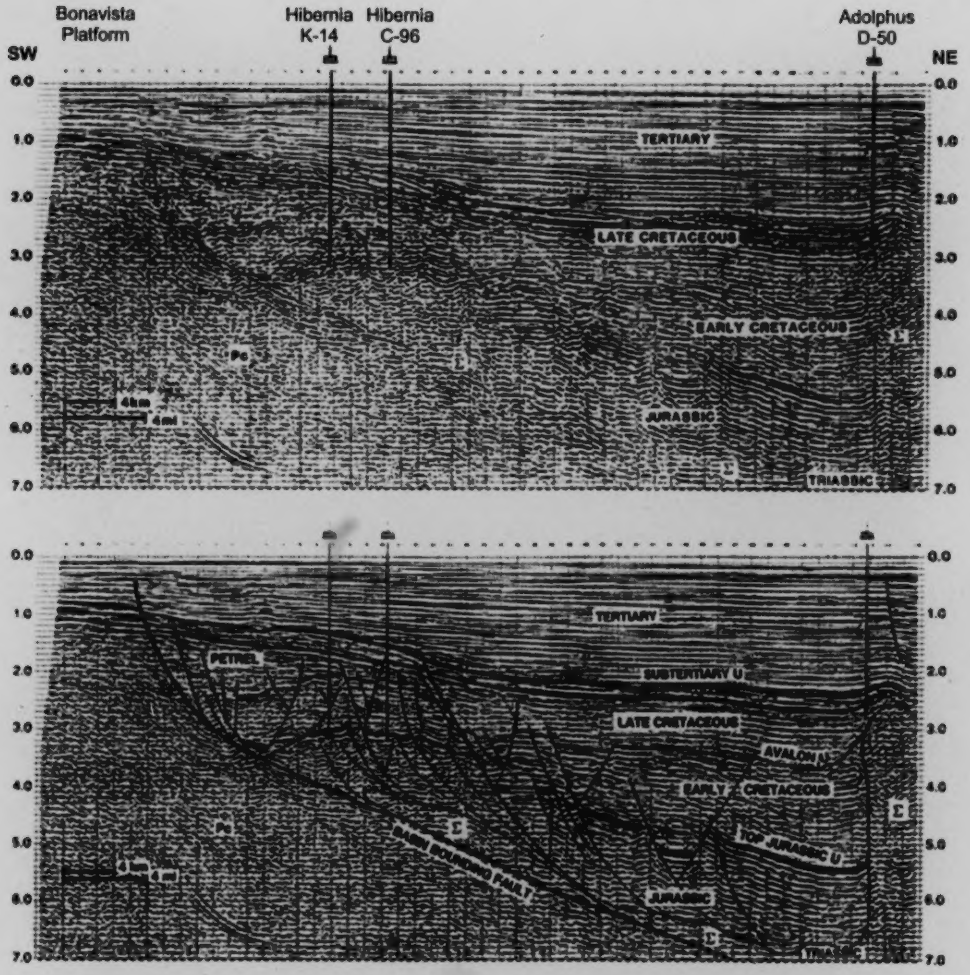
Bonavista Platform
Hibernia K-14
Hibernia C-96
Adolphus D-50
SW
NE
0.0
1.0
2.0
3.0
4.0
5.0
6.0
7.0
TERTIARY
LATE CRETACEOUS
EARLY CRETACEOUS
JURASSIC
TRIASSIC
Pc
Σ
4km
4mi
PETREL
SUBTERTIARY U
AVALON U
EARLY CRETACEOUS
TOP JURASSIC U
BASIN BOUNDING FAULT

Figure 1.4: Migrated time seismic section oriented SW to NE across the Jeanne d'Arc Basin. The basin-bounding fault is the Murre Fault. The section also shows the Hibernia rollover anticline, salt diapir and swell (Σ) and major unconformities: top of the Jurassic, the Barremian/Aptian Avalon Unconformity and the base of the Tertiary. Note that the Avalon/Ben Nevis sedimentary package, which at the level of the Avalon Unconformity, is wedge-shaped over the Hibernia structure. Also, in the vicinity of the Hibernia K-14 and C-96 wells, reflectors are rather flat, revealing an overall thin sedimentary package. The orientation of the seismic line is shown in Figure 1.3. (Modified from Enachescu, 1987)

normal faults transect the Hibernia area and define rhombohedral-shaped fault blocks (Sinclair *et al.* 1999). These transecting faults also divide the field into two main structural provinces, an axial high that encompasses the area between the Nautilus Fault and J-34 fault trend and a trough located along the southernmost extent of the Murre Fault and the entirety of the Rankin Fault. On the axial

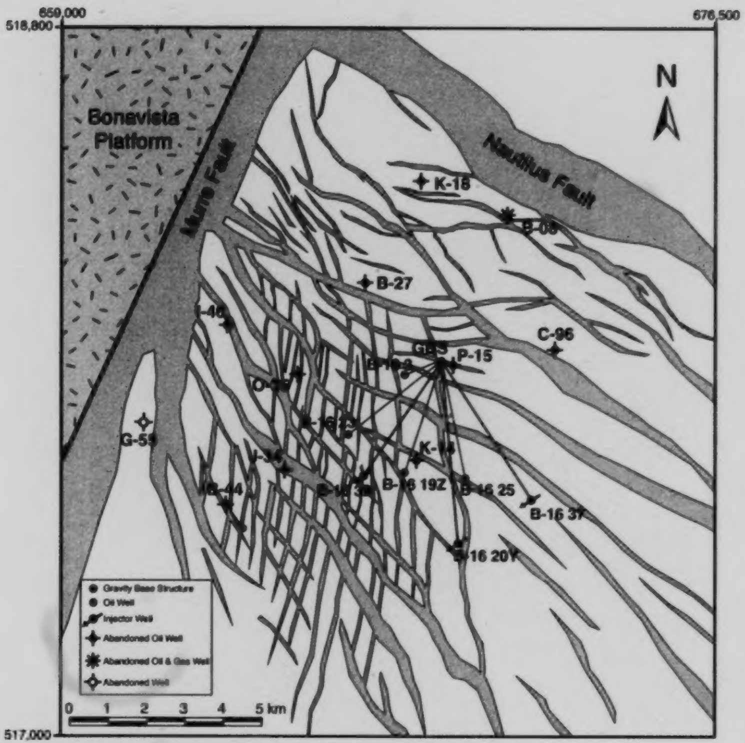
659,000
676,500
518,800
517,000
Bonavista Platform
Murre Fault
Nautilus Fault
N
K-18
B-08
B-27
I-46
C-96
GBS
P-15
B-16 2
O-35
B-16 23
G-55
J-34
K-14
B-16 38
B-16 19Z
B-16 25
B-16 37
B-16 20Y
K-44
Gravity Base Structure
Oil Well
Injector Well
Abandoned Oil Well
Abandoned Oil & Gas Well
Abandoned Well
0 1 2 3 4 5 km

Figure 1.5: Structure of the Hibernia Field. Faults are mapped at the Avalon/Ben Nevis reservoir level.

high, a field transecting "paleo-low" is delineated by the B-08 horst along the Rankin Fault to the north and the J-34 fault trend to the southwest (Figure 1.6). The overall sedimentary package defined as the Avalon/Ben Nevis interval thickens in a southwesterly direction. Seismic sections reveal that the two major structural provinces are associated with characteristically different sedimentary packages in the Avalon/Ben Nevis interval (Figures 1.7 and 1.8). Reflectors over the axial high are flat, varying in thickness only slightly, and denote a relatively thin succession of rocks. Along the Murre Fault, south of the Hibernia G-55 well location, a rather thick sedimentary wedge, which onlaps the axial high and the Murre Fault, is observed (Figure 1.7). Above this wedge and within the trough located along the Rankin Fault, the sedimentary package is lens-shaped, with the greatest thickness occurring just south-southeast of the J-34 fault trend (Figure 1.7). The sediments within this package onlap the sedimentary wedge to the southwest, the Rankin Fault to the south/southwest, the axial high to the north and older strata to the east.

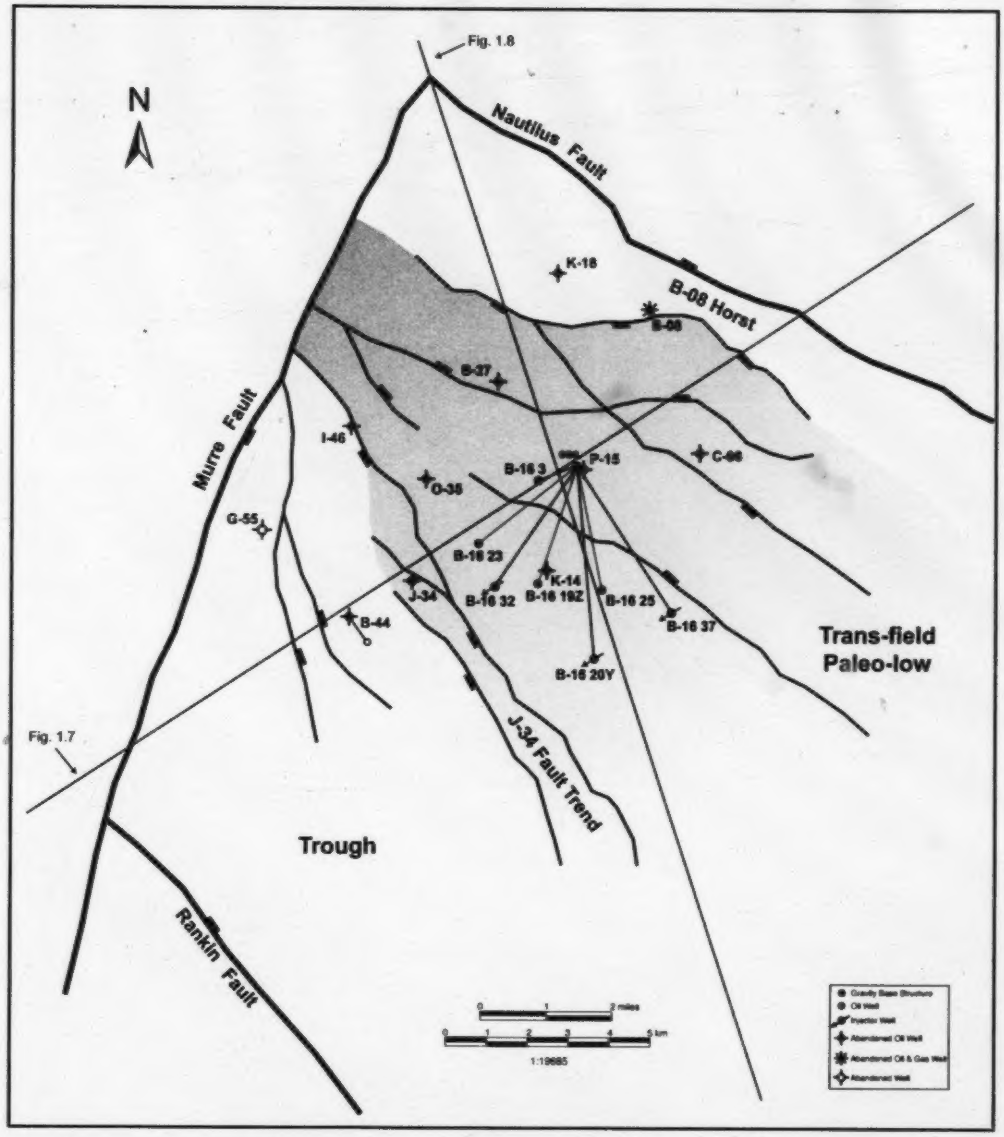
Fig. 1.8
N
Nautilus Fault
K-18
B-08 Horst
B-08
B-37
Murre Fault
I-46
O-35
B-16 3
P-15
C-96
G-55
B-16 23
K-14
J-34
B-16 32
B-16 19Z
B-16 25
B-16 37
B-44
B-16 20Y
Trans-field Paleo-low
Fig. 1.7
J-34 Fault Trend
Trough
Rankin Fault
0 1 2 miles
0 1 2 3 4 5 km
1:19685
Gravity Base Structure
Oil Well
Injector Well
Abandoned Oil Well
Abandoned Oil & Gas Well
Abandoned Well

Figure 1.6: Simplified structure of the Hibernia Field. The J-34 fault trend divides the field into two structural provinces, an axial high to the north and a trough to the southwest. On the axial high, the shaded region corresponds to the trans-field "paleo-low" that is defined by the B-08 horst to the north and the J-34 fault trend to the southwest. Locations of Figures 1.7 and 1.8 are indicated.

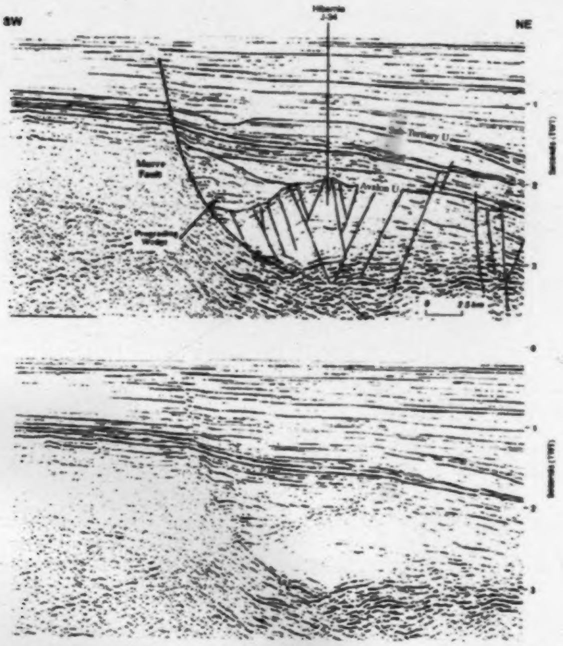
Hibernia
J-34
SW
NE
Murre Fault
Prograding Wedge
Sub-Tertiary U
Avalon U
1
2
3
0
2.5 km
0
1
2
3

Figure 1.7: Seismic reflection profile illustrating the prograding wedge in the vicinity of the Hibernia G-55 well. The trans-field paleo-low is also visible NE of the J-34 well location. The orientation of the seismic line is shown in Figure 1.6. (Modified from Driscoll *et al.*, 1995)

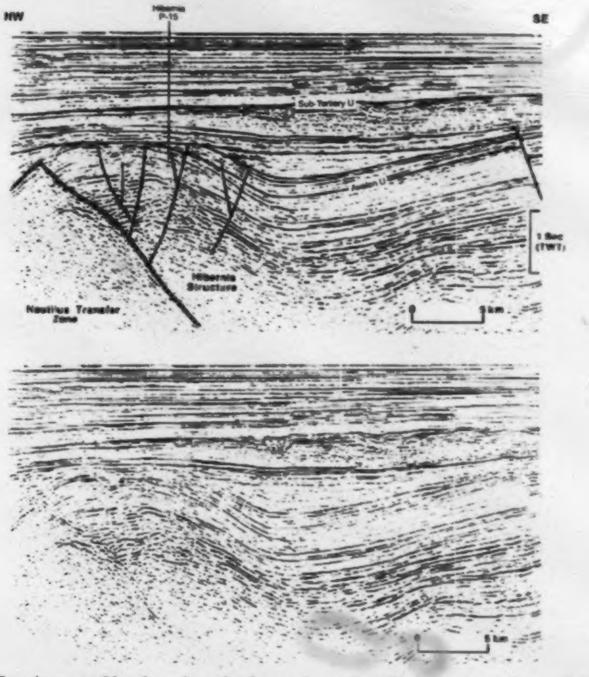
Hibernia
P-15
NW
SE
Sub-Tertiary U
Avalon U
1 Sec
(TWT)
Hibernia
Structure
Nautilus Transfer
Zone
0
5 km
0
5 km

Figure 1.8: Seismic reflection profile showing the lens-shaped sedimentary package that onlaps the Hibernia structure to the NW and uplifted older strata to the SE. The location of the seismic line is given in Figure 1.6. (Modified from Driscoll *et al.*, 1995)

Basin Evolution and Lithostratigraphy

A complete tectonic history of the break-up of Pangea and opening of the Atlantic Ocean is recorded in the thick depositional sequences in the rift basins of the Grand Banks. The Jeanne d'Arc Basin is host to a thick sedimentary fill, Triassic up to Recent in age, reflecting at least two, possibly three, episodes of ocean opening, with associated phases of extensional rifting and passive margin subsidence. The stratigraphy of the Jeanne d'Arc Basin is shown in Figure 1.9; the lithostratigraphic scheme follows that of Sinclair (1988; 1993). The following discussion describes the tectonic history and depositional record of the Grand Banks area and the Jeanne d'Arc Basin as summarized from Grant *et al.* (1986), Enachescu (1987), Tankard and Welsink (1988), Sinclair (1988), Tankard (1990), McAlpine (1990), Mackay and Tankard (1990), Enachescu and Dunning (1994) and Sinclair (1995a).

Initial Rifting

The first episode of rifting occurred in the Late Triassic from Early Carnian to approximately the Mid-Pliensbachian. Continental plate separation along the Atlantic coastline progressed sequentially from south to north around the Grand Banks. During initial extension, conglomerates and siliciclastic red beds of the Eurydice Formation were deposited in the newly created valleys under arid continental conditions. A halite-rich evaporite sequence, the Argo Formation, was then precipitated within the narrow fault-controlled basins. Marine limestones of the lower Iroquois Formation were deposited above the thick halite beds and subsequently were altered to anhydritic dolomites with thin evaporite layers. The later Iroquois limestones experienced much less dolomitization. The emplacement of igneous dykes also occurred during this stage. By the end of the first phase of rifting, the tectonic framework of the Grand Banks was in place and almost all the present day basins and sedimentary troughs had been initiated (Enachescu and Dunning, 1994).

First Thermal Sag

From Mid-Pliensbachian to Kimmeridgian time, a broad epicontinental sea occupied the Grand Banks. Thick successions of shales and limestones of the Downing, Voyager and Rankin Formations blanketed the area. Environments of deposition range from marginal marine deltaic to deeper marine. The Whale Member, a limestone unit within the Downing Formation, is a good Mid-

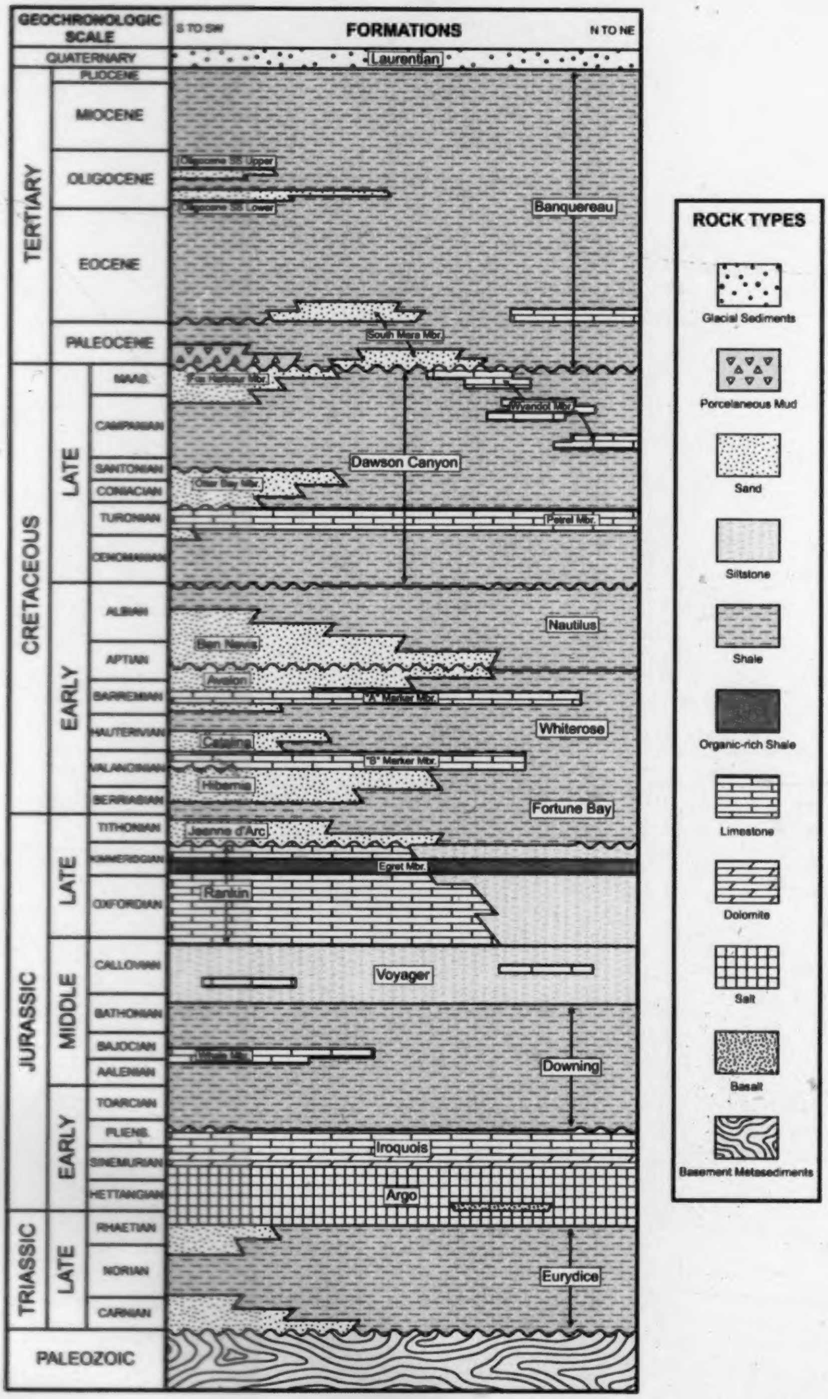
GEOCHRONOLOGIC SCALE
S TO SW
FORMATIONS
N TO NE
QUATERNARY
Laurentian
TERTIARY
PLIOCENE
MIOCENE
OLIGOCENE
Oligocene SS Upper
Oligocene SS Lower
Banquereau
EOCENE
PALEOCENE
South Mara Mbr.
CRETACEOUS
LATE
MAAS.
Fox Harbour Mbr.
Wyandot Mbr.
CAMPANIAN
Dawson Canyon
SANTONIAN
CONIACIAN
Otter Bay Mbr.
TURONIAN
Petrel Mbr.
CENOMANIAN
EARLY
ALBIAN
Nautilus
APTIAN
Ben Nevis
Avalon
BARREMIAN
"A" Marker Mbr.
HAUTERIVIAN
Catalina
Whiterose
VALANGINIAN
"B" Marker Mbr.
Hibernia
BERRIASIAN
Fortune Bay
JURASSIC
LATE
TITHONIAN
Jeanne d'Arc
KIMMERIDGIAN
Egret Mbr.
OXFORDIAN
Rankin
MIDDLE
CALLOVIAN
Voyager
BATHONIAN
BAJOCIAN
Whale Mbr.
AALENIAN
Downing
EARLY
TOARCIAN
PLIENS.
Iroquois
SINEMURIAN
HETTANGIAN
Argo
TRIASSIC
LATE
RHAETIAN
NORIAN
Eurydice
CARNIAN
PALEOZOIC
ROCK TYPES
Glacial Sediments
Porcelaneous Mud
Sand
Siltstone
Shale
Organic-rich Shale
Limestone
Dolomite
Salt
Basalt
Basement Metasediments

Figure 1.9: Lithostratigraphy for the entire sedimentary column hosted in the Jeanne d'Arc Basin. (Modified from Sinclair, 1988)

Jurassic seismic marker extending across most of the basin. Distinctive organic-rich shale of Early Kimmeridgian age represents the major oil source in the basin. The Egret Member was deposited in a basin with restricted, anoxic bottom waters. Due to subsequent erosion, the depositional area south of the Egret Fault is uncertain. This episode of sag marks a hiatus in continental crust extension between the initial rifting event and Late Jurassic reactivation of the rift system.

Reactivation and Syn-rift Deposition

The near base Tithonian (or middle Kimmeridgian *sensu anglico*) unconformity marks the renewal of extension and initial development of the Avalon Uplift. Consequently, rift shoulders suffered erosion, contributing substantial amounts of clastic debris into the rejuvenated grabens. Three of the four main reservoirs were developed at this time: the Jeanne d'Arc, Hibernia and Catalina reservoirs. The Jeanne d'Arc Formation consists of coarse clastics deposited during Tithonian time within fluvial-dominated incised valleys. Shale and siltstone of the overlying Fortune Bay Formation provide a suitable seal for this oldest syn-rift reservoir. The Fortune Bay shale-dominated sediments were deposited in a progradational marginal marine to neritic environment, possibly as a result of long-term subsidence variations, combined with eustatic sea level change. Most production in the Hibernia Field is currently confined to the Hibernia Formation. This deposit consists of medium to coarse-grained sandstones alternating with shales and siltstones deposited in a northward prograding fluvial-deltaic system. There is evidence of multiple periods of incision resulting in development of broad stacked valleys in the Hibernia area. This package of syn-rift strata is characterized by the development of syn-tectonic structures related to the synchronous continuation of basement stretching, formation of salt diapirs and sedimentary faulting.

Second Thermal Sag

The "B" Marker, a limestone unit indicating initiation of a second period of basin stability, lies above the Hibernia Formation. This unit provides an excellent regional stratigraphic and seismic marker. Fine-grained sandstones, siltstones, shales and minor limestones of the Catalina litho-unit signify a return to deposition in nearshore marine to possibly paralic environments. Thick silty shales of the Whiterose Formation were deposited distally to, and above, the interbedded Catalina sandstones and shales. Another laterally persistent limestone, the "A" Marker, lies above silty shales of the Whiterose Formation at the Hibernia and Whiterose localities, while a thick accumulation of oolitic and bioclastic-rich sandstones and limestones was deposited in the central to southern portions of the Jeanne d'Arc basin (Eastern Shoals Formation of McAlpine, 1990). The coarsening-upward marine sandstones and shales of the Avalon Formation represent a regressive phase of basin infilling, possible in response to renewed uplift of the southern end of the Jeanne d'Arc Basin.

Final Reactivation and Syn-rift Deposition

A final episode of large-scale, widespread structural deformation in the Jeanne d'Arc Basin occurred during Barremian or Aptian time (see Biostratigraphy section). This event was characterized by growth of dominantly NW-SE-trending normal faults. Though there is considerable range of opinion on the driving mechanism for this faulting (see review in Sinclair, 1993), this interval is interpreted to be the final episode of rifting to affect the continental crust of the northern Grand Banks region. The presence of numerous "plastic" layers within the Jeanne d'Arc stratigraphic column (salt of the Argo Formation, and shales of the Downing, Fortune Bay and Whiterose Formations), however, did result in many of the Aptian-Albian faults soling out in detachment horizons above synchronously extending basement (Sinclair, 1995b). Salt diapirism also appears to have been widely active during this period of fault growth resulting in initiation of a number of salt ridges and pillars.

Whatever the driving mechanism, this episode of faulting had a crucial effect on Aptian-Albian stratigraphic stacking patterns in the Jeanne d'Arc Basin. That is, it induced highly variable rates of accommodation space creation. Consequently, deposition representing the Avalon Formation was terminated and a long-term transgression above an unconformity referred to as the "Avalon Unconformity" (Grant and McAlpine, 1990; McAlpine, 1990) or "Mid-Aptian Unconformity" (Sinclair, 1993) began. The combination of increasing accommodation space with large volumes of siliciclastic sediment shed from the raised rift margins resulted in deposition of variable marginal to shallow marine sandstones of the Ben Nevis Formation under overall transgressive conditions. Tankard and Welsink (1988) reported that these Aptian-Albian sediments represent a transitional period between the final rifting event and the final thermal sag phase. Abundant syn-sedimentary faults throughout the interval support syn-tectonic deposition.

Together, the Avalon and Ben Nevis formations make up the youngest and most common hydrocarbon-bearing interval in the Jeanne d'Arc Basin. The Ben Nevis grades laterally and vertically into the Nautilus Formation, shale that was continuously deposited in the deepest portions of the basin.

Final Thermal Sag

During Cenomanian time, the fault-bounded margins of the Jeanne d'Arc Basin were flooded and the widely subsiding region became starved of clastics, leading to deposition of the Petrel Member lime mudstones. Subsequently, outbuilding of the shelf occurred, resulting in development of a prominent shelf-slope break at the leading edge of the Otter Bay sandstones and again at the leading edge of the Fox Harbour sandstones. These broad patterns of Dawson Canyon Formation deposition above both the Jeanne d'Arc rift basin and the adjacent Bonavista Platform marked initiation of the most recent episode of thermal sag to affect the Grand Banks region. At the top of this Cretaceous package is a regional unconformity (base Tertiary Unconformity), exhibiting channeling and canyons on the shelf edge margins. This indicates a marked relative sea level drop at this time, which resulted in deposition of submarine fans at the toe of the Upper Cretaceous slope (South Mara Member sandstones). Throughout the Tertiary, depositional patterns over the Grand Banks were typical of a passive margin flanking the spreading Atlantic Ocean. Low sediment influx, long-term thermal subsidence and tilting led to the deposition of a structurally undisturbed marine succession (McAlpine, 1990). The Banquereau Formation is largely composed of deep marine shale and minor chalks with additional siliceous muds and silts. In the Oligocene, a possible change to shallow, neritic environments can be recognized in the presence of two regressive sandstone units. The youngest sediment package on the Grand Banks are paralic glacial sediments deposited by shield ice masses during the Quaternary.

Hydrocarbon Migration and Trapping

Due to its complex tectonic history, the movement of hydrocarbons within the Jeanne d'Arc Basin has likely followed a variable and intricate path. All oils, however, have been geochemically traced almost exclusively to one source rock, the Kimmeridgian-aged Egret Member (Swift and Williams, 1980; Grant *et al.*, 1986; Creaney and Allison, 1987). This sequence of calcareous, organic-rich shales was deposited under euxinic conditions in partially restricted epicontinental basins. The thickness of the Egret Member varies from 40 to 80 m; in the center of the basin it has been estimated to get up to 200 m (Enachescu and Dunning, 1994). This source, buried to depths ranging from 3,300 to 5,000 m, contains oil-prone Types I and II kerogen and an average total organic content of 3% (going as high as 9%) (Grant *et al.*, 1986). Oils are typically light (30-35° API) but several heavy oil pools have been encountered at shallow depths, possibly indicating biogenic alteration.

Hydrocarbons were generated over a wide spectrum of maturation levels and can differ in maturity in stacked pools of the same field. Currently, central and northern parts of the basin are overmature and thus tend to be more gas prone. Vertical variation within fields implies that several episodes of oil migration and emplacement have taken place (Grant and McAlpine, 1990). Migration began in the Mid-Cretaceous and peaked in the Middle Eocene (Grant *et al.*, 1986).

Seals are abundant in the basin; they occur as interbedded intervals encasing reservoirs shortly after deposition and as massive packages providing regional cap rocks. Important regional seals include the Fortune Bay, Whiterose, Nautilus, Dawson Canyon and Banquereau Formations. Trapping is strongly influenced by the structural framework developed during the long and complex geologic history of the Grand Banks area. Traps may also have a stratigraphic component where the pool edge is defined by the depositional limit of the reservoir facies. Structural traps include full/half grabens, horsts, tilted blocks, rollovers, transfer faults, folds and salt domes/diapirs. Sedimentary traps include pinch-outs, sub-crops below unconformities and shale-encased sandstones. The major reservoirs in the Jeanne d'Arc Basin are all composed of siliciclastics deposited within syn-rift sequences. These include the Jeanne d'Arc, Hibernia, Catalina and Ben Nevis/Avalon Formations. Discoveries have also been made in the Rankin and Eastern Shoals Formations, as well as the Otter Bay and South Mara Members.

The Ben Nevis/Avalon Reservoir

The Avalon/Ben Nevis reservoir consists of the older Avalon Formation unconformably overlying the younger Ben Nevis Formation. The Avalon is an upward-coarsening, progradational body whereas the Ben Nevis is an upward-fining, transgressive package. Both formations exhibit a high degree of bioturbation that occurs ubiquitously across the basin, suggesting that these units likely represent a variety of marginal marine to shallow marine environments (Sinclair, 1993). The reservoir is variably calcite cemented; however, the cements are not assumed to be laterally continuous or pose any major problems for production (Hurley *et al.*, 1992). In the reservoir facies of both units, porosities have been found to range up to about 30%. Measured permeabilities to air can get as high as multi-darcy in the cleanest, highest energy intervals, but are generally in the 10s to 100s of millidarcies in thinly interbedded sandstone facies and less than 10 millidarcies in bioturbated muddy to silty sandstone facies. The Avalon/Ben Nevis interval contains hydrocarbons in most of the delineated fields in the basin; in the Hibernia Field it has been targeted for production only recently (CNOPB, 2004). All delineation wells except Hibernia G-55 encountered oil; a gas cap is located in the vicinity of the B-08 well.

The Avalon/Ben Nevis interval contains two hydrocarbon-bearing zones in the Hibernia Field, both of which are assigned to the Ben Nevis Formation. Although shallow marine sandstones are assigned to the Avalon Formation in other parts of the basin (Sinclair, 1995a), in the Hibernia area the Avalon consists of silty to sandy mudstone of very poor reservoir quality. The lower hydrocarbon-bearing zone, also known as the B-27 Basal Sands (CNOPB, 2003), is a relatively thin sandstone (net pay averages 35 m) that is effectively confined to the delineated portion of the Hibernia area (i.e. it is absent south of the Hibernia J-34 well location). The upper hydrocarbon-bearing zone, which contains the B-27 Upper Sands, J-34 Sands, O-35 Basal Sands and O-35 Upper Sands as indicated by CNOPB (2003), is a southward and southwestward-thickening package of clean, well sorted sandstone and bioturbated, muddy to silty sandstone. Although clean sandstones are the primary target in this zone (net pay at least 100 m), substantial hydrocarbon accumulations are contained within the bioturbated, muddy to silty sandstones. Over the delineated portion of the field, this upper zone is rarely greater than 150 m; however, it has the potential to be 2-3 times thicker along the Murre and Rankin faults (CNOPB, 2003). It is assumed that bioturbation will have a considerable effect on hydrocarbon production from this reservoir. However, no studies on the relationship between bioturbation and reservoir quality have been attempted to date.

Biostratigraphy

Dating of the Avalon and Ben Nevis formations, and thus placement of the "Avalon Unconformity" in the sedimentary succession, remains a matter of debate amongst industry geologists. They have conventionally used the highest occurrences of dinoflagellates species belonging to what they call the "Speeton Assemblage" or an ostracod subzone (*Hutsonia* sp.) to mark the top of the Barremian Stage and what is termed "*C. tabulata* Assemblage" and "*C. dampieri* Assemblage" to designate the top of the Aptian (Soliman, 1995). Biostratigraphic studies, to date, have agreed on the existence of at least one significant hiatus (associated with the Avalon Unconformity), but they have been unsuccessful in determining whether it is Late Barremian or Aptian in age because multiple extinction events of the same species can be found throughout the interval in question (Jenkins, 1984; Jenkins, 1993). This may be attributable to the repetitive occurrence of the microfossil-hosting facies in a marginal marine system or fossil recycling due to erosion of Avalon sediments and their incorporation into Ben Nevis sediments. Biostratigraphic work soon to be made accessible to the public may possibly clear up this issue (I. Sinclair, pers. comm.).

Previous Work: Petrography, Diagenesis, Facies and Depositional Environments

Lee (1987) described sandstones of the Avalon/Ben Nevis interval as mineralogically mature sublitharenites to quartz arenites; accessory components include bioclastic fragments, siderite rhombs that bind the detrital framework grains and pyrite. In addition to quartz overgrowths, Lee reported three phases of calcite cementation, one phase of dolomitization and at least one phase of dissolution. At least two phases of cementation, circumgranular calcite cement and pore-filling, poikilotopic, ferroan calcite cement, have been reported (Soliman, 1995); however, discrepancy exists in the interpretation of the timing and origin of these cements. Hutcheon *et al.* (1985) suggested that cementation took place during meteoric water influx at the mid-Cretaceous unconformity and Abid (1988) reported that the cement precipitated as a result of upward-moving, hot shale waters mixing with meteoric waters. Soliman (1995) indicated a much shallower freshwater origin for the poikilotopic ferroan calcite cement. He suggested that the cement represents freshwater recharging during cessation of fault activity, regional uplift and emergence of the Hibernia rollover.

Soliman (1995) conducted the only known detailed facies analysis of the Avalon/Ben Nevis interval over the Hibernia area to date. He concluded that the Avalon/Ben Nevis interval (his Avalon Formation) represents the repetitive development of estuarine and barrier island depositional systems. Although Soliman provided an excellent synopsis of the sedimentary facies, he did not acknowledge fault displacement in several of the key wells and confined his interpretation to structurally controlled valleys on the Hibernia rollover structure. Other interpretations encountered in the literature constitute only minor references in otherwise stratigraphy-oriented studies. Grant and McAlpine (1990) and McAlpine (1990) suggested that the sandstones were deposited in an estuarine environment and that the shales represented lagoons and tidal flats. Lee (1987) suggested a range of settings from supratidal to basinal offshore. Hurley *et al.* (1992) reported that the Avalon Formation was deposited in a shallow bay environment that was then subaerially exposed and gradually transgressed, giving way to shoreline sandstones and finer grained shelf shales. He also suggested that conglomerates overlying coal and red mudstone in the Hibernia G-55 well likely represent alluvial fan sedimentation adjacent to the basin margin. Sinclair (1988; 1993) interpreted the Ben Nevis interval as a locally preserved basal association representing interfingering backbarrier environments (his Gambo Member) and an upper ubiquitous facies association comprising tidal inlet channel, shoreface and lower shoreface/offshore transition sandstones. Industry geologists have slightly modified the interpretation of Sinclair (1988; 1993) more recently (CNOPB, 2003). In this government report, they suggested that the lowermost interval of the Ben Nevis was deposited in incised valleys. Although a common theme resonates through all of the aforementioned stratigraphy-based studies (regarding the likely depositional environments represented in the Avalon/Ben Nevis interval), a workable depositional model remains elusive.

1.6 Rationale

The two main goals of this study are aimed at outlining the ichnology of the Avalon and Ben Nevis formations, which apart from internal reports conducted by S.G. Pemberton (1984; 1985) has never been formally pursued. With this end result in mind, this project was initiated by the Hibernia Management and Development Company (HMDC) as a mutually beneficial, joint academic-industry venture. Facies analysis and reservoir characterization from an ichnological viewpoint will provide unique insight into the nature and distribution of the depositional systems of the Avalon/Ben Nevis in order to improve the model currently used by industry geologists. Information gathered and concepts developed in this study will also contribute to the ever-expanding ichnological database and advance the awareness of this relatively young discipline and its application in paleoenvironmental analysis and reservoir characterization.

Chapter 2

Facies Descriptions and Interpretations

2.1 Introduction

A total of 15 facies (F1 through F15) are identified within the Avalon/Ben Nevis interval (Table 2.1). The facies are presented in succession according to overall grain size (generally, finest to coarsest grained). Each facies description presents a synopsis of the physical and biogenic sedimentary structures contained within it. Petrographic properties of sandstones are excluded since all sandstones were found to be of similar composition by Lee (1987). And, since no definite relationship is recognized between facies and calcite cementation (Hurley *et al.*, 1992), the petrographic properties of the pore-occluding calcite cement are also excluded. However, accessory cements such as siderite, pyrite and other carbonates are included because their occurrence and distribution varies between facies. The interpretation for each facies concentrates on processes of deposition and biological alteration. A brief synopsis of the environmental parameters represented by each facies is included. The characteristics of burrow-demarcated surfaces are also discussed.

2.2 Facies Descriptions and Interpretations

Facies 1 – Dark, Organic-rich Mudstone

Description

Facies 1 consists of dark grey to black mudstone that is confined to sharp-bounded beds averaging 2 to 3 cm in thickness (Figure 2.1). Given the dark color of this facies, organic content is assumed to be quite high. Facies 1 is typically massive or structureless and rarely associated with bioclastic fragments. Faint, planar lamination is visible in some beds.

For the most part F1 is unburrowed, but the bounding surfaces are locally protruded by traces originating from underlying or overlying facies, such as fugichnia, *Chondrites*, *Teichichnus* or *Planolites*.

Of all facies, F1 is the thinnest (maximum of 10 cm thick), and is found interbedded with bioturbated muddy to silty sandstones of Facies 6 and massive to laminated sandstones of Facies 9.

Table 2.1a: Summary of facies characteristics. The key sedimentary structures and trace fossils of each facies are shown in bold type.

Facies	Facies Description	Sedimentary Structures & Accessories	Biogenic Structures		Depositional Environment
1	Dark, organic-rich mudstone	Massive to faint planar laminae, **sharp boundaries**	**Ch** (r), **Pl** (r)		Hyperpycnal Flow
2	Multicolored mudstone & siltstone	**Multicolored**, fissile to massive or **chaotic**, **carbonate stringers & nodules**, pyrite nodules, **turreted gastropods** & bioclasts, plant remains, carbonaceous debris	**Roots** (c), Pl (r), Te (r), Ch (r), Th (r), Pa (r)		Soils/Marsh/ Floodplain
3A	*Teichichnus*, *Asterosoma* & *Scolicia*-dominated silty to sandy mudstone	Planar laminae, wavy to low-angle cross stratification, **wave ripples**, mud clasts, bioclasts & calcareous worm tubes, **siderite**, rare carbonaceous debris & pyrite	**Te** (a), **As** (a), **Sc** (a), Ch (c), Pl (c), **Zo** (m), Th (m), Ph (r), Ro (r), Pa (r), Rh (r), fu (r)		Deltaically Influenced Distal Lower Shoreface/ Muddy Proximal Embayment (Delta Front)
3B	*Chondrites* & *Planolites*-dominated silty to sandy mudstone		**Ch** (a), **Pl** (a), Th (m), **As** (r), Zo (r), **Sc** (r), Ph (r), Pa (r)		
4	Wavy to lenticular-bedded mudstone	Planar to wavy laminae, current & wave ripples, **lenticular to wavy bedding**, **load casts**, rare pyrite, **siderite**, **syneresis cracks**	Ch (a), Pl (a), **Te** (a), **Th** (c), **As** (f), Sc (f), **Zo** (f), Op (r), Rh (r), Pa (r), Sk (r), **fu** (r)		Deltaically Influenced Offshore/ Distal Embayment (Prodelta)
5A	Bioclastic mudstone	Fissile or blocky, planar to wavy laminae, **chaotic**, abundant **gastropods & oysters**, carbonaceous & wood debris, pyrite	**Mottling** (a), Ch (m), Pl (m), Th (f), Te (r)		Deep Lagoon, Mudflat, Oyster Reefs
5B	Bioclastic silty sandstone	Chaotic, Low-angle to wavy cross stratification, **current & wave ripples**, scours with **pelecypod/oyster lags**, plant remains, wood, carbonaceous debris, pebbles	**Op** (c), **Th** (c), **Mottling** (c), Pa (m), Sk (f), Ar (f), Pl (r), **Te** (r), **Ch** (r), **Roots** (r)		Shallow Lagoon, Sandflat, Tidal Creek
6A	*Scolicia*, *Asterosoma* & *Teichichnus*-dominated muddy to silty sandstone	Planar laminae, low-angle cross stratification, **wave ripples**, mud clasts, pelecypods, **echinoids**, calcareous worm tubes, **oysters**, gastropods, carbonaceous debris & wood fragments, rare pyrite, **common siderite**	**Sc** (a), **As** (a), **Te** (a), **Th** (m), Op (m), Ph (m), Pe (r)	Pl (c), Ch (c), Pa (m), Rh (f), Cy (r), Ro (r), Di (r), Sk (r), Zo (r), fu (r)	Deltaically Influenced Proximal Lower Shoreface/ Sandy Proximal Embayment (Delta Front)
6B	*Phycosiphon* & *Pelosichnus*-dominated muddy to silty sandstone		**Pe** (a), **Ph** (a), **Th** (c), **Sc** (c), Op (f), Te (r), As (r)		
6C	*Ophiomorpha* & *Thalassinoides*-dominated muddy to silty sandstone		**Op** (a), **Th** (c), Sc (m), Ph (m), As (r), Te (r), Pe (r)		

Ar – *Arenicolites*, As – *Asterosoma*, Ch – *Chondrites*, Co – *Conichnus*, Cy – *Cylindrichnus*, Di – *Diplocraterion*, fu – Fugichnia, La – *Pelosichnus mumorpha* n. ichnogen., n. ichnosp., Ma – *Macaronichnus*, Op – *Ophiomorpha*, Pa – *Palaeophycus*, Ph – *Phycosiphon*, Pl – *Planolites*, Rh – *Rhizocorallium*, Ro – *Rosselia*, Sc - *Scolicia*, Sk – *Skolithos*, Te – *Teichichnus*, Th – *Thalassinoides*, Zo – *Zoophycos*, a – abundant, c – common, m – moderate, f – few, r – rare

Table 2.1b: Continuation of summary of facies characteristics. The key sedimentary structures and trace fossils of each facies are shown in bold type.

Facies	Facies Description	Sedimentary Structures & Accessories	Biogenic Structures	Depositional Environment
7	Ripple cross-laminated sandstone with mudstone	**Wavy to flaser bedding**, **wave & current ripples**, **convolute**, planar to low-angle cross stratification, carbonaceous debris, wood, plant remains, mud clasts	**Di** (f), **fu** (f), **Roots** (f), Op (r), Pa (r), Th (r), Sk (r), Te (r), Pl (r), Ch (r)	Crevasse Splay/ Channel Levee/ Washover Fan
8	Massive to mottled sandstone	**Massive**, planar to low-angle cross stratification, **multicolored**, **chaotic**, pebbles, carbonaceous debris, siderite, carbonate stringers	Pa (r), Sk (r), Di (r), Mottling?	Subaerially Exposed Channel?
9	Massive, planar to low-angle laminated sandstone	**Clean, well-sorted, massive**, convolute, **faint planar to low angle cross stratification**, trough to high-angle cross bedding, wave ripples, **graded laminae**, **scours with mud clasts, pebbles & bioclasts**, **carbonaceous laminae**	**Op** (r), As (r), Ph (r), **fu** (r), Pa (r), Sk (r), Ma (r), Ch (r)	Upper Shoreface/ Sandbar, Shoal/ Distributary Mouth Bar
10	Wavy to low-angle laminated sandstone	Massive, **planar to wavy laminae (HCS)**, low-angle cross stratification, **wave ripples**, **undulatory scours** with mud clasts & bioclasts	**Op** (m), **fu** (m), **As** (m), **Ph** (m), Pa (m), Th (m), Sk (r), Cy (r), Ar (r), Co (r)	Storm/Tempestite
11	Trough to high-angle cross-bedded sandstone	Well-sorted, **high-angle to trough cross bedding**, low-angle to wavy cross stratification, convolute, **mud flasers & couplets**, **current & wave ripples**, scours with mud clasts, pebbles & bioclasts, wood	Op (r), Sk (r), Pa (r), Ma (r), fu (r)	Active Tidal Channel/ Sandbar/ Shoal/Inlet
12	Bioturbated sandstone	Planar to low-angle cross stratification, **wood**, **coal laminae, pyrite, carbonaceous debris, scattered pebbles & bioclasts**	**Op** (a), **Th** (a), **Pa** (a), fu (f), Sk (f), Te (r), Ch (r)	Inactive Tidal Sandbar/Shoal/ Pointbar/Tidal Flat
13	Coaly to muddy sandstone	**Coal & mud lenses, flasers & wavy beds**, trough cross bedding, **current ripples**, planar to low-angle cross stratification, **soft sediment deformation**, pyrite, **load casts**, rare scours with pebbles and bioclasts	Pa (m), Pl (m), Th (f), Ch (f), Op (r), fu (r)	Crevasse Channel/ Abandoned Tidal Channel
14A	Sand-supported conglomerate	**Rounded to well rounded, pebbles & cobbles**, crude normal grading, weak imbrication, low-angle laminae, **bioclasts & mud clasts**, carbonaceous debris, wood	No trace fossils noted	Channel Lag
14B	Mud-supported conglomerate		**As** (r), **Te** (r), Pa (r), Sc (r), **Ph** (r), Pl (r), **Rh** (r), Ch (r), Op (r)	Transgressive Lag
15	Pebbly, carbonaceous sandstone	**Chaotic/deformed**, low-angle cross stratification, trough to high-angle cross lamination, **scours with pebbles**, **coal beds, mud laminae/beds**, carbonaceous debris	Mottling (a), **Pa** (c), **Op** (c), Sk (m), **fu** (f), **Pl** (f), Th (f), Ch (r), Te (r), **Roots** (r)	Bayhead Delta/ Fan Delta

Ar – *Arenicolites*, As – *Asterosoma*, Ch – *Chondrites*, Co – *Conichnus*, Cy – *Cylindrichnus*, Di – *Diplocraterion*, fu – Fugichnia, Pe – *Pelosichnus mumorpha* n. ichnogen., n. ichnosp., Ma – *Macaronichnus*, Op – *Ophiomorpha*, Pa – *Palaeophycus*, Ph – *Phycosiphon*, Pl – *Planolites*, Rh – *Rhizocorallium*, Ro – *Rosselia*, Sc - *Scolicia*, Sk – *Skolithos*, Te – *Teichichnus*, Th – *Thalassinoides*, Zo – *Zoophycos*, a – abundant, c – common, m – moderate, f – few, r – rare

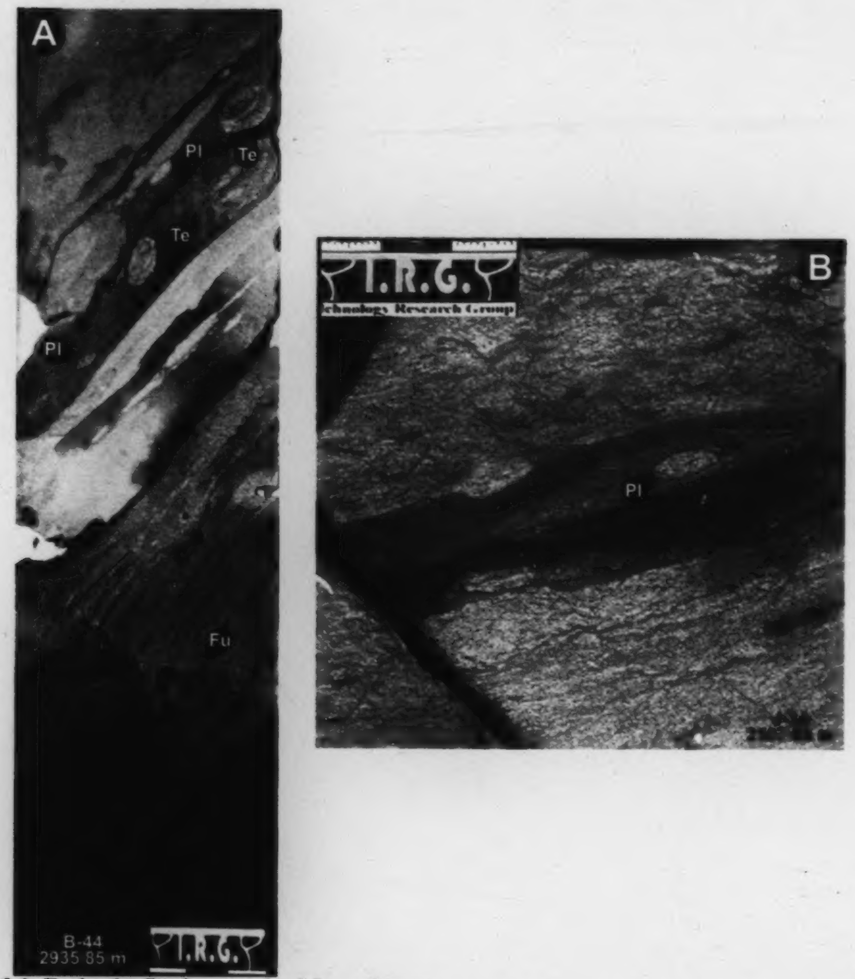

Figure 2.1: Facies 1 – Dark, organic-rich mudstone
A) Note the sharp upper and lower boundaries of the dark grey to black mudstone bed (although the lower boundary is partially interrupted by bioturbation; Fu = fugichnia). *Planolites* (Pl) and *Teichichnus* (Te) are contained within the bed. In this photo, F1 occurs at the contact between bioturbated muddy to silty sandstone of F6 (above) and low angle to wavy laminated sandstone of F9 (below). B) An example of F1 containing very rare bioturbation; *Planolites* (Pl).

Interpretation

Clay-sized particles of F1 were deposited from high-concentration sediment flows. Facies 1 sediments were likely deposited relatively rapidly, of very soupy consistency and accompanied by inhospitable interstitial waters, impeding colonization by organisms during and immediately after deposition. The biogenic penetration that is present is post-depositional, and even then very limited. The dark to black color of F1 suggests that is consists mainly of phytodetrital material. The sharp basal contacts possibly indicate a component of erosion. The limited occurrence and thickness of

F1 mudstone beds suggest that these events were short-lived and rare. Facies 1 is interpreted as fluid mud deposits sourced from a nearby fluvial output as hyperpycnal flows (Rice *et al.*, 1986). Saunders *et al.* (1994), Gingras *et al.* (1998), Bann and Fielding (2004) and MacEachern *et al.* (in press - 2005) described similar deposits within subaqueous deltaic successions.

Facies 2 – Multicolored Mudstone and Siltstone

Description

This facies contains an eclectic mixture of red to brown-colored, and less commonly grey to green-colored, mudstones and siltstones (Figure 2.2). Individual beds are accentuated by color variations across gradational or diffuse boundary transitions. While some intervals are fissile, most intervals are massive or chaotically bedded. Stringers and veins composed of carbonate material highlight deformed intervals. Nodular calcium carbonate accumulations, which range in size from a few millimeters to a few centimeters in diameter, are in great abundance and commonly occur in and around root traces. Pyrite nodules are rare to moderate in occurrence within grey to green-colored mudstone and siltstone intervals. Facies 2 contains approximately 5-10% bioclastic material, which consists of intact turreted gastropods as well as oyster and other pelecypod valve fragments. This material is typically concentrated in shell hash layers associated with green mudstone and siltstone intervals. Plant remains and carbonaceous material is locally abundant.

Evidence of bioturbation in F2 largely exists in the form of root traces that are light grey to blue in color and only rarely carbonatized. Traces produced by macrofauna are very low in abundance. In addition to rootlets, the trace fossil assemblage of F2 includes *Planolites, Teichichnus, Chondrites, Thalassinoides* and *Palaeophycus*.

Facies 2 most commonly underlies bioclastic sediments of Facies 5 and overlies massive to mottled sandstone of Facies 8. In some cores, it occurs intercalated with Facies 5, 11 and 12. Facies 2 intervals range in thickness from 1 to 12 m; the thickest accumulations occur in Hibernia B-16 23, B-27 and K-14.

Interpretation

The predominance of red and brown coloration within F2 is an indication of oxidization, suggesting that this facies was subaerially exposed. The lack of carbonaceous material implies arid

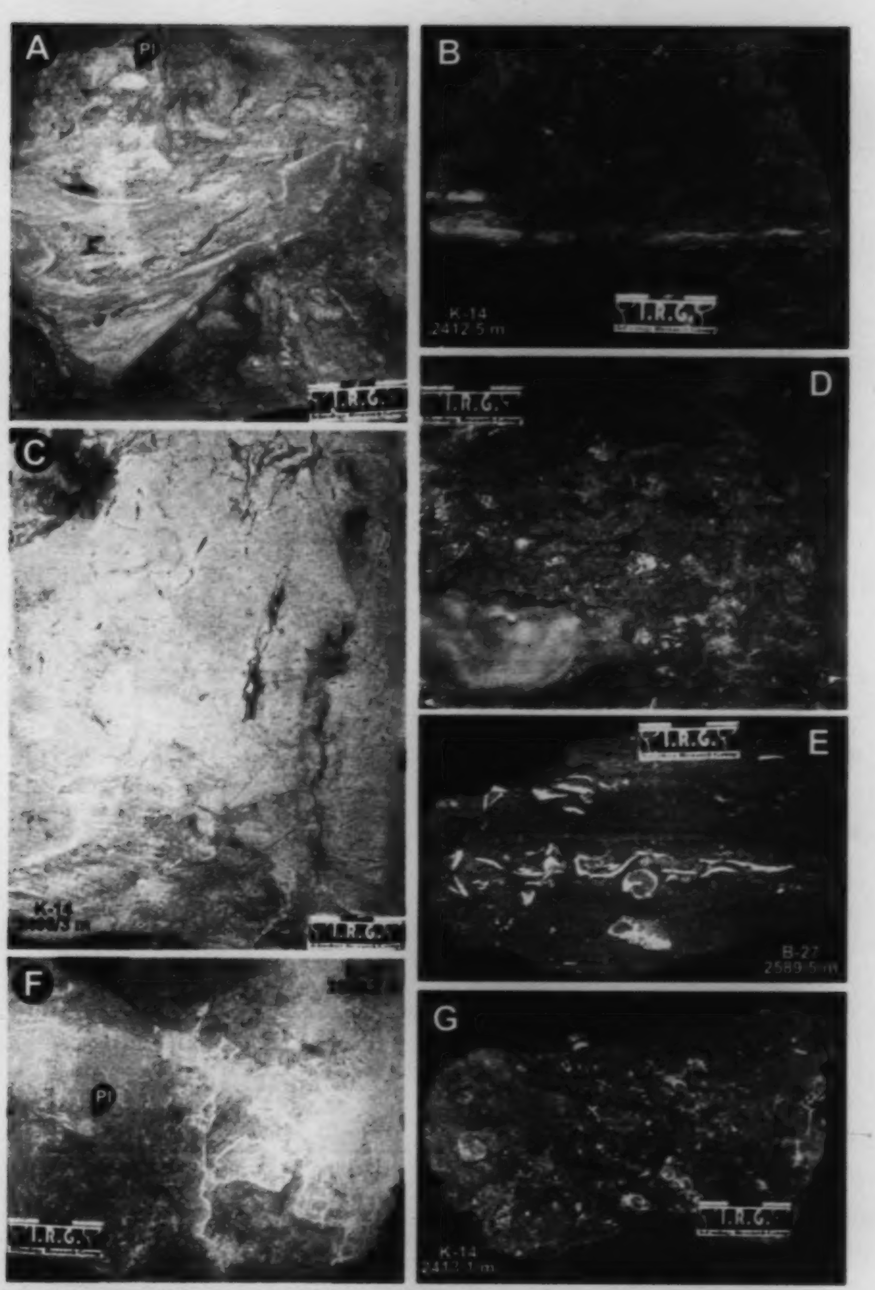

Figure 2.2: Facies 2 – Mulitcolored mudstone and siltstone

A) Example of soft sediment deformed or chaotic, greenish siltstone; *Planolites* (Pl). B) Dark red, root-mottled mudstone containing a thin, finely laminated, green silt layer. C) Carbonate nodules and rootlets within siltstone. D) Siderite concretions and fine bioclastic debris within a pedogenically altered mudstone. E) Dark grey mudstone/siltstone exhibiting fine, planar parallel laminations and a lag of bioclastic material composed predominantly of gastropods and pelecypod fragments. F) Silt-filled roots within red and green-colored mudstone; a possible *Planolites* (Pl) is also visible. G) An interval of blocky, red shale containing abundant gastropods.

conditions persisted; however, limited concentrations of plant remains and carbonaceous debris support localized swamp development (most likely in low lying areas). Paleosol development is supported by the presence of diffuse color variations, root traces and carbonate veins/globules, as well as chaotic textures resulting from disruption by plants (Fenwick, 1985; Retallack, 1988). Pyritic, green-colored mudstone and siltstone intervals are indicative of reducing conditions and deposition within stagnant, ponded waters. In conjunction with brackish fauna shell hash layers, these "ponds" represent periodic influx of water and shell material from adjacent marginal marine settings, probably via storm activity. As such, F2 represents ancient soil development and isolated ponds or lakes within a coastal marsh, flood plain or supratidal flat setting.

Facies 3 – Bioturbated Silty to Sandy Mudstone

Description

Facies 3 consists of intensely bioturbated, brownish to dark grey, silty to sandy mudstone that is interbedded with sporadic very fine-grained sandstone beds (Figures 2.3, 2.4). Silt and sand constitutes 10 to 30% of the facies. The sandstone interbeds range in thickness from 2 to 10 cm, contain planar parallel laminations, wavy to low-angle cross stratification and symmetrical ripple-cross laminae, have bioturbated upper and lower contacts, and are typically greater in abundance toward the top of F3 intervals. Beds containing scattered, randomly oriented pelecypod fragments and calcareous worm tubes account for less than 10% of the deposit. Carbonaceous debris, in the form of fine-grained particles and wispy flakes, and pyrite are rare. Siderite nodules and layers are moderate to common in occurrence.

The degree of bioturbation within this facies is high to intense as primary physical sedimentary structures are absent apart from the intermittent sandstone beds. Two very distinct ichnologic signatures can be discerned within this facies. As such, it can be divided into two subfacies: *Teichichnus*, *Asterosoma* and *Scolicia*-dominated Silty to Sandy Mudstone (F3A) and *Chondrites* and *Planolites*-dominated Silty to Sandy Mudstone (F3B).

Facies 3A – *Teichichnus*, *Asterosoma* and *Scolicia*-dominated Silty to Sandy Mudstone

In addition to *Teichichnus*, *Asterosoma* and *Scolicia*, the representative trace fossil assemblage of F3A includes *Chondrites*, *Planolites*, *Zoophycos*, *Thalassinoides*, *Phycosiphon*, *Rhizocorallium*, *Rosselia* and *Palaeophycus*, which are rare to moderate in occurrence. Because the most common trace fossils are spreitenated, the overall biogenic fabric is dominated by concentric and meniscate structures (Figure 2.3). Silt and sand, which occur mainly within spreiten, constitute 20-30% of F3A.

Facies 3B - *Chondrites* and *Planolites*-dominated Silty to Sandy Mudstone

A much less diverse trace fossil assemblage characterizes this subfacies, as *Chondrites* and *Planolites* are most common (Figure 2.4). *Teichichnus, Asterosoma, Zoophycos* and *Scolicia* are also present, however they occur in reduced abundance compared to F3A. Other traces in low to moderate occurrence include *Phycosiphon, Palaeophycus* and *Thalassinoides*. In F3B, sand and silt, which constitute 10-20% of the deposit, fill burrows (such as *Chondrites* and *Planolites*) and highlight spreiten.

Facies 3 intensely bioturbated mudstone intervals are tens of centimeters to several meters thick. They occur interbedded with sand-dominated sediments of Facies 6, 9 and 10. Facies 3 also gradationally overlies conglomerate of F14B.

Interpretation

Mud comprising F3 was deposited from suspension in a generally low energy environment. Trace fossil assemblages consisting mostly of deposit-feeding structures (indicating that substrates were nutrient-rich) characterize both subfacies. Facies 3A is an intensely bioturbated deposit, reflecting a moderate to high diversity assemblage characteristic of the archetypal to distal *Cruziana* ichnofacies. Although moderate in diversity, Facies 3B contains a predominance of morphologically simple, deposit-feeding traces over comparatively systematic feeding traces, reflecting a distal or stressed representation of the *Cruziana* ichnofacies. Sandstone interbeds represent periodic influx of sand; where not preserved as complete beds, the sand was mixed into the muddy substrate by bioturbation. These remnant beds contain wave-generated sedimentary structures and thus represent periodic disruption of the setting by wave activity. The predominance of mud and deposit-feeding structures within moderate to high diversity assemblages of trace fossils, coupled with intermittent to rare wave activity, places F3 within the distal lower shoreface to offshore realm. This unit is analogous to open marine deposits reported by Howard and Frey

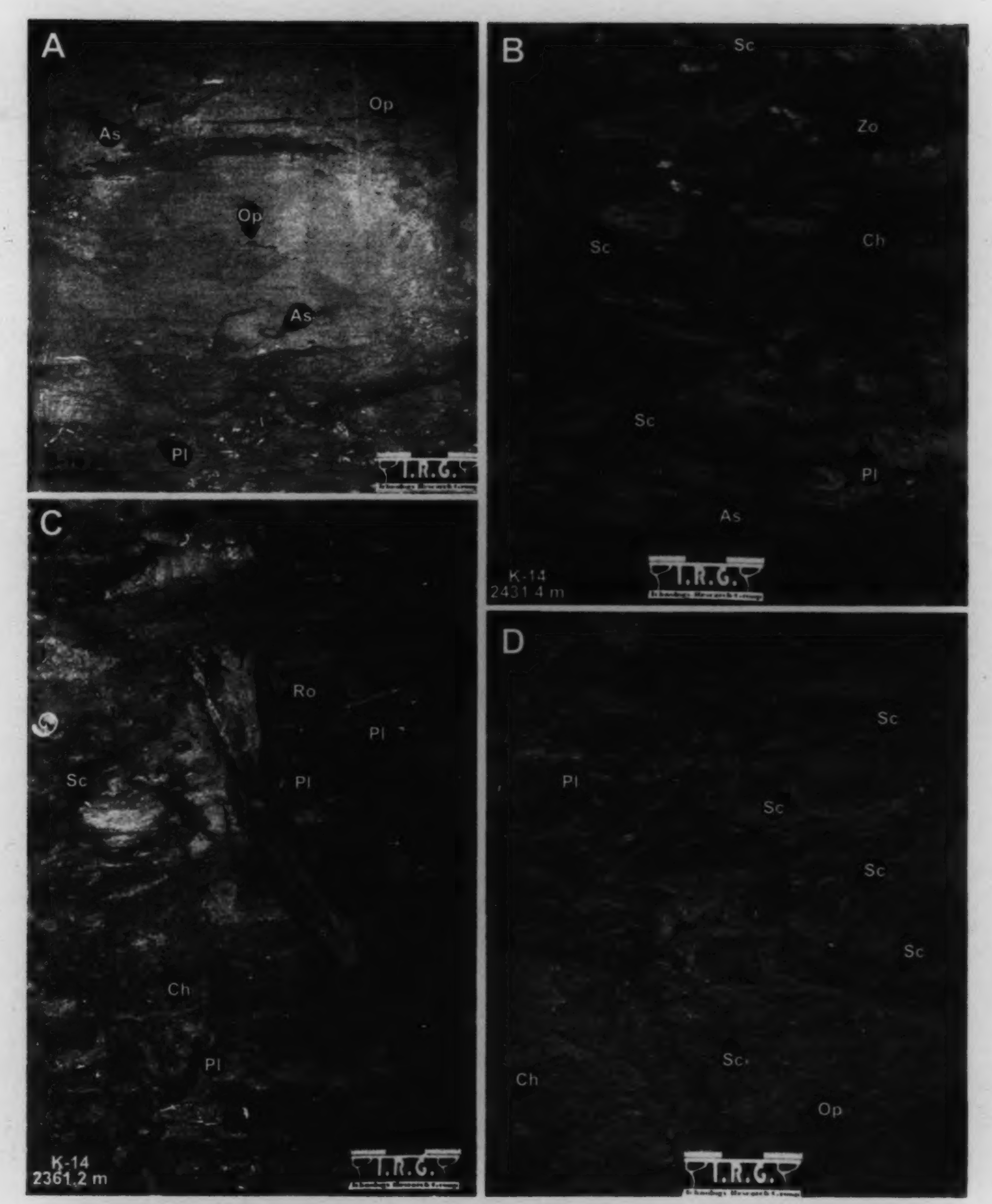
A
As
Op
Op
As
Pl
I.R.G.
B
Sc
Zo
Sc
Ch
Sc
Pl
As
K-14
2431.4 m
I.R.G.
C
Ro
Pl
Sc
Pl
Ch
Pl
K-14
2361.2 m
I.R.G.
D
Sc
Pl
Sc
Sc
Sc
Ch
Sc
Op
I.R.G.

Figure 2.3: Facies 3A – *Teichichnus*, *Asterosoma* and *Scolicia*-dominated silty to sandy mudstone
A) Remnant planar parallel to low-angle cross laminae. Note the partial preservation of its lower scoured boundary; *Asterosoma* (As), *Ophiomorpha* (Op), *Planolites* (Pl). B) *Asterosoma* (As), *Chondrites* (Ch), *Planolites* (Pl), *Scolicia* (Sc) and *Zoophycos* (Zo). C) *Chondrites* (Ch), *Planolites* (Pl), *Rosselia* (Ro) and *Scolicia* (Sc). D) Red-colored siderite staining within F3 is typically diffuse and closely associated with mud in spreiten. This photo also shows an excellent representation of the bioturbate texture of F3; *Planolites* (Pl), *Scolicia* (Sc), *Ophiomorpha* (Op), *Chondrites* (Ch).

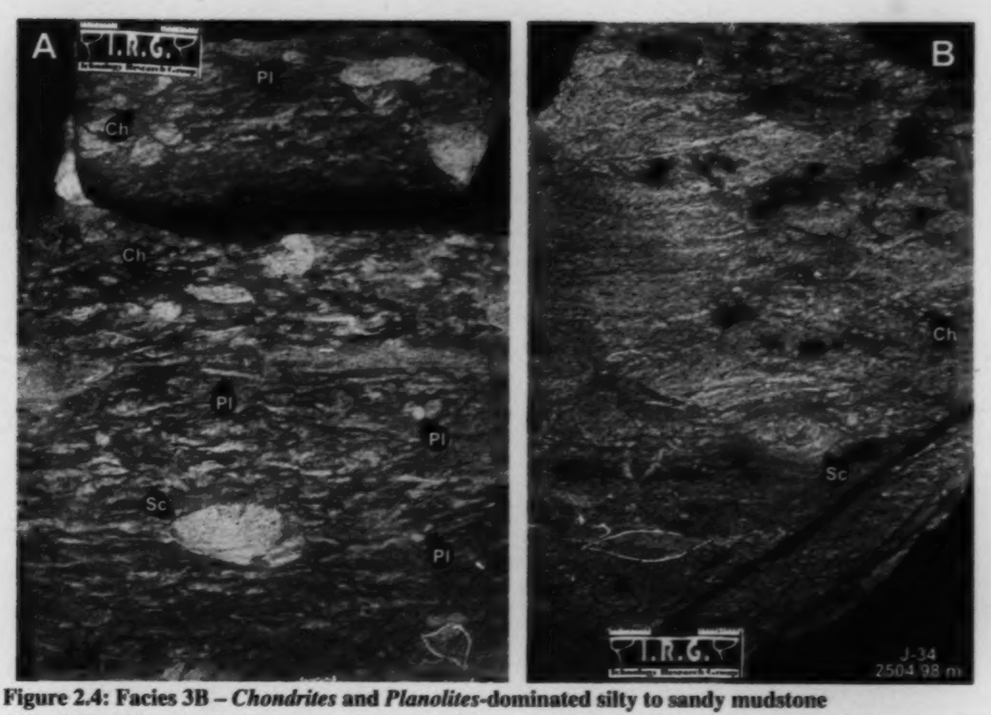

Figure 2.4: Facies 3B – *Chondrites* and *Planolites*-dominated silty to sandy mudstone
A) and B) Although the bioturbate texture of F3B is dominated by *Chondrites* (Ch) and *Planolites* (Pl), *Scolicia* (Sc) commonly cross-cuts the earlier emplaced *Planolites* texture. Note the echinoid fragments in both core photos.

(1984), Bhattacharya and Walker (1991) and MacEachern and Pemberton (1992). However, periodic freshwater influx into the depositional setting is indicated by siderite accumulations and cemented horizons. In addition, heterogeneity in the ichnologic signature reflects considerable environmental fluctuations (as in Facies 6). Such fluctuation is not expected in a normal marine or fully marine offshore setting where conditions are expected to be stable. Thus, this facies was likely deposited in an embayment or a deltaically influenced shoreface system, distal to fluvial sources. Facies 3 represents the "muddier" version of Facies 6; apart from a greater ratio of mud and silt in F3, they both contain similar trace fossil assemblages and multiple bioturbate textures.

Facies 4 – Wavy to Lenticular-bedded Mudstone

Description

Facies 4 is heterolithic in nature, as it consists of dark grey mudstone thinly interbedded with grey to tan-colored, very fine-grained sandstone and siltstone (Figure 2.5). Mudstone intervals generally exhibit a moderate to high degree of bioturbation; some residual planar to wavy, parallel laminae are present. Sandstone beds, which are very fine-grained at the base and grade upward into siltstone, are largely unburrowed, lenticular to wavy, generally 1 to 5 cm thick and represent 10–20% of F4 intervals. Although load structures are commonly present, these beds exhibit sharp to erosive lower boundaries. Most beds are bioturbated at the top and along the edges. Shell material is largely absent and carbonaceous debris and pyrite nodules are rare. However, some laminae/beds are completely sideritized. Internally, sandstones exhibit undulatory or planar to low-angle cross stratification. Some appear to be ripple-cross-laminated within symmetrical and asymmetrical ripple forms. Structures resembling syneresis cracks are rare to moderate in abundance.

Chondrites, Planolites, Thalassinoides and *Teichichnus* are common to abundant within the intensely bioturbated finer grain intervals. *Asterosoma, Scolicia* and *Zoophycos* are also present; however, these traces are diminuative and subordinate elements that occur sporadically. Although upper and lateral boundaries of sandstone/siltstone lenses/beds are burrow-mottled, the lenses/beds themselves are only slightly bioturbated. In addition to fugichnia and *Teichichnus*, they contain rare isolated occurrences of *Ophiomorpha, Palaeophycus, Skolithos* and *Cylindrichnus*.

Facies 4 occurs interbedded with Facies 9 and rarely overlies conglomerate of F14B. The thickest accumulations of this facies are cored at Hibernia B-16 23, B-27, J-34 and K18.

Interpretation

The prevalence of mud-sized particles is indicative of deposition from suspension under quiescent, low energy conditions. Ripple cross-laminated sandstone/siltstone lenses and wavy beds with localized loading are indicative of periodic influx of sand/silt into a mud-dominated setting under low flow regime conditions. Although this material was likely brought in by currents, symmetrical ripple forms indicate intermittent wave activity. The near complete preservation of the lenses and beds suggests that ambient physical processes were not competent to modify them (Wheatcroft, 1990). In addition, the trace fossil suite contained within mudstone intervals is dominated by deposit-feeding and grazing structures that do not achieve significant vertical penetration of the beds. Based on these characteristics, Facies 4 would likely have been deposited below fairweather wavebase and possibly storm wavebase. However, sandstone/siltstone lenses/bed are typically disrupted by isolated occurrences of vertically oriented, suspension-feeding

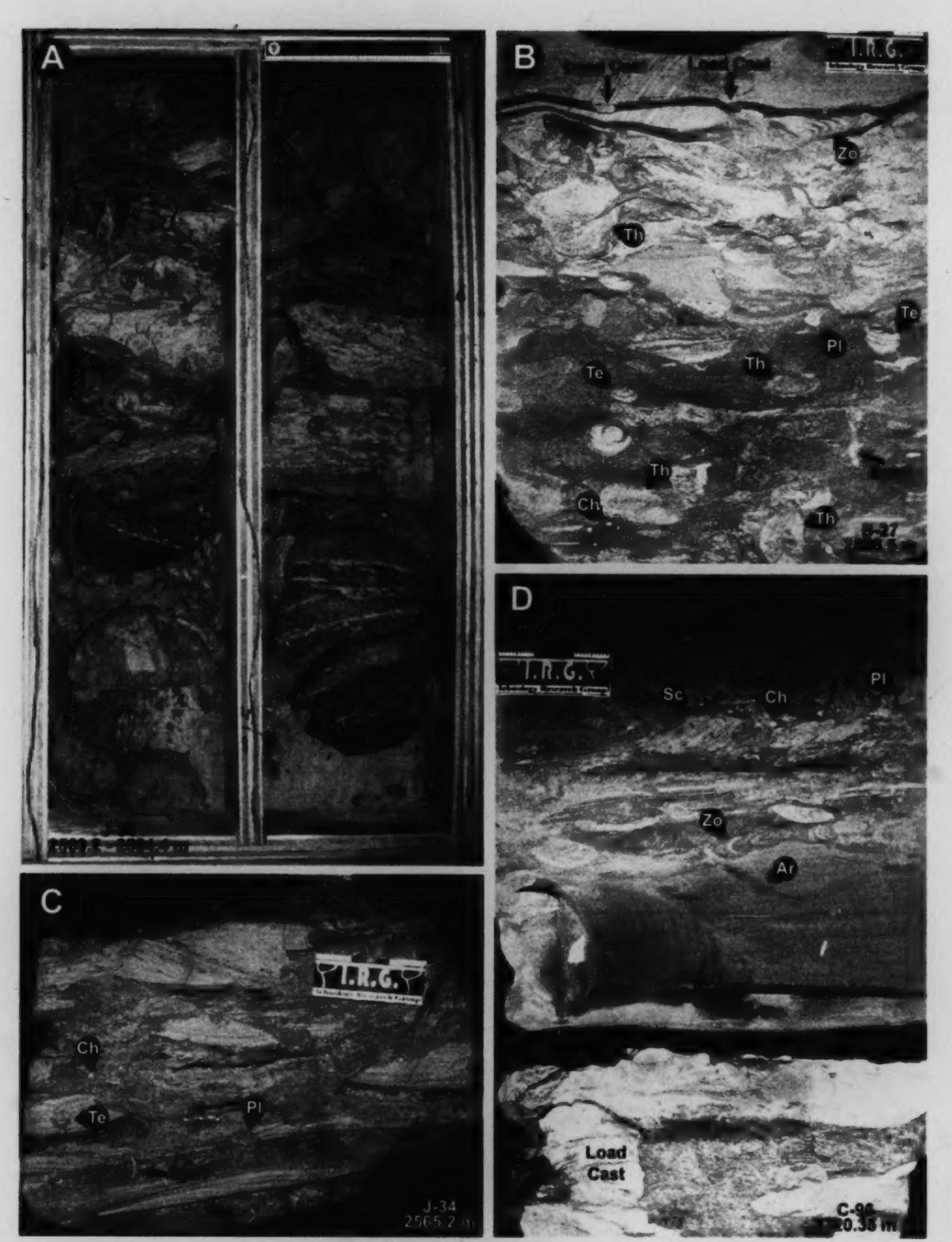
A
B
Load Cast
T.R.G.
Zo
Th
Te
Pl
Th
Te
Th
Ch
Th
C
T.R.G.
Ch
Te
Pl
J-34
2565.2 m
D
T.R.G.
Sc
Ch
Pl
Zo
Ar
Load
Cast
C-96

Figure 2.5: Facies 4 – Wavy to lenticular-bedded mudstone
A) Cored interval showing the fissile nature of F4. In addition to sandstone lenses, sideritized laminae are also visible (Sid). B) Example of load casts and moderate bioturbation dominated by *Teichichnus* (Te); *Chondrites* (Ch), *Planolites* (Pl), *Thalassinoides* (Th) and *Zoophycos* (Zo) are also present. A possible syneresis crack is highlighted. C) Lenticular bedding within F4; the mudstone interbeds appear to be completely bioturbated, while the sandstone lenses remain virtually untouched; traces include *Chondrites* (Ch), *Planolites* (Pl) and *Teichichnus* (Te); a syneresis crack and sideritized laminae (Sid) are also visible. D) Note the load structure at the base of the photo; *Scolicia* (Sc), *Chondrites* (Ch), *Arenicolites* (Ar), *Planolites* (Pl) and *Zoophycos* (Zo).

and domicile traces from the *Skolithos* ichnofacies. Thus, the overall ichnologic assemblage is moderate in diversity and representative of an impoverished mixture of traces from the *Cruziana* and *Skolithos* ichnofacies (Pemberton *et al.*, 2001b). Intermittent fresh water influx is supported by the presence of sideritized laminae/beds and possible syneresis cracks. The above characteristics indicate that Facies 4 was deposited distal to a source of freshwater influx on the shelf. In deltaic settings, this facies would be located within the prodelta zone. Thin interbeds of sandstone represent storm-induced influx of coarse material during periods of high fluvial discharge, probably in the form of short-lived, relatively low energy turbidites. Facies 4 is similar to central bay or embayment deposits described by Pattison (1992). Thus it is possible that F4 was deposited in central to distal portions of a large embayment, especially considering that the presence of marine trace fossils such as *Asterosoma, Zoophycos* and *Scolicia* indicates that F4 was not entirely restricted in terms of its connection to the marine realm.

Facies 5 – Bioclastic Mudstone and Silty Sandstone

Description

Facies 5 consists of dark grey mudstone and light grey silty sandstone, both sediment types contain 20–50% bioclastic material on average (Figures 2.6, 2.7, 2.8). Bioclastic-rich intervals consist of *Turritella* gastropods, oysters, or a mixture of gastropods, oysters and other pelecypods. Some intervals are composed of up to 70% oyster shells (Figure 2.6). Although no shells appear to remain in their original life position, it is not uncommon for near-complete valves to be cemented to one another. Facies 5 is divisible into two subfacies based on grain size, texture, accessory components and trace fossil assemblages: Bioclastic Mudstone (F5A) and Bioclastic Silty Sandstone (F5B).

Facies 5A – Bioclastic Mudstone

This finer grained subfacies of F5 is composed of dark grey shale and mudstone, where some intervals appear planar to wavy laminated and fissile, while others are burrow-mottled, deformed or blocky (Figure 2.7). Although both pelecypod and gastropod material is present, turreted gastropods and oyster valve fragments are most abundant. They are typically found in thin accumulations at localized horizons. Carbonaceous debris, in the form of granular particles, wispy flakes and woody

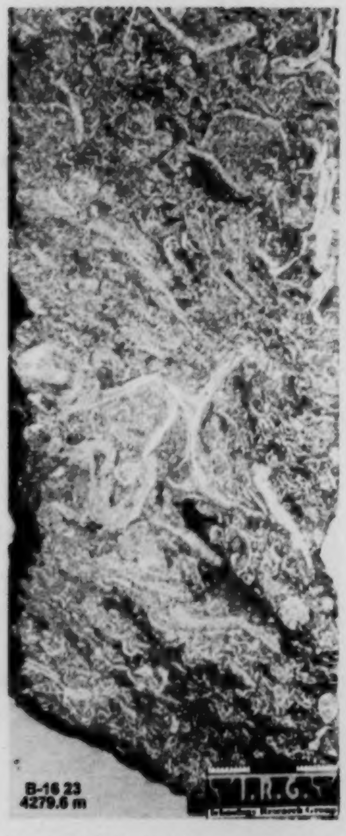

Figure 2.6: Example of the accumulation of oysters that can occur within Facies 5. Some oysters remain cemented to one another. Other bioclastic material present includes gastropods and pelecypods.

coal pieces are present in moderate to high abundance. Pyrite nodules are very common, whereas siderite accumulations are rare. Although some F5A intervals are completely burrow-mottled, recognizable macrofaunal traces are very rare in occurrence. The texture appears to be well mixed or churned; some intervals appear to consist mainly of spreite structures while others more closely resemble soft sediment deformation. *Thalassinoides, Planolites, Chondrites,* and *Teichichnus,* the only recognizable trace fossils, occur sporadically in low to moderate abundance.

Facies 5B – Bioclastic Silty Sandstone

Facies 5B consists of light to medium grey, silty, lower very fine-grained sandstone (Figure 2.8). Beds of Facies 5B are moderately to highly bioturbated and contain rare occurrences of wavy

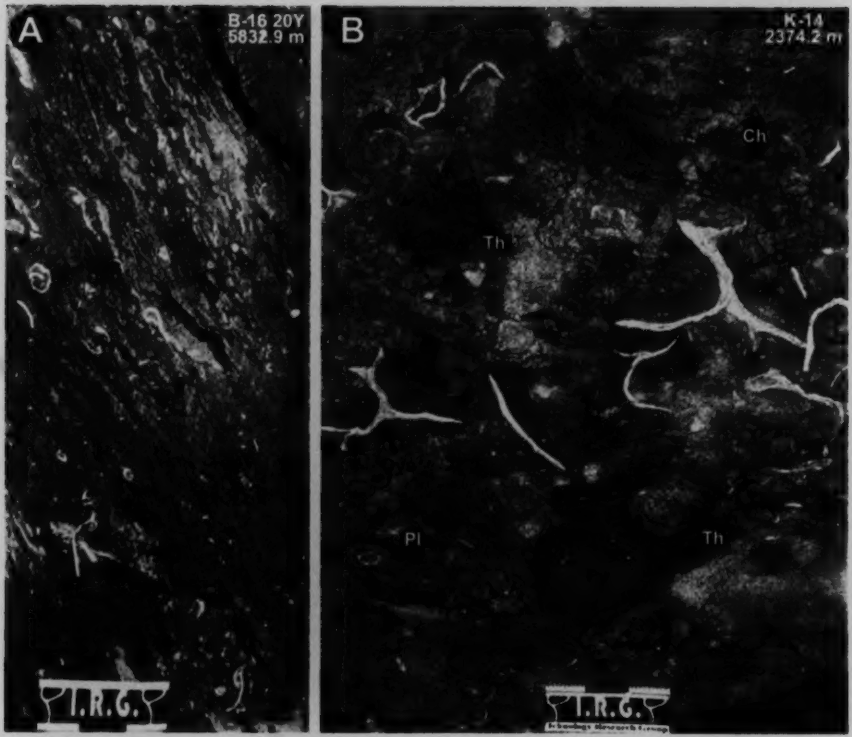

Figure 2.7: Facies 5A – Bioclastic mudstone
A) Laminated interval that is slightly fissile in nature. Laminations are highlighted by the alternation of mud and silt sized particles and possibly some siderite cement. Also visible in this photo is fine gastropod debris (Gas). B) Intensely bioturbated version of F5A. In this photo, the bioturbate texture is well mixed or churned. Forms that are visible include *Thalassinoides* (Th), *Planolites* (Pl) and *Chondrites* (Ch). A pyrite nodule (Py), a gastropod (Gas) and oyster valves (Oys) are also indicated.

to ripple-cross stratification (symmetrical and asymmetrical forms) and soft sediment deformation in the form of convolute laminae and chaotic textures. Sharp, irregular surfaces overlain by shell fragments and low angle cross stratification also occur in moderate abundance. In these layers, pelecypod valves are either randomly or concave/convex-upward oriented. Woody coal debris, plant remains and carbonaceous material are much more common in F5B than in F5A. In addition, small pebbles composed of quartz, chert or rock fragments and mud clasts (less than 5 mm) are present in rare abundance. Both pyrite and siderite nodules are prolific. *Ophiomorpha* and *Thalassinoides* are most commonly recognized within Facies 5B. *Palaeophycus, Skolithos, Arenicolites, Planolites, Teichichnus,* possible *Chondrites* and arthropod burrows are also present in low to moderate abundance. Root traces are present as well, but are very rare in occurrence.

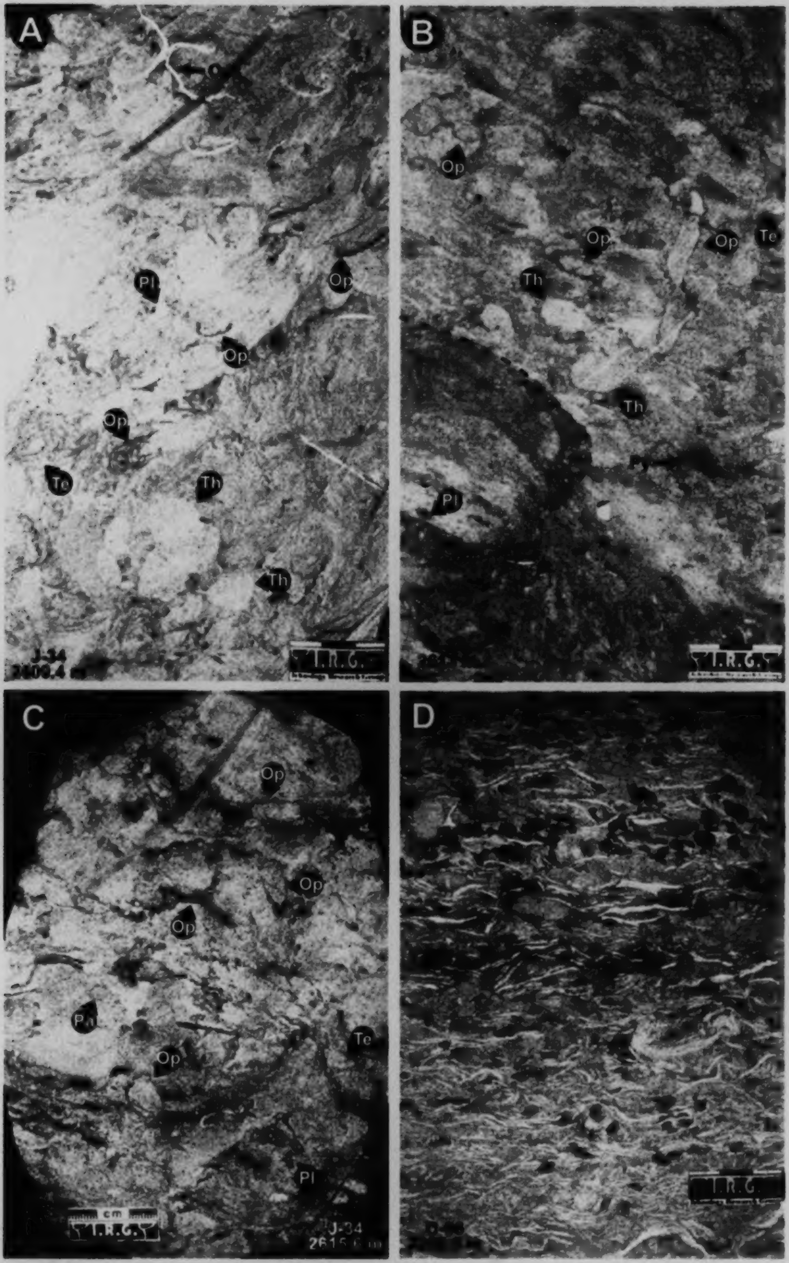
A
B
Op
Op
Op
Te
Pl
Op
Op
Th
Op
Th
Te
Th
Th
Pl
J-34
2400.4 m
I.R.G.
I.R.G.
C
D
Op
Op
Op
Pa
Op
Te
Pl
cm
I.R.G.
J-34
I.R.G.

Figure 2.8: Facies 5B – Bioclastic silty sandstone
A) and B) The bioturbate texture of F5B predominantly consists of *Thalassinoides* (Th) and *Ophiomorpha* (Op); oysters (Oys) and pyrite (Py) are common in this subfacies as well; *Planolites* (Pl), *Teichichnus* (Te). In B, a possible arthropod burrow is outlined (dashed line). C) Some intervals of F5B contain abundant organic matter in the form of disseminated carbonaceous debris; *Ophiomorpha* (Op), *Palaeophycus* (Pa), *Planolites* (Pl), *Teichichnus* (Te). D) Example of the bioclastic lag accumulations at the base of some beds within F5B. The lag predominantly consists of oyster and other pelecypod fragments and valves. Carbonaceous debris and mud clasts, which are commonly sideritized, also make up part of the lag.

Both subfacies occur interbedded with varicolored mudstone of Facies 2, rippled sandstone of Facies 7 and sandstones of Facies 11 and 12. Intervals of F5 display either stacked sets, in which each set consists of F5B overlying F5A, or a single coarsening upward succession, where F5A grades upward into F5B.

Interpretation

Facies 5 was deposited under brackish water conditions in a potentially stressed environment. Oysters and *Turritella* present within F5 are able to tolerate fluctuating salinity conditions, ranging from brackish to open marine (Hudson, 1963; Root, 1983; Allmon, 1988). As well, both subfacies are moderately to highly bioturbated but contain very low diversity ichnofossil assemblages. Mudstones of F5A are characterized by an impoverished *Cruziana* ichnofacies, while silty sandstones of F5B contain elements from both the *Cruziana* and *Skolithos* ichnofacies that are reduced in size compared to less stressed facies such as F6A, F6C or F12. Pyrite nodules, more commonly found in F5A, reflect organic-rich, stagnant and reducing waters, whereas siderite accumulations common to F5B are indicative of organic-rich, low sulfate fresh to brackish waters. As such, Facies 5A and 5B are representative of deep and shallow lagoonal settings, respectively. Mud deposition predominates in central zones of the lagoon, whereas silt and sand are concentrated along lagoonal margins, which include sandy intertidal flats and tidal creeks. Some mud deposition may have also taken place on muddy intertidal flats. Shell fragments and thin hash layers found within F5A were likely brought into the lagoon by storm activity. Oyster-rich intervals represent oyster reefs, while lags containing oriented bioclastic material (overlying scoured surfaces and underlying cross laminated intervals) were hydrodynamically aligned at the base of tidal creeks. The degree of bioturbation impedes further subdivision of F5 into these more specific subenvironments, especially since tidal creek migration and the translation of tidal creek point bar deposits into intertidal flats typically results in the amalgamation of facies characteristics (Reineck and Singh, 1980).

Facies 6 – Bioturbated Muddy to Silty Sandstone

Description

Brownish-grey, muddy to silty, very fine to fine-grained sandstone of Facies 6 is highly to intensely bioturbated (Figures 2.9, 2.10, 2.11). The percentage of silt and mud ranges from 10% to 40%. Although F6 is nearly completely bioturbated, thin intervals of remnant planar parallel to low-angle laminae and symmetrical ripple-cross stratification are present. Randomly oriented shelly material, including thin-shelled pelecypod valves and fragments, echinoid pieces, calcareous worm tubes, thick-shelled oyster valves and fragments, and whole gastropods, can be found scattered and in local accumulations throughout the unit. Carbonaceous debris and wood fragments (up to 4 cm in length) are also variably distributed. Pyrite nodules and siderite staining occur in rare to moderate abundance. Intervals of F6 are hydrocarbon-stained.

In addition to indistinguishable burrow mottling, the trace fossil assemblage of F6 consists of at least 16 morphologically distinct ichnogenera. The assemblage includes *Planolites, Palaeophycus, Cylindrichnus, Rosselia, Diplocraterion, Skolithos, Zoophycos, Chondrites, Asterosoma, Ophiomorpha, Phycosiphon, Rhizocorallium, Scolicia, Teichichnus, Thalassinoides* and *Pelosichnus mumorpha* n. ichnogen., n. ichnosp. (see Appendix 1). Although these traces are found throughout F6 intervals in varying abundance, certain intervals are dominated by one to three ichnogenera over all others. As such, Facies 6 can be divided into three subfacies largely based on the resident bioturbate texture: *Asterosoma, Scolicia* and *Teichichnus*-dominated Muddy to Silty Sandstone (F6A), *Phycosiphon* and *Pelosichnus*-dominated Muddy to Silty Sandstone (F6B) and *Thalassinoides* and *Ophiomorpha*-dominated Muddy to Silty Sandstone (F6C).

Facies 6A – *Asterosoma, Scolicia and Teichichnus*-dominated Muddy to Silty Sandstone

This bioturbate texture is dominated by robust (2–4 cm in diameter), horizontal, inclined and vertical representations of *Asterosoma, Scolicia* and *Teichichnus* (Figure 2.9). Despite the predominance of spreiten and concentric structures, the biogenically modified sedimentary fabric of F6A appears heterolithic in nature. Spreiten and concentric structures form the background, which is cross cut by traces such as *Chondrites, Planolites, Paleophycus, Thalassinoides* and *Ophiomorpha*. Mud and silt particles account for 30-40% of the sedimentary texture; their distribution is highly variable. Some intervals contain diffuse siderite staining as the cement exhibits an affinity toward

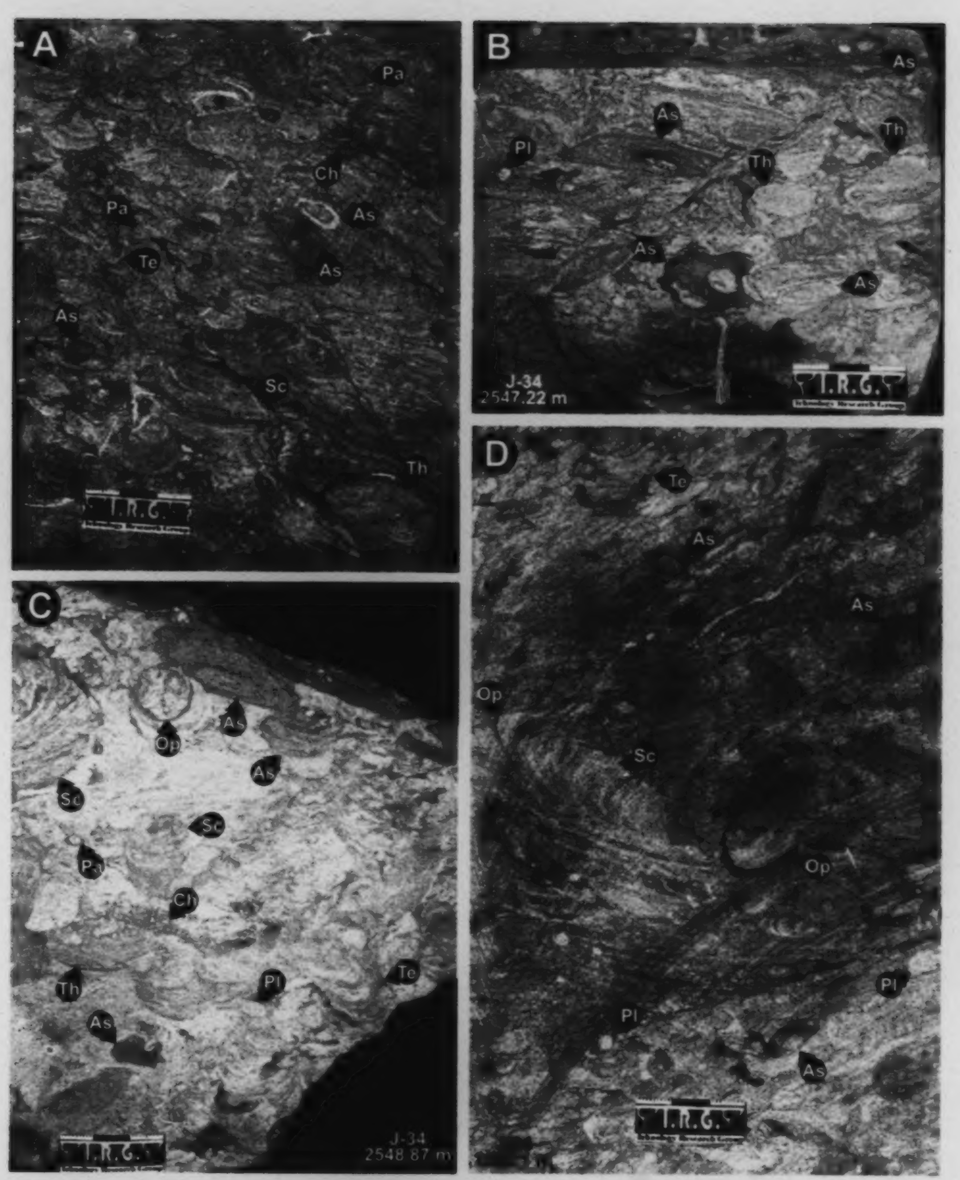
A
Pa
Ch
Pa
As
Te
As
As
Sc
Th
T.R.G.
B
As
As
Th
Pl
Th
As
As
J-34
2547.22 m
T.R.G.
C
As
Op
As
Sc
Sc
Pa
Ch
Te
Th
Pl
As
T.R.G.
J-34
2548.87 m
D
Te
As
As
Op
Sc
Op
Pl
Pl
As
T.R.G.

Figure 2.9: Facies 6A – *Asterosoma, Scolicia* and *Teichichnus*-dominated muddy to silty sandstone
A) The representative bioturbate texture within F6A contains *Scolicia* (Sc), *Asterosoma* (As), *Teichichnus* (Te), *Palaeophycus* (Pa), *Planolites* (Pl) and *Thalassinoides* (Th). B) The sedimentary texture of F6A is sand-dominated; mud more commonly appears associated with trace fossils such as *Asterosoma* (As); also present are *Thalassinoides* (Th) and *Planolites* (Pl). C) F6A is characterized by a high diversity assemblage of trace fossils, including *Asterosoma* (As), *Scolicia* (Sc), *Ophiomorpha* (Op), *Teichichnus* (Te), *Planolites* (Pl), *Thalassinoides* (Th), *Palaeophycus* (Pa) and *Chondrites* (Ch). D) Siderite cementation within F6A is similar to that expressed in F3; the reddish coloration occurs diffusely throughout the bioturbate texture; *Asterosoma* (As), *Teichichnus* (Te), *Planolites* (Pl), *Ophiomorpha* (Op) and *Scolicia* (Sc).

the muddy component of spreite structures. Shell material, carbonaceous debris and woody coal pieces are rare to moderate in abundance.

Facies 6B – *Phycosiphon* and *Pelosichnus*-dominated Muddy to Silty Sandstone

Facies 6B displays a unique distribution of sediment, with sand comprising the framework and silt/mud within biogenic structures (Figure 2.10). The percentage of mud and silt in F6B ranges from 10-30%; these fine-grained particles are mostly contained within the muddy fill of

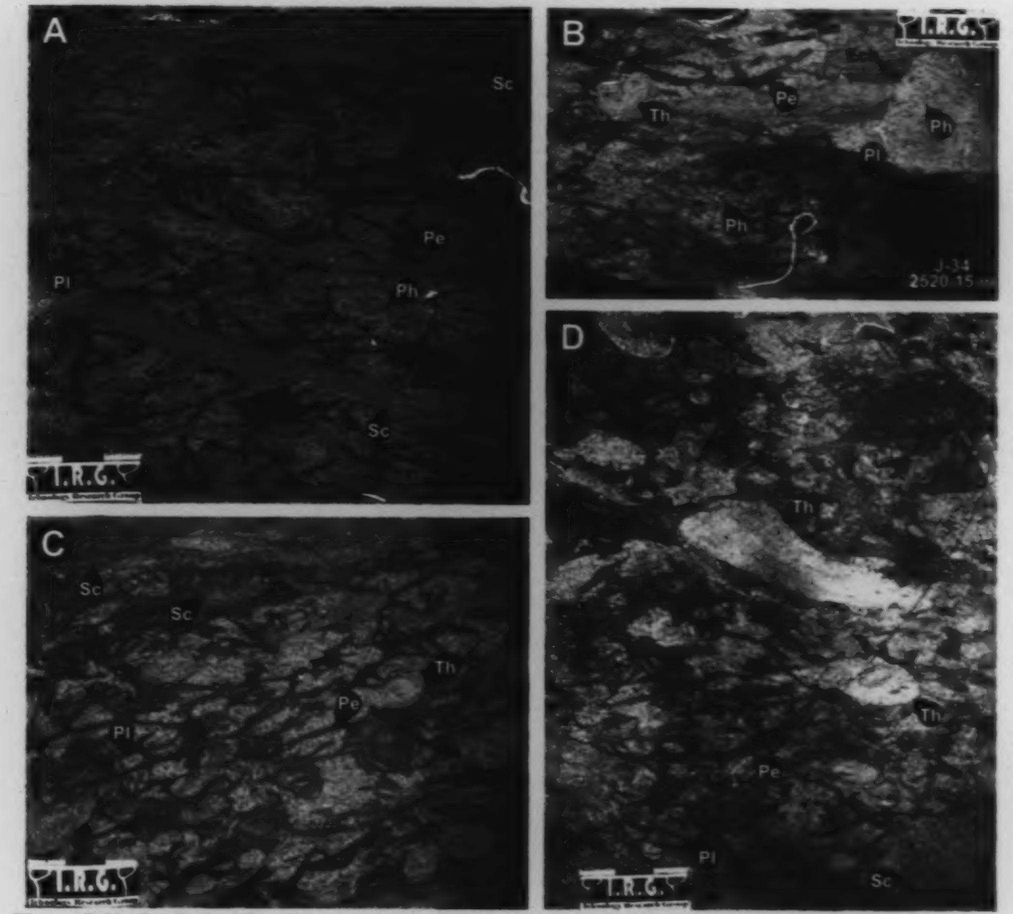

Figure 2.10: Subfacies 6B – *Phycosiphon* and *Pelosichnus*-dominated muddy to silty sandstone
A) Mud-filled burrows here named *Pelosichnus mumorpha* n. ichnogen., n. ichnosp., (Pe) are cross cut by *Scolicia* (Sc) and *Thalassinoides* (Th); *Phycosiphon* (Ph) occur within *Thalassinoides* and patches of sandy framework in between mud burrows. B) *Phycosiphon* (Ph) is even found within the sandy fill of an echinoid (Ech); *Thalassinoides* (Th), *Planolites* (Pl) and *Pelosichnus* n. ichnogen. (Pe). C) *Scolicia* (Sc), *Pelosichnus* n. ichnogen. (Pe), *Planolites* (Pl) and *Thalassinoides* (Th). D) Siderite cementation occurs within the mud-filled burrows; a dense, interpenetrating fabric of *Pelosichnus* n. ichnogen., n. ichnosp. (Pe) is well developed at this level; *Thalassinoides* (Th), *Scolicia* (Sc), *Planolites* (Pl).

Phycosiphon and U-shaped to branching, concentrically walled burrows interpreted as *Pelosichnus mumorpha* n. ichnogen., n. ichnosp. Relatively robust *Thalassinoides, Scolicia* and *Planolites* are locally moderate to common in abundance as well. Shelly material is slightly more abundant than in F6A, however carbonaceous debris appears to be slightly less abundant. Siderite cementation is concentrated within the mud-filled burrows.

Facies 6C – *Ophiomorpha* and *Thalassinoides*-dominated Muddy to Silty Sandstone

The sedimentary fabric of this subfacies is somewhat "nodular" in nature owing to both the distribution of mud and silt and dominant type of trace fossils (Figure 2.11). The matrix is sandy and large-scale burrows are sand-filled, with mud and silt (10-20% of the sedimentary texture) occurring in pelleted linings, as isolated pellets or clasts, and as mud stringers. Mud also alternates with sand and silt to form meniscate or spreite structures associated with some burrows. The nodular appearance of F6C is largely due to the prevalence of large-scale burrows (1 to 3 cm in diameter) such as *Thalassinoides* and *Ophiomorpha*. Although excellent examples of *Ophiomorpha irregulaire* are preserved, *Ophiomorpha nodosa* is relatively more abundant. All forms are dominantly horizontal, lined with a thin ring of mud or rounded to wedge-shaped pellets and are circular to lenticular in cross-section. Some thinly lined smaller transects (<1 cm in diameter) are interpreted as *Palaeophycus*. Both shell material and carbonaceous debris occur in slightly higher concentrations within this subfacies of F6. Woody coal pieces and thick-shelled oysters are very common in abundance. Siderite occurs with the pelleted linings of burrows and as nodules.

The thickest F6 cored intervals exist at Hibernia B-44 and J-34. In these wells and elsewhere, Facies 6 occurs interbedded with muddy deposits of Facies 1, 3 and 4, as well as sand-dominated Facies 9 and 10. Facies 6 may also gradationally overlie conglomerate of Facies 14B.

Interpretation

The ratio of very fine-grained sand to silt and mud in Facies 6 suggests that deposition took place under moderate energy conditions at or just below fair-weather wavebase. The specific mode of sediment emplacement is ambiguous due to the very high degree of bioturbation. The only evidence of wave activity is in the form of planar to low-angle cross-laminated sandstone

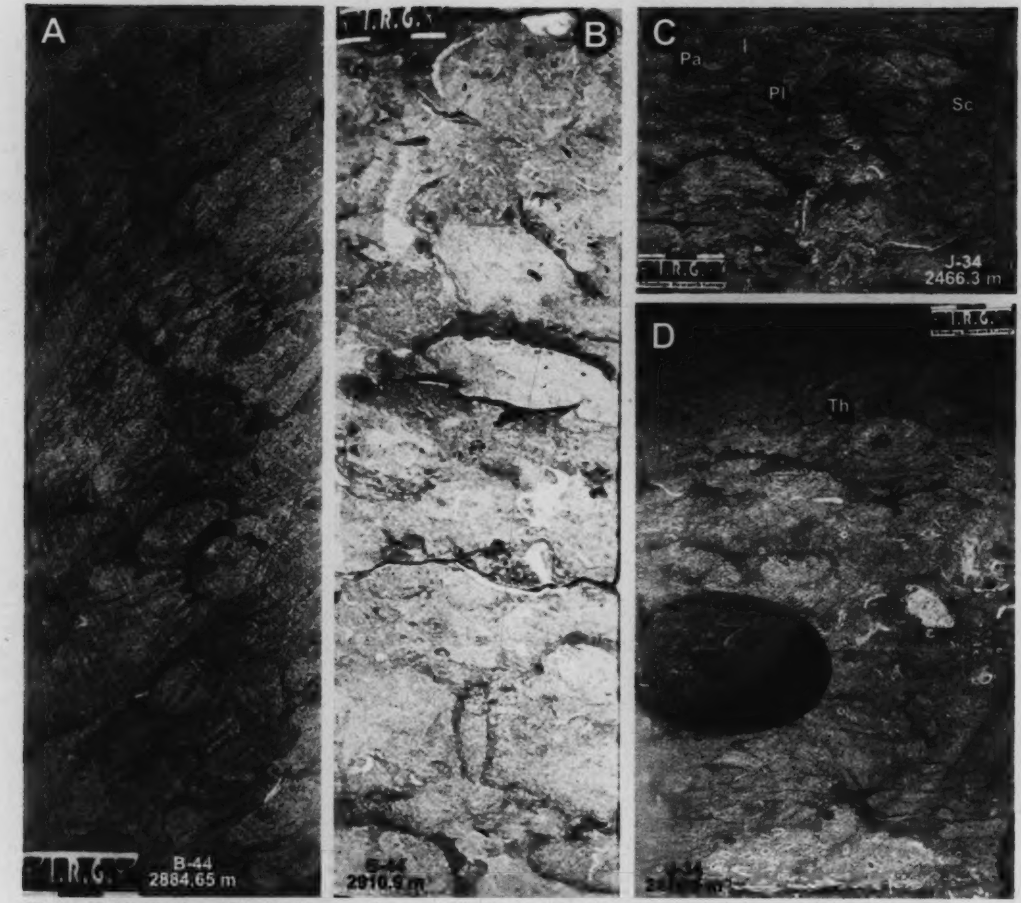

Figure 2.11: Facies 6C – *Ophiomorpha* and *Thalassinoides*-dominated muddy to silty sandstone
A), B) and D) Subfacies 6C exhibits a nodular bioturbate texture owing to the predominance of *Ophiomorpha*. C) The lenticular burrow lined with wedge-shaped mud pellets in the lower left hand corner is a prime example of *Ophiomorpha irregulaire*; *Scolicia* (Sc), *Planolites* (Pl) and *Palaeophycus* (Pa) are also present.

beds that also contain some wave ripple-cross stratification. However, their thin nature and limited occurrence is related to high rates of biogenic reworking. Facies 6 is characterized by a consistent tier structure, in that the cross cutting relationships revealed are constant, irrespective of the bioturbate texture (see Chapter 4, Figure 4.4). Each bioturbate texture is dominated by key or "elite" trace fossils from the middle tier. Traces belonging to the deep tier, such as *Zoophycos* and *Chondrites*, are much more limited in occurrence. The preferential preservation of the middle tier and poor development of deeper tier specialists likely reflects high rates of deposition in an overall low energy environment (Bromley, 1996). A high diversity ichnologic assemblage, representing deposit-feeding, grazing, passive carnivore and suspension-feeding/dwelling behaviors mostly from the archetypal *Cruziana* ichnofacies with some from the *Skolithos* ichnofacies, places Facies 6 within the marine realm (Pemberton *et al.*, 2001b). A high diversity macrofossil assemblage including echinoids also supports this conclusion. However, the presence of a heterogeneous pattern of bioturbation, as exemplified by three very distinct bioturbate textures, suggests that at certain times (or in particular locations) environmental conditions were more favorable to one or a few bioturbators over all others. As such, Facies 6 was likely deposited within a proximal lower shoreface zone subject to periodic or localized environmental fluctuations (i.e. deltaically influenced) or in a sandy bay or embayment. Widespread carbonaceous debris, wood fragments and siderite cementation suggest that these environmental fluctuations are likely due to freshwater influx.

Each subfacies represents slightly different environmental conditions according to their characteristic sedimentary and ichnologic fabric. In particular, the nature of sediment distribution and energy within the system is recorded by the behaviors represented in each bioturbate texture. For example, F6A reflects a predominance of deposit-feeding strategies, where mud is found within spreite structures, thereby suggesting that mud particles were largely deposited. Facies 6B is dominated by mud burrows interpreted as combined dwelling and suspension or detritus-feeding structures similar to modern burrows constructed by the polychaete *Nereis* (Schäfer, 1972; Howard and Frey, 1975; Trevor, 1977; Hertweck, 1986; Davey, 1994). The mud-lined and mud-filled nature of these burrows suggests that the organism fed at the water-sediment interface then stored waste material at depth. Also common in F6B is *Phycosiphon*, which is interpreted as a mud-filled, deposit-feeding structure. Since both deposit and suspension-feeding strategies are prevalent, turbid conditions prevailed only intermittently. The sedimentary fabric observed in F6C suggests that mud-sized particles were kept in suspension. Mud is contained within pellets of *Ophiomorpha*, which are interpreted as the dwelling burrows of suspension-feeding crustaceans. The distribution of mud directly translates into degrees of energy. Where mud is deposited (i.e. F6A) energy is overall low and where mud is kept in suspension (i.e. F6C) energy is overall high. Considering that F6 experienced environmental fluctuations related to freshwater influx, this energy distribution is likely related to the positioning of the bioturbate texture in relationship to distributary mouths bars on a deltaically influenced shoreface or within a relatively large embayment.

Facies 7 – Ripple Cross-laminated Sandstone with Mudstone

Description

Light to medium brown, lower fine-grained sandstone interlaminated with mudstone is characteristic of Facies 7 (Figure 2.12). Mudstone occurs as wavy to flaser laminae and thin beds ranging from 1 mm to 5 cm in thickness. Sandstone beds are typically sharp-based, wavy to lenticular, and vary in thickness from a few millimeters to several tens of centimeters. They also contain asymmetrical to symmetrical ripple-cross stratification. In some instances, the ripple crests appear to migrate along an inclined pathway. Planar to low-angle cross stratification and deformation structures are also present. Facies 7 is rich in carbonaceous debris; fine-grained particles highlight the ripple-cross laminae, while woody coal fragments and plant remains are found on bedding planes. Mud clasts and shell fragments are rare. Sandstone beds of F7 are hydrocarbon-stained.

Facies 7 is only slightly bioturbated. Most traces, including carbonaceous root traces, appear toward the top of sandstone beds as isolated occurrences. Sandstone beds exhibit pitted tops, most likely representing surficial bioturbation. The most common macrofaunal forms present in F7 include fugichnia, *Diplocraterion, Ophiomorpha, Palaeophycus, Thalassinoides, Skolithos* and/or *Teichichnus*. *Planolites* and *Chondrites* are more closely associated with mudstone interbeds.

The maximum thickness of F7 intervals approaches 2 m. Facies 7 occurs interbedded within Facies 5.

Interpretation

Sandstones of F7 are predominantly composed of current ripples produced under low flow regime conditions. Structures that exhibit more symmetrical forms are likely combined flow ripples that reflect a component of wave action. Migrating ripple crests (interpreted as climbing ripples), soft sediment deformation and biogenic escape structures suggest that sedimentation rates associated with the sandstone depositional events were relatively high. Mudstone laminae and thin beds were deposited from suspension; they are preferentially preserved in ripple troughs where they were subsequently covered by new migrating ripples. The interlayering of mud and sand reflects tidal influence or at least the alteration of slack water conditions and current activity. Root traces commonly found at the upper surface indicate that plants colonized F7 intervals subsequent to deposition (i.e. F7 sandstone beds were commonly subaerially exposed). Trace fossils observed

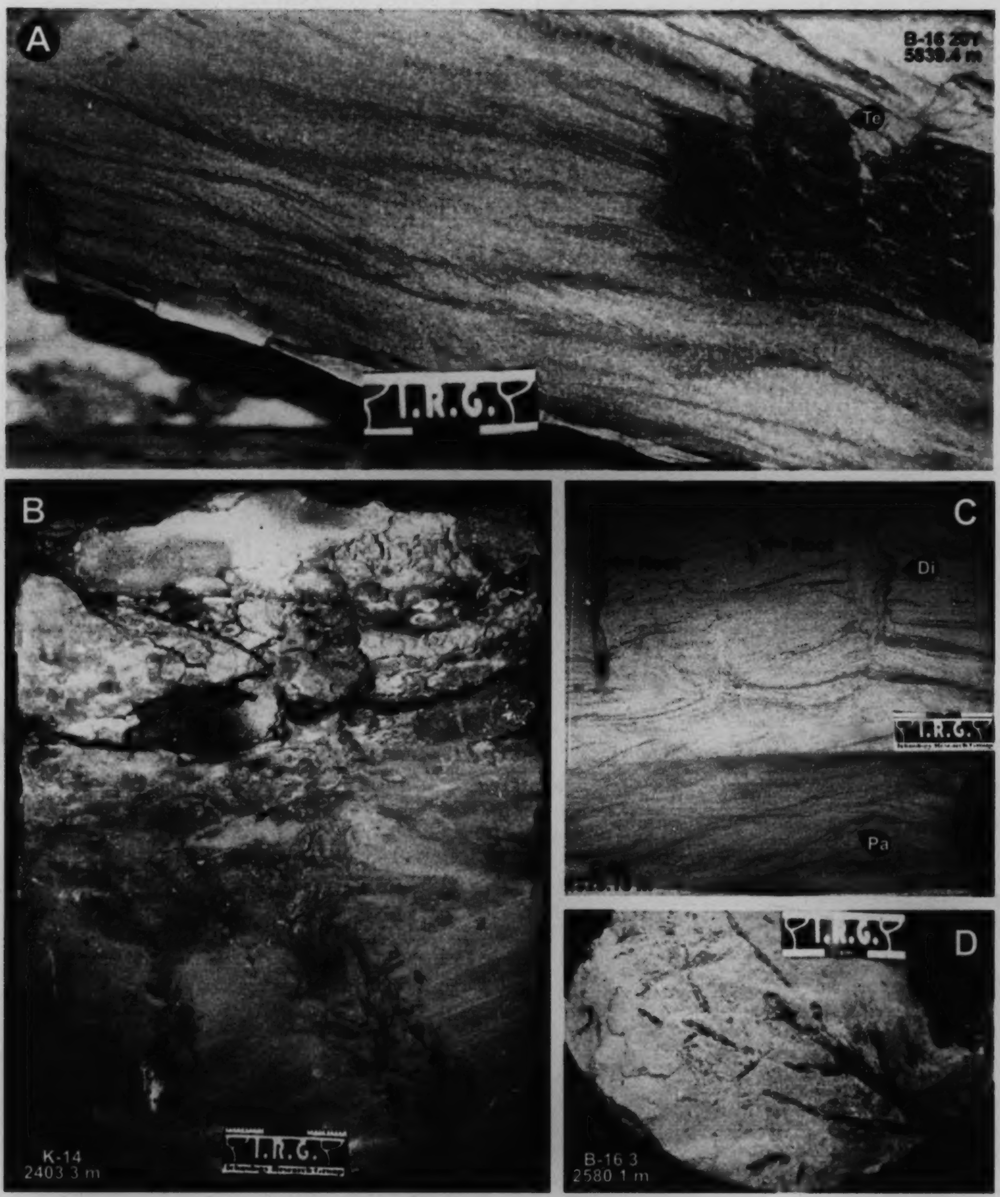
A
B-16 2??
5839.4 m
Te
I.R.G.
B
K-14
2403.3 m
I.R.G.
C
Di
I.R.G.
Pa
D
I.R.G.
B-16 3
2580.1 m

Figure 2.12: Facies 7 – Ripple cross-laminated sandstone with mudstone
A) Current ripples highlighted by mud laminae and cross cut by meniscate-filled *Teichichnus* (Te). B) Ripple cross-laminated sandstone containing root traces; the overlying mudstone appears to be completely burrowed or pedogenically altered. C) The upper bedding surface of a F7 sandstone, which contains rootlets and *Diplocraterion* (Di); *Palaeophycus* (Pa) is also present in the rippled sandstone below. D) Plant remains (of a vascular plant) found on a bedding surface.

within Facies 7 represent a low diversity assemblage with elements common to both the *Cruziana* and *Skolithos* ichnofacies. Vertical suspension-feeding and domicile burrows are associated with sandstone beds while grazing and deposit-feeding traces are found in the mudstone layers. The low degree of bioturbation coupled with low diversity supports deposition within a stressed environment. In addition, the sandstones contain a great abundance of carbonaceous material in a variety of forms, suggesting that the source of these sediments is in close proximity to a vegetated area. Possible environments of deposition include splays and levees associated with channelized flow and washover fans (Reineck and Singh, 1980; Coleman and Prior, 1982; Reinson, 1992).

Facies 8 – Massive to Mottled Sandstone

Description

Grey, green, tan and sometimes reddish-colored, moderately to well-sorted, fine-grained sandstone is characteristic of Facies 8. Although planar to low-angle cross lamination is present, this facies is predominantly massive or chaotic in texture (Figure 2.13). The style of bedding is masked by the rubbly nature of the core; however, intermittent stringers of rounded pebbles (3–8 mm in diameter) suggest that F8 may possibly consist of amalgamated sandstone bodies. Fine-grained carbonaceous particles and flakes are locally abundant and sometimes found highlighting laminae and mottled intervals. Siderite nodules 0.5–2 cm in diameter are rare while irregular, off-white carbonate stringers 1–2 mm in thickness are very common. Only the uppermost tens of centimeters of F8 are hydrocarbon-stained.

Facies 8 contains root traces near its upper boundary and very little evidence of macrofaunal bioturbation (although some intervals appear to be completely burrow-mottled). Identifiable traces include sporadically distributed *Palaeophycus, Skolithos* and possibly *Diplocraterion.*

Core coverage of this facies is limited. It is only found in Hibernia B-16 3, B-27 and K-14. In K-14 and B-27, it sharply overlies Facies 3; the lower contact of F8 is not captured in the B-16 3 cored interval. In B-27, the upper contact of Facies 8 is demarcated by a highly irregular, erosive surface that is immediately overlain by large pebbles (up to 2.5 cm in diameter) and a calcite-cemented layer containing white calcite veins 1 cm in thickness. In K-14 and B-16 3, the nature of the upper contact is uncertain; however carbonized root traces are present. Facies 8 is overlain by mulitcolored mudstone and siltstone of Facies 2 at all three well locations.

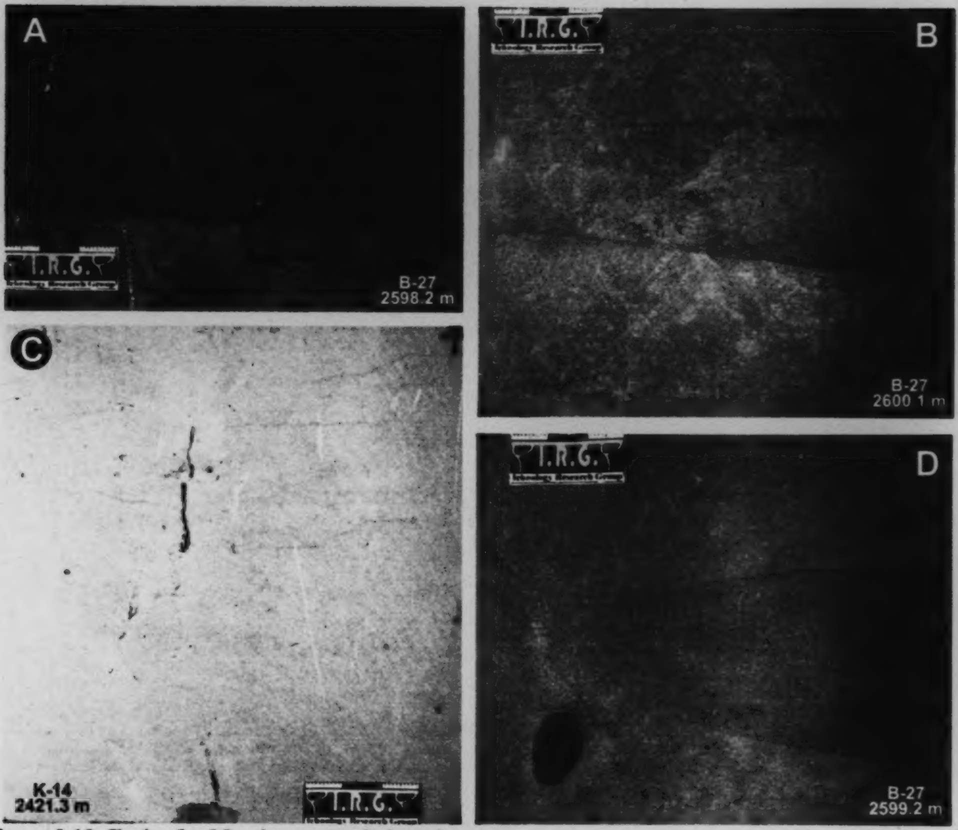

Figure 2.13: Facies 8 – Massive to mottled sandstone
A) The uppermost portion of F8 is hydrocarbon stained; this photo reveals and root and its mottled appearance, which may be due either to rapid sedimentation (e.g. dewatering) or bioturbation. B) Light-colored calcium carbonate stringers are an indication of diagenetic alteration of the sediment in the subaerial realm. C) Carbonized roots within textureless sandstone. D) Siderite nodules.

Interpretation

The limited and rubbly appearance of F8 in core and strong (subaerial) diagenetic overprints lend a certain degree of uncertainty to its interpretation. Color variations, calcite stringers, root traces, siderite nodules and a mottled texture suggest that Facies 8 experienced subaerial exposure and pedogenic alteration. This post-depositional alteration sufficiently masks the true nature of F8's bedding style and constituent physical sedimentary structures. Homogeneous stratification, intermittent pebbles, high abundance of carbonaceous material, overall lack of bioturbation and a very low diversity trace fossils assemblage suggest that these sands were deposited in continental to possibly marginal marine channels. At any rate, F8 contains enough paleosol-like qualities to render it part of a subaerially exposed succession.

Facies 9 – Massive, Planar to Low-angle-laminated Sandstone

Description

Facies 9 is composed of relatively clean and well sorted, tan to grey, lower fine to upper fine-grained sandstone that exhibits (apparently) massive to (faintly) laminated textures (Figure 2.14). Amalgamated bedsets are delineated by intermittent sharp, erosive surfaces, which are overlain by sub-rounded to rounded, commonly sideritized and poorly sorted mud clasts and more rarely, pebbles (up to 2 cm in diameter) and bioclastic debris. Although physical sedimentary structures are faint, planar parallel and low-angle cross stratification is most common. Trough to high-angle cross bedding, wavy to symmetrical ripple-cross stratification, and convoluted or deformed laminae are rare to common. Graded laminae, which are up to 2 cm in thickness and accentuated by granules and/or coarse sand, occur sporadically. Rhythmically distributed carbonaceous laminae are locally abundant. Pelecypod valves, oyster fragments, calcareous worm tubes, rounded wood debris and gastropods occur in low to moderate abundance. Hydrocarbon staining is extensive in this facies.

Most Facies 9 intervals are unbioturbated except for very rare, typically isolated occurrences of fugichnia, *Palaeophycus, Phycosiphon, Skolithos, Ophiomorpha, Asterosoma* and/or *Macaronichnus* at upper boundaries. In addition, the linings of *Ophiomorpha* commonly contain *Chondrites.*

Although intervals of F9 average 1 to 4 m in thickness, more expansive sections (12 to 15 m thick) are found in cored intervals at the Hibernia B-44 and J-34 well locations. Lower boundaries of F9 are commonly sharp and erosive. Upper boundaries are sharp apart from sporadic bioturbation. Facies 9 is found interbedded with muddy sediments of Facies 1, 3 and 4, as well as sandstones of Facies 6. Thin interbeds of Facies 14A also occur within F9 intervals.

Interpretation

The clean, well-sorted and biogenically sterile nature of this facies suggests that it has experienced a considerable amount of physical reworking. Sedimentary structures recognized with F9 indicate that it was subjected to continuous reworking by both currents and waves. In addition, the presence of homogeneous textures, soft sediment deformation and poorly sorted mud clasts suggests that deposition occurred relatively rapidly from high-energy, sediment-laden currents. Sporadic graded laminae are event deposits produced by sedimentation of suspension clouds under

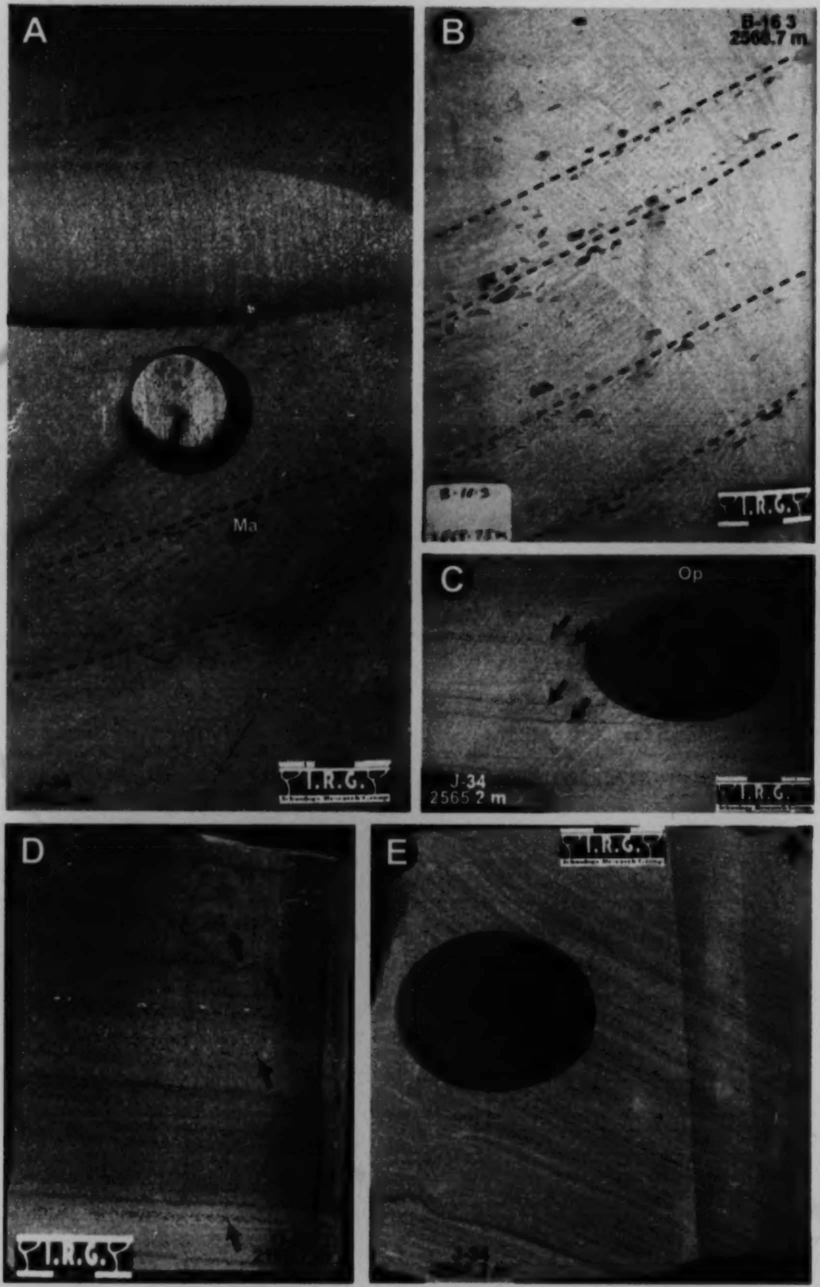

Figure 2.14: Facies 9 – Massive, planar to low-angle laminated sandstone
A) and B) Many cored intervals of this well sorted, very fine to fine-grained facies appear massive or textureless. Faint laminae are visible especially if flat mud clasts and carbonaceous debris is present. Possible *Macaronichnus* (Ma) is highlighted. C) Isolated occurrence of *Ophiomorpha* (Op) within low-angle cross-laminated sandstone; some laminae are paired and highlighted by fine-grained carbonaceous debris (arrows). D) Graded laminae (arrows). E) Convoluted laminae (left side of the photo).

waning flow conditions (Reineck and Singh, 1980). Carbonaceous laminae also are interpreted to accumulate from organic-rich plumes during periods of physical inactivity. A low diversity trace fossil assemblage containing elements of the archetypal *Skolithos* ichnofacies and some marine forms (i.e. *Asterosoma*, *Macaronichnus* and *Phycosiphon*), places this unit within a marginal marine or marine setting (Pemberton *et al.*, 2001b). Sharp-based, sharp-topped, unbioturbated, planar to low-angle laminated sandstones of Facies 9 are interpreted to occur in the upper shoreface zone. Considering the presence of carbonaceous laminae and graded beds, it is also possible that F9 was deposited near the point where channelized flow becomes unconfined in a deltaic setting, including channel breaches into interdistributary bays and bars or shoals located at the mouth of distributary channels. Although stream currents predominate, both of these areas are susceptible to post-depositional wave and biogenic activity. Bhattacharya and Walker (1991) described similar deposits within their mouthbar/delta front succession.

Facies 10 – Wavy to Low-angle Laminated Sandstone

Description

Sandstone beds of this facies are tan to grey-colored and very fine to lower fine-grained. These beds are discrete, relatively thin (10 cm to 1 m), sharp-based and moderately bioturbated near their upper contact (Figure 2.15). Basal surfaces truncate underlying deposits and are sometimes undulatory to irregular. Lower portions of the beds are composed of massive to planar parallel laminae and low-angle cross stratification. Some intervals also exhibit low-amplitude, symmetrical structures with wavelengths greater than the diameter of the core. Symmetrical ripple-cross stratification is rarely found in upper portion of F10 beds. Thin accumulations of pelecypod shell fragments, calcareous worm tubes and sub-angular to sub-rounded, locally sideritized mud clasts (ranging from 5–10 mm in diameter) are found on the lower boundary of most sandstone beds. These hash layers exhibit normal particle size grading, although bioclastic material typically overlies mud clasts. Sandstone beds of F10 are variably stained by hydrocarbons.

Facies 10 sandstones exhibit an upward increase in the degree of bioturbation and diversity of the resident trace fossil assemblage. Middle portions contain vertical to sub-vertical, isolated occurrences of *Ophiomorpha, Skolithos, Cylindrichnus, Arenicolites* and fugichnia. A greater

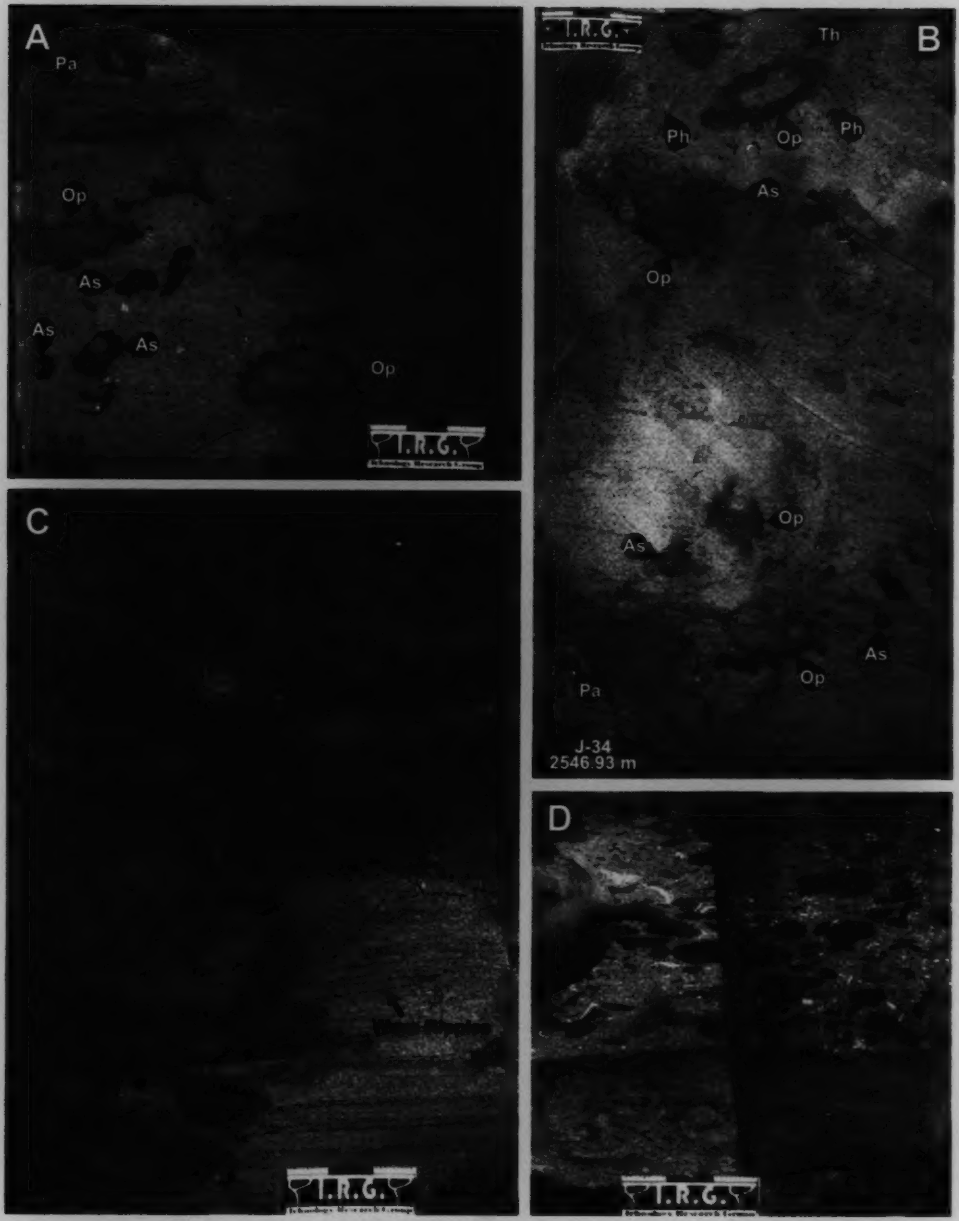

Figure 2.15: Facies 10 – Wavy to low-angle laminated sandstone
A) Planar to low angle-cross stratification with wave ripples at the top; traces include *Asterosoma* (As), *Ophiomorpha* (Op) and *Palaeophycus* (Pa). B) Interval of low-angle laminated sandstone that contains slight to moderate bioturbation; traces include *Ophiomorpha* (Op), *Asterosoma* (As), *Phycosiphon* (Ph), *Thalassinoides* (Th) and *Palaeophycus* (Pa). C) Upper boundary of a F10 interval in which the degree of bioturbation increases upward into the overlying facies; wave ripples are present near the top. D) Lower boundary of a F10 interval; these boundaries commonly exhibit a sharp, erosive nature and are overlain by a lag composed of bioclastic debris and mud clasts; in this lag, the mud clasts display crude normal grading.

variety of ichnogenera are recognized near the upper boundary of the bed, including *Asterosoma, Phycosiphon, Thalassinoides, Palaeophycus* and *Conichnus*.

This facies is found interbedded within bioturbated mudstone intervals of Facies 3, heterolithic mudstone of Facies 4 and bioturbated muddy to silty sandstone of Facies 6.

Interpretation

Episodic, relatively thin, very fine to fine-grained sandstone deposits of Facies 10 are interpreted as event beds. Sharp, sometimes undulatory basal surfaces are erosionally produced under high-energy conditions, as they are commonly overlain by a lag of intraclastic material. Normal grading of the lag, including the transition from massive to laminated to rippled structures in the main sand body itself, is indicative of a single, waning flow event. Sedimentary structures within this facies possess a strong oscillatory flow component. Planar parallel to low-angle cross stratification with intermittent low-amplitude wavy laminae are characteristic of hummocky cross stratification, which is considered representative of storm deposits or tempestites (Dott and Bourgeois, 1982; Dott, 1983; Walker, 1984; Duke, 1985; Duke *et al.*, 1991). In addition, a low diversity ichnologic signature consisting of escape, dwelling and suspension-feeding structures from the archetypal *Skolithos* ichnofacies reflects opportunistic colonization of these storm beds (Seilacher, 1982; Vossler and Pemberton, 1988; Frey and Goldring, 1992; Pemberton *et al.*, 1992; Pemberton and MacEachern, 1997). The upward increase in bioturbation coincides with waning storm conditions and the return to fair-weather conditions.

Facies 11 – Trough to High-angle Cross-laminated Sandstone

Description

Well-sorted, tan to grey, lower fine to lower medium-grained sandstones of Facies 11 are ubiquitously cross-laminated (Figure 2.16). Stratification style includes abundant high-angle and trough cross bedding and rare low-angle to wavy cross stratification. Deformed laminae and ripple-cross stratification are also rare; however, where present, ripples exhibit both symmetrical and asymmetrical forms and are highlighted by mud or carbonaceous flasers and thin lenses. This facies typically consists of amalgamated, sharp-based sandstone bedsets that are up to 3 m in thickness. Lower bed boundaries are commonly associated with rounded pebbles and cobbles (up to 4 cm

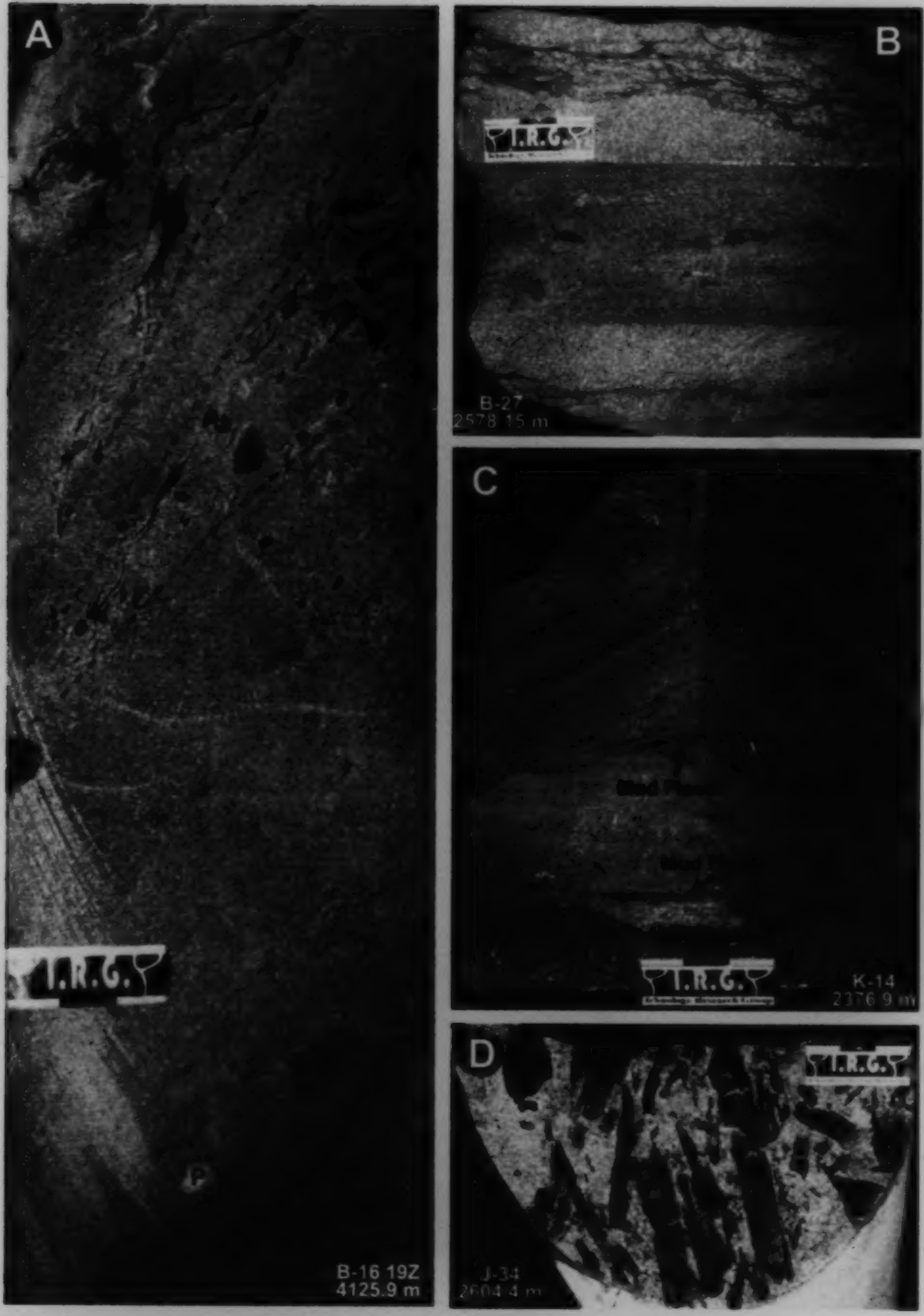
A
B
C
D
P
B-16 19Z
4125.9 m
B-27
2578.15 m
K-14
2376.9 m
J-34
2604.4 m

Figure 2.16: Facies 11 – Trough to high-angle cross-bedded sandstone
A) Trough cross bedding highlighted by wispy coal flakes and pebbles (P). B) Ripples highlighted by fine grain carbonaceous particles. C) Ripple cross-laminated interval containing mud drapes. D) Large pieces of wood aligned on bedding planes.

in diameter), rounded to flat mud clasts that are sometimes sideritized, and bioclastic debris, which consists of oysters, thin-shelled pelecypods, oysters and more rarely, turreted gastropods and calcareous worm tubes. Flat wood pieces, which can get up to 5 cm long, are aligned along some bedding planes. Mud laminae, taking the form of mud drapes or mud couplets, are moderate to common in occurrence. Grain size profiles are generally blocky, but subtle fining-upward or coarsening-upward trends are recognizable. Facies 11 is prolifically hydrocarbon-stained.

Facies 11 is largely unbioturbated. Isolated occurrences of *Ophiomorpha, Skolithos, Palaeophycus, Macaronichnus* or fugichnia can be found at various horizons throughout the deposit.

Lower and upper boundaries of Facies 11 intervals are sharp to erosive. F11 is very closely associated with bioturbated sandstone of F12 and coaly to muddy sandstone of F13. It may also occur intercalated with Facies 2, 5 and 14A.

Interpretation

Physical structures were mainly developed by dune migration under low flow regime conditions. Facies 11 shows evidence of deposition within channels, including fining upward grain-size trends and internal erosive surfaces overlain by pebble, mud clast and shell lags. In addition, mud drapes and mud or carbonaceous couplets are common components of tidally influenced settings (Reineck and Singh, 1980; Weimer *et al.*, 1982). However, the presence of wavy to low-angle cross stratification and symmetrical ripple forms suggests that wave activity was partially responsible for deposition. The mixture of macrofossil fragments from both brackish and marine habitats also suggests that sediment was sourced from both the marginal marine and marine realms. Considering that F11 exhibits both current and wave-derived structures, tidal influence, a mixture of variably sourced bioclastic material, large wood debris, mud/carbonaceous drapes/couplets and internal scour surfaces, it is interpreted as mid-channel tidal bar, tidal delta shoal and/or tidal inlet deposits. Tidal channel, delta and inlet deposits are characterized by closely related facies with regard to their internal sedimentary structures and textures (Boothroyd, 1985). In addition, Facies 11 has a very strong ichnologic signature representative of the *Skolithos* ichnofacies. High-energy conditions and nutrient-rich marine waters required to sustain the suspension-feeding tracemakers are best satisfied near the estuary or bay mouth (Gingras *et al.*, 1999b).

Facies 12 – Bioturbated Sandstone

Description

Facies 12 consists of fine-grained, carbonaceous, grey and tan to brown-colored sandstone that is highly bioturbated (Figure 2.17). Although F12 is highly to intensely bioturbated overall, intervals characterized by inclined planar laminae occur sporadically. Oyster valves and pieces, gastropods, carbonaceous debris and pebbles are found sporadically in horizons and randomly dispersed throughout F12. Carbonaceous material typically occurs as disseminated fine-grained particles and wispy flakes that highlight burrows. Wrinkly coal laminae and woody pieces are rare. Pyrite nodules occur in moderate abundance and appear to be closely associated with accumulations of carbonaceous material. Facies 12 is heavily stained with hydrocarbons.

The trace fossil assemblage of F12 predominantly consists of *Ophiomorpha, Thalassinoides* and *Palaeophycus*. Other traces found in rare to isolated occurrences include fugichnia, *Skolithos, Teichichnus* and *Chondrites*. Some of the larger wood pieces are bored as well. Most intervals are *Ophiomorpha*-dominated, lending the sedimentary fabric a nodular appearance similar to F6C. The fabric also contains mudballs (portions of the horizontal tunnels that are surrounded by mud accumulations 2 to 6 cm thick exhibiting concentric rings), meniscate structures and pellet-rich zones in addition to the passively filled pelleted shafts and tunnels.

Facies 12 is closely associated with cross-laminated sandstones of Facies 11 and coaly to muddy sandstones of Facies 13. In addition, bioclastic deposits of Facies 5, and more rarely multicolored mudstone of Facies 2 and conglomerate of Facies 14A, occur as interbeds within Facies 12 intervals. Lower boundaries of F12 intervals are sharp, commonly erosive and overlain by rounded mud clasts, bioclastic debris and rare pebbles.

Interpretation

Physical sedimentary structures and bedding style are virtually absent in F12 as bioturbation resulted in near complete mixing and the dispersion of shelly material, organics and pebbles throughout the deposit. Although Facies 12 contains a very low diversity trace fossil suite representing the *Cruziana* and *Skolithos* ichnofacies, *Ophiomorpha* is predominant and therefore represents opportunistic colonization of F12 sandbodies. These thickly lined burrows represent the tunnels and shafts of suspension-feeding crustaceans such as shrimp, which are highly adapted

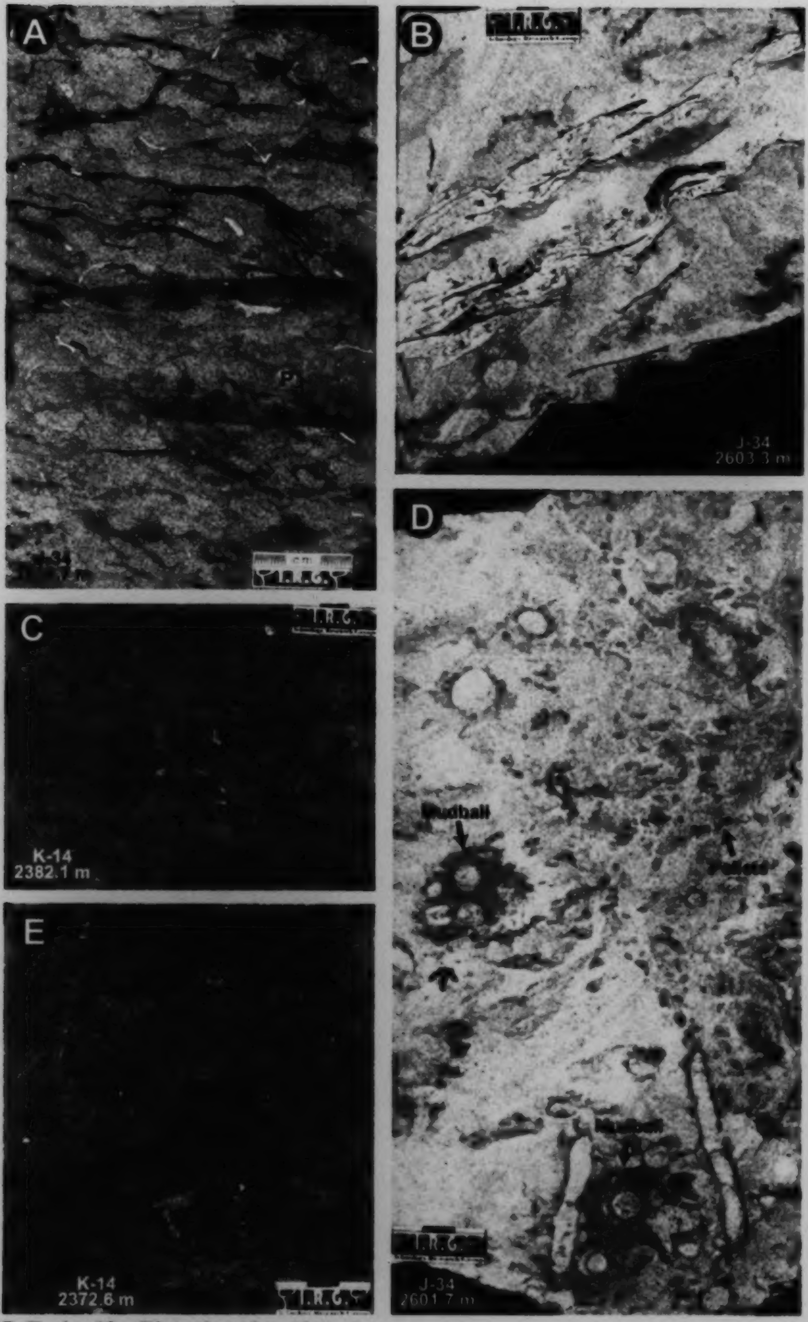
A
B
C
D
E
P
J-34
2603.3 m
K-14
2382.1 m
Mudball
Pellets
Mudball
K-14
2372.6 m
J-34
2601.7 m
I.R.G.

Figure 2.17: Facies 12 – Bioturbated sandstone
A) and B) Mixture of *Ophiomorpha*, pebbles (P) and coal. C) In F12, the degree of bioturbation is high to intense resulting in the distribution of pebbles (P) throughout the interval. D) The bioturbate texture of F12 consists almost entirely of *Ophiomorpha*; in this photo mudballs, interpreted as storage structures, and areas containing an abundance of reworked pellets are highlighted. E) Passive meniscate fill or active backfill within *Ophiomorpha*.

to exploit high-energy, unstable substrates. A variety of behaviors attributable to a shrimp-like organism can be recognized. In addition to domicile networks, mudball structures and meniscate fills are used for storage of organic/fecal matter and excavated material, respectively (Tom Saunders, pers. comm.). Pellet-rich zones represent areas that were reworked by the crustaceans; the pellets are remnants of either recycled burrow networks or deposit-feeding ventures. High individual densities of *Callianassa*, a modern shrimp that produces burrows with knobby exteriors and is known to employ both suspension and deposit-feeding strategies, are commonly reported from tidal flats and the inactive portions of tidal sand ridges/bars or the banks and laterally accreted point bar deposits of tidal channels (Howard and Frey, 1975, 1985; Gingras *et al.*, 1999b). The sporadic occurrence of inclined laminations in F12 could represent remnant pointbar stratification.

Facies 13 – Coaly to Muddy Sandstone

Description

Facies 13 consists of tan to grey-colored, moderately to poorly sorted, very fine to lower medium-grained sandstone intercalated with coal and dark grey to black mud, both of which occur as flasers (Figure 2.18), flat lenses and wavy laminae/beds. Sandstone layers range in thickness from a few millimeters to several tens of centimeters and are predominantly trough cross-bedded to ripple cross-laminated, where most ripple forms are asymmetrical. Planar parallel laminae and low-angle cross stratification are rare. Certain intervals exhibit wavy to lenticular bedding as they are dominated by coal or mud laminae that are wavy or wrinkled (i.e. draped over ripples). Coal and mud laminae also define deformation and load structures; broken coal laminae are common as well. Pyrite nodules occur within mudstone and coal or carbonaceous laminations. Although F13 contains multiple curved, erosional surfaces commonly overlain by bioclastic debris and more rarely pebbles, an overall fining upward and muddier upward trend is recognized. Sandstones of F13 are stained with hydrocarbons.

Bioturbation is mainly confined to mud laminae and intervals dominated by mud laminae. Recognizable traces include *Planolites*, *Palaeophycus*, *Thalassinoides* and *Chondrites*; *Ophiomorpha* and fugichnia are rare.

Facies 13 is limited in occurrence. It occurs intercalated with sandstones of Facies 11 and 12 at the Hibernia B-16 23 location. The lower and upper boundaries of this interval are erosive.

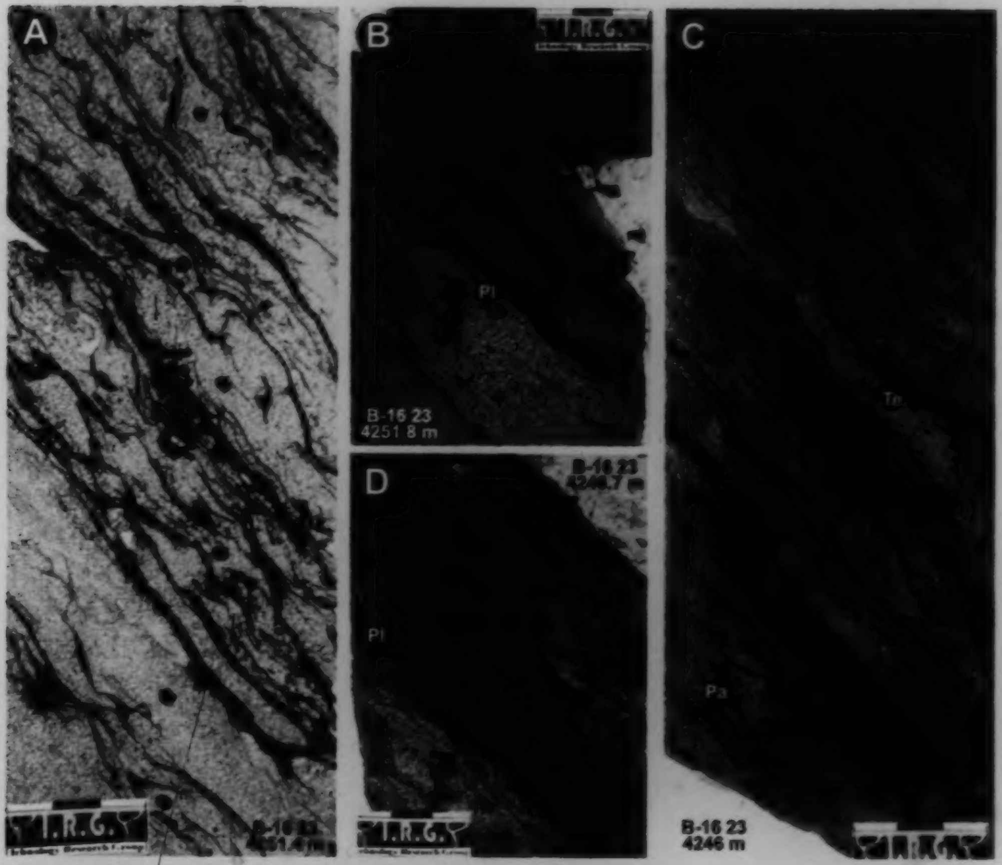

Figure 2.18: Facies 13 – Coaly to muddy sandstone
A) Coal occurs as wavy irregular laminae within a lenticular-bedded sandstone; the coal highlight intervening deformation and load structures. B) Ripples draped by mud; *Planolites* (Pl) is visible within a mud laminae. C) Flaser bedded interval characterized by an abundance of mud laminae, which also exhibit soft sediment deformation structures, *Teichichnus* (Te) and *Planolites* (Pl). D) Mudstone intervals are bioturbated (Pl = *Planolites*); however, it is difficult to differentiate these structures from deformation.

Interpretation

Alternation of sand with mud or coal represents periodic influx of coarser grain material into a quiescent, low energy setting. Trough cross-bedded intervals overlain by ripple cross-laminated layers formed under low to moderate flow regime conditions, while organic and dark mud laminae, which drape ripple forms, were deposited from suspension during periods of slack water. The abundance of organics and fine-grained clastics in the water column during these periods is indicative of low tidal flushing. Deformed intervals and load structures suggest that sand deposition occurred on water-saturated, soupy organic/mud substrates. Some coal or carbonaceous laminae are broken due to gases escaping from decomposing organic accumulations (which also could have cause the observed deformation). Although Facies 13 is sand-dominated, it closely resembles crevasse channel deposits described by Reineck and Singh (1980) and abandoned tidal channel sequences described by Reinson (1992).

Facies 14 – Conglomerate

Description

This facies consists of matrix-supported, pebble and cobble conglomerate, in which the clasts are rounded to well rounded and of various composition (Figure 2.19). Some beds are crudely normally graded and some clasts are weakly imbricated. Although quartz and chert clasts are most common, mudstone and sandstone rock fragments are also present. Because this conglomerate can be either sand or mud-supported, Facies 14 is divided into two subfacies: Sand-supported Conglomerate (F14A) and Mud-supported Conglomerate (F14B).

Facies 14A – Sand-supported Conglomerate

While clasts range in diameter from 0.5–3 cm, the sand supported matrix of F14A varies in grain size from fine to medium (Figure 2.19A). It commonly displays planar to inclined laminae and may host horizontal layers of crudely aligned, small shell fragments or mud clasts, which are sometimes sideritized. Carbonaceous debris and wood pieces also occur in rare to high abundance. Facies 14A intervals range in thickness from a few centimeters to several tens of centimeters.

Facies 14B – Mud-supported Conglomerate

Pebbles and cobbles of this subfacies are situated within a sandy to silty mudstone matrix (Figure 2.19B, C). The sand/silt content of the matrix is highly variable; although it averages 10-30%, it can get up to 60-70%. Facies 14B also commonly contains mud clasts that are sometimes sideritized and a mixture of bioclastic material that includes oysters, thin-shelled pelecypods, gastropods, echinoids and calcareous worm tubes. The matrix of F14B is burrow mottled. The most common trace fossils recognized include *Asterosoma, Teichichnus, Palaeophycus, Rhizochorallium, Ophiomorpha, Chondrites, Scolicia, Phycosiphon* and/or *Planolites*. Facies 14B intervals are generally tens of centimeters thick.

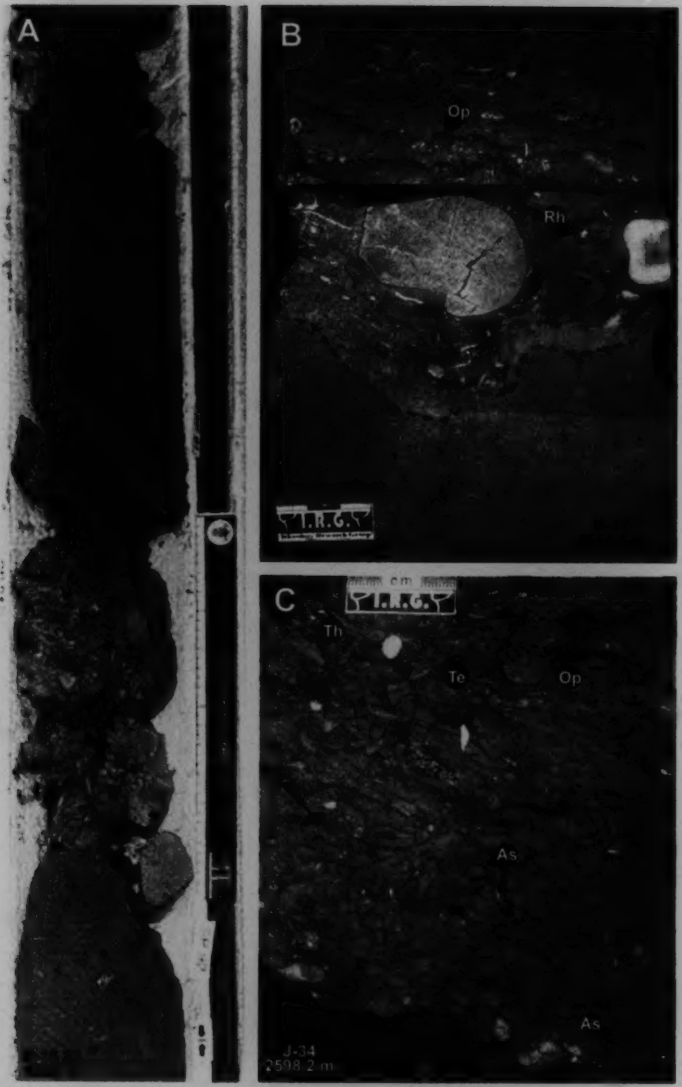

Figure 2.19: Facies 14 – Conglomerate
A) Example of Facies 14A; it contains a sand matrix and is immediately overlain by carbonaceous, cross-laminated sandstone of F11. B) and C) Examples of Facies 14B; this facies is commonly irregularly and sharply based (dashed line), only a few 10s of centimeters thick and contains a muddy matrix that is typically highly to intensely bioturbated; *Rhizocorallium* (Rh), *Asterosoma* (As), *Ophiomorpha* (Op), *Teichichnus* (Te) and *Thalassinoides* (Th); the conglomeratic lag is commonly redistributed by bioturbation.

Lower boundaries of F14 beds are always sharp, irregular and erosive; upper boundaries of F14A are gradational. Facies 14A occurs interbedded within sandstones of Facies 9, 11, 12 and 15. Mudstones of F3 or F4 and sandstone of F6 gradational overlie F14B. Facies 14B erosively overlies sandstone of Facies 11 or 12 and more rarely, bioclastic deposits of Facies 5.

Interpretation

Both subfacies of F14 accumulated via winnowing processes under high-energy conditions. The rounded nature of the clasts and presence of fragmented shell material indicates that the lag components underwent bedload transit for long periods of time, either by currents or oscillatory motion. Since F14A occurs repeated within physically reworked sandstones of Facies 8, 9, 11 and 12, this subfacies likely represents basal channel lags or bar-trough accumulations. The lags demarcate bedset boundaries and do not signify major shifts of the depositional system. Similar deposits are described from fluvial and deltaic successions by Cant (1982) and Coleman and Prior (1982). Conversely, F14B represents a transitional phase indicative of relatively abrupt deepening of the depositional system. In consensus with Soliman (1995), F14B constitutes a transgressive lag deposit. During transgression, a surf-winnowed lag collects behind the landward-advancing sea; once water depths are great enough that fine sediments begin to accumulate on the lag gravel, waves are no longer able to rework the deposit (Clifton, 1981). This process was originally described as "ravinement" by Stamp (1921). Bioturbation occurs in conjunction with the accumulation of fine sediments immediately post-ravinement. The presence of complex deposit-feeding structures most commonly associated with the archetypal to distal *Cruziana* ichnofacies supports placement of this facies within a distal lower shoreface to offshore setting (Pemberton *et al.*, 2001b).

Facies 15 – Pebbly, Carbonaceous Sandstone

Description

Facies 15 consists of grey, carbonaceous, upper fine to upper medium-grained sandstones with locally abundant granules. pebbles and rare interbeds of coal and black to dark grey, laminated mudstone (Figure 2.20). Sandstone beds are defined by sharp, erosive lower boundaries. Bed thickness ranges from a few tens of centimeters to 1-2 m and subtle fining upward and coarsening-upward trends are noted. Coal interbeds are less than 10 cm thick and generally poorly preserved; where present, they cap sandstone beds and immediately underlie scours. Mudstone laminae and beds (at most 20 cm thick) occur sporadically. The thicker mudstone beds show good development of planar lamination. Although F15 is bioturbated, some sandstone beds exhibit soft sediment deformation, massive textures or well-developed physical sedimentary structures. Recognizable structures include rare planar to low-angle cross stratification and more rarely, high-angle and

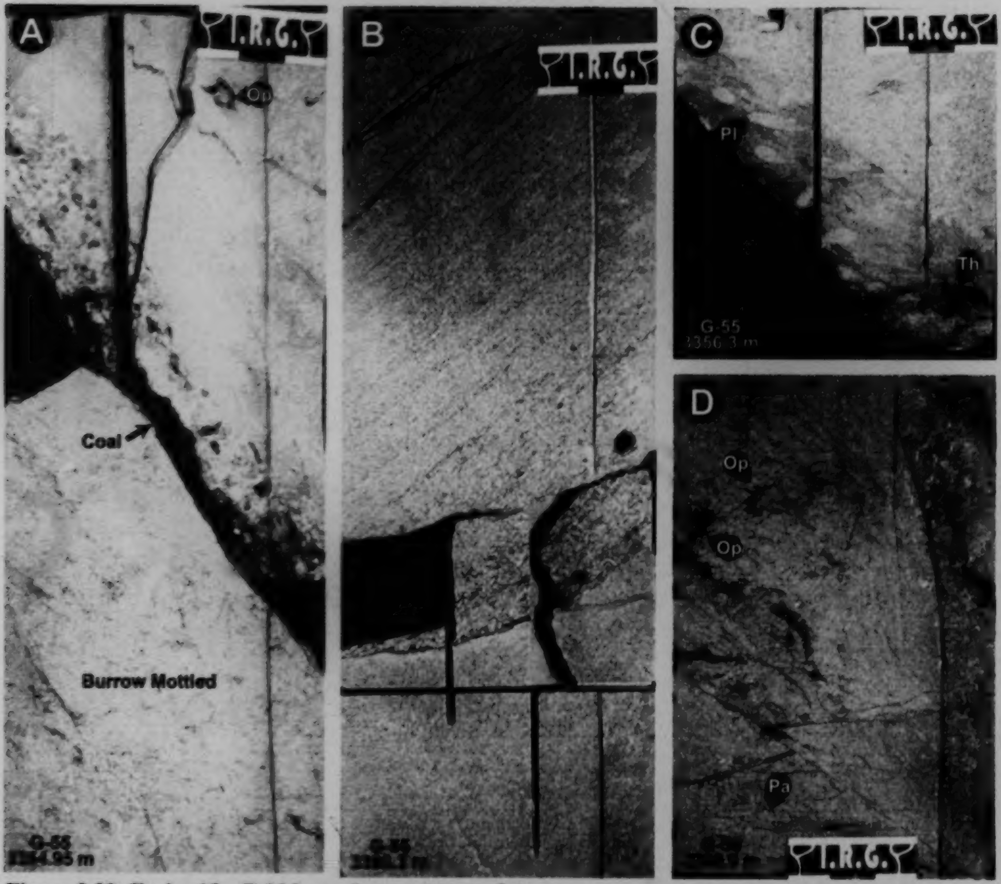

Figure 2.20: Facies 15 – Pebbly, carbonaceous sandstone
A) Conglomerate of F14A immediately overlying a coal bed; the hosting sandstones appear to be burrow mottled by *Palaeophycus*. The uppermost portion of the core photo contains syn-sedimentary faulting and *Ophiomorpha* (Op). B) Trough cross bedding highlighted by carbonaceous debris and granules. C) Muddy interval containing *Planolites* (Pl) and *Thalassinoides* (Th). D) *Ophiomorpha* (Op) and *Palaeophycus* (Pa) adjacent to soft sediment deformation (right side of the core).

trough cross bedding. Carbonaceous flakes and granules highlight laminations and biogenic structures. Large coal chunks are rare to moderate in occurrence. Thin-shelled pelecypod fragments and valves are rare and commonly associated with pebble lags.

The degree of bioturbation in this facies is moderate to high. Lower portions of sandstone beds are cross-laminated while upper portions are more commonly bioturbated. The representative trace fossil assemblage includes *Palaeophycus*, *Skolithos*, *Ophiomorpha nodosa*, *Ophiomorpha irregulaire* and fugichnia; these traces occur in moderate abundance. The bioturbate texture is predominantly composed of a chaotic or mottled fabric. Muddier intervals and mud beds contain rare to moderate occurrences of *Planolites, Chondrites, Thalassinoides* and possibly *Teichichnus*. Root traces are locally preserved.

Facies 15 contains interbeds of Facies 14A; in addition, it is only found in core #2 from the Hibernia G-55 well. Neither its upper or lower contact is captured.

Interpretation

The physical sedimentary structures described represent dune migration in unidirectional currents under low flow regime conditions. Sharp, erosive surfaces overlain by F14A represent intermittent scour and channel development. The transition from lag material into cross-laminated and bioturbated beds records one cycle of deposition corresponding to waning flow and the reduction in energy conditions. The stacked nature of these cycles indicate repeated cut and fill processes. Soft sediment deformation and textureless intervals are indicative of high rates of sedimentation. In addition to displaying the coarsest grain size of all sandstone facies, coal beds, high amounts of carbonaceous debris and root traces indicate that deposition occurred in close proximity to a vegetated area. Coals commonly form the base of a channel fill indicating that organic accumulation was sufficient to form a layer impenetrable to erosion (i.e. local development of mire or swamp conditions). Mud laminae and beds reflect periodic current inactivity corresponding to the lowest energy in the waning flow cycle. These commonly planar laminated intercalations represent the accumulation of fine-grained material from suspension. A trace fossil assemblage containing deposit-feeding structures of limited diversity and simple morphology is locally developed. Although sandstones of F15 are moderately to highly bioturbated, they also exhibit very low diversity. However, the assemblage of traces in the sandstone beds is predominantly composed of dwelling structures representing the *Skolithos* ichnofacies. Both ichnologic suites are impoverished and indicative of stressed environmental conditions – limited food supply and/or oxygen in the muddy substrates and relatively unstable and shifting sandy substrates. Cut and fill cycles representing channel migration and fill, sub-angular to sub-rounded basement pebbles, an abundance of carbonaceous material and coal, root traces and intermittent slack water conditions, coupled with a typical brackish water ichnologic signature, suggests that F15 was likely deposited within a fluvial/alluvial system, but proximally to the marginal marine realm. Possible environments of deposition include a bayhead delta or a fan delta.

2.3 Burrow-demarcated Surfaces

Numerous facies contacts are associated with a unique trace fossil signature. These boundaries are sharp, erosive and commonly overlain by a lag consisting of mud clasts, pebbles, carbonaceous debris and/or bioclastic debris. Robust, sharp-walled, unlined, vertical to sub-vertical burrows extend downward, sometimes up to 50 cm, from these surfaces (Figure 2.21). The burrows, which include *Thalassinoides* and *Skolithos*, are passively filled with material from the overlying unit, including lag material where present. If the underlying unit is bioturbated, the sharp-walled burrows ubiquitously cross cut the trace fossil assemblage of the host substrate.

These burrow-demarcated surfaces most commonly occur where Facies 5 overlies Facies 2, 7, 11 or 12, Facies 11 or 12 overlies Facies 5, Facies 9 or overlie Facies 3 or 4, and Facies 14B overlies Facies 12.

The sharp-walled, unlined nature of *Thalassinoides* and *Skolithos* indicate that the host substrate was firm at the time of excavation and colonization. Further evidence is the passive burrow fill, demonstrating that the structure remained open after burrow evacation allowing material from the subsequent depositional event to enter the open burrow network (MacEachern *et al.*, 1992). If these unlined, domicile burrows had been excavated in loose sand or soupy mud, they would have collapsed upon departure of the tracemaker. Firm substrates, or firmgrounds, form when unconsolidated sediment is buried, dewatered, compacted, exhumed under high-energy conditions and then made available for colonization. The presence of vertical and open-network dwelling burrows exists in contrast to the softground trace fossil suite and readily corresponds to the higher energy conditions; thus, these surfaces signify a depositional hiatus (MacEachern *et al.*, 1992). Seilacher (1967) proposed the *Glossifungites* ichnofacies for trace fossils assemblages emplaced in firm substrates. Since then, modern and ancient examples of *Glossifungites* trace fossil assemblages similar to those described above have been widely recognized (Frey and Seilacher, 1980; Frey and Pemberton, 1985; MacEachern *et al.*, 1992; Gingras *et al.*, 2001b).

Three types of *Glossifungites*-demarcated surfaces are recognized within the Avalon/Ben Nevis interval. Each type of surface formed under a characteristic set of conditions and thus represents a certain degree of temporal significance. These surfaces may represent important time lines within the succession, depending on the contrasting facies across the surface. *Glossifungites* surfaces underlying storm-deposited sandstones of Facies 10, which are contained within offshore

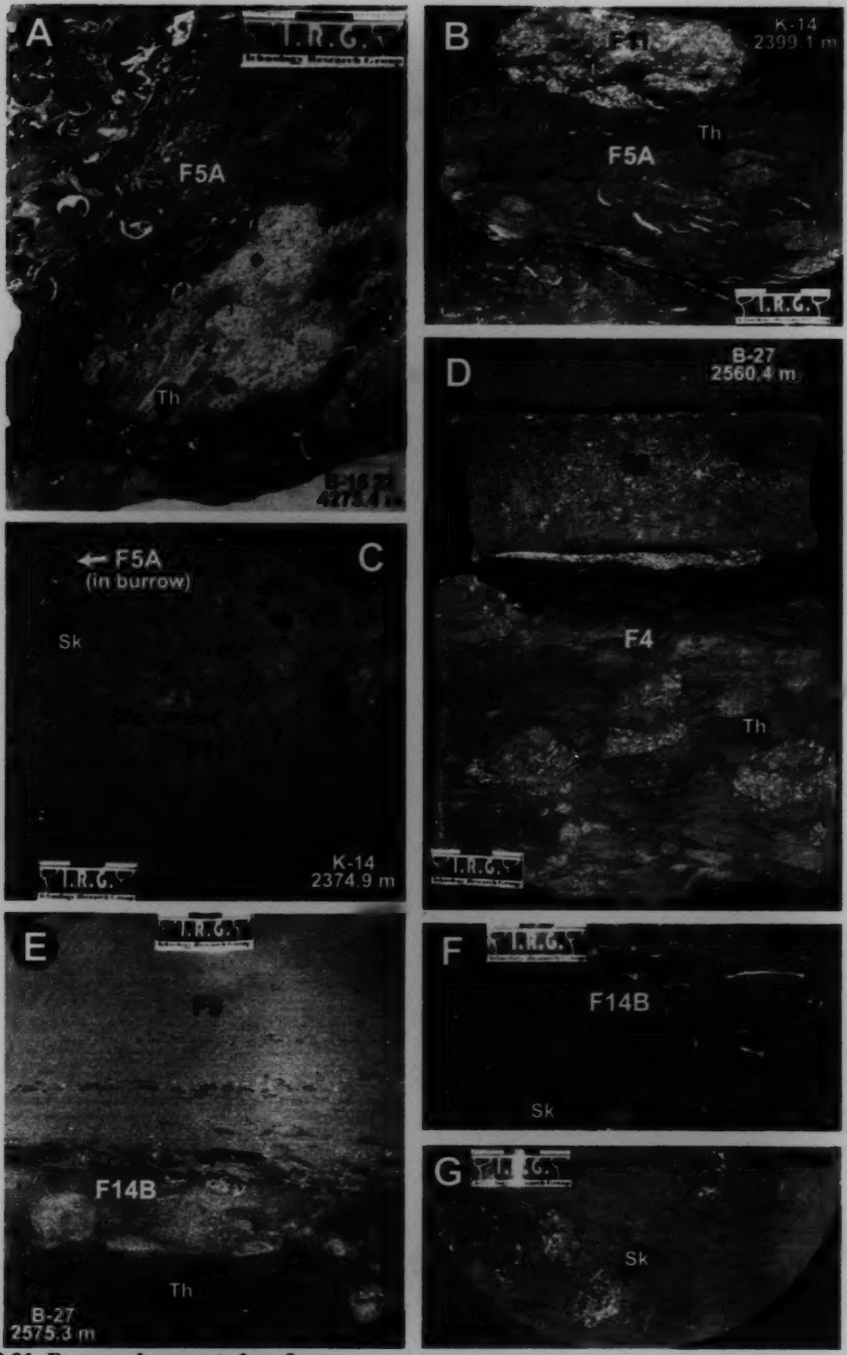
A
I.R.G.
F5A
Th
B
K-14
2399.1 m
Th
F5A
I.R.G.
D
B-27
2560.4 m
F4
Th
I.R.G.
C
F5A
(in burrow)
Sk
I.R.G.
K-14
2374.9 m
E
I.R.G.
F14B
Th
B-27
2575.3 m
F
I.R.G.
F14B
Sk
G
Sk

Figure 2.21: Burrow-demarcated surfaces
On A - F, the overlying and underlying facies, as well as the type of trace fossil that colonized the intervening contact (dashed lines), are highlighted. Photo G is the plan view of photo F; *Thalassinoides* (Th), *Skolithos* (Sk). In C, the burrow may actually be an *Arenicolites*.

or lower shoreface sediments of F6 and F3, are of the least temporal significance. Submarine erosion by wave activity in the shallow marine realm is localized, as some areas experience erosion while others undergo deposition. Thus correlation of these surfaces is unsubstantiated, even within the confines of the offshore or lower shoreface zones. The second type of surface occurs between the marginal marine facies: F2, F5, F7, F11 and F12. Excavation of the firm substrate is facilitated by autocyclic events, such as tidal channel migration, in marginal marine zones. Although these surfaces may be traceable between two particular subenvironments, they typically do not translate into adjacent facies tracts. The most temporally significant *Glossifungites* surface exist where conglomerate of Facies 14B overlies sandstone of F11 or F12 and where sandstones of Facies 9 overly bioturbated sediments of F3A or F6. F14B represents a depositional hiatus coupled with a substantial change in energy and depositional conditions. The lower surface formed via excavation of the firmground substrate due to transgression and erosive shoreline retreat. The upper surface records a depositional hiatus most likely related to low rates of deposition and maximum flooding prior to the establishment of shallower water conditions represented by F9. Therefore, it may be possible to correlate both surfaces over a variety of facies tracts and a wide areal extent.

2.4 Summary

The physical and biogenic sedimentary structures noted in the facies descriptions and interpretations are supportive of marginal marine to marine conditions. Physical sedimentary structures and macrofossil components indicate a mixture of both marine and terrestrial sources. Widespread siderite development and abundance of terrestrial-derived organic matter (carbonaceous debris, wood fragments, plant remains) indicate a strong freshwater influx. A variety of ichnologic signatures suggest the depositional system contained numerous subenvironments representing fully marine, stressed marine and brackish water conditions. These environments include soils, marsh, fluvial channel, bayhead delta or fan delta, lagoon, tidal flat, tidal channel, tidal delta, inlet channel, distributary mouth bar, delta front/lower shoreface and prodelta/offshore. Wave and current-derived structures are present but not persistent, while tidal indicators (e.g. profuse wavy/lenticular/flaser bedding) are rare. Thus apart from a few stratigraphic levels, the depositional system is assumed to be located along a partially restricted coastline under microtidal to mesotidal conditions for much of the succession.

Chapter 3

Facies Associations, Stratigraphy, Paleogeography and Depositional History

3.1 Introduction

This chapter presents an integrative approach to the interpretation of the depositional systems characterizing the Avalon/Ben Nevis interval. This task is accomplished beginning with the assignment of the facies discussed in Chapter 2 into eight facies associations (FAØ through FA7). Each facies association is described in terms of its constituent facies, representative facies successions, distribution and thickness as determined from core and well logs, bounding surfaces, gamma ray log signature, and relationship to overlying and underlying associations. Diagnostic criteria supporting the paleoenvironmental interpretation and a representative litholog (see Appendix 2, page 167, for legend of symbols) of each facies association are supplied. These criteria are based on the unified physical and biological processes presented in the facies, relationships between the constituent facies, relationships to underlying and/or overlying facies associations, and other information from previous studies that remained out of scope in this study. The stratal relationships between facies associations are illustrated in three stratigraphic cross sections. These cross sections highlight the stratal architecture of the Avalon and Ben Nevis formations and provide insight into the depositional systems that are present. Isopach mapping of the lower reservoir sandstone facies serves to illustrate its distribution and orientation. All available data is then integrated to construct paleogeographic maps and provide a depositional history, which is discussed with regards to the tectonic evolution and configuration of the Hibernia area.

3.2 Facies Associations

FAØ – Fan Delta/Bayhead Delta

Facies Association Ø only occurs in core from the Hibernia G-55 well location (Figure 3.1); its upper and lower contacts are not captured. In this association, Facies 15 occurs interbedded with conglomerate of Facies 14A. Although a gamma ray log is not available for this interval, from core it is likely that FAØ would exhibits a blocky signature, subtle fining-upward trends and intermittent inflections corresponding to coal beds, muddy intervals and conglomerate basal lags.

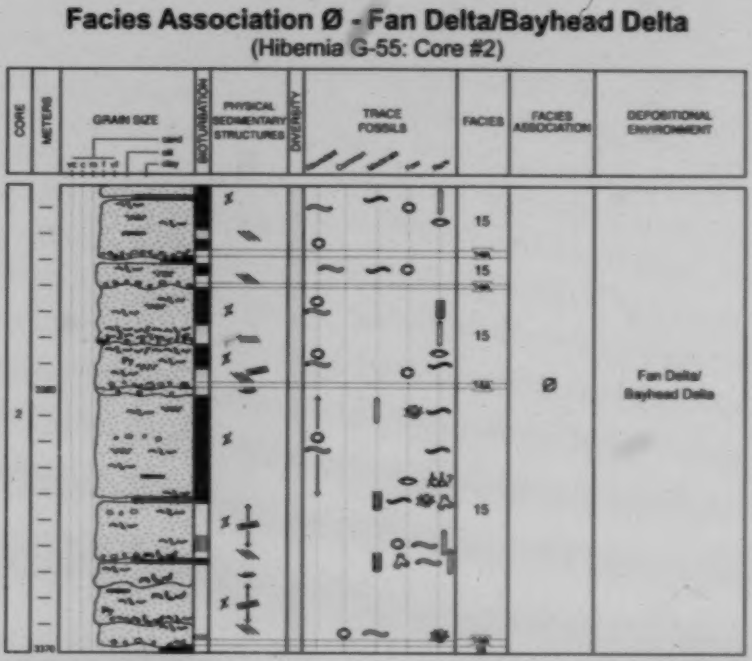

Facies Association Ø - Fan Delta/Bayhead Delta

(Hibernia G-55: Core #2)

CORE
METERS
GRAIN SIZE
BIOTURBATION
PHYSICAL SEDIMENTARY STRUCTURES
DIVERSITY
TRACE FOSSILS
FACIES
FACIES ASSOCIATION
DEPOSITIONAL ENVIRONMENT
2
15
Ø
Fan Delta/
Bayhead Delta

Figure 3.1: Representative litholog for Facies Association 0 – Fan Delta/Bayhead Delta. See Appendix 2 for legend of symbols.

Given its limited occurrence in core, the depositional environment of FAØ remains speculative. However certain characteristics indicate that it was deposited in close proximity to a sediment source but within a marginal marine setting. As such, it is interpreted as fan delta or bayhead delta deposits for several key reasons.

1) Coal beds present within the succession represent the accumulation of terrestrial organic matter in swampy areas. Such coal beds commonly form the base of channels due to the inability of currents to erode the peat material. Deltaic sediments are very commonly found intercalated with coal originating on the upper delta plain (Coleman and Prior, 1982).

2) Hurley *et al.* (1992) and Driscoll *et al.* (1995) noted that these deposits overlie coal and red mudstones, supporting a continental setting for its location. In support of this interpretation they noted no significant bioturbation. However, the deposit was found to be high to intensely bioturbated in this study. In particular, the presence of *Ophiomorpha*, which to date has only been recognized in marginal marine and marine environments, suggests that depostion took place at least near the fluvial-influenced zone (i.e. bayhead delta) or directly within a marginal marine to marine zone (i.e. fan delta).

3) The coarse-grained nature of this facies association, along with low flow regime dune migration and poorly sorted, rounded pebbles, indicates short transport distances by currents followed by periods of quiescence, as indicated by intermittent mud deposition. The presence of bioturbation also supports this conclusion. In such high energy, high sedimentation settings, trace makers only gain access to the substrate once depositional processes have been turned off. Settings exhibiting sediment flux in relation to precipitation or variable sediment supply are prime for the development of a laminated to scrambled appearance.

FA1 – Coastal Plain

Facies Association 1 occurs in the lower portion of most cored intervals; as a result, its lower contact is rarely captured in core. Where it is captured, FA1 erosively overlies shallow marine sediments of FA7; in turn, FA1 is sharply overlain by brackish deposits of FA2. The lower contact of FA1 is therefore interpreted as an unconformity, while the upper contact represents a flooding surface. The thickness of FA1 varies considerably over the Hibernia area; however, the thickest accumulations (up to 40 m) are found in the O-35 and B-27 well locations.

FA1 predominantly consists of Facies 2 and 8; F5 is less common (Figure 3.2). The typical facies succession begins with sandstone of Facies 8, which is sharply overlain by marsh or floodplain soils, mudstones and siltstones of Facies 2. Interbeds of Facies 8 and lagoonal mudstones of Facies 5 are found within Facies 2 (F8 lower in the succession and F5 in upper portions). Thus, the succession is characterized by a lower sand-dominated interval overlain by a mud-dominated interval, giving the appearance of a fining upward gamma ray log response.

This facies association was deposited in a coastal plain setting. There are several lines of evidence that support this interpetation.

1) Both F8 and F2 contain a number of features indicative of subaerial exposure, including soil development, anomalous color variations, root traces and carbonate accumulations (Retallack, 1988; Boggs, 1995).
2) Guilbault (1986) stated that sediments contained within this facies association contain a reduced content and diversity of forams and ostracods that are essentially arenaceous and involve species found in modern intertidal marsh environments.

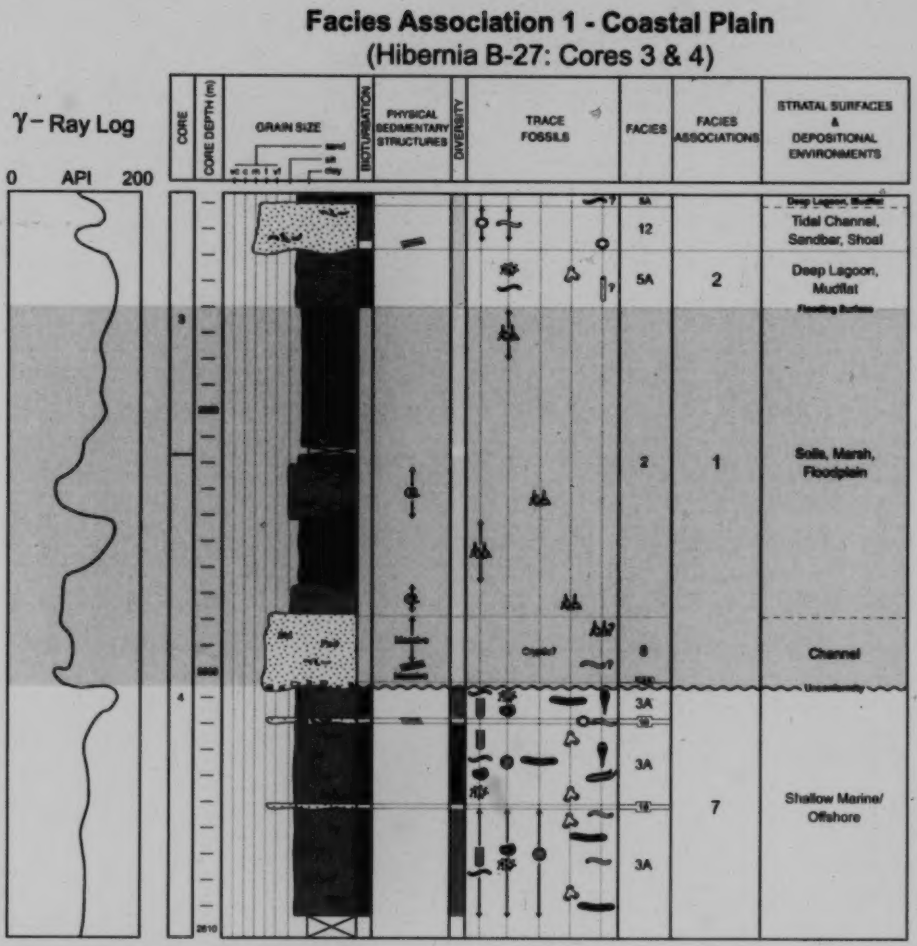
Facies Association 1 - Coastal Plain
(Hibernia B-27: Cores 3 & 4)
γ - Ray Log
0 API 200
CORE
CORE DEPTH (m)
GRAIN SIZE
sand
silt
clay
BIOTURBATION
PHYSICAL SEDIMENTARY STRUCTURES
DIVERSITY
TRACE FOSSILS
FACIES
FACIES ASSOCIATIONS
STRATAL SURFACES & DEPOSITIONAL ENVIRONMENTS
3
4
2610
5A
12
5A
2
8
3A
3A
3A
2
1
7
Deep Lagoon, Mudflat
Tidal Channel, Sandbar, Shoal
Deep Lagoon, Mudflat
Flooding Surface
Soils, Marsh, Floodplain
Channel
Unconformity
Shallow Marine/ Offshore

Figure 3.2: Representative litholog and gamma ray log for Facies Association 1 – Coastal Plain. See Appendix 2 for legend of symbols.

3) Brackish water gastropods and oysters that occur in storm-derived shell hash layers, thin interbeds of Facies 5, and overlying brackish water deposits of FA2 support a coastal position over a fully continental floodplain setting.

4) The thickest sections of FA1 are preserved in the topographically lowest portion of the trans-field half-graben; the thinnest successions occur up on the B-08 horst. Due to their pore preservation potential in the subaerial realm, the thickest accumulations of soils are typically found in areas prone to subsidence.

FA2 – Brackish Bay

Facies Association 2 sharply overlies coastal plain deposits of FA1 and is most commonly sharply overlain by carbonaceous sandstones of FA3. The lower contact is interpreted as a flooding surface. The upper contact is erosive and commonly demarcated by a *Glossifungites* trace fossil suite. FA2 is also rarely overlain by shallow marine sediments of FA7 (Figure 3.3). In this case, the intervening contact is interpreted as a transgressive surface of erosion. The thickness of FA2 ranges from 3 m to over 20 m; it thins toward the north and south and appears to be absent south of the I-46 and J-34 well locations.

FA2 consists of four intercalated facies: F5 and F7 are most common while F2 and F12 are more rare in occurrence. On gamma ray logs, this facies association is represented by a highly serrated pattern that is overall cleaner or sandier upward. Lagoon deposits of Facies 5 most commonly lie at the base of FA2. In a typical succession, F5B usually overlies F5A in a single cycle or several stacked F5B to F5A cycles. Thin interbeds of F2 marsh mudstones are rarely found lower

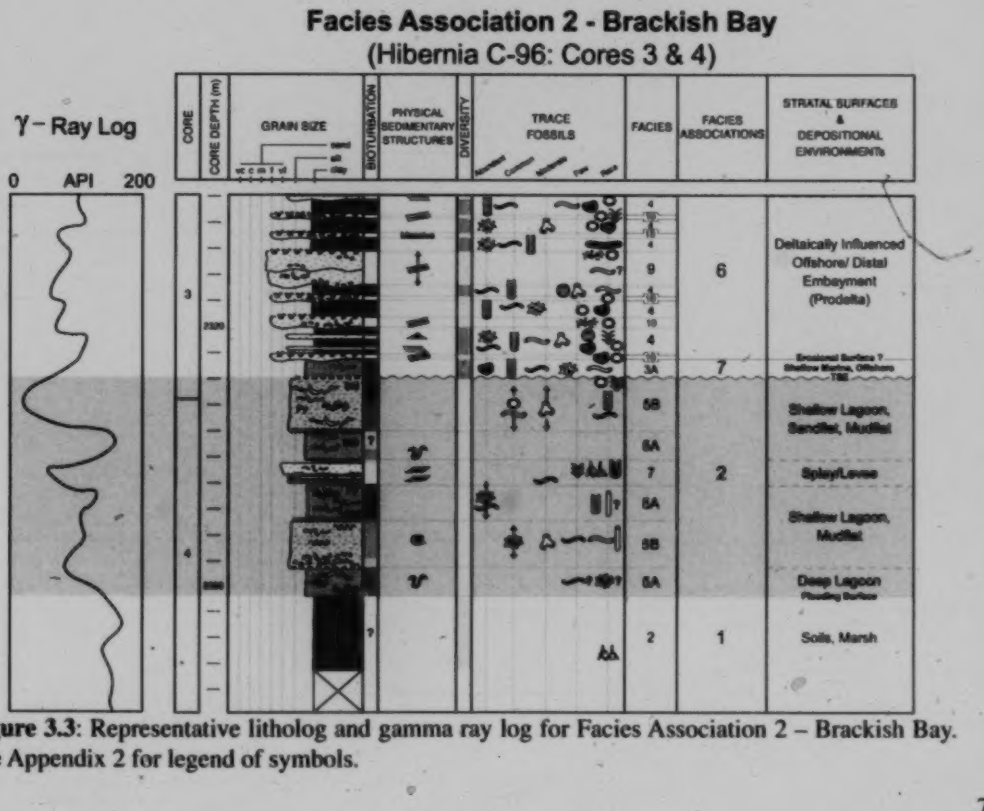
Facies Association 2 - Brackish Bay
(Hibernia C-96: Cores 3 & 4)
γ - Ray Log
0 API 200
CORE
CORE DEPTH (m)
GRAIN SIZE
BIOTURBATION
PHYSICAL SEDIMENTARY STRUCTURES
DIVERSITY
TRACE FOSSILS
FACIES
FACIES ASSOCIATIONS
STRATAL SURFACES & DEPOSITIONAL ENVIRONMENTS
3
4
9
10
3A
5B
5A
7
2
6
1
Deltaically Influenced Offshore/ Distal Embayment (Prodelta)
Erosional Surface ?
Shallow Marine, Offshore
TSE
Shallow Lagoon, Sandflat, Mudflat
Splay/Levee
Shallow Lagoon, Mudflat
Deep Lagoon
Flooding Surface
Soils, Marsh

Figure 3.3: Representative litholog and gamma ray log for Facies Association 2 – Brackish Bay. See Appendix 2 for legend of symbols.

in the succession, while F7 ripple cross-laminated sandstones, representing splays or washover fans, occur in the middle or toward the top of FA2.

FA2 represents interfingering subenvironments of a brackish bay due to:

1) the predominance of *Turritella* and oysters. These species are able to tolerate fluctuating salinity conditions (Hudson, 1963; Allmon, 1988). In addition, oyster beds are commonly reported from Cretaceous lagoon deposits (Land, 1972; Howard and Frey, 1985).
2) deformational structures. Soft sediment deformation and chaotic bedding are fairly common in muddier brackish water settings (Clifton, 1982).
3) localized concentrations of coal debris, plant remains and wood fragments, as well as interbeds of F2 marsh deposits. Intercalations of these deposits within lagoonal mudstones indicate proximity to vegetated supratidal areas or the stabilization of marginal bay facies (Reinson, 1992).
4) a high degree of bioturbation coupled with low diversity trace fossil assemblages and high individual densities. This combination reflects stressed environment conditions within a brackish water setting (Pemberton *et al.*, 2001b).
5) a facies succession representing the complex interfingering of low energy (deep lagoon/ mud flats/plain) with higher energy (shallow lagoon/tidal creeks/sand flats and splays/ washover fans) subenvironments. Such high variety in juxtaposed facies is typical of estuarine central basins or backbarrier lagoons (Reinson, 1992).

FA3 – Bay Mouth Complex

Facies Association 3 predominantly consists of carbonaceous sandstones of Facies 11 and 12. It sharply overlies brackish bay deposits of FA2 (Figure 3.4). The upper contact of FA3 is sharp, irregular and overlain by conglomerate of Facies 14B; it is interpreted as a transgressive surface of erosion or ravinement surface. The lower contact of FA3 is erosive. Both upper and lower contacts may be associated with firmground colonization (i.e. demarcated by *Glossifungites* assemblages). The thickest FA3 intervals occur in the vicinity of Hibernia K-14. As in FA2, this facies association appears to be absent south of the I-46 and J-34 well location; it is also absent in the northeast corner of the field.

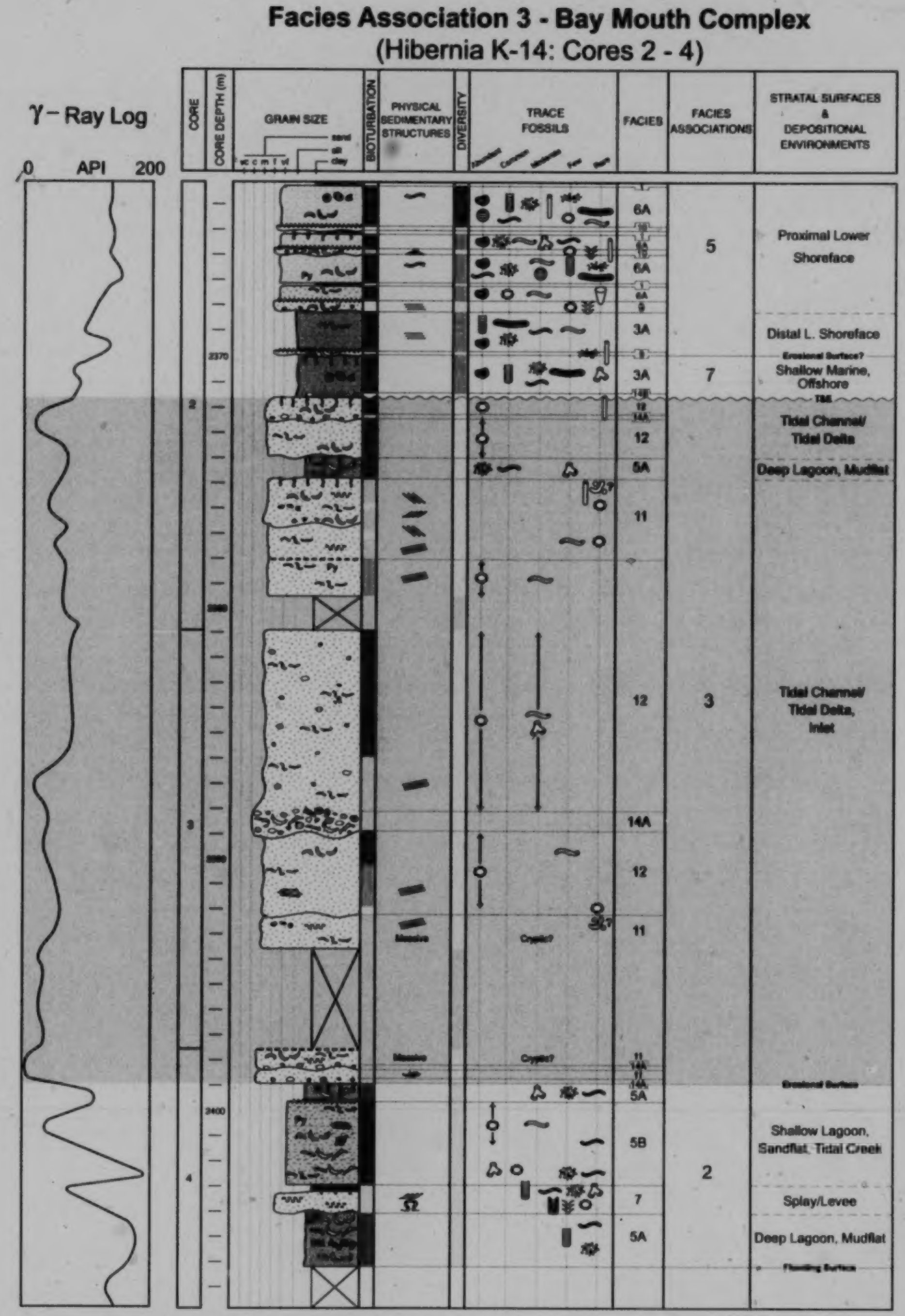

Facies Association 3 - Bay Mouth Complex
(Hibernia K-14: Cores 2 - 4)

γ - Ray Log
0
API
200
CORE
CORE DEPTH (m)
GRAIN SIZE
sand
silt
clay
BIOTURBATION
PHYSICAL SEDIMENTARY STRUCTURES
DIVERSITY
TRACE FOSSILS
FACIES
FACIES ASSOCIATIONS
STRATAL SURFACES & DEPOSITIONAL ENVIRONMENTS
2
3
4
2370
2380
2390
2400
6A
3A
14A
12
5A
11
5B
7
5
7
3
2
Proximal Lower Shoreface
Distal L. Shoreface
Erosional Surface?
Shallow Marine, Offshore
TSE
Tidal Channel/ Tidal Delta
Deep Lagoon, Mudflat
Tidal Channel/ Tidal Delta, Inlet
Massive
Cryptic?
Erosional Surface
Shallow Lagoon, Sandflat, Tidal Creek
Splay/Levee
Deep Lagoon, Mudflat
Flooding Surface

Figure 3.3: Representative litholog and gamma ray log for Facies Association 3 – Bay Mouth Complex. See Appendix 2 for legend of symbols.

In addition to Facies 11 and 12, FA3 also contains interbeds of F2, F5, F13 and F14A. The typical gamma ray log signature of FA3 is blocky to funnel-shaped; the latter indicating a slight cleaning-upward trend. Both patterns are slightly serrated; most inflections coincide with internal erosion surfaces, which are overlain by shell and mud clast lags or conglomerate of F14A and separate fining-upward or coarsening-upward bedsets. Interbeds of F5 lagoonal deposits generally occur at one or both of two horizons, located either near the base or top of the succession. Marsh mudstones of Facies 2 are rare in occurrence and closely associated with Facies 5.

Facies Association 3 is interpreted as a bay mouth complex as indicated by five pieces of evidence.

1) Physical structures are indicative of persistent physical reworking by both waves and currents (well-sorted, clean sands, trough and high-angle cross bedding, low-angle cross stratification, rounded mud clasts and only rare rippled intervals with mud/carbonaceous drapes).
2) Sandstones deposited from dune migration within active channels and sandbars/shoals (F11) interbedded with inactive sandbar or channel bank/pointbar deposits colonized by *Ophiomorpha* (F12) represent the high-energy and low-energy components of a tidal delta/inlet complex, respectively. Because the depth of the inlet channel may exceed the depth of adjacent environments, lateral migration of the inlet channel (and associated flood and ebb deltas) may be so extensive as to completely rework all other facies in close proximity (i.e. beach, dunes, marsh) (McCubbin, 1982; Reinson, 1992).
3) Coaly to muddy sandstone of F13 represents an abandoned tidal channel. Reinson (1992) stated that "channel fills resulting from abandonment should be present in flood tidal delta regions of mesotidal estuaries where tidal switching is common".
4) An isopach map of the FA3 interval (Figure 3.5) reveals that the deposit is confined to the trans-field paleo-low and is lobe-shaped. The lobe thins toward the northwest and is thickest in the central to southeast portions of the Hibernia area. This is consistent with the configuration recognized within modern tidal delta complexes (Coleman and Prior, 1982). The sediment lobe of the tidal delta is thickest nearest to the inlet/barrier and thins in a backbarrier direction.

5) This facies association contains interbeds of lagoonal facies (F5) and is positioned stratigraphically above the brackish bay facies association. If the bay mouth complex is undergoing transgression, the flood tidal delta should be preferentially preserved over the ebb tidal delta, as ebb tidal sediments become reincorporated into the longshore drift system (Boothroyd, 1985; Reinson, 1992). Thus, the sandy sediments of the bay mouth complex share a common facies contact with quiescent, backbarrier lagoon or bay deposits and are sharply overlain by marine sediments (beach, dune and upper shoreface deposits of the barrier proper are removed upon transgression) (Rampino and Sanders, 1980; Elliot, 1986).

6) Barwis (1990), Cheel and Leckie (1990), Boersma (1991) and Murakoshi and Masuda (1991) described similar successions that they interpreted as tidal delta/inlet complexes.

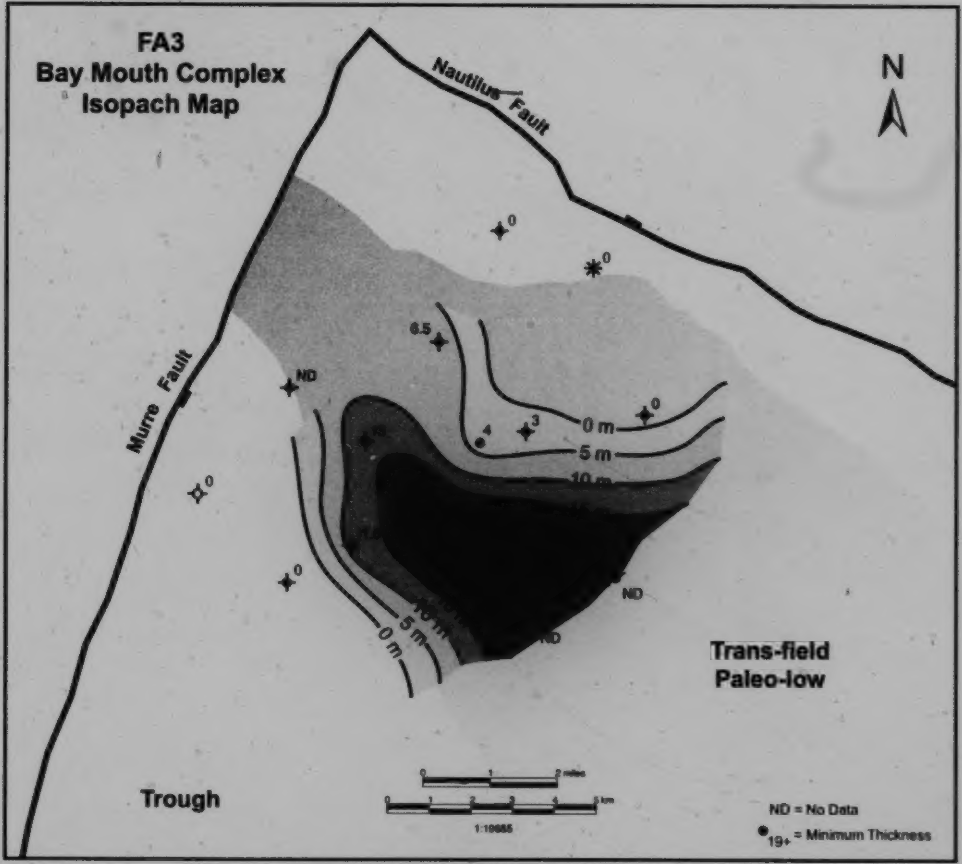
FA3
Bay Mouth Complex
Isopach Map
N
Nautilus Fault
Murre Fault
0
0
6.5
ND
0 m
5 m
10 m
4
3
0
0
0
ND
ND
10 m
5 m
0 m
Trans-field
Paleo-low
Trough
0
1
2 miles
0
1
2
3
4
5 km
1:19665
ND = No Data
19+ = Minimum Thickness

Figure 3.5: Isopach map of the FA3 interval (thickness measured from top of FA2 to the TSE as indicated on gamma ray logs and lithologs). Contour interval is 5 m.

FA4 – Upper Shoreface/Distributary Mouth Bar

Facies Association 4 occurs interbedded with bioturbated deposits of FA5 and mudstone deposits of FA6. Lower boundaries of this facies association are always sharp and sometimes erosive. FA4 commonly overlies conglomerate of F14B; in this case, the intervening contact is interpreted to be a transgressive surface of erosion. Either bioturbated sandstone of FA5 or heterolithic mudstone of FA6 overlies FA4. Upper boundaries are typically sharp and interpreted as flooding surfaces. The thickest accumulations of this association are found at the B-44, G-55, J-34 and O-35 well locations.

Massive to laminated sandstones of F9 form the bulk of FA4 (Figure 3.6); interbeds of F1 mudstone, F6 bioturbated muddy to silty sandstone, F10 sandstone and F14A conglomerate occur locally. The gamma ray log signature for FA4 is blocky and only slightly serrated; no discernable trends are noteworthy as it is primarily made up of clean, well-sorted sandstones of Facies 9.

FA4 is interpreted as a series of stacked bars or shoals within the upper shoreface zone and possibly near mouths of distributary channels. Evidence supporting this interpretation includes:

1) the predominance of features indicative of high sedimentation rates (e.g. massive bedding, convolute bedding) and extensive physical reworking by unconfined outflow (e.g. planar parallel and low-angle cross lamination). At the mouth of distributary channels, river output mixes with marine waters resulting in reduced momentum and loss of transporting ability (Elliot, 1986); thus, it is here that the thickest accretionary bar sediments will accumulate.
2) graded beds, which are produced as suspended particles settle from high concentration sediment clouds. These beds correspond to peak flood and ensuing waning flow conditions and are deposited by either unidirectional currents or high energy waves (Reineck and Singh, 1980).
3) thin muds interpreted as fluid mud event beds. These mud layers, which are deposited during the low-river stage, may escape erosion and be well preserved in distributary mouth bar deposits (Reineck and Singh, 1980).
4) absent to sparse bioturbation. The occurrence of trace fossils solely at the top of F9 beds indicates that environmental conditions were unfavorable to colonization during deposition (e.g. high turbidity, shifting substrates, fresh water influx). These sandbodies are poor in organics and only became available to infaunal organisms subsequent to deposition.

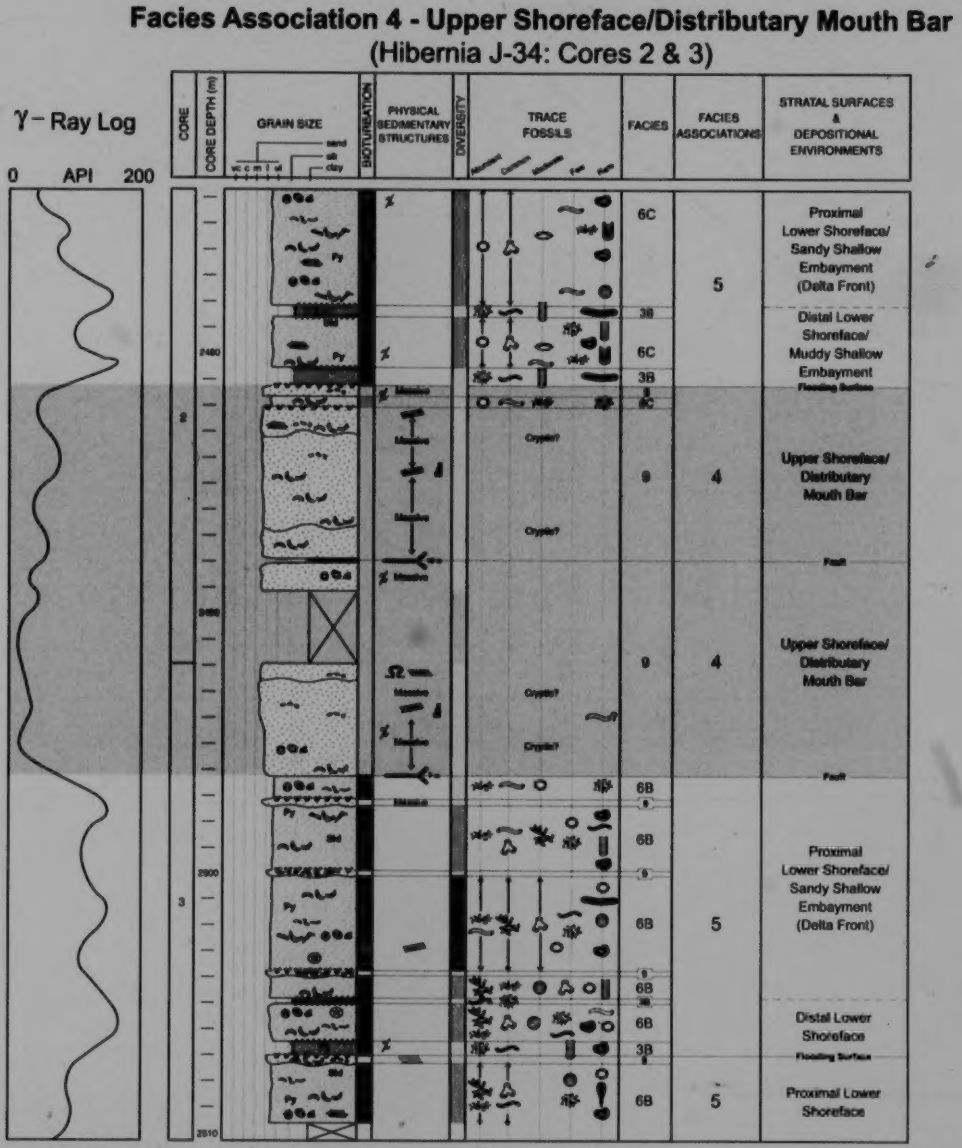
Facies Association 4 - Upper Shoreface/Distributary Mouth Bar
(Hibernia J-34: Cores 2 & 3)
γ- Ray Log
0 API 200
CORE
CORE DEPTH (m)
GRAIN SIZE
sand
slt
clay
BIOTURBATION
PHYSICAL SEDIMENTARY STRUCTURES
DIVERSITY
TRACE FOSSILS
FACIES
FACIES ASSOCIATIONS
STRATAL SURFACES & DEPOSITIONAL ENVIRONMENTS
2
3
2480
2490
2500
2510
Py
Sid
Massive
Cryptic?
6C
3B
9
6B
5
4
Proximal Lower Shoreface/ Sandy Shallow Embayment (Delta Front)
Distal Lower Shoreface/ Muddy Shallow Embayment
Flooding Surface
Upper Shoreface/ Distributary Mouth Bar
Fault
Distal Lower Shoreface
Proximal Lower Shoreface

Figure 3.6: Representative litholog and gamma ray log for Facies Association 4 – Upper Shoreface/ Distributary Mouth Bar. See Appendix 2 for legend of symbols.

FA5 – Deltaically Influenced Lower Shoreface/Shallow Embayment

Facies Association 5 occurs interbedded with sandstones of FA4 and heterolithic mudstone of FA6. It may lie directly above conglomerates of Facies 14B; in this case the contact is interpreted as a transgressive surface of erosion. Where FA5 overlies FA4, the sharp, intervening surface is interpreted as a flooding surface; the contact is conformable where FA5 overlies FA6. The upper surface is interpreted as a flooding surface where FA5 is overlain by F6 and as a surface of erosion where it is overlain by F4. The thickest and best-developed successions of this facies association are found in Hibernia B-16 19Z, B-16 25, B-44, K-14 and J-34.

The most common occurring facies within FA5 are bioturbated mudstones of Facies 3 and bioturbated muddy to silty sandstones of Facies 6 (Figure 3.7). Massive to laminated sandstones of Facies 9 are relatively less common; F1, F10 and F14A also occur sporadically. The typical facies succession of FA5 consists of Facies 3 overlain by Facies 6; interbeds of Facies 9 can sometimes be found toward the top of the succession. This succession may occur repeatedly. As such, the gamma ray log signature appears slightly serrated and overall cleaning or coarsening upward. Where sandstones of F6 and F9 are most abundant, the pattern takes on a more blocky appearance (e.g. J-34) and when mudstones of F3 predominate, the gamma ray response exhibits high radioactivity and low amplitude serration with a low radioactivity spike near the top of the succession (e.g. K-14). Storm deposits (F10) occur as thin isolated beds within and sometimes between F3 and F6. Facies 1 mudstones can occur within either F6 or F9; F14A is found interbedded within F9.

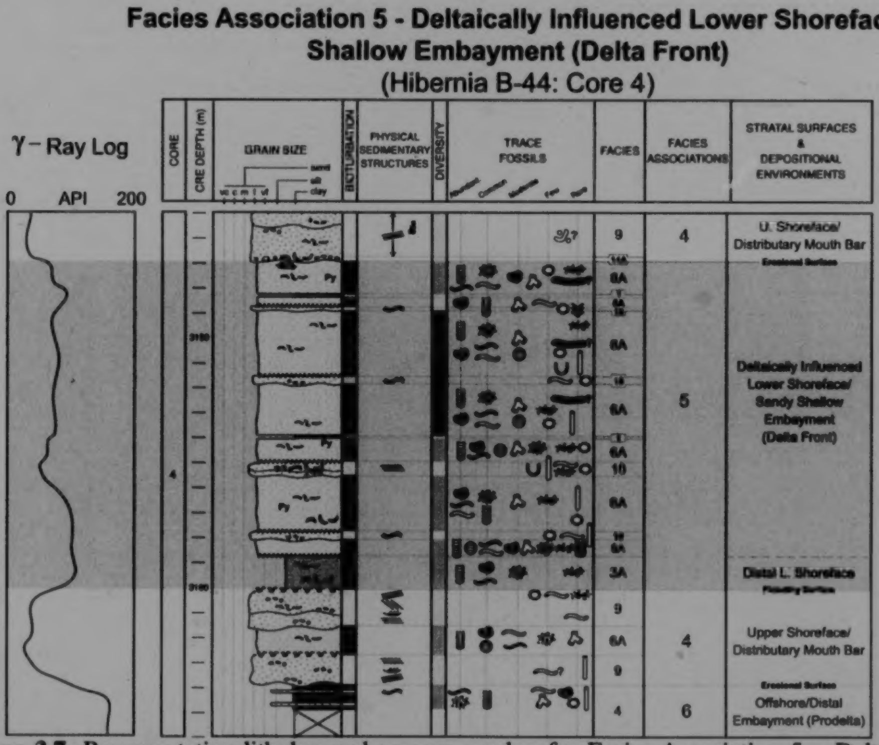
Facies Association 5 - Deltaically Influenced Lower Shoreface/
Shallow Embayment (Delta Front)
(Hibernia B-44: Core 4)
γ - Ray Log
0 API 200
CORE
CRE DEPTH (m)
GRAIN SIZE
sand
silt
clay
BIOTURBATION
PHYSICAL SEDIMENTARY STRUCTURES
DIVERSITY
TRACE FOSSILS
FACIES
FACIES ASSOCIATIONS
STRATAL SURFACES & DEPOSITIONAL ENVIRONMENTS
4
9
6A
3A
10
4
5
6
U. Shoreface/ Distributary Mouth Bar
Erosional Surface
Deltaically Influenced Lower Shoreface/ Sandy Shallow Embayment (Delta Front)
Distal L. Shoreface
Flooding Surface
Upper Shoreface/ Distributary Mouth Bar
Erosional Surface
Offshore/Distal Embayment (Prodelta)

Figure 3.7: Representative litholog and gamma ray log for Facies Association 5 – Deltaically Influenced Lower Shoreface/Shallow Embayment. See Appendix 2 for legend of symbols.

Facies Association 5 was deposited within a deltaically influenced lower shoreface or a shallow embayment (equivalent to the delta front). The lower muddy deposits represent the distal lower shoreface, while upper sandy deposits represent the proximal lower shoreface. This interpretation is support by five main pieces of evidence.

1) The common occurrence of siderite staining, nodules and layers within F3 and F6. Such an early occurrence of siderite cement is common in deltaic settings (MacEachern *et al.*, in press - 2005); is indicative of periodic freshwater influx, concomitant dilution of marine waters and reduction in sulphate activity.
2) Interbeds of F1, interpreted as hyperpycnal or fluid muds, are present within many FA6 intervals. These mudstones are depositional event beds representing influx of phytodetrital material from a nearby fluvial source.
3) The transition from F3 to F6 and F9 represents progradational parasequences. In a deltaic system, once a lobe becomes inactive, subsequent subsidence results in deepening and re-establishment of more distal F3. The supply of (coarser) sediment increases as distributary channels migrate back into the area (establishment of more proximal F6). The succession may or may not contain or be capped by ichnologically sterile deposits of F9, which are tongues of distributary mouth bar sands that extend into the interdistributary areas.
4) FA 5 is interbedded with and adjacent to thick intervals of FA4, which is interpreted as distributary mouth bars. Together, they represent delta front sheet sands that contain distributary mouth bar finger sands, which are described by Reineck and Singh (1980) as elongated sand bodies resulting from continual deposition at the mouth of distributaries as the delta advances seaward. These sand bodies eventually become encased by lower shoreface or delta front successions (or shallow embayment deposits).
5) Facies 3 and 6 comprise a number of ichnologic signatures. As a result, the overall bioturbate texture of both deposits is heterogeneous in nature. On an open or fully marine shoreline (i.e. strandplain or barrier island), uniformity of environmental conditions, within the lower shoreface and offshore zones in particular, is expected (Ekdale *et al.*, 1984; Howard and Frey, 1984; Pemberton *et al.*, 1992). Because this uniformity represents a stable niche, a wide variety of organisms can readily adapt. Over prolonged periods of accumulation time, which can range from 10,000 to 100,000 years for fair-weather deposits

of the lower shoreface and offshore zones (Soliman, 1995), a fairly complex but consistent and homogeneous texture will develop. Since F3 and F6 do not follow this rationale, other environmental or configurational factors must come into play in determining the stability of the sublittoral zone. These include dissection of the shoreline by the distributary channels of a delta and restricted marine conditions as observed in embayments.

FA6 – Deltaically Influenced Offshore/Distal Embayment

FA6 occurs interbedded with bioturbated sediments of FA5 and sandstones of FA4 (e.g. Hibernia J-34 and B-16 23 cored intervals). The lower boundaries of FA6 intervals are interpreted as flooding surfaces. FA6 commonly overlies conglomerate of Facies 14B; in this case, the intervening contact is interpreted as a transgressive surface of erosion. Where FA6 is overlain by FA4 or FA5, the upper contact is conformable to sharp and erosive. The thickest accumulations of FA6 occur in the northern parts of the Hibernia Field, in the vicinity of K-18 and C-96.

Facies Association 6 is largely composed of heterolithic mudstones of Facies 4; sandstone interbeds of Facies 9 and 10 occur locally (Figure 3.8). The typical gamma ray log signature is only slightly serrated and offset toward higher radioactivity compared to all other facies.

Facies Association 4 represents a deltaically influenced offshore setting (equivalent to the prodelta). It also may have been deposited in central or distal portions of an embayment. The line of evidence that supports this interpretation includes:

1) the presence of both wave and current activity. The ambient setting represented by mudstone-dominated F4 is characterized by quiescent, low-energy, shallow water conditions that are intermittently modified by wave activity (sand lenses) and storm activity (Facies 10). Interbeds of F9 are deposited from high energy currents (possibly turbidites) induced by storm activity (i.e. represents periods of high fluvial output).
2) siderite nodules/cemented layers and syneresis cracks. These sedimentary structures are associated with the influx of fresh water into more saline, offshore waters.
3) a trace fossil assemblage consisting of diminutive forms, predominantly grazing and deposit-feeding structures (stressed representation of the *Cruziana* ichnofacies) in the mudstone layers and equilibrium or escape structures in the sandstone layers. This combination reflects conditions conducive to the deposition of abundant foodstuffs that

are intermittently interrupted by higher energy events associated with increased sediment influx The juxtaposition of these two behaviors is indicative of environmental instability.

4) presence of marine forms such as *Asterosoma, Zoophycos* and *Scolicia*. FA6 very closely resembles the central bay deposits described by Pattison (1992). In conjuntion with reduced size and rare occurrence, such complex, deposit-feeding traces indicate that the depositional setting was restricted but not entirely isolated from the marine realm.

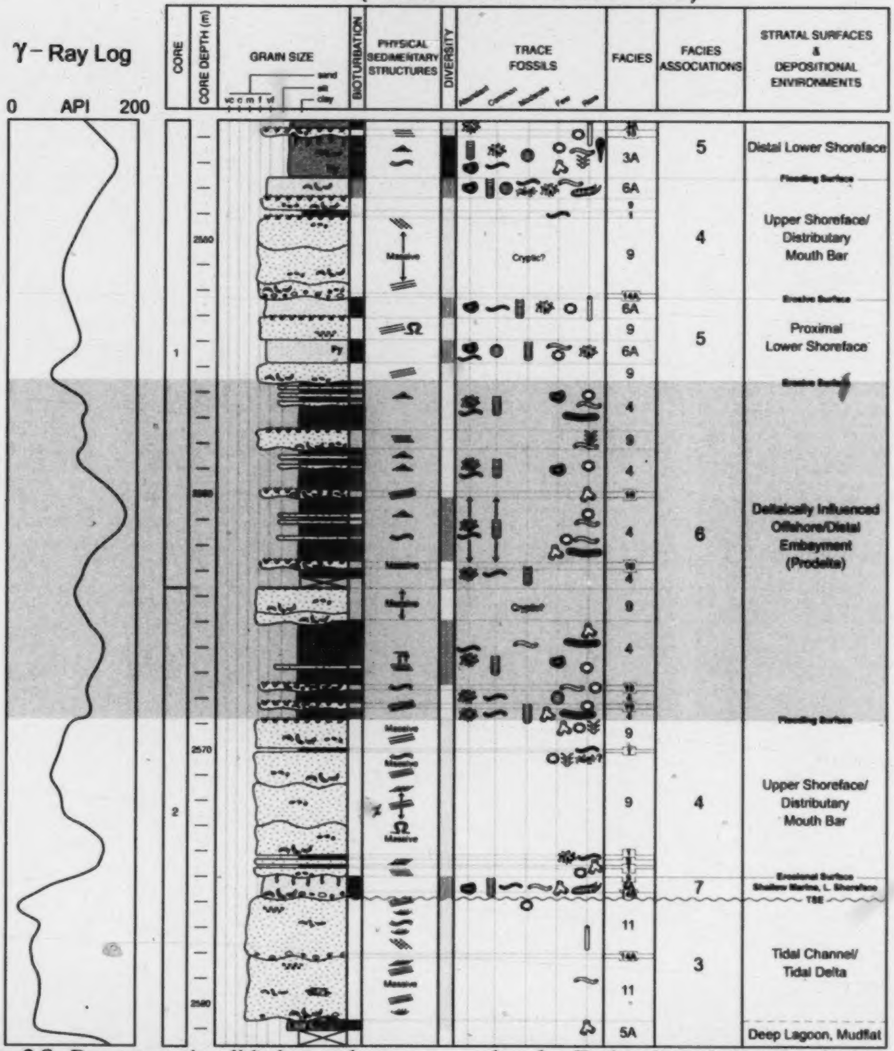

Facies Association 6 - Deltaically Influenced Offshore/
Distal Embayment (Prodelta)
(Hibernia B-27: Cores 1 & 2)

γ - Ray Log
0 API 200
CORE
CORE DEPTH (m)
GRAIN SIZE
sand
silt
clay
vc c m f vf
BIOTURBATION
PHYSICAL SEDIMENTARY STRUCTURES
DIVERSITY
TRACE FOSSILS
FACIES
FACIES ASSOCIATIONS
STRATAL SURFACES & DEPOSITIONAL ENVIRONMENTS
2560
2565
2570
2580
1
2
Massive
Cryptic?
3A
6A
9
6A
9
6A
9
4
9
4
4
9
4
9
11
11
5A
5
4
5
6
4
7
3
Distal Lower Shoreface
Flooding Surface
Upper Shoreface/ Distributary Mouth Bar
Erosive Surface
Proximal Lower Shoreface
Erosive Surface
Deltaically Influenced Offshore/Distal Embayment (Prodelta)
Flooding Surface
Upper Shoreface/ Distributary Mouth Bar
Erosional Surface
Shallow Marine, L. Shoreface
TSE
Tidal Channel/ Tidal Delta
Deep Lagoon, Mudflat

Figure 3.8: Representative litholog and gamma ray log for Facies Association 6 – Deltaically Influenced Offshore/Distal Embayment (Prodelta). See Appendix 2 for legend of symbols.

FA7 – Shallow Marine

FA7 occurs at two stratigraphic levels (Figure 3.9). A thick succession of Facies Association 7, which is predominantly contains silty to sandy mudstone of Facies 3A and interbeds of F10 storm deposits, occurs at the base of three cored intervals (Hibernia B-16 3, B-27 and K-14). Subaerially exposed deposits of FA1 erosively overlie FA7; as such, the contact is interpreted as an unconformity. The lower contact of this association is not captured in core; however, as observed on well logs, this interval can get up to 20 m thick in the Hibernia area. A very thin occurrence of FA7 (maximum 5 m) also occurs immediately above the transgressive surface of erosion. At this level, FA7 mainly consists of Facies 14B, 3A and 6A. On gamma ray logs, FA7 is overall high in radioactivity; in addition, it has a weakly serrated signature with very few, relatively small spikes.

FA7 represents deposition within the shoreface to offshore realm (i.e. mostly above storm wavebase) along an open marine coastline.

1) The lower occurrence of this association consists of a rather thick accumulation of Facies 3A that is commonly interrupted by storm deposits. Such prolonged, consistent deposition represents stable environmental conditions within a wave-dominated marine setting.
2) The thinner, but ubiquitous occurrence of FA7 higher up in the succession is related to abrupt deepening and transgression above a ravinement surface. This occurrence of FA7 is indicative of increased rates of subsidence coupled with low sedimentation rates. The presence of a *Glossifungites* surface at the base of FA7 supports the interpretation of an abrupt change in the depositional setting corresponding to abrupt deepening.
3) Although FA3 is considered to have rather common occurrence of siderite, accumulations of this cement are rather limited in FA7. Thus, deltaic influence is interpreted to be minimal at the stratigraphic levels of FA7.
4) Because FA7 is predominantly composed of F3A and F6A, both of which exhibits a homogeneous ichnologic signature, high to intense bioturbation and a high diversity trace fossil assemblage. This combination reflects relatively stable environmental conditions and is characteristic of the archetypal to distal *Cruziana* ichnofacies, which is typically associated with lower shoreface to offshore settings (Pemberton *et al.*, 2001b).
5) FA7 contains storm deposits of Facies 10, which are rather sporadic and thin, indicating that they were deposited below fair-weather wavebase but above storm wavebase.

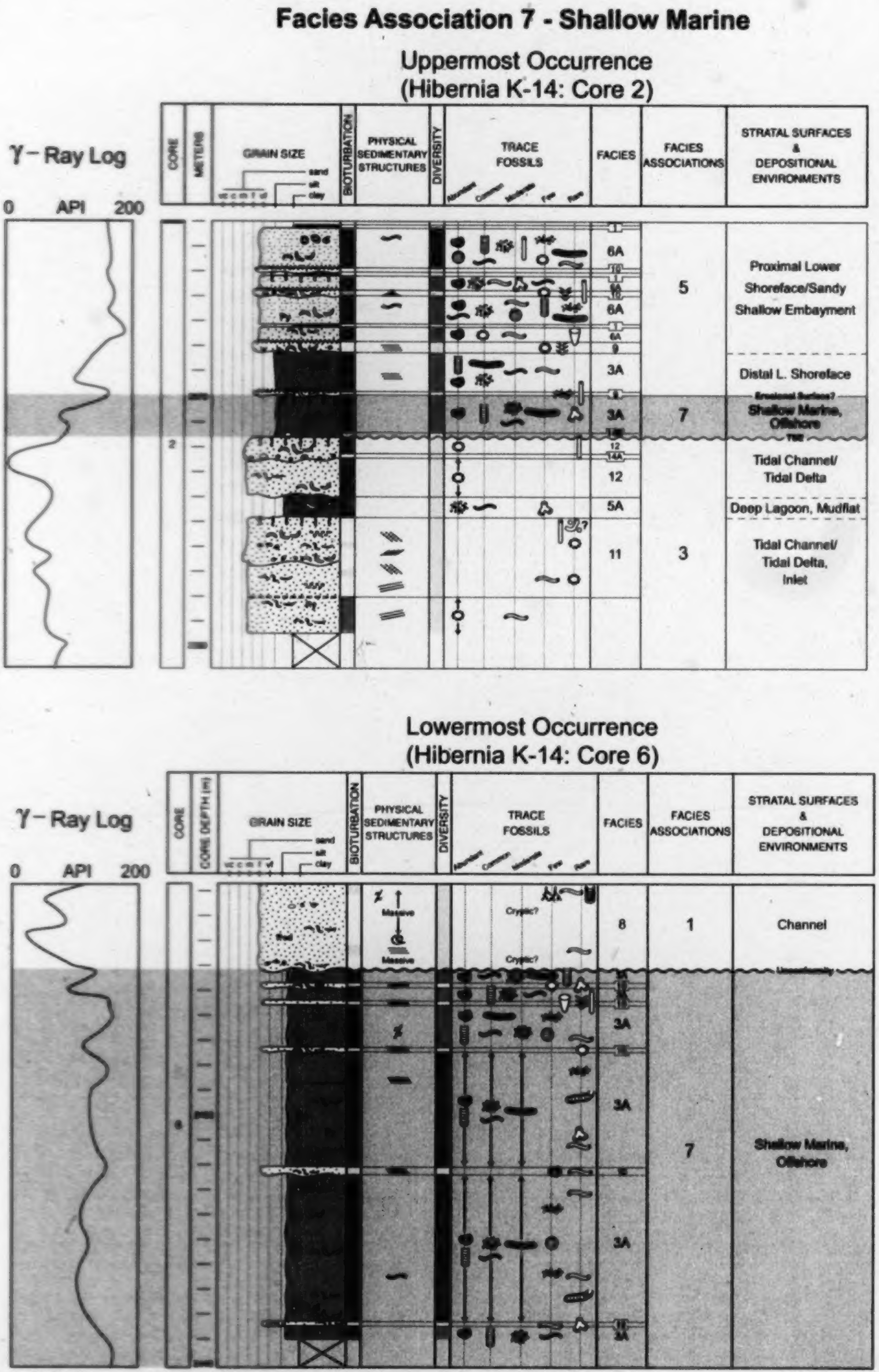
Facies Association 7 - Shallow Marine
Uppermost Occurrence
(Hibernia K-14: Core 2)
γ - Ray Log
0 API 200
CORE
METERS
GRAIN SIZE
sand
silt
clay
BIOTURBATION
PHYSICAL SEDIMENTARY STRUCTURES
DIVERSITY
TRACE FOSSILS
FACIES
FACIES ASSOCIATIONS
STRATAL SURFACES & DEPOSITIONAL ENVIRONMENTS
6A
6A
3A
3A
12
14A
12
5A
11
5
7
3
Proximal Lower Shoreface/Sandy Shallow Embayment
Distal L. Shoreface
Erosional Surface?
Shallow Marine, Offshore
TSE
Tidal Channel/ Tidal Delta
Deep Lagoon, Mudflat
Tidal Channel/ Tidal Delta, Inlet
2
Lowermost Occurrence
(Hibernia K-14: Core 6)
γ - Ray Log
0 API 200
CORE
CORE DEPTH (m)
GRAIN SIZE
sand
silt
clay
BIOTURBATION
PHYSICAL SEDIMENTARY STRUCTURES
DIVERSITY
TRACE FOSSILS
FACIES
FACIES ASSOCIATIONS
STRATAL SURFACES & DEPOSITIONAL ENVIRONMENTS
Massive
Massive
Cryptic?
Cryptic?
8
3A
3A
3A
3A
1
7
Channel
Unconformity
Shallow Marine, Offshore
6

Figure 3.9: Representative lithologs and gamma ray logs for both occurrences of Facies Association 7 – Shallow Marine. See Appendix 2 for legend of symbols.

3.3 Stratigraphy

Three stratigraphic cross sections utilizing gamma ray logs in conjunction with cored intervals were constructed in order to delineate the stratal relationships between the aforementioned facies associations over the Hibernia area (Figure 3.10).

A-A' and B-B' (Figures 3.11 and 3.12, respectively) illustrate the distribution of the lower reservoir sandstone (i.e. Facies Association 3). All three cross sections illustrate the relationships within the upper reservoir interval (FA 4, 5 and 6); however, cross section C-C' (Figure 3.13)

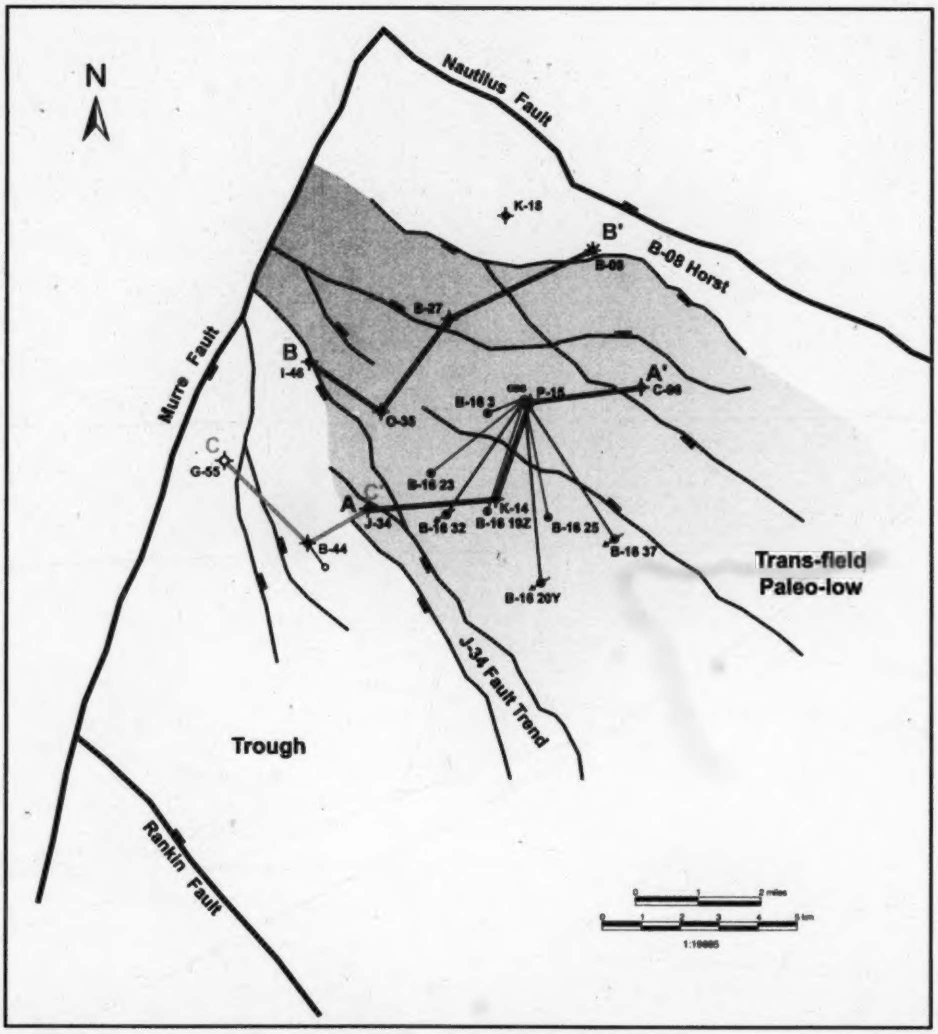
N
Nautilus Fault
K-18
B'
B-08
B-08 Horst
B-27
Murre Fault
B
I-46
O-35
A'
C-96
P-15
B-16 3
C
G-55
B-16 23
A
C'
J-34
B-16 32
B-16 19Z
K-14
B-16 25
B-16 37
B-44
B-16 20Y
Trans-field
Paleo-low
J-34 Fault Trend
Trough
Rankin Fault
0
1
2 miles
0
1
2
3
4
5 km
1:19985

Figure 3.10: Location map showing the lines of cross section for Figures 3.11, 3.12 and 3.13.

approximates depositional strike while A-A' and B-B' run approximately parallel to depositional dip. Note that the position of faults are indicated (displacements approximately 10 m and greater); however, only displacements of major faults that influence correlation of the "A" Marker carbonate unit are taken into consideration. Also note that inter-well spacing is constant and B-44 is of a different vertical scale because it is a deviated well.

Three depositional packages and three marker horizons are delineated on each cross section. Depositional Package A contains FA7 and older Avalon sediments (not represented in core) and is defined by the "A" Marker and the Avalon Unconformity. Depositional Package B contains FA1, FA2, and FA3 and is defined by the Avalon Unconformity and a transgressive surface of erosion (TSE). Depositional Package C, which contains FA4, FA5, FA6 and FA7, overlies the transgressive surface of erosion.

Cross Sections A-A' and B-B' (Figures 3.11 and 3.12)

Cross section A-A' runs SW-NE and contains J-34, K-14, P15 and C-96. Cross section B-B' also runs SW-NE, but is located closer to the Murre Fault. It consists of I-46, O-35, B-27, K-18 and B-08. The datum used in both cross sections is the transgressive surface of erosion. This surface is sometimes demarcated by a *Glossifungites* surface (e.g. Hibernia K-14), but is everywhere overlain by conglomeratic lag of Facies 14B and shallow marine deposits of FA7. Other marker horizons visible include the carbonate unit known as the "A" Marker and the Avalon Unconformity (a.k.a. Mid-Aptian Unconformity). In both cross sections, Depositional Package A gets increasingly thicker toward the SW. Depositional Package B displays axial thickening at K-14 and O-35. Within Depositional Package B, FA3 is absent in the C-96 well on A-A' and in the K-18 and B-08 wells on B-B'. FA2 is also absent in the B-08 well on B-B'. Depositional Package C gets increasingly thicker toward the SW in both cross sections. Within this interval, it is apparent that mud-dominated FA6 dominates in the NE while sand-dominated FA4/FA5 persists toward the SW. Also, FA4 is greater in abundance in B-B' than in A-A'. The number and extent of FA6 interbeds is highly interpretive due to the lack of core coverage. However, their existence is supported through comparison of the well log signature between cored and uncored intervals.

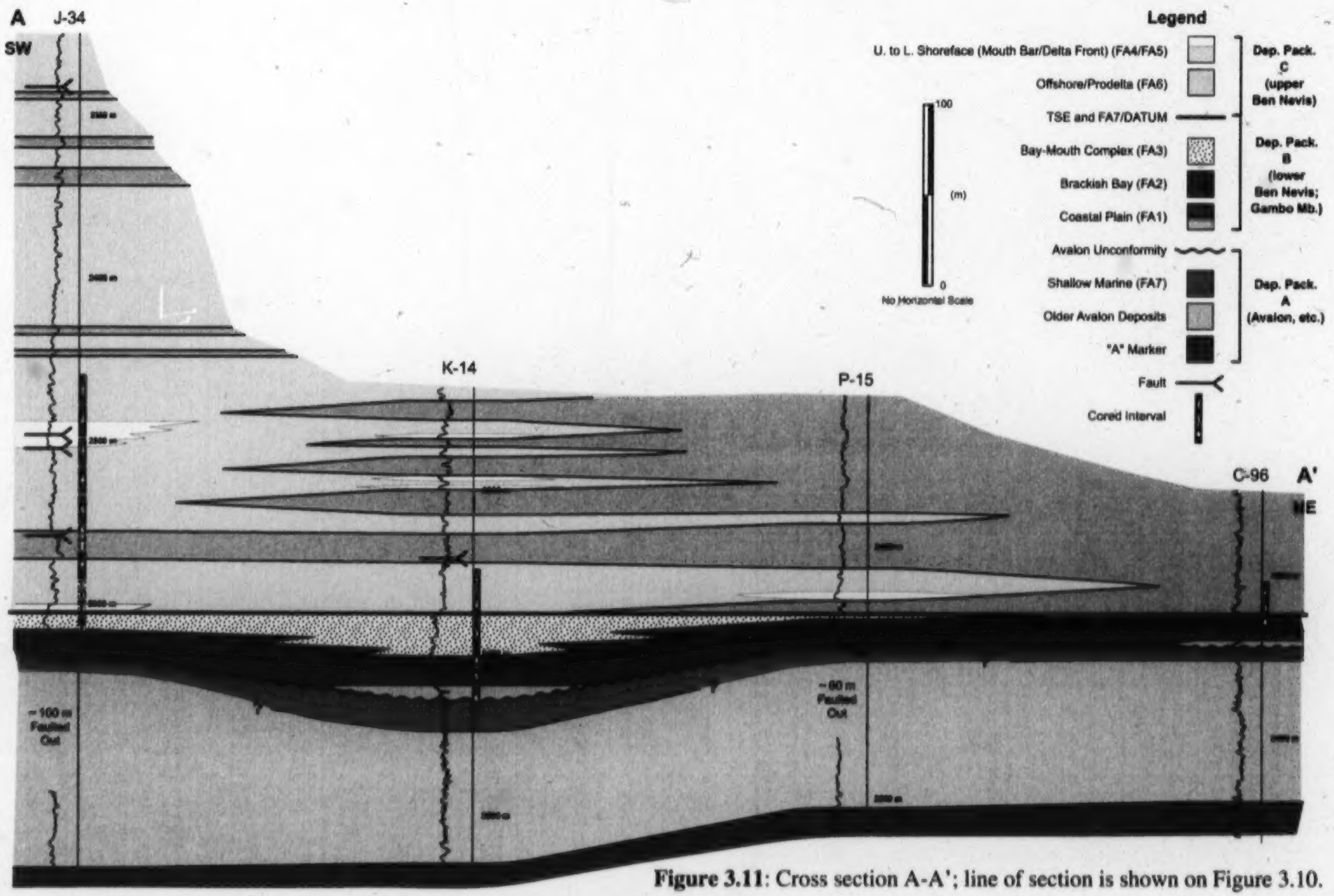
A
SW
J-34
K-14
P-15
C-96
A'
NE
Legend
U. to L. Shoreface (Mouth Bar/Delta Front) (FA4/FA5)
Offshore/Prodelta (FA6)
TSE and FA7/DATUM
Bay-Mouth Complex (FA3)
Brackish Bay (FA2)
Coastal Plain (FA1)
Avalon Unconformity
Shallow Marine (FA7)
Older Avalon Deposits
"A" Marker
Fault
Cored Interval
Dep. Pack. C (upper Ben Nevis)
Dep. Pack. B (lower Ben Nevis; Gambo Mb.)
Dep. Pack. A (Avalon, etc.)
100
(m)
0
No Horizontal Scale
~100 m Faulted Out
~60 m Faulted Out

Figure 3.11: Cross section A-A'; line of section is shown on Figure 3.10.

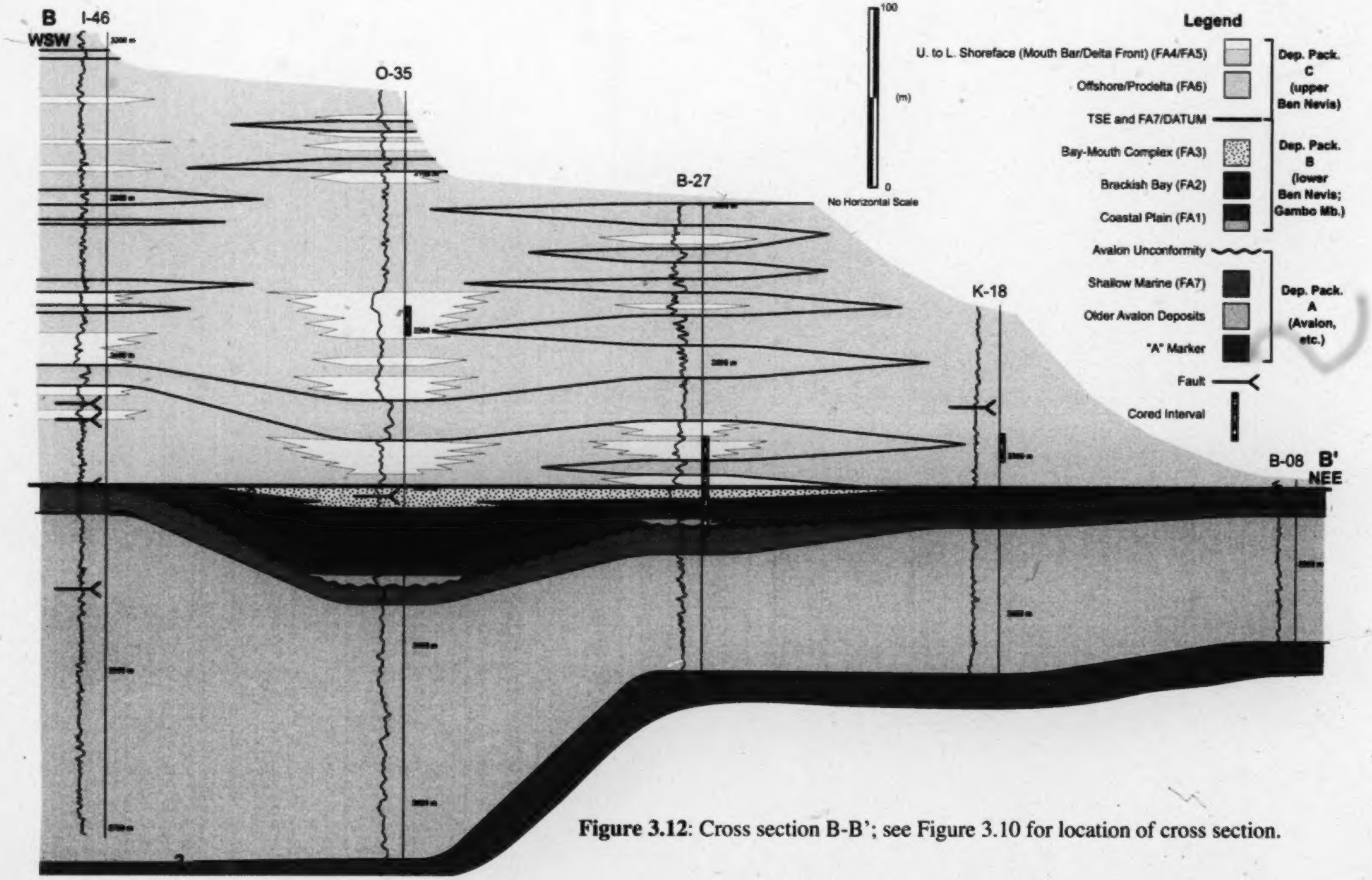
B
WSW
I-46
O-35
B-27
K-18
B-08
B'
NEE
100
(m)
0
No Horizontal Scale
Legend
U. to L. Shoreface (Mouth Bar/Delta Front) (FA4/FA5)
Offshore/Prodelta (FA6)
Dep. Pack. C (upper Ben Nevis)
TSE and FA7/DATUM
Bay-Mouth Complex (FA3)
Brackish Bay (FA2)
Coastal Plain (FA1)
Dep. Pack. B (lower Ben Nevis; Gambo Mb.)
Avalon Unconformity
Shallow Marine (FA7)
Older Avalon Deposits
"A" Marker
Dep. Pack. A (Avalon, etc.)
Fault
Cored Interval

Figure 3.12: Cross section B-B'; see Figure 3.10 for location of cross section.

Cross Section C-C' (Figure 3.13)

Cross section C-C' is oriented roughly W-E; it includes the G-55, B-44 and J-34 wells. The datum used in this cross section is a major flooding surface located at the base of a rather thick interval of FA6. A portion of the prograding sedimentary wedge located at the Hibernia G-55 well is indicated and placed within Depositional Package B. Note that Depositional Package C onlaps this wedge to the west and the topographic high located near the J-34 well to the east. In this cross section, FA 2 and 3 of Depositional Package B are absent in B-44 and G-55 and the transgressive surface of erosion lies directly above an interpreted soil horizon in B-44. Depositional Package C is thickest at Hibernia B-44 and also exhibits a highly interfingering pattern expressed as FA6 interbedded within FA4/FA5. The more continuous layers of FA6 demarcate at least three hierarchies of depositional cycles within Depositional Package C (described as major, medium and minor in C-C', Figure 3.13). The smallest or minor cycle is on the order of 10s of meters, the medium cycle averages 100 m in thickness and the major cycle can get up to 400 m in thickness. Two large-scale cycles are divided by a rather thick interval of FA6 that extends across the entire Hibernia Field. Sand-dominated FA4 is also more common in the west than in the east. As in A-A' and B-B', the extent and abundance of FA6 interbeds is highly interpretive due to the lack of core control.

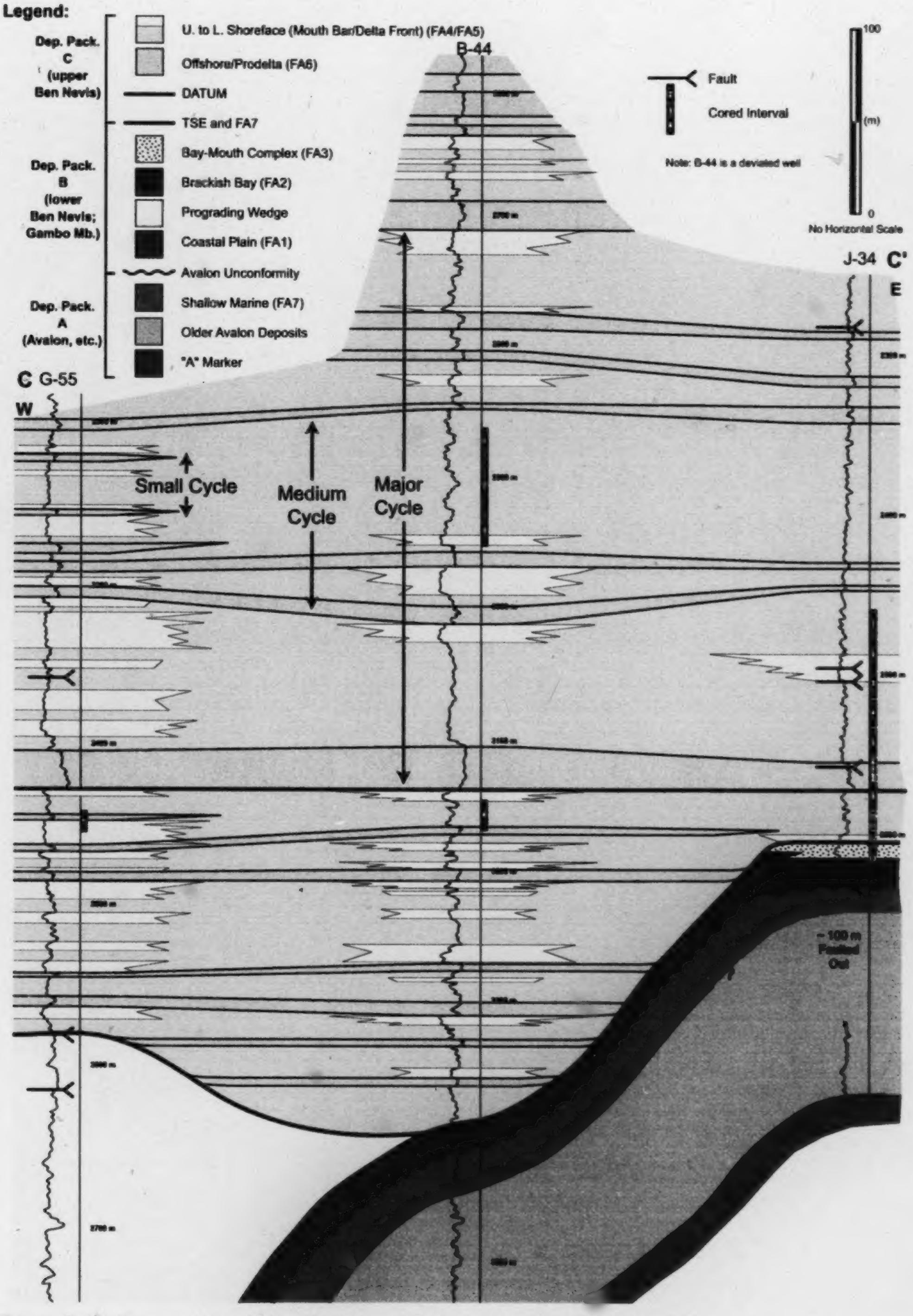
Legend:
Dep. Pack. C (upper Ben Nevis)
U. to L. Shoreface (Mouth Bar/Delta Front) (FA4/FA5)
Offshore/Prodelta (FA6)
DATUM
TSE and FA7
Dep. Pack. B (lower Ben Nevis; Gambo Mb.)
Bay-Mouth Complex (FA3)
Brackish Bay (FA2)
Prograding Wedge
Coastal Plain (FA1)
Avalon Unconformity
Dep. Pack. A (Avalon, etc.)
Shallow Marine (FA7)
Older Avalon Deposits
"A" Marker
Fault
Cored Interval
Note: B-44 is a deviated well
100
(m)
0
No Horizontal Scale
B-44
C G-55
W
J-34 C'
E
Small Cycle
Medium Cycle
Major Cycle
~100 m Faulted Out

Figure 3.13: Cross section C-C'; see Figure 3.10 for location of cross section.

3.4 Paleogeography and Depositional History

The paleogeographic record and depositional history of the Avalon/Ben Nevis interval can be divided into 5 stages. Stages 2 and 4 represent periods of depositional hiatus (i.e. unconformity and TSE). Stages 1, 3 and 5 represent three different depositional systems. The paleogeography and corresponding history of deposition for each stage is described below, starting with the oldest. A paleogeographic map, with a corresponding diagrammatic cross-section, is provided for each stage (Figures 3.14 to 3.18). Stratigraphic relationships reveal that deposition is linked to the tectonic setting, thus the history is described in terms of ambient environmental and tectonic conditions.

Stage 1 – Shallow Marine

Depositional Package A, which consists of a thick succession of FA7 and older deposits down to the "A" Marker carbonate horizon, represents Stage 1. This package is equivalent to the Avalon Formation, for which the upper limit is the Avalon Unconformity. FA7, where cored, is indicative of an offshore marine setting intermittently modified by storms. In gamma ray well logs, this succession appears to be ubiquitous across the Hibernia Field; it corresponds to extension-related subsidence and successive sea level highstand occurring regionally across the basin (Figure 3.14). Carbonate of the "A" Marker and mudstones of the Avalon represent relatively high sea level and inundation of the Hibernia area. Elsewhere in the basin, a shoreface proper is developed at this level, indicating normal regressive conditions. Considering that FA7 is overlain by an unconformity, it is likely that shoreface conditions may have developed in the Hibernia area but were then subaerially exposed and eroded. Although the thickness of FA7 varies over the Hibernia area, Depositional Package A as a whole slightly increases in thickness toward the W and SW (from 100 m in NE to 200+ m in the W-SW) indicating that the Rankin and Murre faults were active at this time. Increased rates of accommodation along the Murre and Rankin Faults, resulting from counterclockwise rotation of the hanging wall, would allow a thicker package of sediment to accumulate. The topography of the rollover structure during Stage 3 would be quite subdued as there is no indication of fault activity within the Hibernia area at this time. Although movement along the Nautilus Fault would also have been initiated at this time, the Hibernia area remained open to the influence of waves and storms tracking southward from the north.

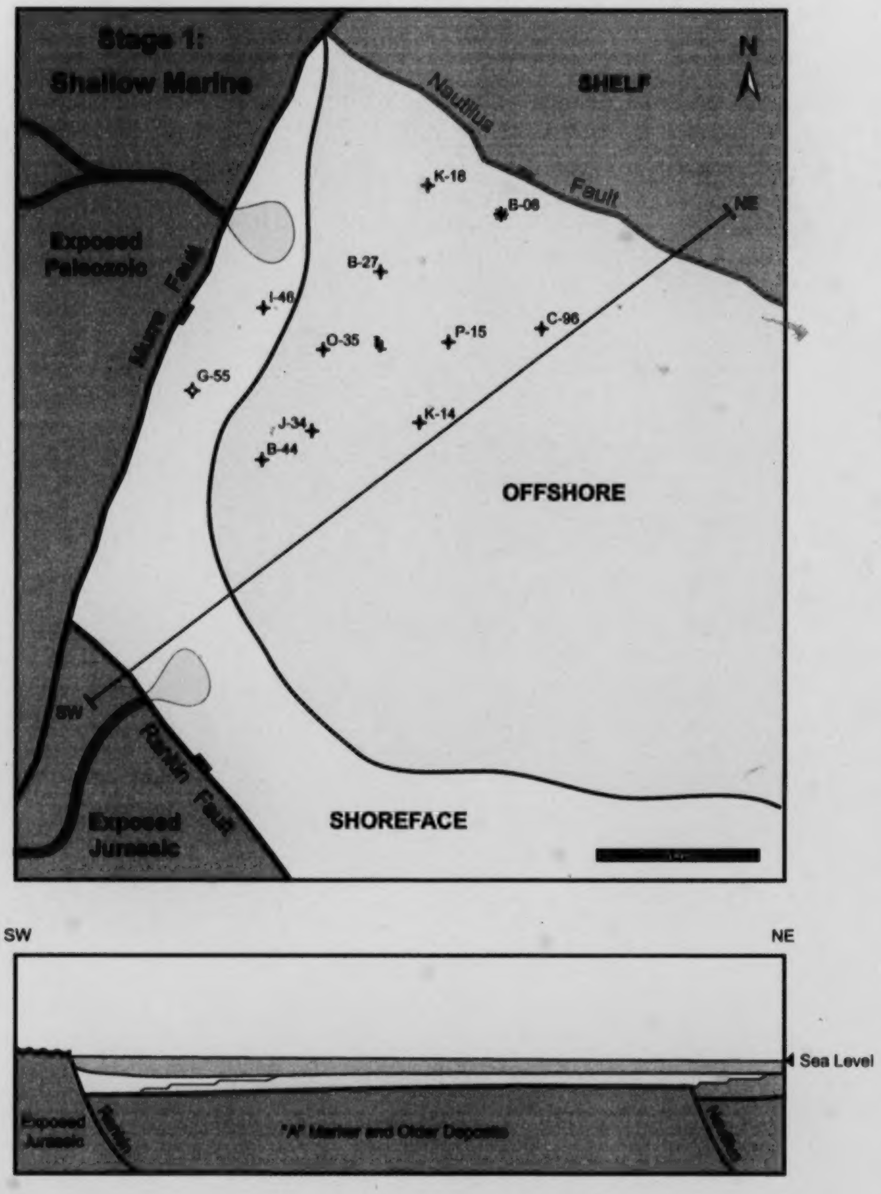
Stage 1:
Shallow Marine
SHELF
N
Nautilus Fault
Exposed Paleozoic
Murre Fault
K-18
B-08
B-27
I-46
O-35
P-15
C-96
NE
G-55
J-34
B-44
K-14
OFFSHORE
SW
Rankin Fault
Exposed Jurassic
SHOREFACE
SW
NE
Sea Level
Exposed Jurassic
Rankin
"A" Marker and Older Deposits
Nautilus

Figure 3.14: Paleogeographic map for Stage 1 - Shallow Marine. The Hibernia area is inundated and deposition is dominated by offshore sediments. Any terrigenous influx (i.e. delta systems) and shoreface zones, are subdued and restricted to areas immediately adjacent to Murre and/or Rankin faults. In cross section, the sedimentary package shows slight thickening toward the southwest as a result of limited hanging wall rotation into the Rankin Fault. Facies tracts will more than likely exhibit progradational stacking patterns.

Stage 2 – Unconformity and Coastal Plain

Stage 2 represents the initiation of the final episode of rifting in the basin. As a result of rifting, basin margins, including the entire Hibernia area, are uplifted and eroded; the Hibernia area becomes a zone of sediment bypass, as recorded by the erosion and subaerial exposure of the Avalon Formation (Figure 3.15). Any lowstand deposits would be located north and east of the Hibernia Field. Multicolored mudstones of FA1, which lie directly over the marine mudstones of the Avalon, are representative of subaerial alteration and soil development; as such, they indicate the development of widespread arid coastal plain conditions over the Hibernia area. Sandstones of FA1 likely represent remnants of the sediment bypass channels, which eventually become exposed and subaerially altered themselves. The thickness of FA1 is fairly consistent over the Hibernia Field except in the vicinity of K-14, B-27 and O-35 where a slight thickening is noted. This indicates that the trans-field faults were possibly activated at this time, allowing thicker channel and soil/coastal plain deposits to accumulate, and therefore be preserved, in subtle paleo-lows. This subaerial event is interpreted as the Avalon or Mid-Aptian Unconformity, reported to represent regional uplift associated with the final episode of rifting in the Jeanne d'Arc Basin (Sinclair, 1993). Although this unconformity is poorly constrained by biostratigraphic data, it appears to be well placed in terms of the juxtaposed facies and their subaerial exposure characteristics.

Stage 3 – Prograding Wedge and Estuary

Stage 3 demarcates the division of the Hibernia area into two tectonically derived depocenters because the Jeanne d'Arc Basin would have experienced considerably increased levels of tectonic activity as the rifted continental margins eventually began to pull apart (Figure 3.16). As such, all major faults in the basin would have likely been reactivated. NW-SE trending listric faults, such as the Rankin and Nautilus, are of no exception. In the Hibernia area, development of the rollover anticline structure is at a climax in Stage 3. The Nautilus and Rankin faults demarcate an approximately 20 km long half-graben structure of which counterclockwise rotation into the Rankin produces relative uplift in proximity to the Nautilus Fault and relative subsidence adjacent to the Rankin Fault. A thick sedimentary package is deposited in the newly forming trough along the Rankin and Murre faults. This wedge of sediment is visible in seismic sections that transect the Hibernia Field in a SW-NE direction (see Figure 1.7). It appears as a prograding wedge of coarse

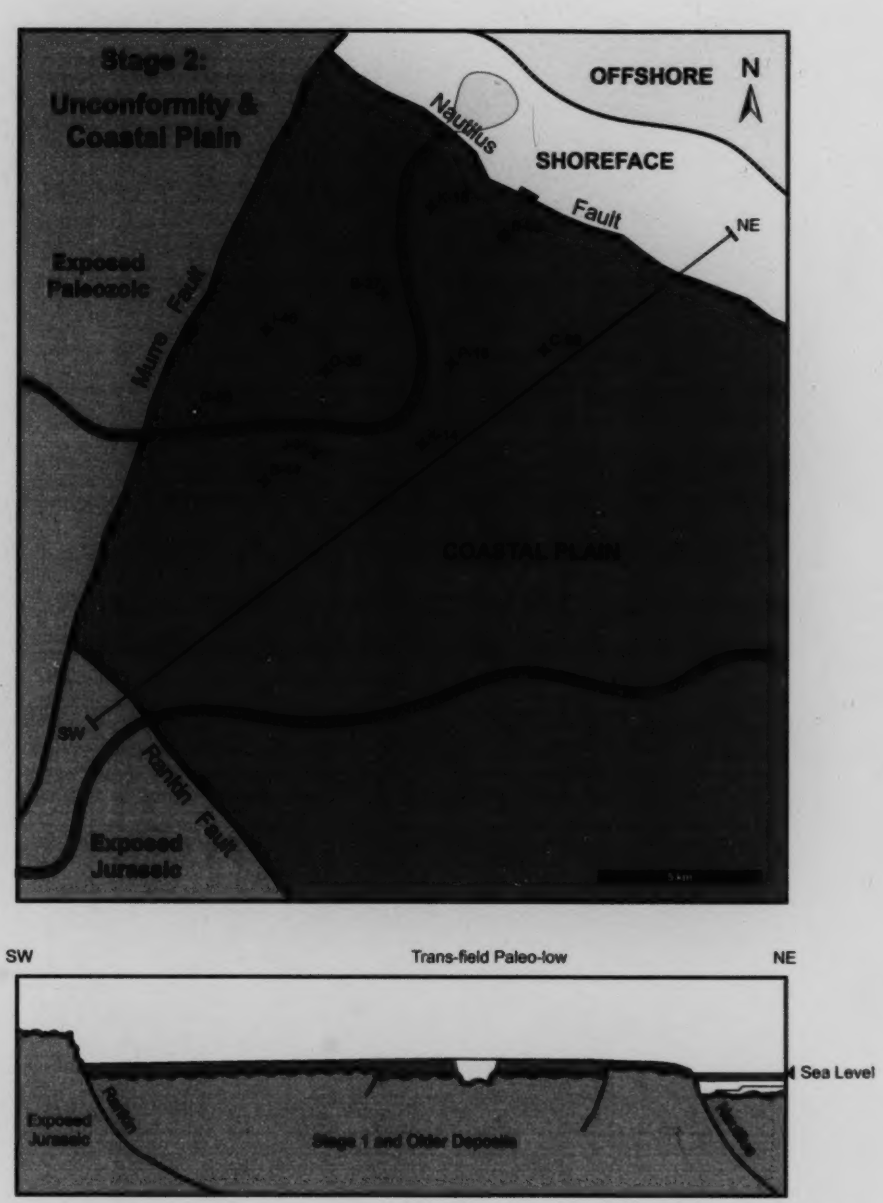
Stage 2:
Unconformity &
Coastal Plain
OFFSHORE
N
Nautilus
SHOREFACE
Fault
NE
Exposed
Paleozoic
Murre Fault
COASTAL PLAIN
SW
Rankin Fault
Exposed
Jurassic
SW
Trans-field Paleo-low
NE
Sea Level
Exposed
Jurassic
Rankin
Stage 1 and Older Deposits
Nautilus

Figure 3.15: Paleogeographic map for Stage 2 - Unconformity and Coastal Plain. In response to renewed rifting, the Hibernia area is exposed and Stage 1 and older deposits of the Avalon Formation are uplifted and eroded creating the Avalon Unconformity (red squiggly line). A widespread, arid coastal plain with soil development and limited channel incision is established in the Hibernia area. Thus, it becomes a zone of sediment bypass and deltaic/shoreface deposits are relocated basinward (i.e. to the east/northeast/north).

sandstones and conglomerates (or series of progradational wedges) that are represented in Facies Association 0 of Core #2 of the Hibernia G-55 well. This sedimentary wedge overlies coal and red mudstones (that are likely associated with the Avalon Unconformity) and is interpreted as bayhead deltas or fan deltas shed from the uplifted basin margins to the west and south (Hurley *et al.*, 1992 and Driscoll *et al.*, 1995). As indicated by its facies characteristics, these sediments would have been fed into a standing body of water that was brackish in nature. Considering that the Hibernia area proper was relatively uplifted at this time, the area adjacent to the Rankin Fault would have experienced reduced circulation and little marine influence. The resulting body of water would resemble a bay or embayment.

While sediments filled the accommodation space represented as troughs along the Murre and Rankin faults, the Hibernia area was sediment starved and subject to very low rates of accommodation space creation. The thickest accumulations of FA2 and FA3, which are deemed representative of Stage 3 in the Hibernia area proper, are found in the paleo-low that is defined by the J-34 fault trend to the south and the B-08 horst along the Rankin Fault to the north. This paleo-valley was created in conjunction with the development of the rollover anticline structure and is host to a micro- to mesotidal estuarine system that reflects the initial transgression of the Hibernia area. Deposits within this paleo-valley are relatively thin, reflecting the reduced amount of accommodation space available in the Hibernia area proper at this time. The cored intervals over the Hibernia Field only record the preservation of the outer estuary subenvironments (i.e. FA2 and FA3). Core is conspicuously lacking in the inner estuary zone, which is located adjacent to the Murre Fault. The mouth of the valley is plugged by sand bars/shoals/channels of FA3. Erosion of coastal headlands (i.e. exposed Avalon and older sediments) and along-shore transport from the north develop a barrier island across the mouth of the valley, which is located near K-14. The thickest accumulations of FA3 are found in the vicinity of the K-14 well. The thickest accumulations of FA2 occur at O-35; these deposits represent interfingering back barrier subenvironments that accumulated behind the barrier. Thus, seaward is to the southeast and landward is to the northwest.

Stage 4 – Transgressive Surface of Erosion and Shallow Marine

Stage 4 represents a landward shift of facies across an erosive surface that can be easily correlated over the entire Hibernia Field. Underlying sediments of Stage 3, which represent

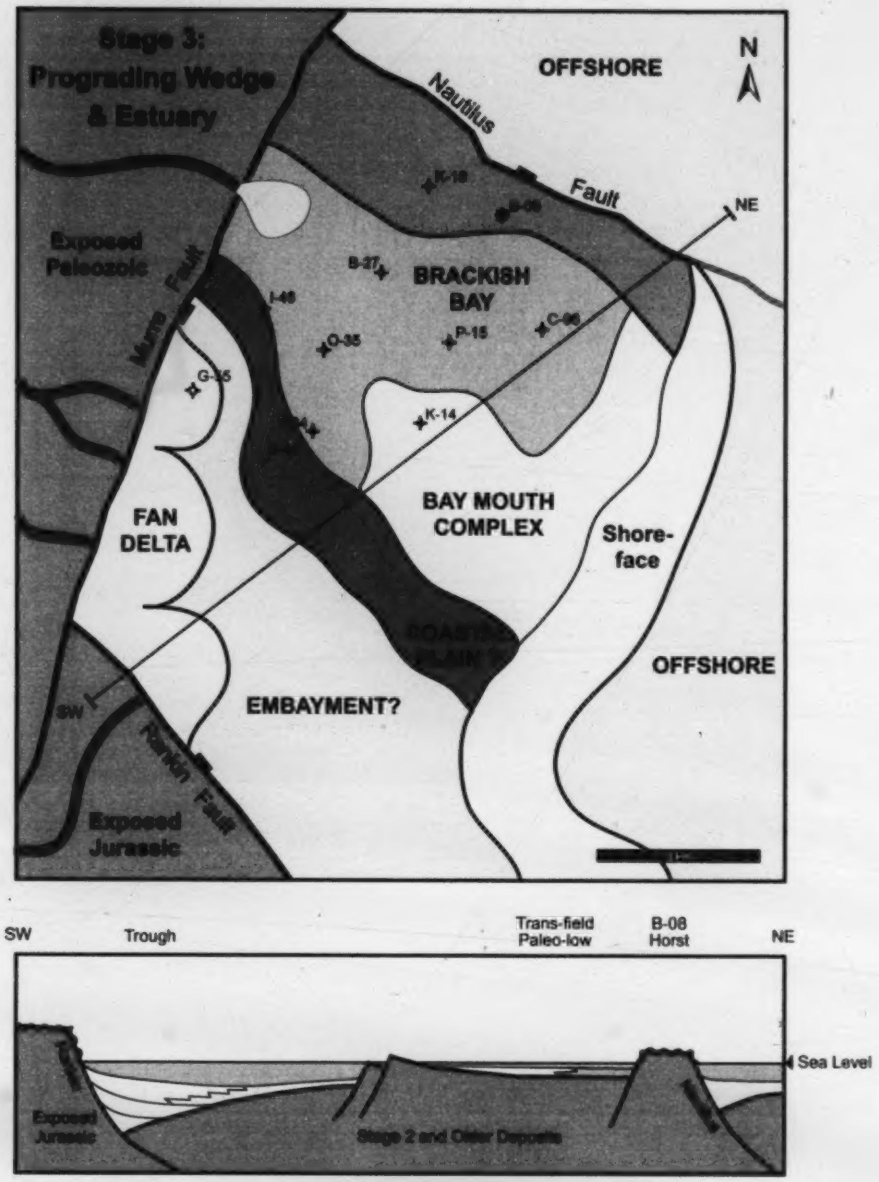
Stage 3:
Prograding Wedge
& Estuary
OFFSHORE
N
Nautilus
Fault
K-18
B-08
NE
Exposed
Paleozoic
Murre Fault
B-27
BRACKISH
BAY
I-46
O-35
P-15
C-96
G-55
K-14
FAN
DELTA
BAY MOUTH
COMPLEX
Shore-
face
COASTAL
PLAIN ?
OFFSHORE
EMBAYMENT?
SW
Rankin Fault
Exposed
Jurassic
SW
Trough
Trans-field
Paleo-low
B-08
Horst
NE
Sea Level
Exposed
Jurassic
Stage 2 and Older Deposits

Figure 3.16: Paleogeographic map for Stage 3 - Prograding Wedge and Estuary. Due to rifting, most basin faults, including the Rankin, Murre and Nautilus faults are reactivated. Subsequent to rifting, during extension, the Rankin and Nautilus faults become major growth faults. Collapse of the hanging wall block into the listric faults creates great accommodation space. A prograding wedge of fan delta or bayhead delta deposits are found in the trough adjacent to the Rankin and Murre faults, which is likely host to restricted marine conditions (i.e. embayment). The Hibernia Field is still relatively uplifted, and thus experiences reduced sedimentation rates and accommodation. The paleo-low confined to the axial high, contains a thin sedimentary package of micro- to mesotidal estuarine deposits reflecting initial transgression in the Hibernia area.

marginal marine deposits of an estuary, are sharply overlain by a bioturbated conglomeratic deposit (Facies 14B); the intervening surface is thus interpreted as a transgressive surface of erosion. Deposits of F14B are interpreted as a transgressive lag that developed in the shallow marine realm, thereby indicating that the Hibernia area was once again inundated (Figure 3.17). A comparatively thin veneer of FA7 bioturbated mudstone immediately overlies this lag. At this time, subsidence rates in the Hibernia area are jump-started, resulting in a relatively abrupt deepening of the depositional system. The presence of a *Glossifungites* surface at this level demonstrates a hiatus between erosion of the surface and deposition of the coarse lag material. As such, erosion likely took place in the high energy upper shoreface realm as wave ravinement processes worked to cannibalize the shoreface and sandstones of the barrier island. Only sandstones deposited behind the barrier in the lagoon are well preserved (i.e. FA3). Colonization of this erosional surface took place either during or shortly after erosional excavation. The emplacement of coarse material took place in a more basinward setting and was facilitated by storms, debris flows or sediment gravity flows induced by erosive shoreface retreat (MacEachern *et al.*, 1992).

The presence of a *Glossifungites* surface at the upper contact of FA7 corresponds to "catch-up" or stillstand conditions. In a sense, deposition over the Hibernia area enters a period of inactivity. For the duration of FA7, sediments are in short supply and bioturbators are free to bioturbate to great intensity. As such, the upper surface at least represents a major marine flooding surface and possibly a maximum marine flooding surface. Cross-laminated sandstones of Facies 9 sharply overlie bioturbated muddy, silty to sandy deposits of Facies 3A or 6A. Erosional exhumation at this level is linked to migration of distributary channels across the shelf.

Stage 5 – Delta within an Embayment

This stage comprises Depositional Package C, which is equal to the Ben Nevis Formation. As illustrated in the cross sections, this package reveals an interfingering relationship between deltaically influenced upper shoreface, lower shoreface and offshore deposits or distributary mouth bar, delta front and prodelta sediments of a deltaic system (Figure 3.18). On cross sections A-A' and B-B', deltaic sediments onlap the TSE toward the north in the Hibernia area. In C-C' and on seismic sections (see Enachescu, 1987; Driscoll *et al.*, 1995; Sinclair *et al.*, 1999) seismic reflectors within this interval onlap the G-55 prograding wedge, the Hibernia axial structure, the

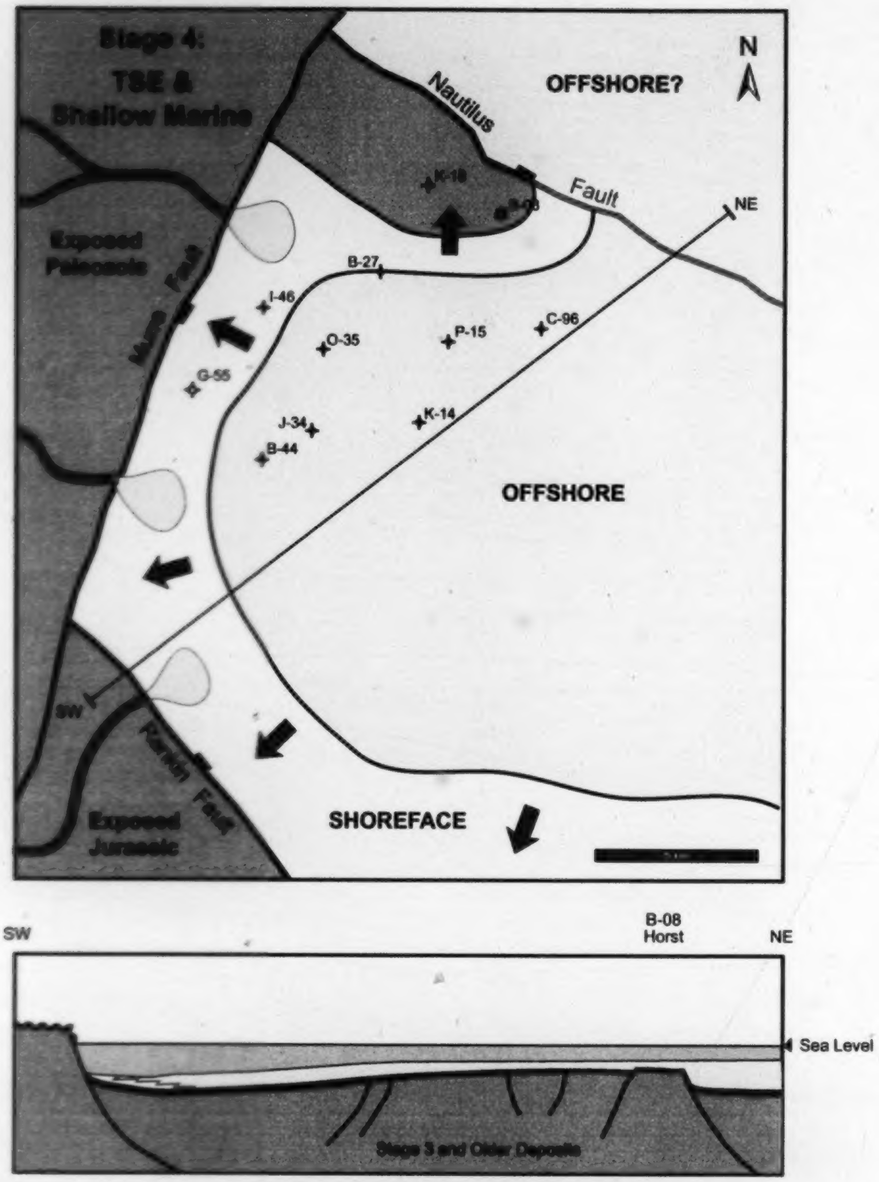
Stage 4:
TSE &
Shallow Marine
N
OFFSHORE?
Nautilus
Fault
K-18
B-08
NE
Exposed
Paleozoic
Murre Fault
B-27
I-46
O-35
P-15
C-96
G-55
J-34
K-14
B-44
OFFSHORE
SW
Rankin
Fault
Exposed
Jurassic
SHOREFACE
SW
B-08
Horst
NE
Sea Level
Stage 3 and Older Deposits

Figure 3.17: Paleogeographic map for Stage 4 - TSE and Shallow Marine. The axial high in the Hibernia area is transgressed and wave ravinement processes in the shoreface zone rework older sediments of the estuarine system into a transgressive lag (blue line), which is immediately followed by shallow marine lower shoreface and offshore sediments. Facies tracts most likely exhibit a retrogradational stacking pattern and onlap the Murre Fault, Rankin Fault and B-08 horst. Offshore sediments predominate in the Hibernia area, but the sedimentary package is very thin due to low sediment influx and reduced accommodation. Any deltaic or shoreface systems are restricted to the zone along the Murre and Rankin faults.

Murre faulted margin to the west and the Rankin faulted margin to the southeast. Thus, the thickest accumulation of sediment (not necessarily the sandiest) at this time is located west and southwest of the Hibernia J-34 well (the thickness of Depositional Package C is nearly doubled in B-44). The onlap patterns observed reflect the filling of this accommodation space in response to increased rates of subsidence. The rate of accommodation space creation eventually outpaces sediment supply, as sediments of the Ben Nevis Formation laterally and vertically shale out into shelf mudstones of the Nautilus Formation.

As observed in cross section, the smallest depositional cycles represent parasequences developed in response to autocyclic fluctuations, such as distributary channel migration and delta lobe abandonment. The larger scale cycles correspond to relative sea-level changes induced by residual tectonic activity. The majority of these cycles display cleaning upward or coarsening patterns on gamma ray logs; this is typical of deltaic successions (Coleman, 1981). The predominance of delta front and distributary mouth bar sands in B-44 and G-55, versus prodelta sediments in K-18, C-96 and B-08, suggests that sediments were shed from the Bonavista Platform to the west and/or uplifted Jurassic highlands to the south. Lack of well control in areas adjacent to the Murre and Rankin faults (i.e. southwest of B-44) precludes identification of the more landward deposits of the upper delta plain.

This delta is probably fluvial-dominated and confined within an embayment, as indicated by the presence of relatively thick and rare distributary mouth bar deposits interspersed amongst delta front and prodelta sediments. The mouth bars do not appear to be redistributed by either wave or tidal activity (as evidenced by their sedimentary characteristics). Thus, with additional well control, these sands may be proven to exhibit linear trends. In addition, delta front sediments are highly to intensely bioturbated. Influx of freshwater, and the environmental havoc it wreaks upon its entrance into a marginal marine or marine body of water, is restricted to the immediate area around a distributary in fluvial dominated deltas (subaqueous levees keep flow confined). In the Ben Nevis, interdistributary areas show relatively little indication of freshwater influx and are essentially protected from the influence of deltaic sedimentation (i.e. these areas are bypassed: Coleman, 1981). This is also supported by minimal evidence of physical modification and development of a variable ichnological signature in lower shoreface, delta front or shallow embayment sediments. However, prodelta or offshore sediments show greater evidence of freshwater influx; this is related

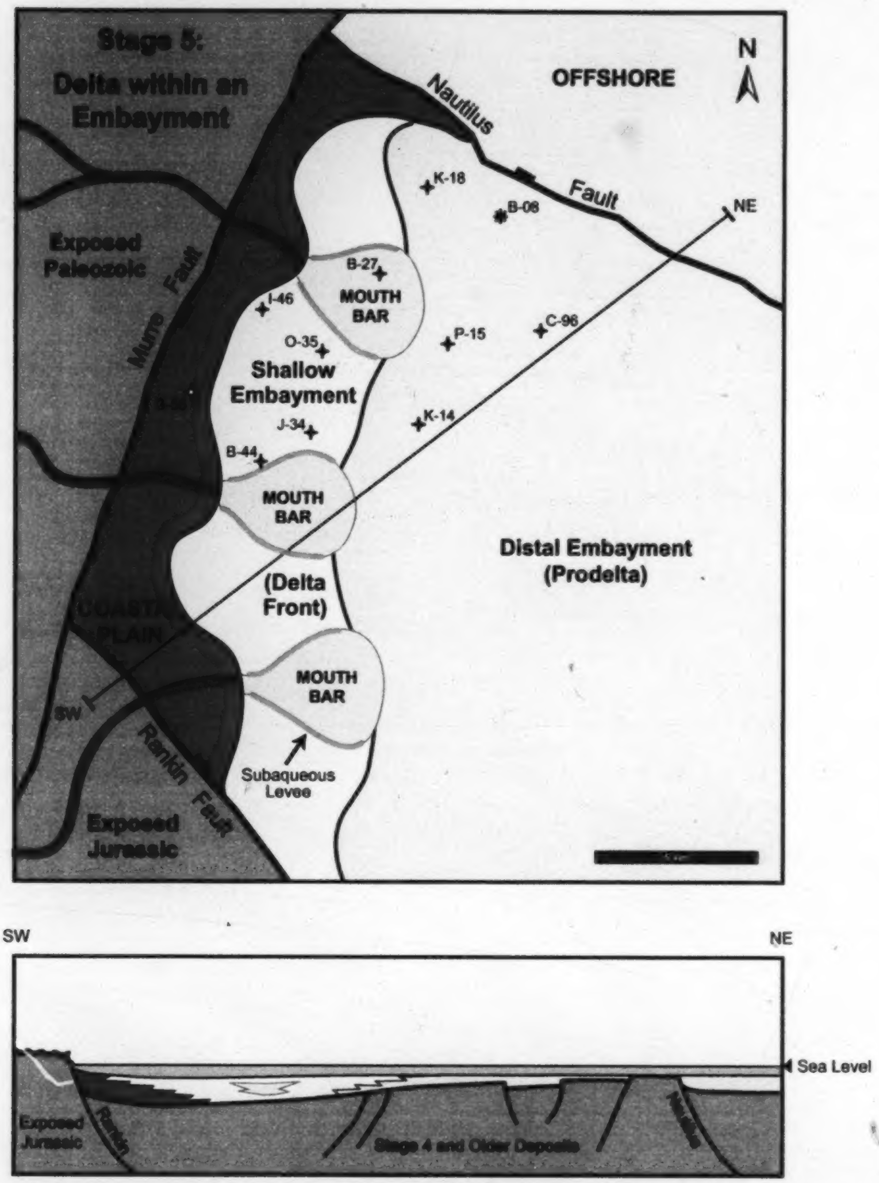
Stage 5:
Delta within an Embayment
N
OFFSHORE
Nautilus Fault
K-18
B-08
NE
Exposed Paleozoic
Murre Fault
B-27
MOUTH BAR
I-46
O-35
P-15
C-96
Shallow Embayment
J-34
K-14
B-44
MOUTH BAR
Distal Embayment (Prodelta)
(Delta Front)
COASTAL PLAIN
MOUTH BAR
SW
Rankin Fault
Subaqueous Levee
Exposed Jurassic
SW
NE
Sea Level
Exposed Jurassic
Rankin
Stage 4 and Older Deposits
Nautilus

Figure 3.18: Paleogeographic map for Stage 5 - Delta within an Embayment. Although fault activity lessens and regional/thermal subsidence sets in, highlands to the west and/or southwest continued to supply sediment to the Hibernia area. The remaining accommodation space is filled with a lens of sediment representing a deltaically influenced shoreface. The system is river-dominated, possibly due to restriction of the area from the full effect of storms tracking south by the topographically high Nautilus Fault zone. Thus, distributary mouth bar sediments are not redistributed by waves (or tides for that matter) and occur encased within delta front deposits. In the cross section, deltaic sediments onlap the Murre Fault to the west, the Rankin Fault to the southwest and the axial high to the north.

to unconfined flow past the distal margins of the distributary channel into the prodelta setting (Wright, 1978). The influence of freshwater influx in the prodelta is marked by the presence of syneresis cracks, abundant siderite cementation, a stressed ichnological signature, load casts and soft sediment deformation, and sand lenses that remain largely unbioturbated and retain their physical structures. In addition, the degree of storm influence is much less in Depositional Package C as compared to Depositional Package A. This is likely a reflection of restriction induced by highlands located in the vicinity of the Nautilus Fault. Although there is no evidence to suggest that these highlands were emergent, they at least played a major role is restricting water circulation into the Hibernia area.

This deltaic system is interpreted to occur during overall transgressive conditions, especially since the Ben Nevis Formation eventually "shales out" into the overlying Nautilus Formation. From cross sections and seismic lines, it is clear that Depositional Package C onlaps land in at least three directions. Also, stratal relationships in a SW direction illustrate a retrogradational stacking pattern of cycles denoted by minor flooding surfaces corresponding to FA6 over FA4 or FA5. The extent and distribution of the delta (or deltas) are been strongly influenced by preexisting topography, especially since the thickest delta front and distributary mouth bar sands are located south of the J-34 fault trend.

3.5 Summary

The variety in the configuration and distribution of depositional packages, in conjunction with the great variety of depositional environments, clearly indicates that the Hibernia area was tectonically active for the duration of Barremian to Aptian deposition. In comparison with other areas of the basin (Sinclair, 1995a), this activity appears to be characteristic of the Hibernia area alone. Thus, understanding the progression of tectonic events and the corresponding changes in basin configuration over this timeframe is key to understanding the distribution of facies and therefore reservoir units. In addition, tectonism in the Hibernia area at this time is integral in deciphering the history of relative sea level fluctuation; as such, it may prove quite difficult to attempt a sequence stratigraphic interpretation as related to global sea level changes. It may also prove to be very difficult to correlate from the Hibernia Field into other adjacent areas and tie its history into the rest of the basin.

Chapter 4

Bioturbate Textures

4.1 Introduction

Many intervals within the Avalon and Ben Nevis are characterized by high to intense bioturbation. These intervals may contain one or several ichnogenera and bioturbation intensity is always such that most or all original physical sedimentary structures are obliterated. This type of ichnologic signature is here defined as a bioturbate texture. In the absence of physical sedimentary structures, it is simply not sufficient to just recognize that the deposit is bioturbated; especially since these highly bioturbated rocks are attributable to a wide range of environmental settings, from brackish bay to tidal channel/shoal complex to delta front to offshore.

This chapter re-examines basic ichnological terminology and the history of the bioturbate texture in order to emphasize its value in trace fossil and facies analysis. It also proposes that the description of a bioturbate texture, especially as an integral part of a facies analysis, should simply reflect its characteristic *texture elements* and *fabric*. These objectives are achieved using examples from the Avalon/Ben Nevis interval.

4.2 Bioturbate Texture: Definition and Usage

The definition, usage and concept of the term "bioturbate texture" has a long and confusing history. According to Schäfer (1972), it was Rudolf Richter (1952) who first introduced the term. He used it to describe mechanical deformations of the sediment; "zooturbate" and "phytoturbate" referred to disruption by animals and plants, respectively. Bioturbate textures were originally intended to include surface and internal traces and the perturbations of the sediment due to burrowing. He used the term "burrowing texture" (sometimes reported as "burrowing fabric") to describe simple deformation of laminae due to locomotion or complete destruction of laminae due to repeated burrowing by either dwelling-producing or sediment-eating organism. Seilacher (1964) introduced the term "biodeformational structures" to describe ill-defined, poorly preserved or obscurely exposed biogenic structures in core, which appear as interruptions or deformations of the original bedding. Frey (1971; 1973) suggested that this term was unnecessary and that the same idea can be expressed in the concepts bioturbate texture and burrow mottle. He redefined "bioturbate texture" as the "gross texture imparted to sediment by extensive bioturbation; consists of dense, contorted, or interpenetrating burrows or other traces, few of which are distinct morphologically" and "burrow mottled" as sediment in which "burrows are somewhat less crowded and are thus more distinct individually". Both definitions were proposed to reflect the most common usages of the terms at the time. However, Frey and Pemberton (1991) suggested that, in historical perspective, these definitions should not be considered definitive, and that usage of "bioturbate texture" should be used for any rock displaying intense bioturbation in any way, shape or form. As such, burrow mottling is a type of bioturbate texture strictly referring to unrecognizable dense, interpenetrating burrows. In 1983, Ekdale and Bromley proposed the term "ichnofabric" for "those aspects of the texture and internal structure of the bed resulting from all phases of bioturbation". In light of the mix-mash of historically established and re-interpreted terms discussed above, many ichnologists deem this newest term a synonym of bioturbate texture (e.g. Frey and Pemberton, 1990; 1991).

A re-examination of all terms pertinent to the process of bioturbation, the degrees of bioturbation and the products of bioturbation is presented in Figure 4.1, which follows logic and the most common or modern usage of each term. The "thought path" presented in Figure 4.1 reveals that "bioturbate texture" is the most appropriate term for use toward the description of a highly bioturbated interval - an honor well deserved considering its thankless and frustrating history. Here, bioturbate texture is defined as an interval characterized by a high to intense degree of bioturbation, and consequently rare to no preservation of physical sedimentary structures, that consists of distinct trace fossils and/or indiscrete burrow mottling. Therefore, the term bioturbate texture should be used to refer to bioturbated intervals that exhibit intense to complete bioturbation (i.e. 90–100% bioturbation (Reineck, 1963) or ichnofabric indices (ii) 5 to 6 of Droser and Bottjer (1986) or bioturbation indices (BI) 5 to 6 of Taylor and Goldring (1993)).

The most practical use of "bioturbate texture" is as a descriptive term applied to any volume of sedimentary rock in which all or most physical sedimentary structures are obliterated as a direct result of intense to complete bioturbation. Cryptic bioturbation is the only known exception to this rule. In this special case, a rock or sedimentary package can be 100% bioturbated and still retain all of its physically produced fabric. Cryptic bioturbation deals with microscopic organisms (meiofauna) that inhabit the interstitial spaces between grains and due to their comparable size with the grains, either do not dislodge the grains at all or only slightly (Howard and Frey, 1975;

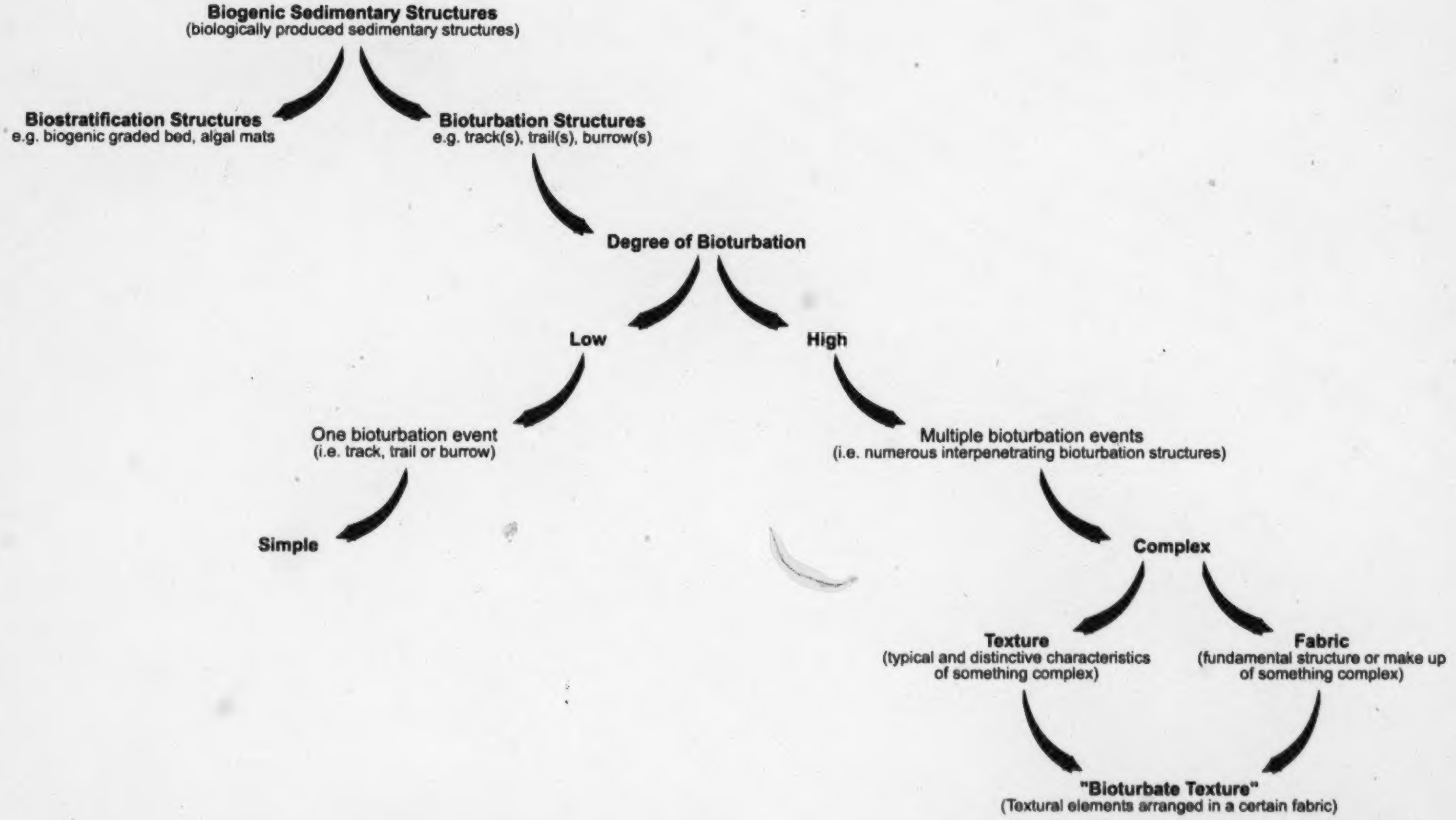
Biogenic Sedimentary Structures
(biologically produced sedimentary structures)
Biostratification Structures
e.g. biogenic graded bed, algal mats
Bioturbation Structures
e.g. track(s), trail(s), burrow(s)
Degree of Bioturbation
Low
High
One bioturbation event
(i.e. track, trail or burrow)
Multiple bioturbation events
(i.e. numerous interpenetrating bioturbation structures)
Simple
Complex
Texture
(typical and distinctive characteristics of something complex)
Fabric
(fundamental structure or make up of something complex)
"Bioturbate Texture"
(Textural elements arranged in a certain fabric)

Descriptive term said of a rock unit that is highly to intensely bioturbated (i.e. physically produced sedimentary structures are rare to absent) and contains distinct trace fossils and/or indistinct burrow mottling

Burrow mottling: Bioturbate texture in which individual trace fossils are apparent, but not sufficiently well-preserved to be identified

Figure 4.1: Review of terminology pertaining to the bioturbate texture concept. The terminology summarized here is synthesized from Frey (1973), Ekdale *et al.* (1984), Frey and Pemberton (1985), Pemberton (1992), Bromley (1996) and Pemberton *et al.* (2001b).

Pemberton *et al.*, 2001b). A bioturbate texture may consist of only one type of discrete trace fossil, two or more different types of discrete trace fossils, indiscrete burrow mottling or a combination of discrete trace fossils and indiscrete burrow mottling. Each texture is unique in that its general appearance is determined by its constituent trace fossils and/or biogenically modified sedimentary fabric (in the case of indiscrete burrow mottling). Thus, for ease in communication, a modifier should be assigned in naming the bioturbate texture, especially if several different textures are recognized within the sedimentary succession. The modifier can be non-specific (e.g. Bioturbate Texture A) or quantitative (e.g. Bioturbate Texture 1). However, descriptive adjectives are of the greatest merit (e.g. *Skolithos*-dominated Bioturbate Texture). As in facies delineation, the title alone should reveal something about the nature of the texture.

4.3 Bioturbate Textures in Trace Fossil and Facies Analyses

Trace fossil analysis can be conducted on a range of biogenic forms, from a single bioturbation event to complex, multiphase, interpenetrating bioturbation events. Bioturbate textures lie at the latter end of the spectrum. The most fundamental technique used in studying trace fossils of any intensity is simple detailed observation (Ekdale *et al.*, 1984). However, the very nature of a bioturbate texture dictates that it can potentially provide much more information than a single trace fossil occurrence. It may involve one or numerous ichnogenera, may reflect long residence times or opportunistic tendencies, may represent organisms employing the same behavior or a number of different behaviors, etc. Thus, its description is potentially much more involved than that of an isolated occurrence of one or a few trace fossils.

The quality and value of the description is dependent on the source of the data, just as the type of information gathered will vary between outcrop exposures and cored rock. In outcrop, one must be aware of alteration via weathering processes. In addition, preservation is commonly restricted to bedding plane views. However, outcrop is best for observing the entire morphology and extent of biogenic structures. In core, the observer is restricted to the vertical perspective. As such, vertical structures are acutely under represented. Core also represents a two-dimensional view in which the overall morphology may be difficult to ascertain. However, it provides a clean un-weathered surface and is best for observing forms in full relief, and especially their internal structure. Of the two types of material, core is the most amenable to examination of the bioturbate textures contained within it, despite the shortfalls and biases listed above. Bioturbate textures represent a very high degree of bioturbation; given a particular volume of rock, this is best observed and approximated from a vertical section. Clean, unweathered surfaces allow a clear view of the internal structures for identification purposes; complete biogenic forms are rarely preserved in bioturbate textures due to the high degree of reworking. Finally, the vertical continuity provided by core allows recognition of subtle trends and changes in bioturbate texture. This lends great insight into the ecological and depositional stress factors that may be present and the resulting succession of facies and environments.

The description of a sedimentary facies should be based on the total field aspect of the rock, including its lithological, physical, biological and chemical properties (Walker, 1992). Thus, biogenic structures, whether represented by just one trace fossil or a bioturbate texture, constitute only one component of a facies. However, if the facies is intensely to completely bioturbated, the facies description should rightfully focus on the nature of the bioturbate texture, which fundamentally contains *textural elements* displaying a certain *fabric*. *Textural elements* include the biogenic structures and the sediment in which they are emplaced. The relative abundance of each should also be addressed. How these elements are arranged or structured constitute the *fabric*. Its appearance varies accordingly with the type and relative abundance of the textural elements. The variety of bioturbate textures, and the information that can be garnered from them, is potentially limitless. It would be greatly beneficial to at least standardize how they are described, for either trace fossil or facies analysis. This is a timely endeavour, especially considering the ongoing ichnofacies-ichnofabric controversy (Ekdale *et al.*, 1991; Frey and Pemberton, 1990; 1991; Taylor *et al.*, 2003). The basic guidelines that can be used to describe a bioturbate texture are summarized below.

4.4 Textural Elements

Types of Sediment

Any facies description should begin with a description of the sediment types present within it; a facies exhibiting a bioturbate texture is of no exception. Because organisms often introduce material into the substrate (i.e. mucus, detritus, fecal pellets), it is important to document the different types of sediment that make up the bioturbate texture. From this record, inferences regarding the behavior of the organism may be made. Accessory components, such as shell fragments, mud clasts and pebbles should also be documented. Caution must be applied in this task, however. Considering the high degree of bioturbation, these components can be easily overlooked. In addition to a simple list of the sediment types present, the description should also include ratios of each sediment type to one another. Along these same lines, any trends in the types of sediment or their ratio to one another, in either a vertical or horizontal sense, should be noted. For example, in Facies 6, each subfacies is characterized by a slightly different ratio of mud and silt to sand. Upon closer examination of the bioturbate textures, it becomes apparent that this is directly related to the resident trace fossils (Figure 4.2).

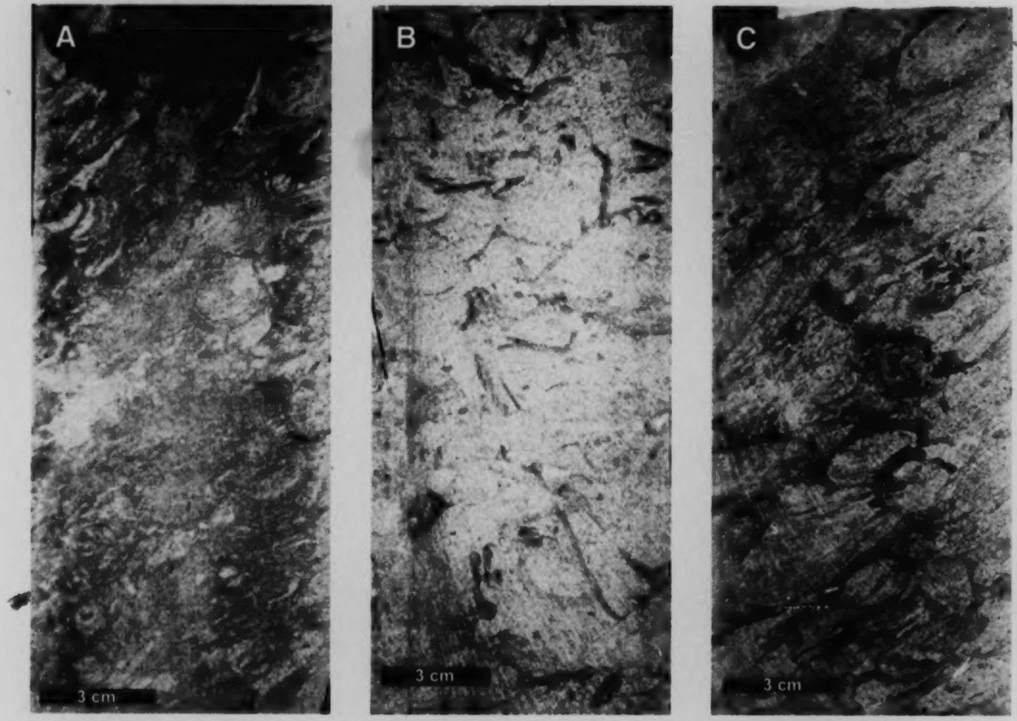

Figure 4.2: Characteristic appearance of the three subfacies of Facies 6, and consequently, the representative bioturbate textures. A) *Asterosoma*, *Scolicia* and *Teichichnus*-dominated bioturbate texture, B) *Phycosiphon* and *Pelosichnus*-dominated bioturbate texture and C) *Ophiomorpha* and *Thalassinoides*-dominated bioturbate texture. All three textures contain the same sediment types, but the ratio of one sediment type to another varies between textures based on the types of trace fossils and consequenly, the behaviors that they represent. In these photos, the darkest shapes represent mud while the lightest shades represent sand grains.

Types of Trace Fossils

The basic taxonomic information regarding the types of trace fossils present (i.e. a trace fossil assemblage) is integral in describing a bioturbate texture. The list should include both ichnogenera and ichnospecies, where possible (some forms may not be possible to formally name due to poor preservation or lack of identifying features). Remember to keep in mind the biases of the host material (e.g. in outcrop, obscurity by weathering; in core, may only see partial representation of a much larger burrow). This list provides the foundation for comparison purposes, whether it is to the archetypal ichnofacies, other textures in the succession or assemblages reported in other ichnological studies.

The relative abundance of each trace fossil in the texture is acquired through visual estimation of occurrence, not cross-sectional area or volume. Caution must be applied when dealing with branched structures such as *Chondrites* or *Phycosiphon* (each "patch", not each "branch" should be considered as one occurrence). Abundance is by no means an absolute account of trace fossil quantity, but rather an approximation of which trace fossil is relatively more or less abundant than another. Results are reported verbally on a scale of relatively less abundant to relatively more abundant (i.e. rare to few to moderate to common to abundant), or vice versa. Relative abundance is not the most accurately derived property, but is nevertheless useful (Bromley, 1996). If the textures occur repeatedly in the succession, abundance of a particular trace fossil may vary slightly from encounter to encounter. Thus, abundance should be averaged over the vertical or lateral extent of the texture. In Facies 6, relative abundance forms the basis for the delineation of three subfacies (Figure 4.3). For example, although *Ophiomorpha* is ubiquitous in F6, it occurs with the greatest frequency in intervals labeled as F6C. And within this subfacies, it just happens to be the most abundant relevant to all other traces.

4.5 Fabric

Arrangement of Sediment

Contrasting sediment types (whether is by grain size, composition, shape, etc.) is required to visualize any sedimentary structure, physical, chemical or biogenic. A sedimentary rock without contrasting sediment types appears massive or structureless, even if sedimentary structures may be present. Benthic and infaunal organisms manipulate the sediment in the production of a biogenic sedimentary structure. In many cases, they actually change the sediment from its original character (e.g. by introducing mud filtered from the water column or organics in the form of faeces). Thus, the distribution of the textural elements in relationship to trace fossil morphology and their interpreted

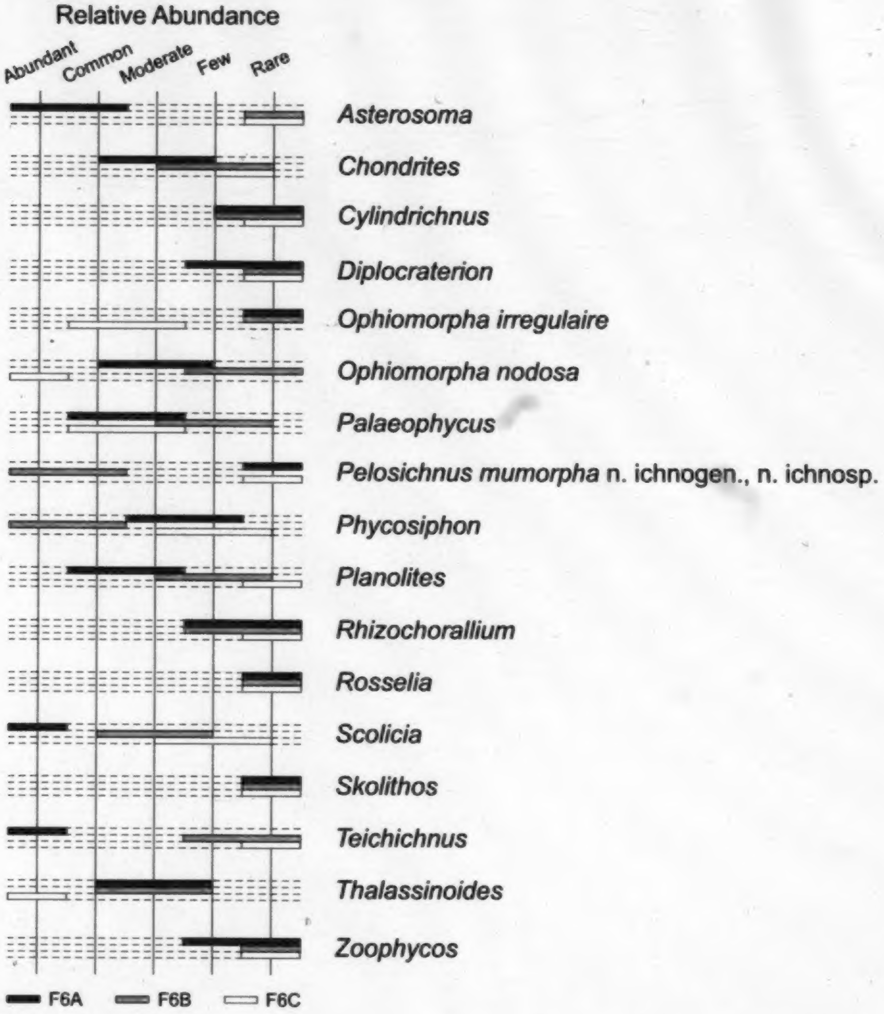

Figure 4.3: Summary of relative abundance for each ichnogenera within Facies 6 as divided into the representative subfacies. Although each texture exhibits an overall high diversity of trace fossils, they are dominated by only a certain few biogenic structures.

behavior can reveal something about the ecological or environmental parameters that influenced them to act that way. In addition to sediment types, the distribution of accessory components (such as intraclasts, macrofossils, cement, fecal pellets, etc.) in the context of the bioturbate texture can provide equally valuable information. For example, the affiliation of cement with a particular burrow type may indicate that early diagenetic processes were directly related to the burrowers and their burrows. The information gathered from biogenically produced textural heterogeneity might also be applied in the development of economically important deposits. Chapter 5 deals with the textural heterogeneity observed in Facies 6B and its direct influence on fluid flow pathways and hydrocarbon production.

Arrangement of Trace Fossils

Every bioturbate texture exhibits a characteristic fabric or pattern that is directly controlled by the type and abundance of its constituent trace fossils and their tiering structure. If the assemblage is dominated by one or few bioturbators behaving in a similar manner or contained within the same tier, the fabric should consist of one basic shape or morphology in a repetitive random or structured distribution. If the assemblage consists of a mixture of trace fossils representing variable behavioral strategies of numerous different tiers, the fabric will appear heterogeneous. For example, Facies 3A and 6A are dominated by the same middle tier, deposit-feeding traces (*Asterosoma, Teichichnus* and *Scolicia)* (Figure 4.4). However, they exhibit different fabrics due to the ethology and tiering

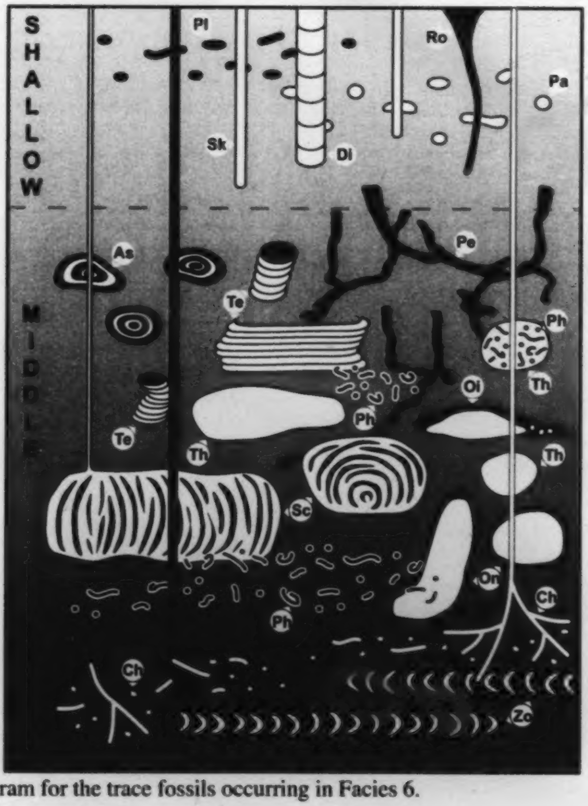

Figure 4.4: Tier diagram for the trace fossils occurring in Facies 6.

structure of other traces in the bioturbate texture. Facies 3A also contains abundant *Zoophycos*, a deep tier, horizontal, spreitenated deposit-feeding trace, while F6A also contains abundant *Thalassinoides* and *Ophiomorpha*, middle to deep tier, sand-filled, domicile tunnels. Deciphering the arrangement of traces within a bioturbate texture can supply detailed information regarding the ichnocoenoses, or benthic community, including the community structure and its response to changes in environmental conditions. As well, a detailed description of the fabric is perhaps of utmost importance when dealing with the part of the texture for which specific trace fossil names cannot be supplied or a texture solely consisting of indiscrete burrow mottling.

4.5 Summary

The amount and type of information that bioturbate textures have to offer is vast. The data actually collected is of course dependent on the capabilities, intentions and methodologies of the investigator. A bioturbate texture can provide specific information pertaining to the environment (e.g. sedimentation rates, salinity, oxygen levels, substrate consistency, energy levels, etc.), emphasize abstract or concealed surfaces, affect diagenetic processes, and influence fluid flow pathways, to name just a few examples. In sedimentary facies analysis, bioturbate textures are commonly ignored by physical sedimentologists, under-examined by ichnologists utilizing the ichnofacies analytical technique and over-scrutinized by proponents of the ichnofabric concept. This is understandable considering that the task of interpreting a bioturbate texture can be quite daunting, especially if the objective is to provide an environmental interpretation from facies analysis. As demonstrated in this chapter, perhaps the best solution is to focus the description of a bioturbate texture on its texture elements and fabric. This technique combines the best attributes of both trace fossil analytical techniques. It may also make it easier for sedimentologists to derive at least some basic information about the bioturbate texture, even if they only have a basic ichnology textbook at their disposal.

Chapter 5

Biogenic Textural Heterogeneity, Fluid Flow and Hydrocarbon Production

5.1 Introduction

This chapter focuses on the characterization of fluid flow through a bioturbated portion of the upper reservoir target within the Ben Nevis Formation. The interval chosen to accomplish this task is Facies 6B, a subfacies within the delta front sandstones of Facies Association 5 (see Figure 2.10). The data utilized in this chapter (thin sections, permeability, porosity, capillary pressure data) originates from the Hibernia J-34 cored interval, between 2498 and 2521 m core depth (see J-34 litholog in Appendix 2; Figure 5.1). Portions of this cored interval are totally occluded by calcite cement, rendering the core a bluish grey color (Figure 5.2). Facies 6B exhibits a very unusual bioturbate texture that is dominated by mud-filled burrows (identified as *Pelosichnus mumorpha* n. ichnogen., n. ichnosp.; see Appendix 1). Although these muddy burrows are predominant, four other trace fossils are common: *Phycosiphon, Thalassinoides, Planolites* and *Scolicia*. As such, the substrate can be divided into two textural categories, mud filled burrows and sandy framework, the latter of which includes the sandy fill of *Thalassinoides* and *Scolicia* and sandy halo surrounding patches of *Phycosiphon*.

The main goal of this chapter is to provide a better understanding of how burrows control effective permeability, which is dependent upon the nature of the reservoir and relative hydrocarbon saturation (Weber, 1986). In both cemented and uncemented intervals, textural properties of the muddy burrows versus the sandy framework are confirmed petrographically and described from hand sample, then compared and discussed in terms of plug and probe permeability data. Textural and reservoir engineering data are then inputted into MPath, numerical modeling software that uses a modified percolation-invasion technique to simulate secondary petroleum migration through bioturbated media (Carruthers, 2003).

5.2 Petrographic Characteristics

Overall, F6B consists of bioturbated, argillaceous, very fine-grained sandstone, in which the matrix (consisting of mud, miscellaneous organics, fecal pellets and siderite) varies from 10 to 40%. The greatest concentration of matrix material exists within burrows (Figure 5.3A), thus

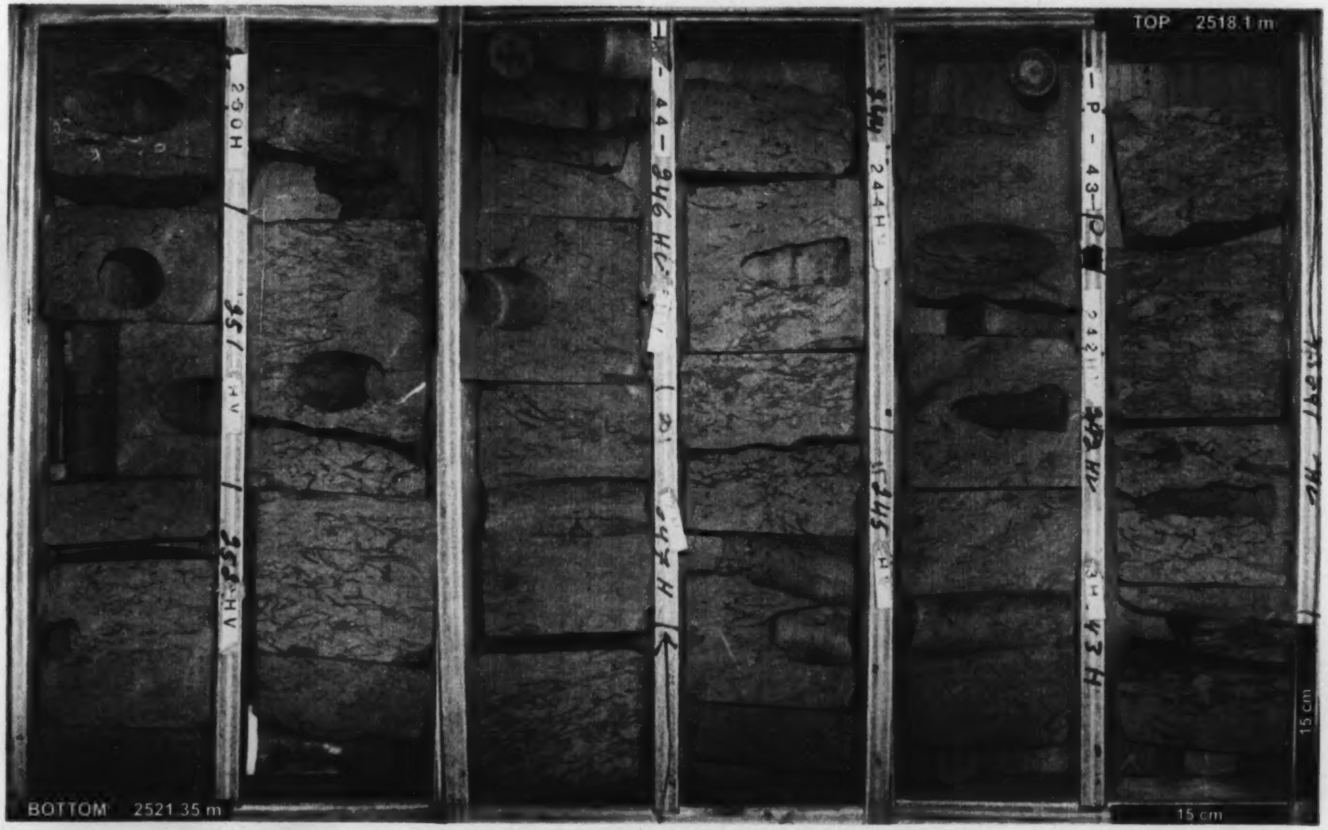
TOP 2518.1 m
BOTTOM 2521.35 m
15 cm
15 cm

Figure 5.1: Core 4, boxes 11, 10 and 9 from within Facies 6B. Core lies in succession (bottom up) from left to right. This portion of F6B is not calcite cemented; the brown coloration is a result of hydrocarbon staining. Dark grey heterogeneities are the mud-filled burrows, *Pelosichnus mumorpha* n. ichnogen., n. ichnosp.

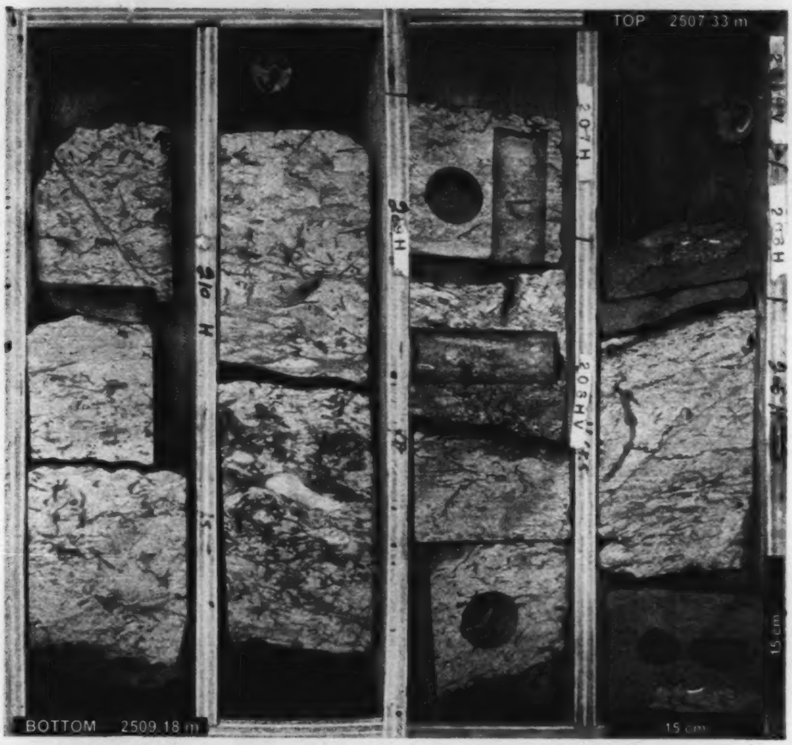

Figure 5.2: Core 3, boxes 18 and 17 from within Facies 6B. Core lies in succession (bottom up) from left to right. This portion of F6B is calcite cemented, as suggested by its light grey-bluish color. Note that some of the mud-filled burrows are stained red by siderite.

matrix content is directly controlled by burrow density. Quartz grains are predominant, although up to 5% of clasts are rock fragments, feldspar grains or bioclastic debris (Figure 5.3B). In certain horizons, sub-angular to sub-rounded pieces of pelecypod valves and calcareous worm tubes are particularly abundant (up to 15-20%). They can range from a few microns to several centimeters in width or diameter. Overall, grain size of quartz, feldspar and rock fragment clasts ranges from 40 to 260 μm (4.5ϕ to 2ϕ). However, approximately 75% of the grains are moderately well sorted within a size range of 85 to 125 μm (3.5ϕ to 3ϕ). Most grains are sub-angular to sub-rounded and randomly oriented (Figure 5.3C). Where present, calcite cement is texturally poikilotopic and confined to the sandy framework (Figure 5.3D). Individual crystals are irregularly shaped, with slightly curved to straight edges, and distributed in a mosaic pattern (Figure 5.3E). Most crystals are larger than the field of view under low power (i.e. greater than 7.5 mm in diameter). Siderite cement is also common. It occurs as interlocking mosaics of rhomb-like microcrystals interstitially between

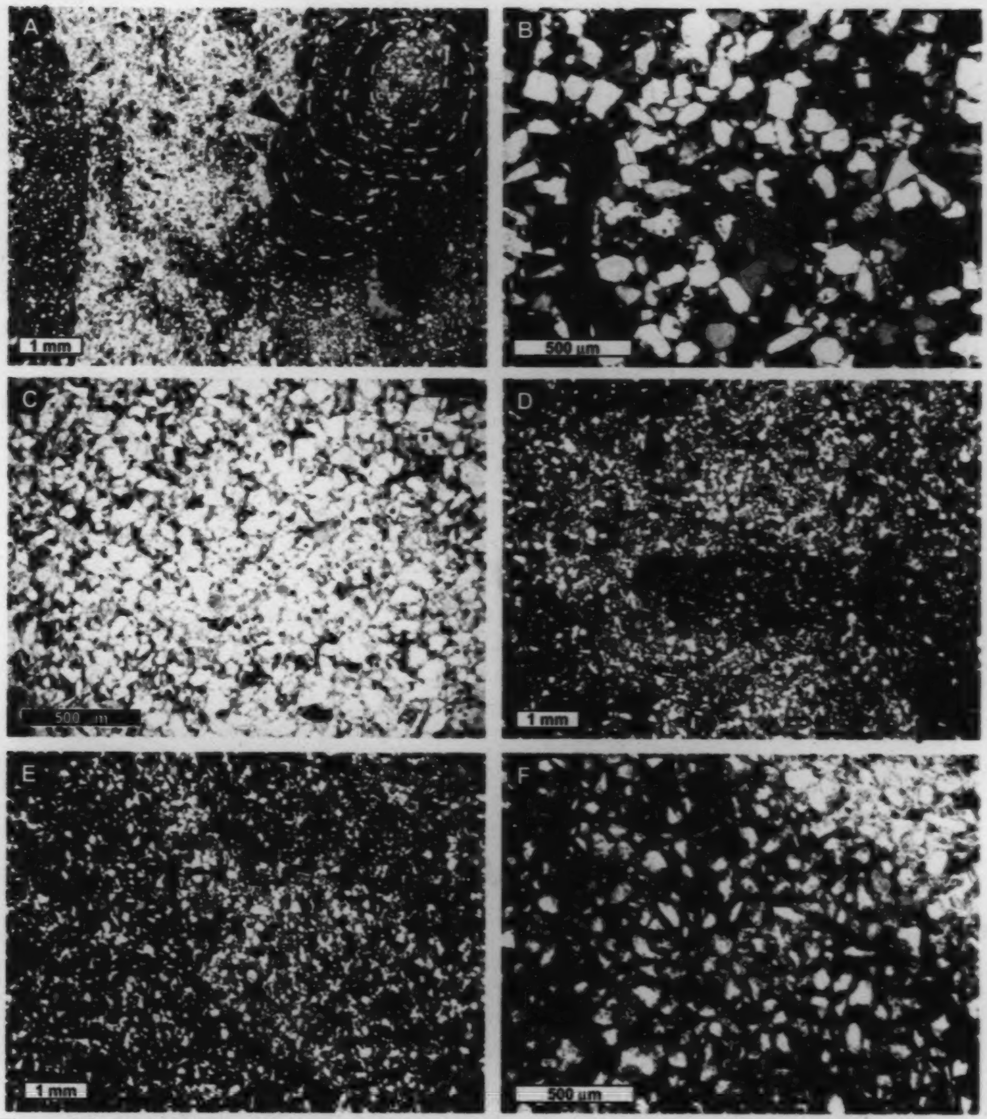

Figure 5.3: A) Matrix material is more concentrated within burrow structures. The area adjacent to the mud burrows (between red dashed lines) corresponds to the sandy framework. Concentric laminae and the sandy core of a mud burrow are also visible in this micrograph (yellow dashed lines). The blue arrows highlight fecal pellets. Normal light; blue corresponds to porosity. B) Rock fragment (red arrow), feldspar grain (yellow arrow) and pelecypod fragment (blue arrow). Crossed-polars. C) Grains are moderately well sorted; most fall within a size range of 85 to 125 µm (3.5ϕ to 3ϕ), are sub-angular to sub-rounded and are randomly oriented. Normal light; blue corresponds to porosity. D) Calcite cement occurs as large, poikilotopic crystals that are confined to the sandy framework (pale red under crossed-polars). Mud burrows are outlined in red dashed lines; these burrows contain a structureless fill with fecal pellets (blue arrows). E) Four calcite crystals in various states of extinction, with slightly curved contacts (outlined in red dashed lines), are visible in this micrograph. Crossed-polars. F) Siderite occurs as mosaic microcrystals interstitially between grains. It appears to replace matrix material, especially within *Pelosichnus* n. ichnogen. Normal light; blue corresponds to porosity.

grains (Figure 5.3F). Because it has an affinity for calcite cement and mud or organic material within burrows, it is likely representative of matrix replacement. Primary physical structures such as remnant low angle planar lamination are very rare to absent, and as such, are not considered to play a major role in textural characterization. Following the scheme of Dott (1964), this sandstone is classified as an argillaceous sandstone or quartz wacke.

Porosity ranges from 3 to 26% and averages 15%, as measured during routine core plug analysis. Detailed review of the values indicates that porosity drops only slightly in cemented intervals. In uncemented intervals, porosity is mainly primary intergranular, and rarely moldic (Figure 5.4A). All porosity in cemented intervals is secondary. The most common types are vuggy and moldic; intercrystalline porosity is very rare (Figure 5.4B). Variation in porosity between sandy framework and muddy burrows could not be accurately determined by point-count due to plucking of mud during polishing. However in largely unaffected thin sections, porosity within muddy burrows is observed to be relative less than in the framework (Figure 5.4C).

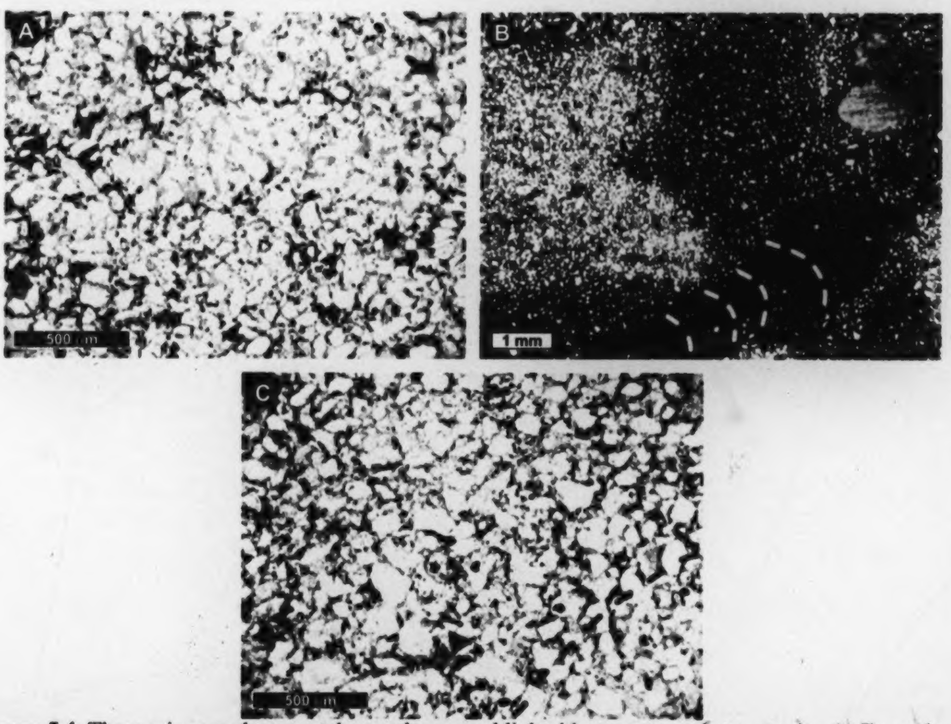

Figure 5.4: These micrographs were taken under normal light; blue corresponds to porosity. A) Example of primary intergranular porosity within the sandy framework. B) Moldic porosity developed within the calcite-cemented portion of the BT2 zone. Meniscate structures (yellow dashed lines) within a mud and pellet-filled burrow exhibiting a club-shaped termination are also visible in this micrograph. C) Note the change in intergranular porosity across the red dashed line, which highlights the edge of a mud-filled burrow.

5.3 Trace Fossil Characteristics

Together, *Thalassinoides*, *Scolicia*, areas containing *Phycosiphon* and burrow mottling make up the sandy framework (Figure 5.5A). *Thalassinoides* are horizontal to slightly inclined, sharp-walled, commonly lined with a thin (up to 1 mm thick) veneer of mud, and average 2 to 4 cm in diameter. *Planolites* average 3 to 6 mm in diameter and are typically contained within single or aggregated muddy burrows. *Phycosiphon* are mud-filled, dominantly horizontal to inclined, sometimes branched micro-burrows that average 1 mm in diameter. *Thalassinoides, Planolites* and areas containing *Phycosiphon* are relatively cleaner than regions of the sandy framework that exhibit burrow mottling (i.e. matrix content drops to 10-15%; Figure 5.5B). *Phycosiphon* are consistently surrounded by a halo of sand that is up to 5 mm thick and largely void of matrix material (Figure 5.5C). In *Scolicia* (horizontal to inclined structures that are 2–3 cm in diameter), matrix content increases to 20–25%. Matrix material occurs as thin (less than 2 mm) spreite or meniscate structures, commonly oriented parallel or tangentially to the base of *Scolicia* tunnels. Matrix material in areas of the sandy framework that are burrow mottled is well mixed and diffuse.

Unique mud-filled burrows classified as *Pelosichnus mumorpha* n. ichnogen., n. ichnosp. represent the muddy burrow textural category. The morphology of these burrows is thoroughly described in Appendix 1. The burrows create a locally dense, interpenetrating 3-D network, through which horizontal and vertical sections are practically identical (Figure 5.6). On average, these mud-filled burrows account for 40–45% of the core volume, as estimated from point counts on vertical and horizontal sections of slabbed core.

5.4 Plug and Probe Permeametry

Methodology and Results

A total of 152 core plug permeability measurements (in millidarcies (mD)) were recorded over the F6B interval as summarized from Corelabs (1982: Table 5.1). Gas flow through plug samples was measured using a conventional Hassler-sleeve permeameter (Corelabs, 1982). Resulting fluid velocities are considered to be in the purely viscous or Darcy flow regime. In uncemented intervals, horizontal permeability measurements (Plug_u-K_{hor}) range from 0.01 to 65.9 mD. The arithmetic mean is calculated as 6.76 mD. Vertical permeability measurements (Plug_u-K_{vert}) range from 0.04

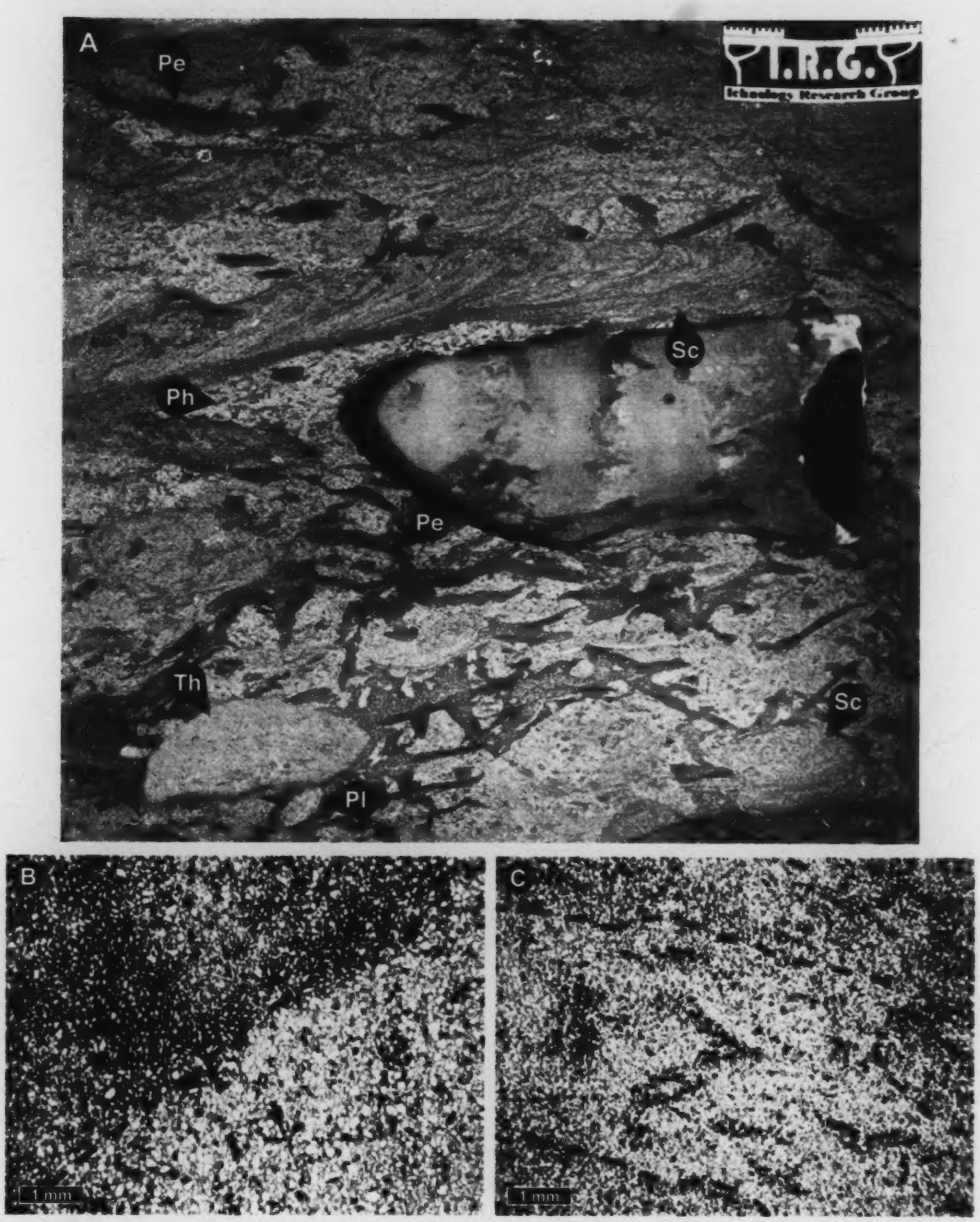
A
Pe
I.R.G.
Ichnology Research Group
Sc
Ph
Pe
Th
Sc
Pl
B
1 mm
C
1 mm

Figure 5.5: A) Characteristic trace fossils of Facies 6B: *Scolicia* (Sc), *Phycosiphon* (Ph), *Thalassinoides* (Th), *Pelosichnus* n. ichnogen. (Pe) and *Planolites* (Pl). B) Relatively clean fill of *Thalassinoides* compared to the sandy framework. Red dashed line denotes the boundary of *Thalassinoides*. C) Red dashed lines highlight the area containing *Phycosiphon*. These micro-burrows are surrounded by conjoined sandy halos that are relatively free of matrix material.

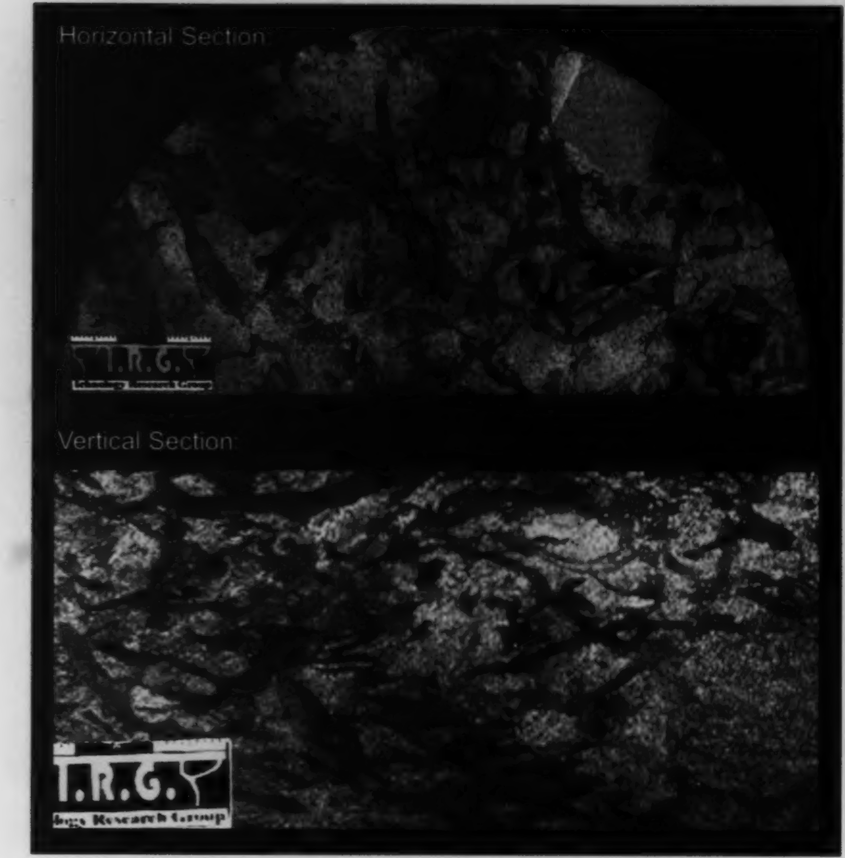

Figure 5.6: Comparison of horizontal and vertical cross-sections revealing similar configuration of the mud-filled burrow systems.

Table 5.1: Summary of arithmetic mean, minimum and maximum, plug and probe permeabilities. Values are reported in millidarcys (mD). "*n*" corresponds to the number of measurements utilized in this study. See text for explanation of permeability nomenclature.

	Plug$_u$-K$_{hor}$ (mD)	Plug$_u$-K$_{vert}$ (mD)	Plug$_c$-K$_{hor}$ (mD)	Plug$_c$-K$_{vert}$ (mD)	Probe-K$_{us}$ (mD)	Probe-K$_m$ (mD)	Probe-K$_{cs}$ (mD)
Mean*	**6.76**	**1.82**	**0.59**	**0.21**	**7.87**	**2.55**	**0.18**
Min	0.01	0.04	0.001	0.01	1.39	0.712	0.0826
Max	65.9	20.8	1.94	0.41	73.5	7.18	0.548
n	86	41	18	7	54	83	20

*Arithmetic Mean

to 20.8 mD and average 1.82 mD. In cemented intervals, horizontal permeability measurements (Plug$_c$-K$_{hor}$) range from 0.001 to 1.94 mD; the mean is 0.59 mD. Vertical permeability measurements (Plug$_c$-K$_{vert}$) range from 0.01 to 0.41 mD and average 0.21 mD.

Probe permeability measurements were collected using a frame-mounted PDPK-400 Pressure-decay Profile Permeameter by the author in the summer of 2002. With this instrumentation, a known volume of nitrogen gas is injected into the sample and the rate of pressure decay (between two predetermined pressures) is recorded over time, yielding a flow rate from which liquid permeability values corrected for gas slippage and Non-Darcian flow effects are derived (CoreLabs, 1996). A standard rubber O-ring probe tip seal (2-202) was utilized. This tip has an inner diameter of 3.1 mm and an outer diameter of 5.99 mm. Five slabbed core intervals 15 cm in diameter (three uncemented, one cemented and one half and half) formed the sample basis. The slabs ranged in length from 7.3 to 17.1 cm and were selected as representative of the entire F6B interval. On each slab, approximately 20-50 sites were chosen for testing (Figure 5.7). The sites were divided into four categories, uncemented and cemented sandy framework versus uncemented and cemented muddy burrows. A total of 157 probe permeability measurements were collected (Table 5.1; Figure 5.8). The exact location of each measurement was made possible using laser-sighting, thus allowing for repeat analyses. Each site was tested three times to ascertain the accuracy and precision of the equipment and testing method. Non-repeatable values of error ranges greater than 0.3-0.5 mD were disregarded and the remaining values averaged. Disregarded values represent erroneous measurements that record mechanical failure or slippage of the probe tip off of the target site. Uncemented sandy framework permeability values (Probe-K$_{us}$) range from 1.39 to 73.5 mD; the arithmetic mean is calculated as 7.87 mD. Measurements from muddy burrows in uncemented and cemented intervals overlap, thus further distinction between the two categories is not required. Muddy burrow permeability values (Probe-K$_{m}$) range from 0.712 to 7.18 mD and average 2.55 mD. Cemented sandy framework permeability values (Probe-K$_{cs}$) range from 0.0826 to 0.548 mD, with an arithmetic mean of 0.18 mD.

Interpretation

Plug Permeability Measurements in Uncemented Intervals

Several key observations can be made in regard to the plug permeability values. Within uncemented intervals, both horizontal and vertical plug permeability data are exceedingly heterogeneous likely due to variable silt/mud content as determined by mud burrow density. However, the average vertical permeability is considerably lower than the average horizontal permeability, likely reflecting horizontally oriented micro-barriers such as grains and matrix material aligned perpendicular to the direction of compaction, mud meniscae arranged parallel to the bottom of *Scolicia* tunnels, or patches of *Phycosiphon* (a dominantly horizontally oriented deposit-feeding burrow).

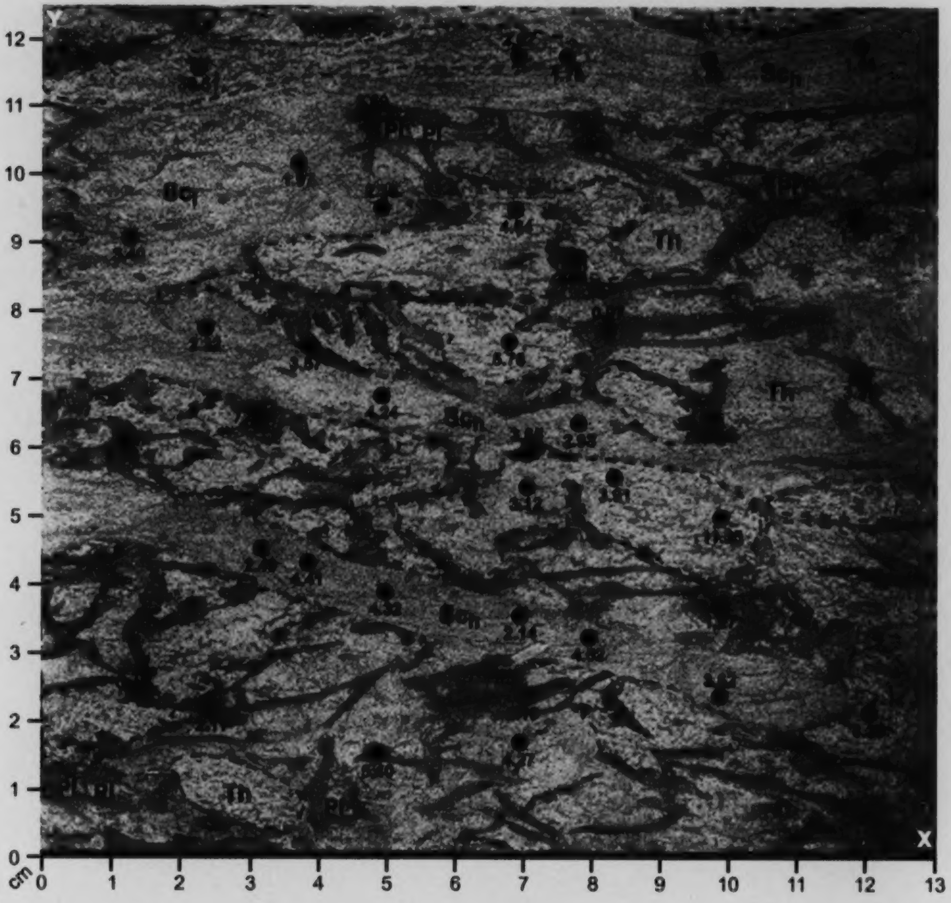

Figure 5.7: Core slab utilized in both probe permeametry and MPath simulation of fluid flow. Points denote the location of probe permeability measurements and the extent of probe-tip coverage; adjacent values are permeabilities in millidarcys (mD). The various types of trace fossils are also labeled in this photo. Dark grey color corresponds to ***Pelosichnus mumorpha*** n. ichnogen., n. ichnosp. Dashed lines highlight areas containing well-developed *Phycosiphon*. In addition to *Thalassinoides* (Th) and *Planolites* (Pl), horizontal (Sc_h) and inclined (Sc_i) cross-sections of *Scolicia* are also indicated. The black line at the base of the photo represents ubiquitous and unlimited hydrocarbon source for the purposes of the simulation only.

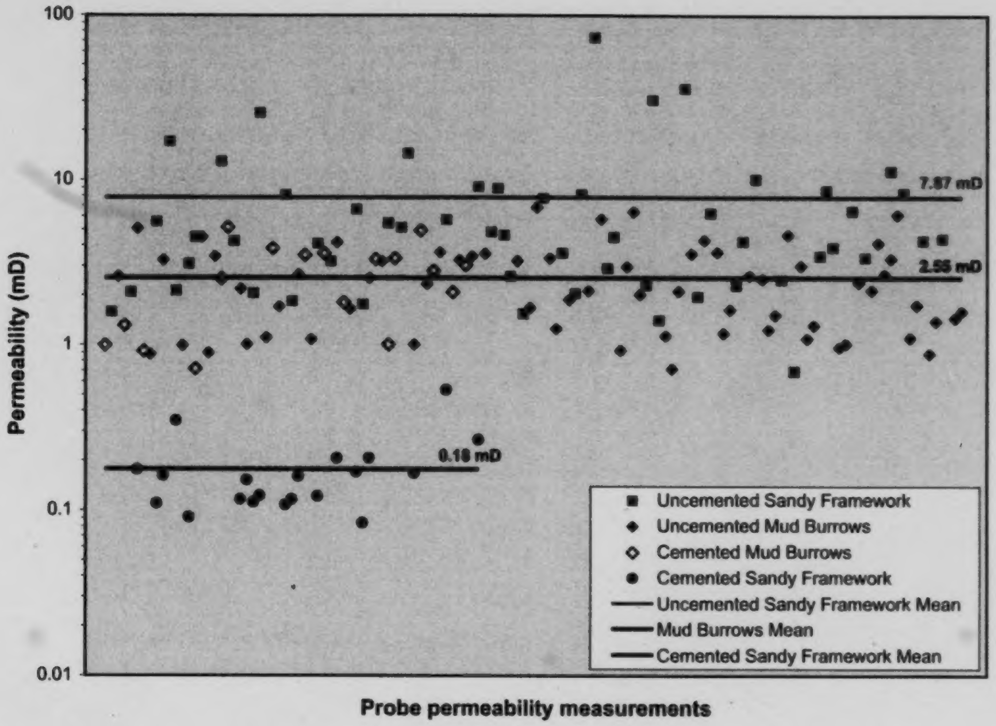

Figure 5.8: Scatter plot of probe-derived permeability measurements and calculated arithmetic means of each textural category.

Probe Permeability Measurements in Uncemented Intervals

Heterogeneity in uncemented sandy framework probe permeabilities is due to the presence of *Scolicia*, *Thalassinoides* or areas containing *Phycosiphon*. Measurements taken within *Scolicia* are at the low end of the spectrum of permeabilities (1 to 4 mD). The higher permeabilities recorded (> 10 mD up to 73.5 mD) are typically recorded within *Thalassinoides* or areas containing *Phycosiphon*. Measurements that are indeterminate with respect to biogenic texture fall within a more restricted range around the mean Probe-K_{us}.

Heterogeneity in mud burrow permeability values (Probe-K_m) is interpreted to reflect either irregular sample surfaces created by the loss of mud during slabbing and washing or slippage of the probe tip "off" of the mud burrow, resulting in the extension of the probe tip past the edges of the mud burrow (i.e. in these cases, inner probe tip diameter is greater than mud burrow width). Abnormally high permeability values may reflect increased sand content within the burrow or the presence of the sandy core of the burrow just beneath the slabbed face.

However, on average, mud burrow permeabilities are lower than uncemented sandy framework permeabilities and show a more consistent range of values. Thus, mud burrows have a more consistent textural character, which is interpreted to be less conducive to fluid flow.

Probe Permeability Measurements in Cemented Intervals

Cemented sandy framework permeabilities (Probe-K_{cs}) are considerably lower than both uncemented sandy framework and mud burrow values, and as such, are barriers to flow. It is currently unknown if these cemented zones are concretions or continuous layers (Hurley *et al.*, 1992); if they are layers, they may add to the degree of reservoir compartmentalization. However, given the density and configuration of the mud burrow networks, it is possible that the mud burrows may actually aid in the communication of fluids across cemented zones.

Comparison of Plug and Probe Permeability Measurements

Both plug and probe measurements reveal that cemented intervals are characterized by a similar mean and range of permeabilities of very low value, indicating that although porosity is comparable to uncemented zones, the cement will not support an open network of conduits for ease of fluid flow. And finally, the range and mean of uncemented plug values is similar to that of uncemented sandy framework probe values, suggesting that flow is concentrated within the more permeable sandy framework.

5.5 Modeling Fluid Flow Through a Bioturbated Reservoir

Rationale

Heterogeneity in plug and probe permeability values is a direct reflection of biogenically produced textural heterogeneity. In particular, the contrast noted in probe permeability measurements of the muddy burrows versus the sandy framework in uncemented intervals indicates that fluids moving through the reservoir will be influenced by the textural and spatial characteristics of the various burrows. Therefore, it is possible to examine the negative influence that the muddy burrows will have on oil migration using simulation techniques that can incorporate burrow morphology, density and connectivity, in addition to burrow-framework permeability contrast. This study uses MPath (Version 4.9), which was developed by Daniel Carruthers of Permedia Research Group Inc., Ottawa, Ontario, Canada. MPath is capable of simulating secondary petroleum migration through two-dimensional or three-dimensional models (at the core-scale up to the basin-scale) containing tens of millions of grid cells in a matter of minutes, while honoring the mechanics of migration transport (Permedia, 2004). In this study, the "model" is a two-dimensional core photograph that is considered to be representative of uncemented portions of the F6B interval (Figure 5.7); it contains all trace fossils that define the characteristic bioturbate texture exuded by Facies 6B as well as the best development of their "ideal" morphology, density and connectivity in cross section.

Domain

As described by Carruthers (2003), MPath uses a modified invasion-percolation (IP) technique based on the premise that flow in porous media can be represented by invasion through a matrix of pores and throats characterized by threshold pressures or probabilities. Invasion occurs along a fluid front by accessing the "pores" with the smallest threshold pressure; fluid flow is deflected around areas of increased threshold pressure. Percolation is achieved once a network of invaded pores spans the media, allowing fluid to flow unimpeded from one boundary to its opposing boundary. The simulation consists of constant composition petroleum flow, or invasion of a non-wetting phase into a water-saturated medium, representing static migration over a geologic timescale. Theoretically, the driving forces of dissipative capillary forces or capillary pressure (as determined by the radius of pore throats, hydrocarbon-water interfacial tension and wettability) are central to IP (Berg, 1975; Schowalter 1979; England *et al.*, 1987). Simply stated, the smaller the pore throat radii (or the smaller the grain size), the higher the threshold pressure. All considering, the key parameters required for MPath are phase densities of the invading and defending fluids, bulk porosity of the media and capillary threshold pressures of the medium. In this study, typical values are utilized for both the invading and defending fluid densities (hydrocarbon = 700 kg/m^3 and brine = 1100 kg/m^3), and an average porosity, determined as 15% from core plug analyses, is assumed. The determination and assignment of capillary pressure, however, is not as straightforward.

Determination and Assignment of Capillary Pressure

Capillary threshold pressures utilized in this study are extrapolated from mercury injection capillary pressure data as reported in the special core analysis for the Hibernia J-34 well (CoreLabs, 1984). Mercury-air capillary pressure values acquired from 25 plug samples over the entire Avalon/Ben Nevis interval were converted into oil-water capillary pressure values using the conversion factor of Vavra *et al.* (1992). Most of the oil-water capillary pressure data falls within a range of approximately 1 to 100 kPa (Figure 5.9). Two extraneous data points, reflecting capillary pressures of 0.164 kPa and 294.337 kPa, correspond to a cemented interval and a vug, respectively. Although the bulk of the data corresponds to a much larger range of permeabilities than that reported from probe permeability analyses (Figure 5.10), the capillary pressure values (extraneous values excluded) are deemed representative of all *possible* capillary pressures present within the Avalon/Ben Nevis reservoir. In assigning capillary pressure data to the medium, it is assumed that the muddy burrows, which just happen to represent the lowest permeability, could possible have a capillary pressure as high as 100 kPa and that the sandy framework, which just happens to represent the highest permeability, could possible have a capillary pressure as low as 1 kPa.

MPath assumes that color approximates lithology; i.e. the darkest shades represent the finest material and the lighter shades represent the coarsest material. The validity of this assumption is questionable; however the margin of error is reasonably small for the medium utilized in this study.

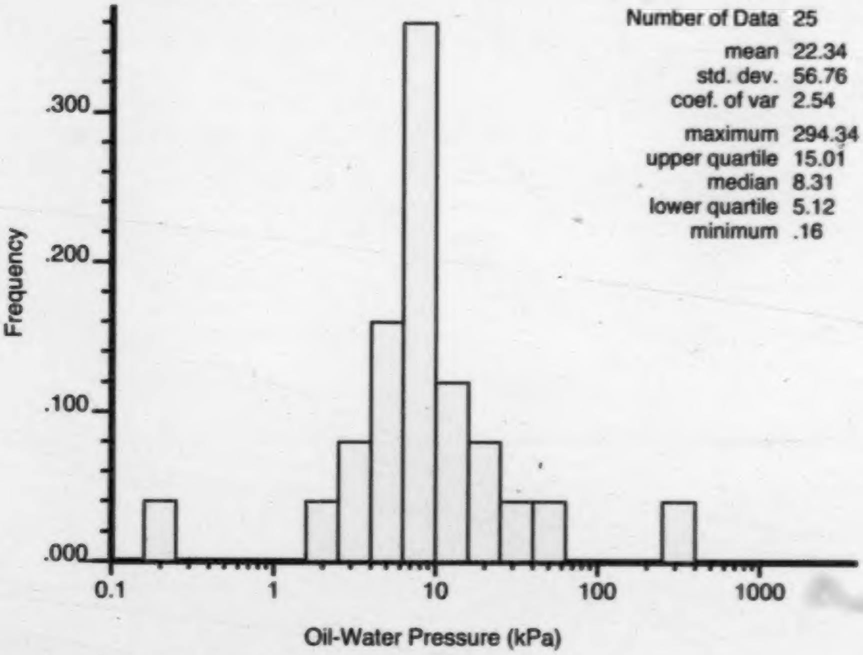

Figure 5.9: Histogram of capillary pressure data.

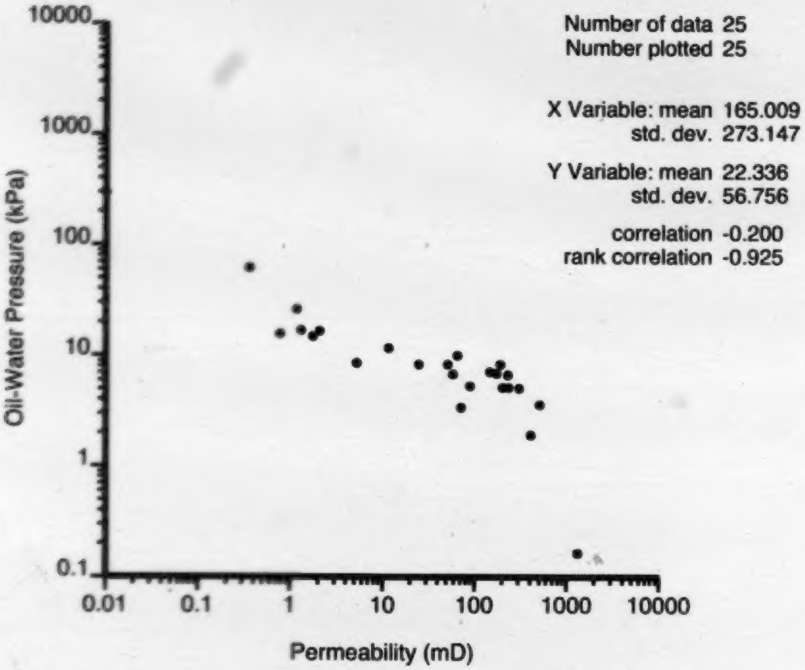

Figure 5.10: Scatter plot of capillary pressure versus permeability as measured from core plugs.

The medium/model (i.e. core photo) exhibits a largely bimodal distribution of "colors" or shades of black and white (Figure 5.7); the muddy burrows, which predominantly contain matrix material, are of the darkest shade, while the sandy framework, which predominantly contains of sand grains, is of the lightest shade. Considering that the muddy burrows are interpreted to exhibit the highest capillary pressure, the assumption that the darkest shades represent the highest capillary pressures is valid. This also holds true in the opposite case for coarser grained material of framework as representative of the lowest capillary pressures. Thus, a value of 1 kPa is assigned to the lightest shade, while a value of 100 kPa is assigned to the darkest shade. Considering the bimodal distribution of colors in the model, values for intermediate shades are exponentially interpolated.

Properties of the Model

The model is a two-dimensional black and white core photo that corresponds to one of the uncemented slabs utilized in the probe permeability analysis (Figure 5.7). The photo is 13 cm wide (x-axis) by 12.5 cm high (y-axis) and contains 2.3 million grid cells. Because MPath requires a third dimension, the z-axis is defaulted to 1 cm thickness. Y-axes (or left and right boundaries) are set to a "closed" state; the top boundary is set to an "open" state. This is necessary in order to simulate flow through the entire column of rock; MPath terminates the simulation once an "open" boundary is breached (i.e. percolation). A black line at the base of the photo represents the hydrocarbon source. This configuration simulates a source rock or layer of hydrocarbon of essentially infinite supply that feeds petroleum into the system at a constant rate, as determined by a default expulsion parameter file that accompanies the software. The model consists of abundant mud-filled burrows juxtaposed with traces of the sandy framework, including areas containing *P. incertum*, four occurrences of *Scolicia* (three horizontal and one inclined), at least three *Thalassinoides* and several *Planolites*.

Simulation Output

The program reports the progression of hydrocarbon migration through the rock volume in successive increments or steps (note that these steps have no connotation of time, *sensu stricto*). The simulation is complete once 50% of grid cells are invaded or percolation is achieved. The hydrocarbon trajectory is marked by a spectrum of colors ranging from blue, through turquoise, green, yellow and orange, to red. Colors represent the invasion sequence (blue to green = early; yellow to red = late); thus, red represents the fluid front or the *latest* pores to be invaded in any particular step. The cross-sectional area of each color changes with each step as the fluid progresses through the medium. And through successive color changes, the simulation demonstrates that flow paths delineating the migration of the oil through the medium are determined by the bioturbate texture. It also reveals which elements of the bioturbate texture are less conducive to flow and highlight areas of "null" flow.

Results and Interpretation

Thirty-six steps are recorded before percolation is achieved, out of which 12 key steps are shown in Figure 5.11. As seen in Figure 5.12A, multiple points of invasion are initiated as the simulation begins (Step 1). By Step 3, the invasion is concentrated into six individual stringers of petroleum (Figure 5.11B). While some stringers meet dead-ends, two columns of advancing petroleum breach the lowermost *Scolicia*, where petroleum then begins to migrate laterally within the confines of the burrow (Step 7; Figure 5.11C). Muddy spreite within *Scolicia* represent subtle variations in threshold pressures, which effectively reduce lateral migration and induce backfilling below *Scolicia* within areas containing *Phycosiphon* (Step 11; Figure 5.11D). By Step 16, the lowermost *Scolicia* is breached and the fluid front moves relatively quickly and uniformly into areas containing *Phycosiphon* (Figure 5.11E). In Step 18 (Figure 5.11F), the middle *Scolicia* is breached and petroleum once again begins to move laterally within the confines of the burrow. Backfilling within patches of sandy framework below the middle *Scolicia* commences (Step 20; Figure 5.11G) and continues into Step 23 (Figure 5.11H), as a zone of mud-filled burrows located above the middle *Scolicia*, representing relatively higher threshold pressures, effectively halts vertical migration. Although the middle *Scolicia* is breached and migration continues upward into areas containing *Phycosiphon* in Step 25, backfilling persists, likely due to matrix heterogeneities within *Scolicia* (Figure 5.11I). Into Step 30, migration continues with relative ease through the inclined *Scolicia* and areas containing *Phycosiphon* (Figure 5.11J). As petroleum invades the uppermost *Scolicia*, it encounters rather continuous mud laminae oriented parallel to the base of the burrow and thus increased threshold pressures (Step 35; Figure 5.11K). This induces multiple points of backfilling along the blue, turquoise and green areas toward the base of the model. Percolation is achieved in the 36th step; however, backfilling continues in areas far from the main fluid front (Figure 5.11L).

5.6 Discussion

Probe permeametry is recognized as an ideal technique for resolving small-scale heterogeneities and anisotropies in porous media (Georgi and Jones, 1992; Meyer and Krause, 1998, 2001; Gingras et al, 2004). It can analyze a much smaller volume relative to plugs and its use is considered to be an accurate (±5% or less), non-destructive, cost-efficient method to gather large amounts of permeability data over a wide range of efficiency (from 0.001 to 20,000 mD) in a short period of time (Jones, 1992; Goggin, 1993). Biogenic textural heterogeneity visible in hand sample and thin section over F6B is reflected in probe permeametry as a marked contrast in permeability between the muddy burrows and sandy framework; however it is effective permeability, which is dependent on the relative saturations of the fluids as well as the nature of the reservoir, that is key in reservoir characterization. For proper assessment of effective permeability in bioturbated reservoirs, trace fossil morphology, including burrow type, density and connectivity, must be taken

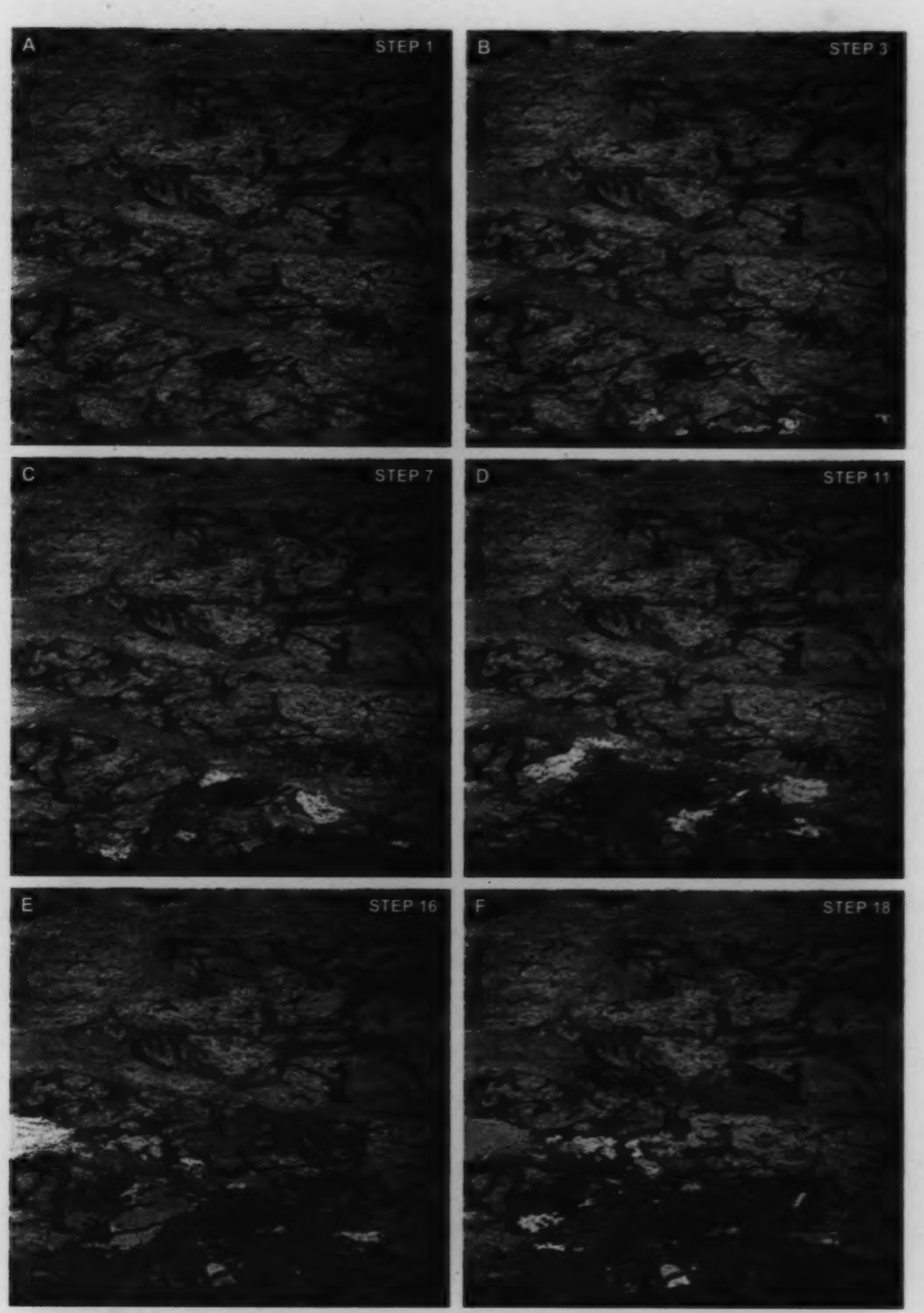
A
STEP 1
B
STEP 3
C
STEP 7
D
STEP 11
E
STEP 16
F
STEP 18

Figure 5.11a: Key increments or steps of the MPath simulation. Colors represent the invasion sequence (blue = early, red = late; thus red represents the hydrocarbon front). See text for interpretation of each step.

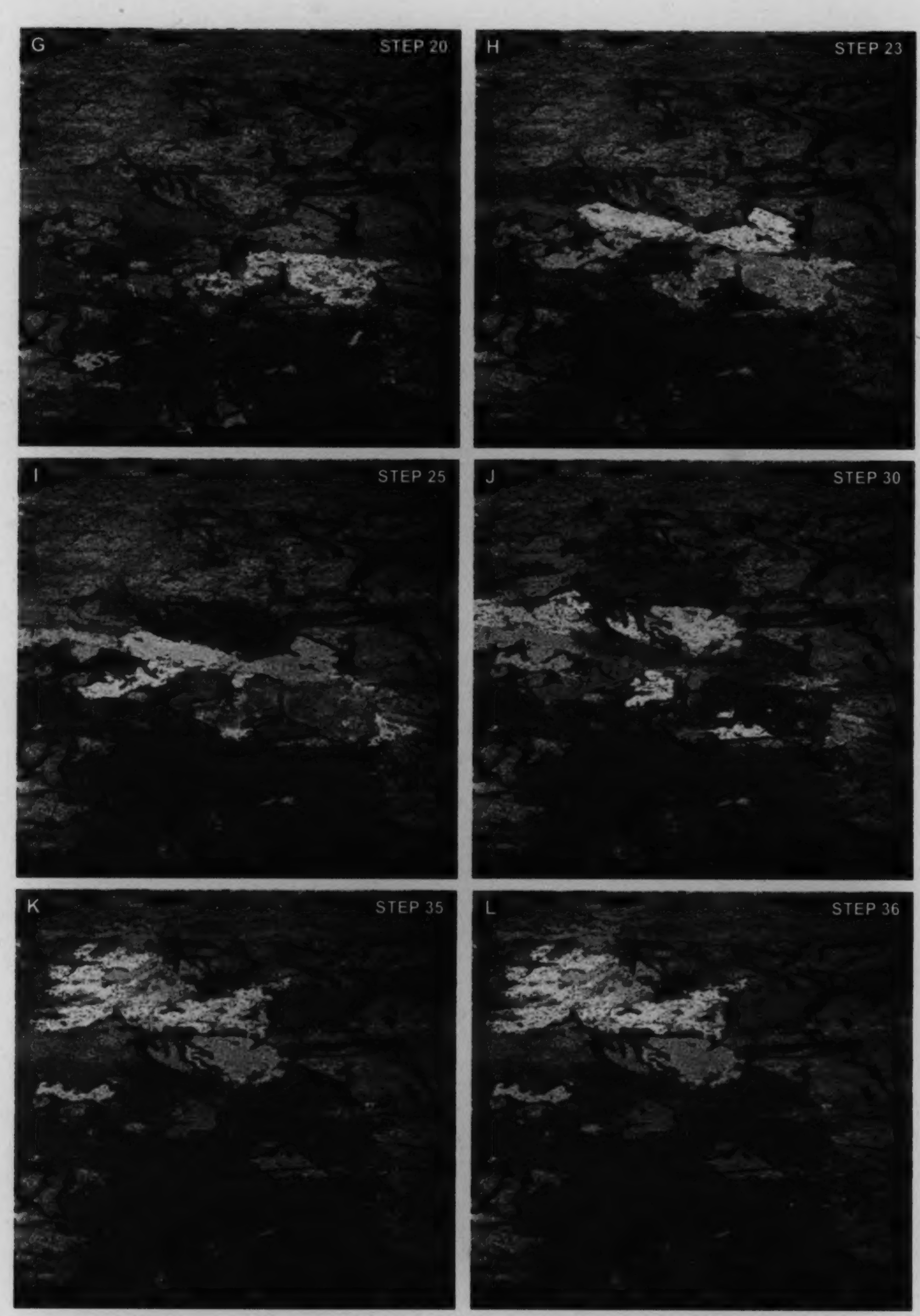

Figure 5.11b: Key increments or steps of the MPath simulation. Colors represent the invasion sequence (blue = early, red = late; thus red represents the hydrocarbon front). See text for interpretation of each step.

into consideration along with the relative contrast in permeability between the framework and the burrows (Gingras *et al.*, 1999a). If effective permeability is assumed from plug permeability data, the influence of burrows on the transmission of fluids through the reservoir remains unrealized. To this end, averaging heterogeneity data from plugs should be done with caution because it can lead to under-estimation of the effect of bioturbation.

In the case of Facies 6B of the upper Ben Nevis, mud-filled burrows, here known as *Pelosichnus mumorpha* n. ichnogen., n. ichnosp., represent a rather intricate, relatively impenetrable three-dimensional network of obstacles or baffles to fluid flow. As seen in the oil migration scenario, the resulting trajectory of petroleum migration is highly sinuous and tortuous as burrows induce dispersion (macroscopic mixing) caused by uneven co-current laminar flow (Figure 5.12). Greenkorn and Kessler (1969) summarized the main mechanisms of dispersion as molecular diffusion, eddies, mixing due to obstructions, incomplete connectivity of the medium, recirculation into regions of reduced pressure, dead-end pores, adsorption and hydrodynamic dispersion (or the adherence of fluid to the capillary wall). Diffusion, adsorption and hydrodynamic dispersion operate on the microscopic level, and therefore, are not observed in this simulation. However, eddies, mixing, and incomplete connectivity of flow conduits (dead-ends) are observable as macroscopic dispersion as petroleum interacts with the mud-filled burrows (Figure 5.12). Mixing is represented as a network of interconnected flow paths. Eddies most commonly occur within *Thalassinoides* or circular areas containing *Phycosiphon*. Dead-ends occur at intersections of mud burrows, which together with *Planolites* represent the incomplete connectivity of the sandy framework. Recirculation or backfilling into regions of reduced pressure are represented by the development of secondary fluid fronts when high threshold pressures are encountered at the main fluid front (e.g. Steps 20, 23, 35, 36 and Figures 5.11J, H, K, L, respectively).

Although mud burrows are key in determining flow pathways, *Scolicia* and *Phycosiphon* also influence petroleum migration. Throughout the simulation it is evident that the fluid front moves more easily into areas containing *Phycosiphon*, reflecting their matrix-reduced nature and higher permeability. In addition, lateral migration is initiated upon breaching of horizontal tunnels of *Scolicia*. The fluid front also moves more slowly due to the greater percentage of matrix material contained within these burrows. Core, petrography and plug/probe permeability analyses alone may give an indication of the effect of mud-filled burrows on the trajectory of petroleum migration;

Figure 5.12: Interpreted fluid flow paths as traced from the MPath simulation. Mixing occurs in areas containing multiple, intertwining flow paths. Location of possible eddy development (E) and dead-ends (D) are also indicated.

however, the microscopic effects induced by matrix material associated with *Phycosiphon* and *Scolicia* would remain unrealized.

Upon percolation (Step 36; Figure 5.11L), it is evident that *Pelosichnus* n. ichnogen., *Phycosiphon* and muddy spreiten of *Scolicia* remain hydrocarbon unsaturated. This end result has two major implications. First, reservoir volumetric calculations may potentially be inaccurate due to the fact that *Pelosichnus* n. ichnogen. accounts for an estimated 40–45% of the reservoir by volume. Although the F6B zone is limited in its vertical and lateral extent, upper Ben Nevis reservoir sandstones include a number of additional bioturbated zones in which mud-filled and mud-lined burrows could promote similar miscalculations. Second, dead-end pores or zones of null flow and the adhesion of petroleum to matrix material associated with these trace fossils may promote serious recovery problems in swept zones, especially if water-flooding is implemented without proper appreciation of the presence of bioturbation. To this end, cores are indispensable for resolving small-scale heterogeneities such as burrows. Ignoring biogenic textural heterogeneity can lead to reduced production rates and low sweep efficiency, increasing the time required to drain the reservoir and the chances of water breakthrough occurring sooner than predicted.

More practically, the simulation outlined here can provide specific information that can be scaled up and applied toward larger and more involved simulations. According to Carruthers (2003), once the volume is spanned vertically, the critical saturation (i.e. the first non-zero oil relative permeability) and the vertical threshold pressure can be calculated. Combined with a separate horizontal invasion simulation, the anisotropic critical parameters for Facies 6B volume and lithotype could then be inputted into reservoir and basin simulators. Scaling up from such a simple simulation, which only requires a core photo, some probe permeability, average bulk porosity and capillary pressure data, can result in much higher resolution of the database that is ultimately used in reservoir and basin simulations.

It is recognized that further work is required to fully realize the value of these simulations. The modeling of fluid flow paths in two dimensions is sufficient to demonstrate how burrows affect petroleum migration (i.e. solves the transport problem for a realistic bioturbated fabric giving an indication of path trajectories and saturations). However, MPath is capable of producing simulations of much more significant value on the production time scale if the parameters of the geologic system are better represented (Carruthers, 2003). For example, three-dimensional models, made possible with advanced imaging techniques such as X-ray computed tomography (CT scans) or magnetic resonance imaging (MRI) (e.g. Gingras *et al.*, 2002a, b), would allow for more accurate determination of saturations, migration efficiencies and emplaced petroleum volumes (Carruthers, 2003).

5.7 Summary

Understanding effective permeability distributions, which are a function of relative saturations and the nature of the reservoir (Weber, 1986), is key for enhanced hydrocarbon recovery strategies. In bioturbated reservoir, the burrows are key to both parameters, thus trace fossils should not be overlooked or ignored. Understanding the nature of bioturbation gives great insight into how petroleum will flow through the reservoir.

Facies 6B within the uppermost Ben Nevis hydrocarbon zone exhibits biogenically produced textural heterogeneity. Petrographically, it can be divided into two textural categories, muddy burrows and sandy framework. The sandy framework is much more variable, as it consists of the relatively cleaner fill of *Thalassinoides* and halos of *Phycosiphon*, the slightly muddier fill of *Scolicia* and areas that are biogenically indeterminate. Although core plug permeability values reflect the heterogeneity, the contrast is subdued; to the untrained geologist, the true significance of this heterogeneity might remain unrealized. Pinpoint measurements resulting from probe permeametry, however, reveal the true nature of the textural disparities. On average, mud-filled burrows are three times lower in permeability than the sandy framework. While mud-filled burrow permeability values are relatively consistent in range, it is evident that the heterogeneity in sandy framework is due to the different types of sand-associated trace fossils.

Although limited in extent and occurrence, interesting conclusions can also be drawn from the cemented intervals. Calcite cement-occluded sandy framework is fourteen times lower in permeability than the muddy burrows. This suggests that where connectivity of the burrows is well developed, the burrows may act as conduits, permitting the transmission of fluids across cemented zones. This is particularly important if these zones turn out to be laterally continuous horizons rather than concretions (i.e. they may not be as impenetrable as previously thought).

One key question remained subsequent to probe permeametry: will simulated flow occur independent of these textural heterogeneities or will they influence it? While honoring the laws of fluid flow through porous media, MPath permits the modeling of secondary petroleum migration through highly bioturbated reservoir rock. As indicated from the results of probe permeametry, the simulation reveals that mud-filled burrows do play a major role in determining petroleum pathways and trajectories. It is also evident that *Scolicia*, *Thalassinoides* and *Phycosiphon* do as well. Flow is slightly impeded and directed laterally within *Scolicia*. When areas containing *Phycosiphon* are breached, fluid flow appears to be uninhibited and the "compartment" is filled more rapidly and ubiquitously. The resulting flow paths are highly tortuous, as burrows induce dispersion at both the microscopic and macroscopic level. The simulation also reveals the effects of macroscopic dispersion and permits the observer to make a saturation forecast. From the simulation, it is obvious that saturation will not be uniform and that some areas will even remain unsaturated. If the nature of bioturbation remains unrealized, reservoir volumetric calculations and water breakthrough predictions may potentially be inaccurate.

A very important tool is introduced in this study – detailed, controlled probe permeametry combined with invasion-percolation modeling software. The methodology outlined holds great potential for resolving reservoir heterogeneities and predicting their effect on hydrocarbon production. In the case of the Ben Nevis/Avalon, the technique utilized here can also be expanded to other bioturbated facies and upscaled for use toward reservoir recovery strategies.

Chapter 6

Conclusion

If used in conjunction with sedimentology and stratigraphy, ichnology can greatly enhance paleoenvironmental interpretation and reservoir characterization. This is especially true for highly bioturbated intervals, like the Avalon and Ben Nevis formations in the Hibernia Field, offshore Newfoundland. This study investigates the sedimentation patterns represented in the Avalon/Ben Nevis interval with respect to its ichnological characteristics and the tectonic conditions present in the Hibernia area at the time of deposition. It also examines the role that biogenic textural heterogeneity has on fluid flow and hydrocarbon production in bioturbated zones of the Avalon/ Ben Nevis reservoir. Several key conclusions can be outlined as a result of this study:

1) Facies analysis, which focused on sedimentological and ichnological characteristics of the cored intervals, resulted in the recognition of fifteen facies. The facies were grouped into eight facies associations, which were deposited in distinct environments including fan delta/bayhead delta, coastal plain, brackish bay, bay mouth complex, upper shoreface/ distributary mouth bar, deltaically influenced shoreface or shallow embayment (delta front), deltaically influenced offshore or deep embayment (prodelta), and shallow marine.
2) Stratigraphic correlation of these facies associations using gamma ray well logs illustrated that these associations can be grouped into three depositional packages. The lowermost depositional package (A) includes FA7 and older sediments down to the "A" Marker; the upper contact is the Avalon Unconformity. This package represents the Avalon Formation. Depositional Package B includes FA1, FA2 and FA3; it unconformably overlies the Avalon Formation and is largely restricted to a trans-field paleo-low in the delineated portion of the Hibernia area. A thick wedge of progradational sediments located at Hibernia G-55, which are interpreted as fan delta/bayhead delta deposits of FAØ, can also be included in this interval. The upper contact of this package is a transgressive surface of erosion (TSE). The uppermost depositional package (C) rests above the TSE and includes FA4, FA5, FA6 and FA7. It grades into overlying shales of the Nautilus Formation. Together, depositional packages B and C make up the Ben Nevis Formation.

3) In the Hibernia area, the overall regressive Avalon Formation culminates in shallow marine offshore deposits. Although shoreface sandstones are found elsewhere in the basin at this time, in the Hibernia area, they were likely removed at the Avalon Unconformity. The Avalon represents the final moments of basin-wide subsidence and initiation of the final rifting event to affect the Jeanne d'Arc Basin, as reflected in the transition from stable platform carbonates of the "A" Marker to offshore siliciclastics of FA7 and increasing depositional thicknesses into the Murre and Rankin faults, respectively.

4) Onset of the final stage of rifting resulted in uplift and erosion of the Hibernia area, and creation of the Avalon Unconformity. At this time, a widespread, arid coastal plain (FA1), characterized by soil development and minor channel incision, is established between the Rankin and Nautilus faults.

5) As extensional forces pull the continental margins of the North Atlantic Ocean apart, faults of the Jeanne d'Arc Basin are reactivated. In the Hibernia area, development of the anticline rollover structure is at a maximum. Vast amounts of accommodation space are created adjacent to the Rankin Fault. While progradational alluvial fan or fan delta sediments (FAØ) fill the trough along the Rankin, the Hibernia area is sediment starved. The thin sedimentary package identified in the paleo-low of the Hibernia Field records the development of a micro to mesotidal estuary. Brackish bay sediments (FA2) accumulated behind a bay mouth barrier complex (FA3) located in the vicinity of the K-14 well. Although thin and limited in its extent, relatively clean and well-sorted sandstones of FA3 represent a primary hydrocarbon-bearing zone of the Avalon/Ben Nevis reservoir.

6) Onset of regional subsidence is recorded as a transgressive surface of erosion that is ubiquitously defined by a transgressive lag and shallow marine deposits overlying estuarine deposits. Any shoreface sediments that may have been present are eroded so that only FA3 sand bodies encased in backbarrier subenvironments of FA2 are preserved. At this time, the Hibernia area is inundated and lower shoreface to offshore sediments of FA7 blanket the area. The deposit is relatively thin, however, reflecting very low rates of sedimentation coupled with low rates in the creation of accommodation space. The presence of a *Glossifungites* surface at the top of FA7 indicates a depositional hiatus that may be associated with maximum flooding.

7) While basin margins remain relatively uplifted during the onset of thermal subsidence in the basin, sediment supply to the basin is maintained and a deltaic system is established within the restricted Hibernia area (i.e. embayment; FA4, FA5, FA6). Deltaic sediments are observed to onlap the sedimentary wedge at G-55, the Rankin Fault to the southwest, the Murre Fault to the west, the rollover structure to the north, and older sediments to the southeast. Sandstones of FA4, which represent a secondary hydrocarbon zone in the Avalon/Ben Nevis reservoir, are found interbedded with highly to intensely bioturbated sediments of FA5 and heterolithic mudstones of FA6. As such, the bioturbated sandstones of FA5 are host to considerable hydrocarbon reserves.

8) As a consequence of facies analysis, it became apparent that bioturbate textures, or intervals comprising 90-100% bioturbation, were integral in the interpretation and delineation of some facies (i.e. F3, F6, F12). These textures developed as a result of intense bioturbation, which annihilated most or even all physically produced sedimentary structures. Thus, it was important to describe these textures in such a way as to obtain the maximum amount of data for use toward paleoenvironmental interpretation or other applications such as reservoir characterization. In order to do this, a bioturbate texture must be described as a function of its textural elements (e.g. sediment types and trace fossils) and their distribution (or fabric). The methodology introduced in this study promotes standardization in the description of bioturbate textures.

9) Hydrocarbon production from the Avalon/Ben Nevis reservoir will be influenced by biogenic textural heterogeneity; especially within highly to intensely bioturbated sandstones that are interbedded with clean, well-sorted distributary mouth bar sandstones of the upper hydrocarbon-bearing zone. Probe permeability analysis conducted on F6B, which consists of dense, interlocking networks of *Pelosichnus mumorpha* n. ichnogen., n. ichnosp., revealed that the burrows induce permeability heterogeneity. As demonstrated by the fluid flow simulation, some forms of bioturbation within this bioturbate texture promote tortuous fluid flow paths, dispersion and adsorption, while others aid migration. If the small-scale effects of bioturbation go unrealized, failure of secondary recovery strategies and reservoir miscalculations are imminent.

10) This study provides unique perspectives into the distribution and configuration of strata that make up the Avalon and Ben Nevis formations; it also lends some insight in the internal structure of hydrocarbon-bearing zones contained within this interval. These realizations afford new prospects in the development of the Avalon/Ben Nevis interval at both the depositional system scale, in terms of tracking reservoir facies trends, and at the reservoir scale, in terms of developing hydrocarbon production procedures.

References

Abid, I.A. 1988. Mineral diagenesis and porosity evaluation in the Hibernia oil field, Jurassic-Cretaceous Jeanne d'Arc graben, eastern Grand Banks of Newfoundland, Canada. Unpublished M.Sc. Thesis, McGill University, Montreal, Quebec, 280 p.

Allmon, W.D. 1988. Ecology of recent Turritelline gastropods (Prosobranchia, Turritellidae): current knowledge and paleontological implications. Palaios, v. 3, p. 259-284.

Amoco Canada Petroleum Company Ltd. and Imperial Oil Ltd. 1973. Regional geology of the Grand Banks: Bulletin Canadian Society of Petroleum Geologists, 21: 479-503.

Bann, K.L. and Fielding, C.R. 2004. An integrated ichnological and sedimentological comparison of non-deltaic and subaqueous delta deposits in Permian reservoir units of Australia. In: The Applications of Ichnology to Palaeoenvironmental and Stratigraphic Analysis. D. McIlroy (ed.). Geological Society of London, Special Publication 228, p. 273-310.

Barwis, J.H. 1990. Flood-tidal delta reservoirs, Medota-Dickinson Trend, North Dakota. In: J.H. Barwis, J.G. McPherson and R.J. Studlick (eds.), Sandstone Petroleum Reservoirs. Springer-Verlag, New York, p. 389-412.

Berg, R.R. 1975. Capillary pressures in stratigraphic traps. American Association of Petroleum Geologists Bulletin, v. 59, p. 939-956.

Bhattacharya, J. and Walker, R.G. 1991. Allostratigraphic subdivision of the Upper Cretaceous Dunvegan, Shaftesbury and Kaskapau formations, northwestern Alberta subsurface. Bulletin of Canadian Petroleum Geology, v. 39, p. 145-164.

Boersma, J.R. 1991. A large flood-tidal delta and its successive slipover apron: detailed proximal-distal facies relationships (Miogene lignite Suite, Lower Rhine Embayment, Germany). In: D.G. Smith, G.E. Reinson, B.A. Zaitlin and R.A. Rahmani (eds.), Clastic Tidal Sedimentology. Canadian Society of Petroleum Geologists Memoir 16, p. 227-254.

Boggs, S. Jr. 1995. Principles of Sedimentology and Stratigraphy. 2nd Edition. Prentice Hall, New Jersey, 774 p.

Boothroyd, J.C. 1985. Tidal inlets and tidal deltas. In: R.A. Davis Jr. (ed.), Coastal Sedimentary Environments. Springer-Verlag, New York, p. 445-533.

Bromley, R.G. 1996. Trace Fossils: Biology, Taphonomy and Applications – 2nd Edition. Chapman & Hall, New York, 361 p.

Buatois, L.A. and Mángano, M.G. 1995. The paleoenvironmental and paleoecological significance of the *Mermia* ichnofacies: an archetypal subaqueous non-marine trace fossil assemblage. Ichnos, v. 4, p. 151-161.

CNOPB, 2003. Decision 2003.02 Respecting Extension of the Ben Nevis/Avalon Appraisal Period. Canada-Newfoundland Offshore Petroleum Board, St. John's, Newfoundland, 41 p.

CNOPB, 2004. Annual Report of the Canada-Newfoundland Offshore Petroleum Board. 52 p.

Cant, D.J. 1982. Fluvial facies models. In: P.A. Scholle and D. Spearing (eds.), Sandstone Depositional Environments, American Association of Petroleum Geologists Memoir 31, p. 115-138.

Caron, A., Desrosiers, G., Olive, P.J.W., Retière, C. and Nozais, C. 2004. Comparison of diet and feeding activity of two polychaetes, *Nephtys caeca* (Fabricius) and *Nereis virens* (Sars), in an estuarine intertidal environment in Québec, Canada. Journal of Experimental Marine Biology and Ecology, v. 304, p. 225-242.

Carruthers, D.J. 2003. Modeling of secondary petroleum migration using invasion percolation techniques. In: S. Duppenbecker and R. Marzi (eds.), Multidimensional Basin Modeling. American Association of Petroleum Geologists Datapages Discovery Series 7, p. 21-37.

Cheel, R.J. and Leckie, D.A. 1990. A tidal-inlet complex in the Cretaceous epeiric sea of North America: Virgelle Member, Milk River Formation, southern Alberta, Canada. Sedimentology, v. 37, p. 67-81.

Clay, E. 1967. Literature survey of the common fauna of estuaries. 1: *Nereis diversicolor* O.F. Müller 1776. Imperial Chemical Industries Ltd., p. 1-28.

Clifton, H.E. 1981. Progradational sequences in Miocene shoreline deposits, southern Caliente Range, California. Journal of Sedimentary Petrology, v. 51, p. 165-184.

Clifton, H.E. 1982. Estuarine deposits. In: P.A. Scholle and D. Spearing (eds.), Sandstone Depositional Environments, American Association of Petroleum Geologists Memoir 31, p. 179-190.

Coleman, J.M. 1981. Deltas: Processes of Deposition and Models for Exploration. 2nd Edition. Burgess Publishing Company, Minneapolis, MN, 124 p.

Coleman, J.M. and Prior, D.B. 1982. Deltaic environments. In: P.A. Scholle and D. Spearing (eds.), Sandstone Depositional Environments. American Association of Petroleum Geologists Memoir 31, p. 139-178.

Corelabs, 1982. Hibernia J-34 core analysis (core #1-13). File No. 7004-82-42. Canada-Newfoundland Offshore Petroleum Board Report.

Corelabs, 1984. Hibernia J-34 special core analysis study. File No. 7009-312-82-026. Canada-Newfoundland Offshore Petroleum Board Report.

Corelabs, 1996. PDPK – 400 Pressure Decay Profile Permeameter: Operations Manual. Core Laboratories, Calgary Alberta.

Creaney, S. and Allison, B.H. 1987. An organic geochemical model of oil generation in the Avalon/Flemish Pass sub-basins, east coast Canada. Bulletin Canadian Society of Petroleum Geologists, v. 35, p. 12-23.

Davey, J.T. 1994. The architecture of the burrow *Nereis diversicolor* and its quantification in relation to sediment-water exchange. Journal of Experimental Marine Biology and Ecology, v. 179, p. 115-129.

Dott, R.H. Jr. 1964. Wacke, Graywacke and matrix – what approach to immature sandstone classification? Journal of Sedimentary Petrology, v. 34, p. 625-632.

Dott, H.R. Jr. 1983. Episodic sedimentation – how normal is average? How rare is rare? Does it matter? Journal of Sedimentary Petrology, v. 53, p. 5-23.

Dott, H.R. Jr. and Bourgeois, J. 1982. Hummocky stratification: significance of its variable bedding sequences. Geological Society of America Bulletin, v. 93, p. 663-680.

Driscoll, N.W., Hogg, J.R., Christie-Blick, N. and Karner, G.D. 1995. Extensional tectonics in the Jeanne d'Arc Basin, offshore Newfoundland: implications for the timing of break-up between Grand Banks and Iberia. In: R.A. Scrutton, M.S. Stoker, G.B. Shimmerfield and A.W. Tudhope, (eds.), The Tectonics, Sedimentation and Paleooceanography of the North Atlantic Region. Geological Society of London Special Publication 90, p. 1-28.

Droser, M.L. and Bottjer, D.J. 1986. A semiquantitative field classification of ichnofabric. Journal of Sedimentary Petrology, v. 56, p. 558-559.

Duke, W.L. 1985. Hummocky cross-stratification, tropical hurricanes and intense winter storms. Sedimentology, v. 32, p. 167-194.

Duke, W.L., Arnott, R.W.C. and Cheel, R.J. 1991. Shelf sandstones and hummocky cross-stratification: new insites on a storm debate. Geology, v. 19, p. 625-628.

Ekdale, A.A. and Bromley, R.G. 1983. Trace fossils and ichnofabric in the Kjolby Gaard Marl, uppermost Cretaceous, Denmark. Bulletin of the Geological Society of Denmark, v. 31, p. 107-119.

Ekdale, A.A., Bromley, R.G. and Pemberton, S.G. 1984. Ichnology: Trace Fossils in Sedimentology and Stratigraphy. Society of Economic Paleontologists and Mineralogists Short Course Notes 15, 317p.

Ekdale, A.A., Bromley, R.G., Bockelie, J.F., Droser, M.L. and Bottjer, D.J. 1991. "Ichnofabric" it is! Palaios, v. 6, p. 100-101.

Elliot, T. 1986. Clastic shorelines. In: H.G. Reading (ed.), Sedimentary Environments and Facies. Blackwell Scientific Publications, New York, p. 143-177.

Enachescu, M.E. 1987. Tectonic and structural framework of the northeast Newfoundland continental margin. In: C. Beaumont, and A.J. Tankard (eds.), Sedimentary Basins and Basin-forming Mechanisms. Canadian Society of Petroleum Geologists, Memoir 12, p. 117-146.

Enachescu, M. and Dunning, G. 1994. Basin Monitor: Grand Banks Basin, Canada. Petroconsultants International Energy Services, Switzerland.

England, W.A., Mackenzie, A.S., Mann, D.M. and Quigley, T.M. 1987. The movement and entrapment of petroleum fluids in the subsurface. Journal of the Geological Society of London, v. 144, p. 327-347.

Esnault, G., Retière, C. and Lambert, R. 1990. Food resource partitioning in a population of *Nereis diversicolor* (Annelida, Polychaeta) under natural experimental conditions. In: M. Barnes and R.N. Gibson (eds.), Trophic Relationships in Marine Environments. Proceedings of the 24th European Marine Biology Symposium. Oban, U.K., Aberdeen University Press, p. 453-467.

Fenwick, I. 1985. Paleosols: problems of recognition and interpretation. In: J. Boardman (ed.), Soils and Quaternary Evolution. Wiley Interscience, New York, p. 3-21.

Frey, R.W. 1971. Ichnology – the study of fossil and recent lebensspuren. In: B.F. Perkins (ed.), A Field Guide to Selected Localities in Pennsylvanian, Permian, Cretaceous and Tertiary Rocks of Texas and Related Papers. Louisiana State University, Miscellaneous Publication 71-1, p. 91-125.

Frey, R.W. 1973. Concepts in the study of biogenic sedimentary structures. Journal of Sedimentary Petrology, v. 43, p. 6-19.

Frey, R.W. and Goldring, R. 1992. Marine event beds and recolonization surfaces as revealed by trace fossil analysis. Geological Magazine, v. 129, p. 325-335.

Frey, R.W. and Pemberton, S.G. 1985. Biogenic structures in outcrop and cores. 1. Approaches to ichnology. Bulletin of Canadian Petroleum Geology, v. 33, p. 72-115.

Frey, R.W. and Pemberton, S.G. 1990. Bioturbate texture of ichnofabric? Palaios, v. 5, p. 385-386.

Frey, R.W. and Pemberton, S.G. 1991. Or, is it 'bioturbate texture'? Ichnos, v. 1, p. 327-329.

Frey, R.W. and Seilacher, A. 1980. Uniformity in marine invertebrate ichnology. Lethaia, v. 13, p. 183-207.

Frey, R.W., Pemberton, S.G. and Fagerstrom, J. A. 1984. Morphological, ethological, and environmental significance of the ichnogenera *Scoyenia* and *Ancorichnus*: Journal of Paleontology, v. 58, p. 511-528.

Fürsich, F.T. 1981. Invertebrate trace fossils from the Upper Jurassic of Portugal. Communicoes Servicos Geologicos de Portugal, v. 67, p. 153-168,

Georgi, D.T. and Jones, S.C. 1992. Application of pressure-decay profile permeametry to reservoir description. 16th Annual Society of Petroleum Engineers (Nigeria Council) International Conference and Exhibition, SPENC Paper 9212, 12 p.

Gingras, M.K., MacEachern, J.A. and Pemberton, S.G. 1998. A comparative analysis of the ichnology of wave- and river-dominated allomembers of the Upper Cretaceous Dunvegan Formation: Bulletin of Canadian Petroleum Geology, v. 46, p. 51-73.

Gingras, M.K., Pemberton, S.G., Mendoza, C.A. and Henk, F. 1999a. Assessing the anisotropic permeability of *Glossifungites* surfaces. Petroleum Geoscience, v. 5, p. 349-357.

Gingras, M.K., Pemberton, S.G., Saunders, T.D.A., and Clifton, H.E. 1999b. The ichnology of modern and Pleistocene brackish-water deposits at Willapa Bay, Washington: variability in estuarine settings. Palaios, v. 14, p. 352-374.

Gingras, M.K., Pemberton, S.G. and Henk, F. 2001a. Conceptual models for burrow-related, selective dolomitization. Annual Meeting of the American Association of Petroleum Geologists, Abstracts Volume, p. 73.

Gingras, M.K., Pemberton, S.G. and Saunders, T.D.A. 2001b. Bathymetry, sediment texture and substrate cohesiveness; their impact on modern *Glossifungites* trace assemblages at Willapa Bay, Washington. Palaeogeography, Palaeoclimatology, Palaeoecology, v. 169, p. 1-21.

Gingras, M.K., McMillan, B. and Balcom, B.J. 2002a. Visualizing the internal characteristics of carbonate sediments with magnetic resonance imaging and petrography. Bulletin of Canadian Petroleum Geology, v. 50, p. 363-369.

Gingras, M.K., McMillan, B., Balcom, B.J., Saunders, T. and Pemberton, S.G. 2002b. Using magnetic resonance imaging and petrographic techniques to understand the textural attributes and porosity distribution in *Macaronichnus*-burrowed sandstone. Journal of Sedimentary Research, v. 72, p. 552-558.

Gingras, M.K., Mendoza, C.A. and Pemberton, S.G. 2004. Fossilized worm burrows influence the resource quality of porous media. American Association of Petroleum Geologists Bulletin, v. 88, p. 875-883.

Goggin, D.J. 1993. Probe permeametry: is it worth the effort? Marine and Petroleum Geology, v. 10, p. 299-308.

Goldring, R. 1996. The sedimentological significance of concentrically laminated burrows from Lower Cretaceous Ca-bentonites, Oxfordshire. Journal of the Geological Society of London, v. 153, p. 253-263.

Goldring, R., Gruszczynski, M. and Gatt, P.A. 2002. A bow-form burrow and its sedimentological and paleoecological significance. Palaios, v. 17, p. 622-630.

Grant, A.C., McAlpine, K.D. and Wade, J.A. 1986. The continental margin of eastern Canada: geological framework and petroleum potential. In: M.T. Halbouty, (ed.), Future Petroleum Provinces of the World. American Association of Petroleum Geologists, Memoir 40, p. 177-205.

Grant, A.C. and McAlpine, K.D. 1990. The Continental Margin around Newfoundland, Chapter 6. In: M.J. Keen, and G.L. Williams, (eds.), Geology of the Contintal Margin of Eastern Canada. Geological Survey of Canada, Geology of Canada, v. 2, p. 239-292.

Greenkorn, R.A. and Kessler, D.P. 1969. Dispersion in heterogeneous nonuniform anisotropic porous media. Industrial and Engineering Chemistry, v. 61, p. 14-32.

Guilbault, J.P. 1986. Foraminiferal and Ostracodal Paleoecology of 5 Cores from the Avalon Sand, Hibernia Field, Grand Banks. Mobil Internal Report G-19.55, 37 p.

Hertweck, G. 1986. Burrows of the polychaete *Nereis virens* SARS. Senckenbergiana Maritima, v. 17, p. 319-331.

Howard, J.D. and Frey, R.W. 1975. Regional animal-sediment characteristics of Georgia estuaries. Senckenbergiana Maritima, v. 7, p. 33-103.

Howard, J.D. and Frey, R.W. 1984. Characteristic trace fossils in nearshore to offshore sequences, Upper Cretaceous of east-central Utah. Canadian Journal of Earth Sciences, v. 21, p. 200-219.

Howard, J.D. and Frey, R.W. 1985. Physical and biogenic aspects of backbarrier sedimentary sequences, Georgia Coast, U.S.A. In: G.F. Oertel and S.P. Leatherman (eds.), Barrier Islands, Marine Geology Special Issue, v. 63, p. 77-127.

Hudson, J.D. 1963. The recognition of salinity-controlled mollusk assemblages in the Great Estuarine Series (Middle Jurassic) of the Inner Hebrides. Paleontology, v. 6, p. 327-348.

Hurley, T.J., Kreisa, R.D., Taylor, G.G. and Yates, W.R.L. 1992. The reservoir geology and geophysics of the Hibernia field, offshore Newfoundland. In: M.T. Halbouty (ed.), Giant Oil and Gas Fields of the Decade 1977-88. American Association of Petroleum Geologists Memoir 54, p. 35-54.

Hutcheon, I., Nahnybida, C. and Krause, H.R. 1985. The geochemistry of carbonate cements in the Avalon Sand, Grand Banks of Newfoundland. Mineralogical Magazine, v. 49, p. 457-467.

Jenkins, A. 1984. Palynology and Stratigraphy of the Avalon Reservoir Rocks, Hibernia Structure, Grand Banks of Newfoundland. Mobil Internal Report, 57 p.

Jenkins, A. 1993. Age Interpretation and Biostratigraphic Correlation of the Avalon and Ben Nevis Formations at Hibernia, Grand Banks of Newfoundland. Hibernia Management and Development Company Internal Report,

Jones, S.C. 1992. The profile permeameter: a new, fast, accurate minipermeameter. 67th Annual Technical Conference and Exhibition of the SPE, Paper 24757, p. 973-983.

Keen, C.E., Boutilier, R., de Voogd, B., Mudford, B. and Enachescu, M.E. 1987, Crustal geometry and extensional models for the Grand Banks, eastern Canada: constraints from deep seismic reflection data. In: Beaumont, C. and Tankard, A.J. (eds.), Sedimentary Basins and Basin-Forming Mechanisms: Canadian Society of Petroleum Geologists, Memoir 12, p. 101-115.

Land, C.B. Jr. 1972. Stratigraphy of Fox Hills Sandstone and associated formations, Rock Springs uplift and Wamsutter arch area, Sweetwater County, Wyoming: a shoreline-estuary sandstone model for the Late Cretaceous. Colorado School of Mines Quarterly Journal, v. 67, p. 1-69.

Lee, J.M. 1987. Sedimentology and diagenesis of the Avalon Member of the Mississauga Formation, Hibernia Field, Grand Banks of Newfoundland. Unpublished M.Sc. Thesis, University of Calgary, Calgary, Alberta, 132 p.

MacEachern, J.A. and Pemberton, S.G. 1992. Ichnological aspects of Cretaceous shoreface successions and shoreface variability in the Western Interior Seaway of North America. In: S.G. Pemberton (ed.) Applications of Ichnology to Petroleum Exploration: A Core Workshop. . Society of Economic Paleontologists and Mineralogists Core Workshop Notes 17, p. 57-84.

MacEachern, J.A., Raychaudhuri, I. and Pemberton, S.G. 1992. Stratigraphic applications of the Glossifungites ichnofacies: delineating discontinuities in the rock record. In: S.G. Pemberton (ed.) Applications of Ichnology to Petroleum Exploration: A Core Workshop. . Society of Economic Paleontologists and Mineralogists Core Workshop Notes 17, p. 169-198.

MacEachern, J.A., Bann, K.L., Bhattacharya, J.P. and Howell, C.D. in press - 2005. Ichnology of deltas: organism responses to the dynamic interplay of rivers, waves, storms and tides. In: B.P. Bhattacharya and L. Giosan (eds.), Deltas: Past and Present. Society of Economic Paleontologists and Mineralogists, Special Publication.

Mackay, A.H. and Tankard, A.J. 1990. Hibernia Oil Field-Canada Jeanne d'Arc Basin, Grand Banks Offshore Newfoundland. In: N.H. Foster and E.A. Beaumont, (eds.), Structural Traps: Tectonic Fold Traps, v. 3. American Association of Petroleum Geologists, Atlas of Oil and Gas Fields, p. 145-175.

McAlpine, K.D. 1990, Mesozoic stratigraphy, sedimentary evolution and petroleum potential of the Jeanne d'Arc Basin, Grand Banks of Newfoundland. Geological Survey of Canada, Paper 89-17, 50 p.

McCubbin, D.G. 1982. Barrier-island and strand-plain facies. In: P.A. Scholle and D. Spearing (eds.), Sandstone Depositional Environments. American Association of Petroleum Geologists Memoir 31, p. 247-279.

Meyer, R. and Krause, F.F. 1998. Directional permeability anisotropy: a comparison of horizontal and vertical plug- and probe-permeabilities in sandstones. Geo-Triad, Joint Meeting of the CSEG, CSPG and CWLS, Abstracts Volume, p. 406-407.

Meyer, R. and Krause, F.F. 2001. A comparison of plug-derived and probe-permeability in cross-bedded sandstones of the Virgelle Member, Alberta, Canada: the influence of flow direction on probe permeametry. American Association of Petroleum Geologists Bulletin, v. 85, p. 477-489.

Murakoshi, N. and Masuda, F. 1991. A depositional model for flood-tidal delta and washover sands in the late Pleistocene Paleo-Tokyo Bay, Japan. In: D.G. Smith, G.E. Reinson, B.A. Zaitlin and R.A. Rahmani (eds.), Clastic Tidal Sedimentology, Canadian Society of Petroleum Geologists Memoir 16, p. 219-226.

Oglesby, L.C. 1969. Inorganic components and metabolism: ionic and osmotic regulation: Annelida, Sipuncula and Echiura. In: M. Florin and B.T. Scheer (eds.), Chemical Zoology. Academic Press, New York, p. 211-310.

Olivier, M., Desrosiers, G., Caron, A., Retière, C. and Caillou, A. 1995. Résponses comportemantales des polychètes *Nereis diversicolor* (O.F. Muller) et *Nereis virens* (Sars) aus stimuli d'ortre alimentaire: utilisation de la matière organique particulaire (algues et halophytes). Canadian Journal of Zoology, v. 73, p. 2307-2317.

Pak, R., Pemberton, S.G. and Gingras, M.K. 2001. Reservoir characterization of burrow-mottled carbonates: the Yeoman Formation of southern Saskatchewan. In: J.E. Christopher, C.F. Gilboy, F.M. Haidl, and L.K. Kreis (eds.), Summary of Investigations 2001, Volume 1. Saskatchewan Geological Survey, p. 10-13.

Pattison, S.A. 1992. Recognition and interpretation of estuarine mudstones (central basin mudstones) in the tripartite valley-fill deposits of the Viking Formation, Central Alberta. In: S.G. Pemberton (ed.), Applications of Ichnology to Petroleum Exploration. Society of Economic Paleontologist and Mineralogists Core Workshop Notes 17, p. 223-250.

Pemberton, S.G. 1984. Ichnology of the Avalon Cores, Offshore Newfoundland. Mobil Internal Report, 82 p.

Pemberton, S.G. 1985. Synthesis of Ichnology: Hibernia-related Core. Mobil Internal Report, 41 p.

Pemberton, S.G. 1992. Applications of Ichnology to Petroleum Exploration: A Core Workshop. Society of Economic Paleontologists and Mineralogists, Core Workshop Notes 17, 429 p.

Pemberton, S.G. and MacEachern, J.A. 1995. The sequence stratigraphic significance of trace fossils: examples from the Cretaceous foreland basin of Alberta, Canada. In: J.C. Van Wagoner and G. Bertram, (eds.), Sequence Stratigraphy of Foreland Basin Deposits - Outcrop and Subsurface Examples from the Cretaceous of North America. American Association of Petroleum Geologists Memoir 64, p. 429-475.

Pemberton, S.G. and MacEachern, J.A. 1997. The ichnological signature of storm deposits: the use of trace fossils in event stratigraphy. In: C.E. Brett (ed.), Paleontological Event Horizons: Ecological and Evolutionary Implications. Columbia University Press, p. 73-109.

Pemberton, S.G. and Wightman, D.M. 1992. Ichnological characteristics of brackish water deposits. In: S.G. Pemberton (ed.), Applications of Ichnology to Petroleum Exploration: A Core Workshop. Society of Economic Paleontologists and Mineralogists Core Workshop Notes 17, p. 141-167.

Pemberton, S.G., Van Wagoner, J.C. and Wach, G.D. 1992. Ichnofacies of a wave-dominated shoreline. In: S.G. Pemberton (ed.), Applications of Ichnology to Petroleum Exploration: A Core Workshop. Society of Economic Paleontologists and Mineralogists Core Workshop Notes 17, p. 339-382.

Pemberton, S.G., Gingras, M.K. and Henk, F. 2001a. Assessing permeability in bioturbated media. Annual Meeting of the American Association of Petroleum Geologists, Abstracts Volume, p. 156.

Pemberton, S.G., Spila, M.V., Pulham, A.J., Saunders, T.D.A., MacEachern, J.A., Robbins, D. and Sinclair, I.K.. 2001b. Ichnology and Sedimentology of Shallow to Marginal Marine Systems: Ben Nevis and Avalon Reservoirs, Jeanne d'Arc Basin. Geological Association of Canada Short Course Notes 15, 343p.

Permedia, 2005. The Permedia Research Group Inc. Online User Manual for MPath. Viewed July 20, 2005. <http://www.permedia.ca/>

Rampino, M.R. and Sanders, J.E. 1980. Holocene transgression in south-central Long Island, New York. Journal of Sedimentary Petrology, v. 50, p. 1063-1080.

Reineck, H.-E. 1958. Wühlbau-gefüge in abhängigkeit von sediment-umlagerungen. Senckenbergiana Lethaea, v. 39, p. 1-23.

Reineck, H.-E. 1963. Sedimentgefüge im bereich der südlichen nordsee. Abhandlungen der Senckenbergischen Naturforschenden Geseilschaft, no. 505, 137 p.

Reineck, H.E. and Singh, I.B. 1980. Depositional Sedimentary Environments: With Reference to Terrigenous Clastics. Springer-Verlag, New York, 551 p.

Reinson, G.E. 1992. Transgressive barrier island and estuarine systems. In: R.G. Walker and N.P. James (eds.), Facies Models: Response to Sea Level Change. Geological Association of Canada, Geotext 1, p. 179-194.

Retallack, G.J. 1988. Field recognition of paleosols. In: J. Reinhardt and W.R. Sigleo (eds.), Paleosols and Weathering Through Geologic Time. Geological Society of America Special Paper 216, p. 1-20.

Rice, A.L., Billett, D.S.M., Fry, J., John, A.W.G., Lampitt, R.S., Mantoura, R.F.C. and Morris, R.J. 1986. Seasonal deposition of phytodetritus to the deep-sea floot. Proceedings of the Royal Society of Edinburgh, v. 88B, p. 265-279.

Richter, R. 1952. Fluidal-textur in sediment-gesteinen und über sedifluktion überhaupt. Notizblatt des Hessischen Landesamtes für Bodenforschung zu Wiesbaden, v. 3, p. 67-81.

Root, S.A. 1983. Macrofossil Paleoenvironmental Interpretation of 20 Cores from the Mobil Hibernia I-46 Well, Grand Banks, Canada. Mobil Internal Report, 64 pp.

Saunders, T., MacEachern, J.A. and Pembertonm S.G. 1994. Cadotte member sandstone: progradation in a boreal basin prone to winter storms. In: S.G. Pemberton, D.P. James and D.M. Wightman (eds.), Mannville Core Conference. Canadian Society of Petroleum Geologists, p. 331-350.

Scaps, P. 2002. A review of the biology, ecology and potential use of the common ragworm *Hediste diversicolor* (O.F. Müller) (Annelida: Polychaeta). Hydrobiologia, v. 470, p. 203-218.

Schäfer, W. 1972. Ecology and Paleoecology of Marine Environments. University of Chicago Press, Chicago, 568p.

Schowalter, T.T. 1979. Mechanics of secondary hydrocarbon migration and entrapment. American Association of Petroleum Geologists Bulletin, v. 63, p. 723-760.

Seilacher, A. 1957. An-aktualistisches Wattenmeer? Paläontologische Zeitschrift, v. 31, p. 198-206.

Seilacher, A. 1964. Biogenic sedimentary structures. In: J. Imbrie and N. Newell (eds.), Approaches to Paleoecology. John Wiley, New York, p. 296-316.

Seilacher, A. 1967. Bathymetry of trace fossils. Marine Geology, v. 5, p. 389-412.

Seilacher, A. 1982. Distinctive features of sandy tempestites. In: G. Einsele and A. Seilacher (eds.), Cyclic and Event Stratification. Springer-Verlag, Berlin, p. 333-349.

Sinclair, I.K. 1988. Evolution of Mesozoic-Cenozoic sedimentary basins in the Grand Banks area of Newfoundland and comparison with Falvey's (1974) rift model. Bulletin of Canadian Petroleum Geology, v. 36, p. 255-273.

Sinclair, I.K. 1993. Tectonism: the dominant factor in mid-Cretaceous deposition in the Jeanne d'Arc Basin, Grand Banks. Marine and Petroleum Geology, v. 10, p. 530-549.

Sinclair, I.K. 1995a. Sequence stratigraphic response to Aptian-Albian rifting in conjugate margin basins: a comparison of the Jeanne d'Arc Basin, offshore Newfoundland and the Porcupine Basin, offshore Ireland. In: R.A. Scrutton, M.S. Stoker, G.B. Shimmeld and A.W. Tudhope (eds.), The Tectonics, Sedimentation and Palaeoceanography of the North Atlantic Region. Geological Society of London, Special Publication 90, p. 29-49.

Sinclair, I.K. 1995b. Transpressional inversion due to episodic rotation of extensional stresses in Jeanne d'Arc Basin, offshore Newfoundland. In: J.G. Buchanan, and P.G. Buchanan (eds.), Basin Inversion. Geological Society of London Special Publication 88, p. 249-271.

Sinclair, I.K., Evans, J.E., Albrechtsons, E.A. and Sydora, L.J. 1999. The Hibernia oil field – effects of episodic tectonism on structural charater and reservoir compartimentalization. In: A.J. Fleet and S.A.R. Boldly (eds.), Petroleum Geology of Northwest Europe. Geological Society of London, Proceedings of the 5th Conference, p. 517-528.

Sinclair, I.K., McAlpine, K.D., Sherwin, D.F. and McMillan, N.J. 1992. Petroleum Resources of the Jeanne d'Arc Basin and Environs, Grand Banks, Newfoundland, Part 1: Geological Framework. Geological Survey of Canada, Paper 92-8, 48p.

Smith, R.M.H., Mason, T.R. and Ward, L.F. 1993. Flash flood sediments and ichnofacies of the Late Pleistocene Homeb Silts, Kuiseb River, Namibia. Sedimentary Geology, v. 85, p. 579-599.

Soliman, O.M. 1995. Depositional Facies and Calcite Cementation in the Avalon Formation, Hibernia Oil Field, Jeanne d'Arc Basin, Grand Banks of Newfoundland. Unpublished Ph.D. Thesis, Memorial University, Newfoundland, 282 pp.

Stamp, L.D. 1921. On cycles of sedimentation in the Eocene strata of the Anglo-France-Belgium Basin. Geological Magazine, v. 58, p. 108-114.

Swift, J.H. and Williams, J.A. 1980. Petroleum source rocks, Grand Banks area. In: A.D. Miall (ed.), Facts and Principles of World Petroleum Occurrences. Canadian Society of Petroleum Geologists Memoir 6, p. 567-588.

Tankard, A.J. 1990. Extensional basin styles in exploration: Grand Banks of Newfoundland (Eastern Canada). In: B. Pinet and C. Bois (eds.), The potential of Deep Seismic Profiling for Hydrocarbon Exploration. Proceedings of the 5th IFP Exploration and Production Research Conference, p. 219-223.

Tankard, A.J. and Welsink, H.J. 1987. Extensional tectonics and stratigraphy of the Hibernia oil field, Grand Banks, Newfoundland. Bulletin of the American Association of Petroleum Geologists, v. 71, p. 1210-1232.

Tankard, A.J. and Welsink, H.J. 1988. Extensional tectonics and stratigraphy of the Mesozoic Grand Banks of Newfoundland. In: W. Manspeizer (ed.), Triassic-Jurassic Rifting: Continental Breakup and the Origin of the Atlantic Ocean and Passive Margins, Part A. Developments in Geotectonics 22, Elsevier, Amsterdam, p. 129-165.

Taylor, A.M. and Goldring, R. 1993. Description and analysis of bioturbation and ichnofabric. Journal of the Geological Society of London, v. 150, p. 141-148.

Taylor, A.M., Goldring, R. and Gowland, S. 2003. Analysis and application of ichnofabrics. Earth-Science Reviews, v. 60, p. 227-259.

Trevor, J.H. 1977. The burrowing of *Nereis diversicolor* (O.F. Müller), together with some observation on *Arenicola marina* (L.) (Annelida: Polychaeta). Journal of Experimental Marine Biology and Ecology, v. 30, p. 129-145.

Troy, 2005. Troy City Schools, New York, NY. Biology Webpage on Excretion and Locomotion. Viewed July 20, 2005. <http://www.troy.k12.ny.us/thsbiology/skinny/skinny_excreation_locomo.html>

Tsuchiya, M. and Kurihara, Y. 1979. The feeding habits and food sources of the deposit-feeding polychaete, *Neanthes japonica* (Izuka). Journal of Experimental Marine Biology and Ecology, v. 36, p. 79-89.

Tsuchiya, M. and Kurihara, Y. 1980. Effects of the feeding behavior of macrobenthos on changes in environmental conditions of intertidal flats. Journal of Experimental Marine Biology and Ecology, v. 44, p. 85-94.

Vavra, C.L., Kaldi, J.G. and Sneider, R.M. 1992. Geological applications of capillary pressure: a review. American Association of Petroleum Geologists Bulletin, v. 76, p. 840-850.

Vossler, S.M. and Pemberton, S.G. 1988. *Skolithos* in the Upper Cretaceous Cardium Formation: an ichnofossil example of opportunistic ecology. Lethaia, v. 21, p. 351-362.

Walker, R.G. 1984. Shelf and shallow marine sands. In: R.G. Walker (ed.), Facies Models, 2nd Edition, Geoscience Canada Reprint Series 1, p. 141-170.

Walker, R.G. 1992. Facies, facies models and modern stratigraphic concepts. In: R.G. Walker and N.P. James (eds.), Facies Models: Response to Sea Level Change. Geological Association of Canada, Geotext 1, p. 1–14.

Weber, K.J. 1982. Influence of common sedimentary structures on fluid flow in reservoir models. Journal of Petroleum Technology, v. 34, p. 665- 672.

Weber, K.J. 1986. How heterogeneity affects oil recovery. In: L.W. Lake and H.B. Carroll, Jr. (eds.), Reservoir Characterization. Academic Press Inc., Montreal, Quebec, p. 487-544.

Weimer, R.J., Howard, J.D. and Lindsay, D.R. 1982. Tidal Flats. In: P.A. Scholle and D. Spearing (eds.), Sandstone Depositional Environments. American Association of Petroleum Geologists Memoir 31, p. 191-246.

Welsink, H.J., Srivastava, S.P. and Tankard, A.J. 1989. Tectonic linkage between continental crust of the Grand Banks and oceanic crust during extension. In: A.J. Tankard and H.R. Balkwill (eds.), Extensional Tectonics and Stratigraphy of the North Atlantic Margins. American Association of Petroleum Geologists Memoir 46, p. 197-214.

Wheatcroft, R.A. 1990. Preservation potential of sedimentary event layers. Geology, v. 18, p. 843-845.

Wightman, D.M., Pemberton, S.G. and Singh, C. 1987. Depositional modeling of the Upper Mannville (Lower Cretaceous), east central Alberta: implications for the recognition of brackish water deposits. In: R.W. Tillman and K.J. Weber (eds.), Reservoir Sedimentology. Society of Economic Paleontologists and Mineralogists Special Publication 40, p. 189-220.

Wright, L.D. 1978. River deltas. In: R.A. Davis Jr. (ed.), Coastal Sedimentary Environments. Springer-Verlag, New York, 420 p.

Appendix 1

Pelosichnus mumorpha n. ichnogen., n. ichnosp.: Inclined to Branching, Mud-filled Burrows

A1.1 Introduction

Pelosichnus mumorpha n. ichnogen., n. ichnosp. is here proposed for the distinctive mud-filled burrows found in muddy to silty sandstones of the Aptian/Albian Ben Nevis interval, particularly subfacies B of Facies 6. Due to the two-dimensional nature of core, a complete burrow form has not been observed; however, multiple, variably oriented sections of the burrow system are visible due to high burrow density. These vantages allow sufficient representation of the burrow system for ichnotaxonomic classification, description and diagnosis. The generic term "*Pelosichnus*" is from the Greek "pelos" meaning mud and "ichnos" meaning trace. The specific epithet "*mumorpha*", is also Greek; it refers to the burrow's shape or form, which bears an uncanny resemblance to "μ" (or "mu"), the 12th letter of the Greek alphabet. *Pelosichnus mumorpha* is interpreted as a dwelling burrow of a worm-like organism, mostly because it shares many characteristics with modern burrow systems produced by nereid polychaetes.

A1.2 Occurrence

Inclined, mud-filled burrows are preserved in full relief within cored intervals from the Hibernia Field. They are found in all three subfacies of Facies 6 from the Aptian/Albian Ben Nevis interval. Facies 6 consists of muddy to silty sandstone representing the lower shoreface domain on a deltaically influenced shelf; more specifically, it lies within the delta front zone. Some intervals of Facies 6 (especially within F6B) contain such high densities of *Pelosichnus mumorpha* that the bioturbate texture is typically dominated by it (see Figures 5.1, 5.2). Other trace fossils found in close association with *Pelosichnus* n. ichnogen. include *Phycosiphon, Planolites, Scolicia* and *Thalassinoides*; the latter three commonly cross-cut the earlier emplaced mud-filled burrows. Reoccurrence of *Pelosichnus mumorpha* through space and time is not addressed here, as no pertinent descriptions have been encountered in the literature to date; however, comparable mud-filled burrows have been informally recognized in siliciclastic deposits of similar age (M. Gingras, pers. comm.).

A1.3 Description

The trace fossil under consideration consists of a U-shaped tube with a downward extension that is inclined to rarely vertical (Figure A1.1). The paired shafts of the "U" as well as the downward extension are rarely bifurcated. Where present, the bifurcations vary in number and are oblique to the main shaft. Upward-directed branches approach vertical and sometimes flare into a subtle cone, while downward-directed branches are inclined to horizontal and exhibit club-shaped terminations. Burrow diameter averages 3–4 mm and the total length of the structure rarely exceeds 1-20 cm, with the "U" accounting for the uppermost few centimeters. Even though the burrow system appears to be ubiquitously filled with mud-sized particles, the nature of the fill is actually quite variable (Figure A1.1). Some segments of the burrow system are sand-filled and concentrically lined with mud, silt and sand up to 3 mm thick. These linings do not appear to contain fecal pellets. Other segments contain meniscate fill that is highlighted by the alternation of clay, silt or very fine sand grains with fecal pellets. Depending on the line of section, these latter fills can sometimes appear structureless or textureless.

A1.4 Preservation

Trace fossil identification in core can be quite difficult owing to the unique perspective that core provides. The difficulty also increases with increasing rates or degrees of bioturbation. In highly bioturbated units, the lower or deepest portion of a trace fossil is preferentially preserved over the shallow portion (Bromley, 1996). As the organism adjusts its position with respect to the water-sediment interface, it reworks structures that were emplaced earlier. In the case of continuous sedimentation, the deeper tier perpetually cross cuts or eventually obliterates the shallower tier. Diagenetic effects such as cementation, dissolution and compaction also can alter the appearance of the trace fossil from its original form. *Pelosichnus mumorpha* in core from the Ben Nevis interval falls victim to all of these impediments. Its potentially complex, three-dimensional habit has little chance of being preserved, and therefore observed, in its entirety. In addition, the interval in which it is best developed is intensely to completely bioturbated. While lowermost portions of the burrow system are very well preserved, upper portions are much more rare and only partially preserved. Siderite, which is most prolific in calcite-cemented intervals, preferentially invades the muddy matrix of the burrow fill. This process typically includes some replacement, thus the internal

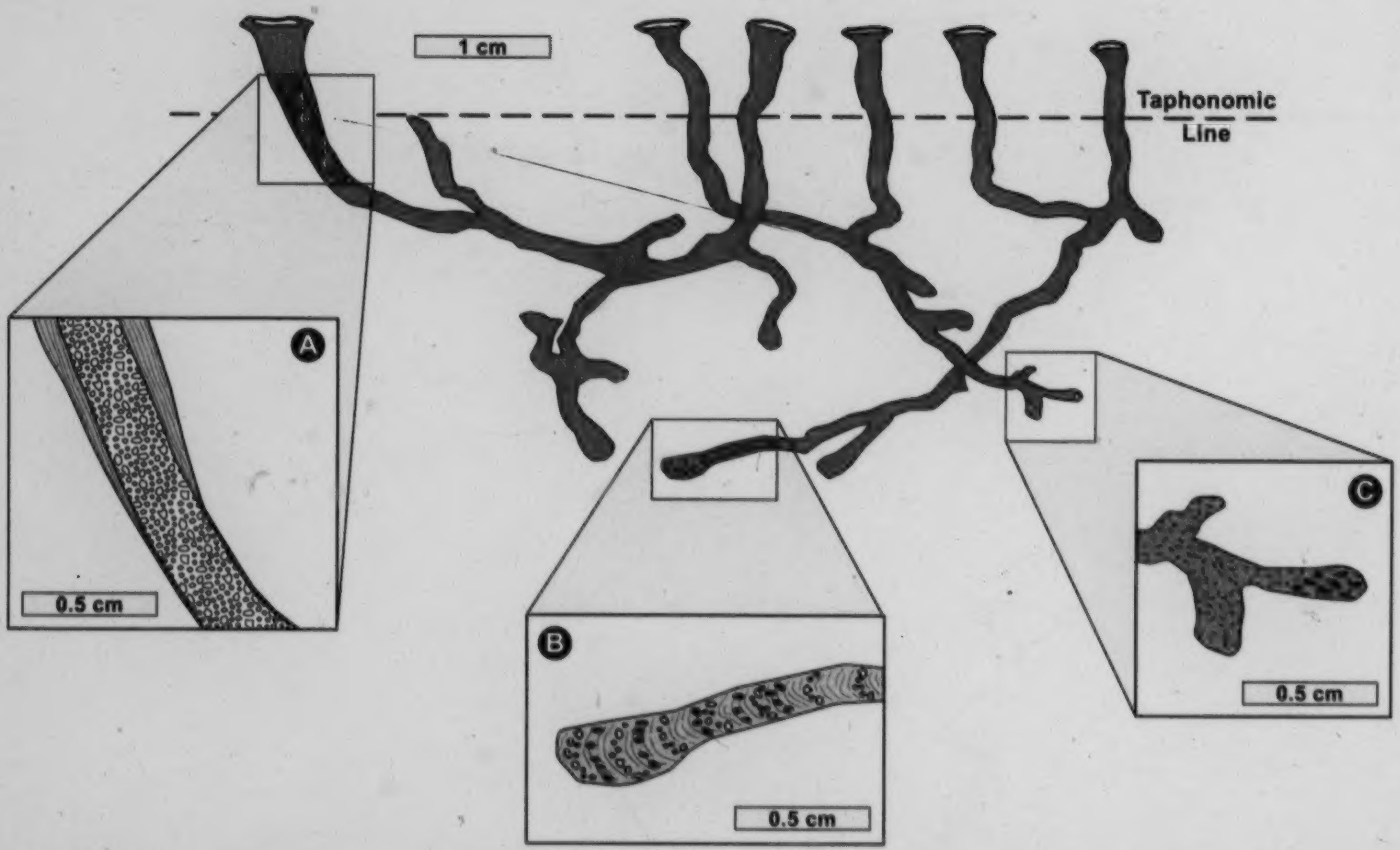

Figure A1.1: Gross morphology of *Pelosichnus mumorpha*, as interpreted from core. The taphonomic line denotes the uppermost limit of the burrow system that is most likely to be preserved in the rock record. A) Sand-filled core surrounded by concentric mud laminae. B) Meniscate back-fill containing mud particles alternating with silt and sand particles as well as fecal pellets. C) Massive or textureless mud fill containing some fecal pellets.

structure of the burrow system may be masked. However, because *Pelosichnus* occurs in such high concentrations over such a substantial interval of core, the burrow system is dissected extensively enough to allow all the "pieces of the puzzle" to be amalgamated into a reasonable representation of the burrow system.

In core, *Pelosichnus mumorpha* is predominantly represented by the lowermost portion of its burrow system (Figure A1.2; A1.3). This includes mud-filled, concave-up arc- or clinoform-shaped tubes that are several centimeters in length and may display Y-shaped, downward-directed bifurcations. Both the tubes and branches exhibit widespread development of club-shaped

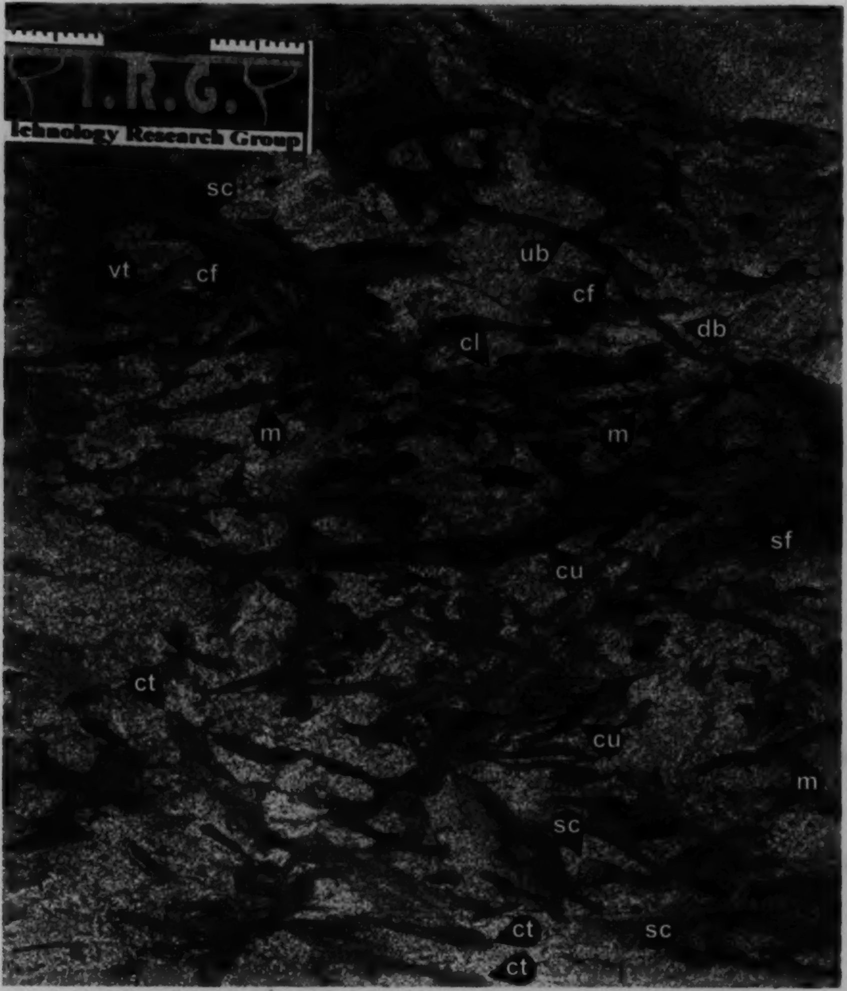

Figures A1.2: Characteristic features of *Pelosichnus* in core: club-shaped terminations (ct), concentric lining (cl), sandy core (sc), upward branching (ub), downward branching (db), meniscate fill or spreiten (m), concave-up arcs (cu), clinoform structures (cf), structureless fill (sf) and vertical mud-filled tube (vt) .

terminations and most commonly exhibit structureless and meniscate fill. Aspects that represent the uppermost portion of the burrow system are more rare in occurrence. These include inclined to vertical tubes that maintain a consistent diameter and are filled with structureless mud, or much more rarely, shafts and tunnels that flare upward and consist of a very fine grain sand core concentrically surrounded by mud and sand layers. With increasing bioturbation intensity or residency, interpenetrations become very common. Where *Pelosichnus* occur in high density, a very characteristic crosshatch pattern consisting of arcs and clinoforms (cross cutting each other obliquely) is produced.

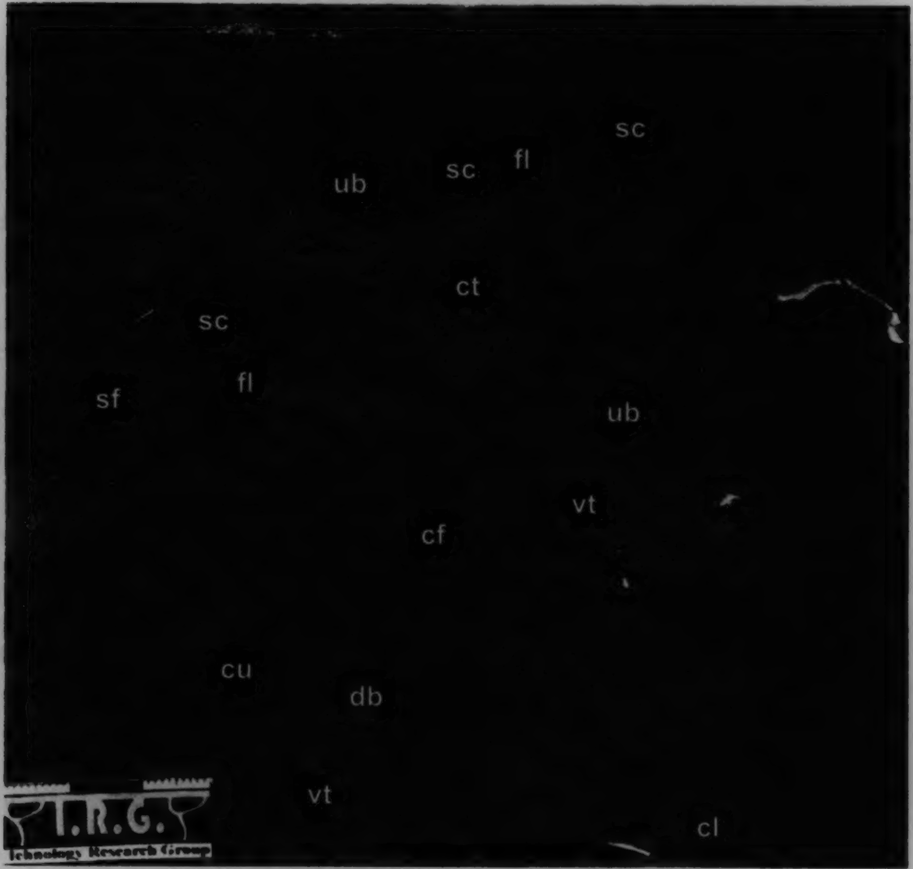

Figures A1.3: Characteristic features of *Pelosichnus* in core: club-shaped terminations (ct), concentric lining (cl), sandy core (sc), upward branching (ub), downward branching (db), concave-up arcs (cu), clinoform structures (cf), structureless fill (sf), vertical mud-filled tube (vt) and flaring upward tube (fl).

A1.5 Comparison to other Trace Fossils

Pelosichnus shares characteristics with several other ichnogenera (Figure A1.4). Depending on the angle of intersection, some vertical sections through concentrically lined portions of the burrow system resemble *Cylindrichnus*. Vertical or oblique sections, through horizontal and vertical segments that are filled with meniscate or massive mud, can appear identical to *Planolites*, *Arenicolites* or *Skolithos*. A section through a sandy core could look like *Palaeophycus*. *Pelosichnus* has the most in common with *Polykladichnus*, a vertical, Y-shaped, upward-branching burrow that has a thick silt lining (Fürsich, 1981). However, key differences preclude placement of the mud-filled burrows into the *Polykladichnus* ichnogenus. These differences include the dominantly inclined to horizontal habit, arc or clinoform-shaped segments, downward branching, club-shaped terminations and variability in burrow fill of *Pelosichnus*. It is important to note that if *Pelosichnus* occurs in low abundance, it may be mistaken as belonging to one of these ichnogenera.

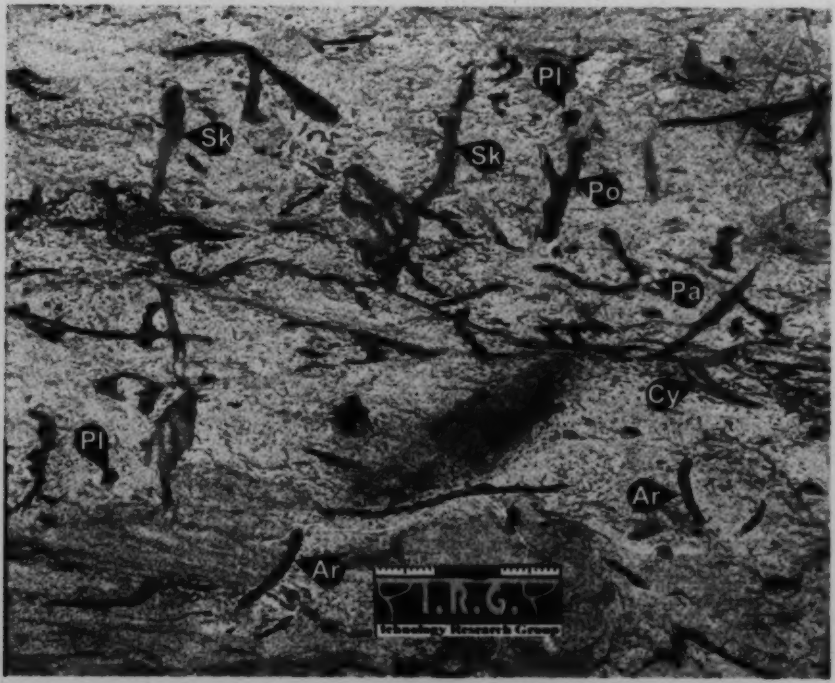

Figure A1.4: *Pelosichnus* shares characteristics with several other ichnogenera and therefore can be misinterpreted as those other ichnogenera in cored intervals. In low density, *Pelosichnus mumorpha* can be mistaken for *Skolithos* (Sk), *Arenicolites* (Ar), *Planolites* (Pl), *Cylindrichnus* (Cy), *Palaeophycus* (Pa) or *Polykladichnus* (Po), depending on where the plane of section intersects the *Pelosichnus* burrow system.

Pelosichnus is also similar to bow-form burrows described by Goldring (1996) and Goldring *et al.* (2002) in some respects. Commonalities include an arc or bow shape, variable fill and local development of a core, although the core is filled with sand in *Pelosichnus* and mud in the bow-form burrows. All other characteristics are unique to each burrow type, thereby prohibiting any further comparison. However, when dense, interpenetrating fabrics of the two traces are juxtaposed, similar crosshatch patterns are recognized (Figure A1.5).

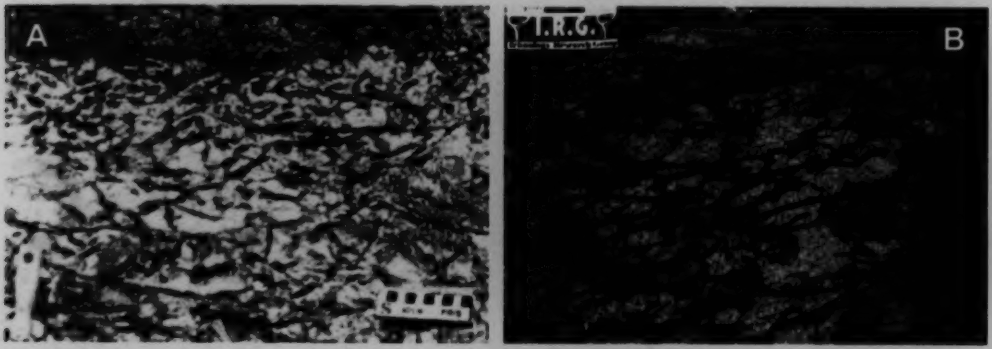

Figure A1.5: In cross section, bow-form burrows described by Goldring (1996) and Goldring *et al.* (2002) (A) appear very similar to intensely bioturbated intervals of F6B containing *Pelosichnus mumorpha* (B).

A1.6 Interpretation of Burrow Morphology

The size and shape of *Pelosichnus mumorpha* suggest that the producer was probably a vermiform organism several millimeters in diameter and several centimeters to tens of centimeters in length. The concentric lining common to the "U" portion of the burrow acted to stabilize the apertures and burrow walls. It is unclear whether the inhabitant intentionally constructed the lining or indirectly created it by pressing the sediment that fell into the burrow onto the wall. In either case, the burrow was obviously kept open by the inhabitant to maintain a permanent connection to the sediment-water interface; additional upward-directed branches provided multiple openings to the sediment water interface. Sand-filled cores reflect passive infiltration subsequent to abandonment of the burrow, while structureless and meniscate fills containing fecal pellets represent active backfill or possibly stowage. An enlarged chamber (as indicated by club-shaped terminations) was produced at the end of downward-directed extensions and branches. Although the organism occupied the U-shaped portion of its burrow system most frequently, it probably retreated into the chamber periodically to escape a predator, rest or consume food. Considering their mud-filled nature, the shafts and tunnels leading to the chamber were more likely used as organic or fecal matter storage areas (Schäfer, 1972). Eventually these shafts and tunnels are filled and new branches are created.

Pelosichnus mumorpha is interpreted as a dwelling burrow of a suspension- or detritus-feeding worm. The "U" shape facilitates irrigation and flushing of the burrow network and multiple upward-directed branches allow easy access to the water-sediment interface. The burrow system is semi-permanent to permanent; deep-seated branches allow the organism to store decomposing matter and faeces at a distance from the U-shaped, irrigated "living room".

A1.7 Modern Analogue

Pelosichnus mumorpha is very similar to the burrow systems produced by polychaetes of the Nereididae family, which in addition to *Nereis* (Figure A1.6) includes the genera *Neanthes* and *Hediste*. The nereids are segmented worms, up to 30 cm in length and 1 cm in diameter, that have a jawed, eversible pharynx or proboscis. Each segment bears a pair of parapodia with setae, which are used for locomotion and anchorage (nereids "grasp" the burrow wall with their setae: Trevor, 1977). Although nereids can potentially inhabit a wide range of marginal marine and marine environments *(Nereis*, for example, can tolerate a great range of salinity conditions, from freshwater to at least 200% of normal seawater (Oglesby, 1969)), they are most commonly found

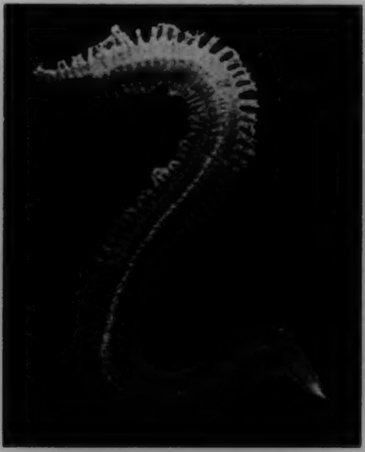

Figure A1.6: *Nereis diversicolor*, a segmented, polychaete worm known to produce burrow systems that are similar to *Pelosichnus mumorpha* (Image modified from Troy, 2005)

in intertidal, estuarine settings (Trevor, 1977; Scaps, 2002).

Nereid worms are omnivorous and reported to collect food in a number of different ways. The three most common methodologies, as reviewed by Esnault *et al.* (1990) and Caron *et al.* (2004), include collecting fine-grained particles and organics near its burrow opening (detritus-feeding), crawling on the sediment surface prospecting for food (predation) and capturing suspended particles with mucous nets either on the sediment-water interface, at the burrow aperture or within the burrow (suspension-feeding). In addition, juveniles have been observed to store plant detritus in their burrow, from which they harvest bacteria (gardening: Olivier *et al.*, 1995). Predation is most likely an aberrant behavior employed by polychaetes under duress. Tsuchiya and Kurihara (1979; 1980) reported a bacteria-rich diet for *Neanthes japonica*, suggesting that detritus or suspension feeding is "normal" behavior for nereid worms.

Nereids inhabits a mucus-lined burrow that is excavated in sandy mud or muddy sand but also gravels, clays and even turf (Clay, 1967). The architecture of nereid burrows is summarized by Schäfer (1972), Hertweck (1986) and Davey (1994). These polychaetes initially produce a U-shaped burrow, to which they add a further downward stem to create a "Y" or "μ" form (Figure

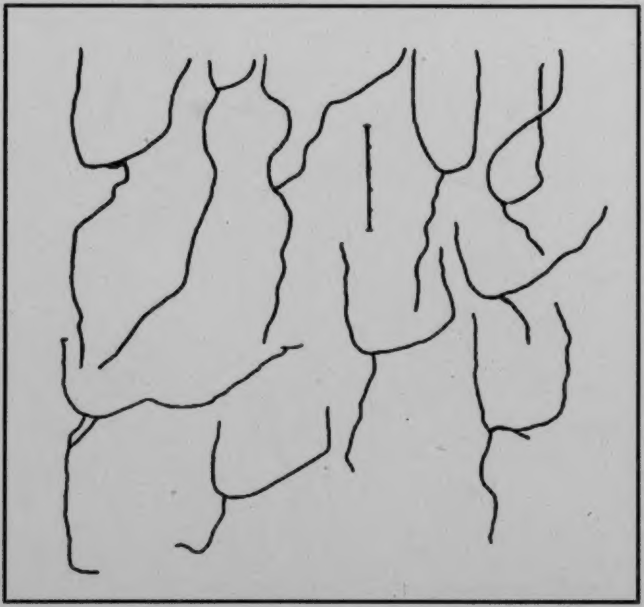

Figure A1.7: Traced radiographic images of U- and Y-shaped burrows each built within 24 hours by 10 different *Nereis diversicolor* in laboratory containers. Scale bar is 5 cm long. (Modified from Davey, 1994)

A1.7). Davey (1994) noted that subsequent development of this Y-shaped burrow resulted in its elaboration into an upward and downward, multi-branched structure with up to 6 openings (Figure A1.8). However, he also suggested that because adult nereids are territorial and defend their burrows against intruders, as population density rises, so logically must the restrictions on the size,

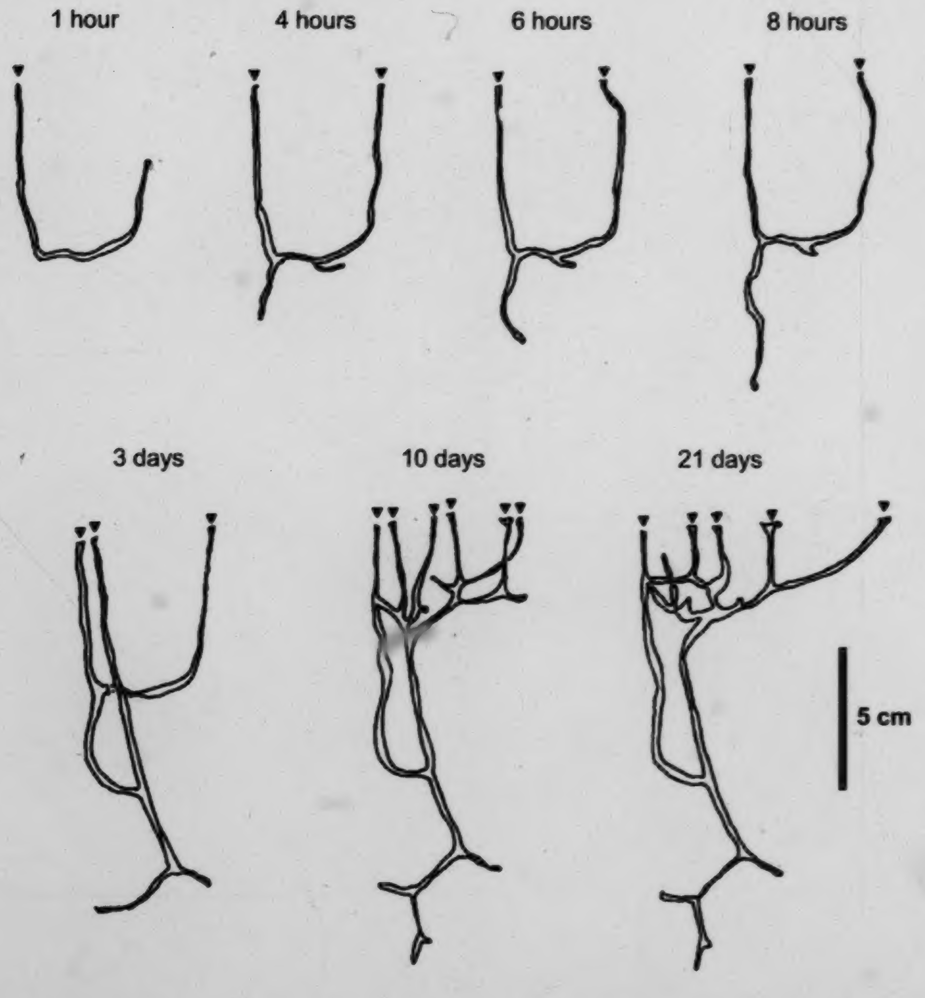

Figure A1.8: Traced series of radiographic images showing the progressive development of a nereid burrow over the time indicated. Arrows at the top of each burrow figure represent open connections to the water-sediment interface. (Modified from Davey, 1994)

extent and degree of branching of an individual's burrow.

Nereids have been observed to carry out several behaviors that are also represented in *Pelosichnus*. The key parallel is that they tend to press sediment that has recently entered the burrow against the wall by peristaltic and undulating movements (Schäfer, 1972, as reported from Reineck, 1958). Seilacher (1957) reported reaming or lining within nereid burrows, which he suggested resulted from stowing activity related to food turn-over (as discussed by Schäfer, 1972 and Bromley, 1996). In addition, casts of modern nereid burrows commonly exhibit enlarged, club-shaped terminations (L. Zabcic, pers. comm.).

Other reported peculiarities in burrow morphology include networks of horizontal burrows preferentially produced in sediment layers that are favourable for digging (Schäfer, 1972) and irregularly meandering branches (Hertweck, 1986). Hertweck (1986) also noted reticulate imprints on the inside of the burrow walls originating from movements of the parapodia.

A1.8 Environmental Significance

Based on its distribution in the Avalon/Ben Nevis interval and similarity to nereid burrows, *Pelosichnus* is interpreted to occur in marginal marine to marine settings. Its presence reflects low to moderate energy conditions, ample supply of suspended particles and detritus, and relatively stable substrates. When *Pelosichnus* appears in high density (as in Facies 6B), its occurrence represents opportunistic behavior in response to stressed environmental conditions, such as fluctuating salinity, oxygen levels, temperature, turbidity, etc. Such instability is most commonly associated with restricted, brackish water settings that include lagoons, bays and tidal flats/deltas/channels within deltaic or estuarine systems.

A1.9 Summary

The description and interpretation of *Pelosichnus* provided here will hopefully lead to future recognition of this trace fossil and vindication of its establishment as a new ichnogenus. It probably already is a part of the ever expanding ichnological database; however, because it bears similarity to *Cylindrichnus, Planolites, Skolithos/Arenicolites* and *Polykladichnus*, it may be unknowingly identified as such.

Appendix 2

Lithologs

Note:

All cored intervals are represented in core depth. The legend for all symbols is provided below.

LEGEND

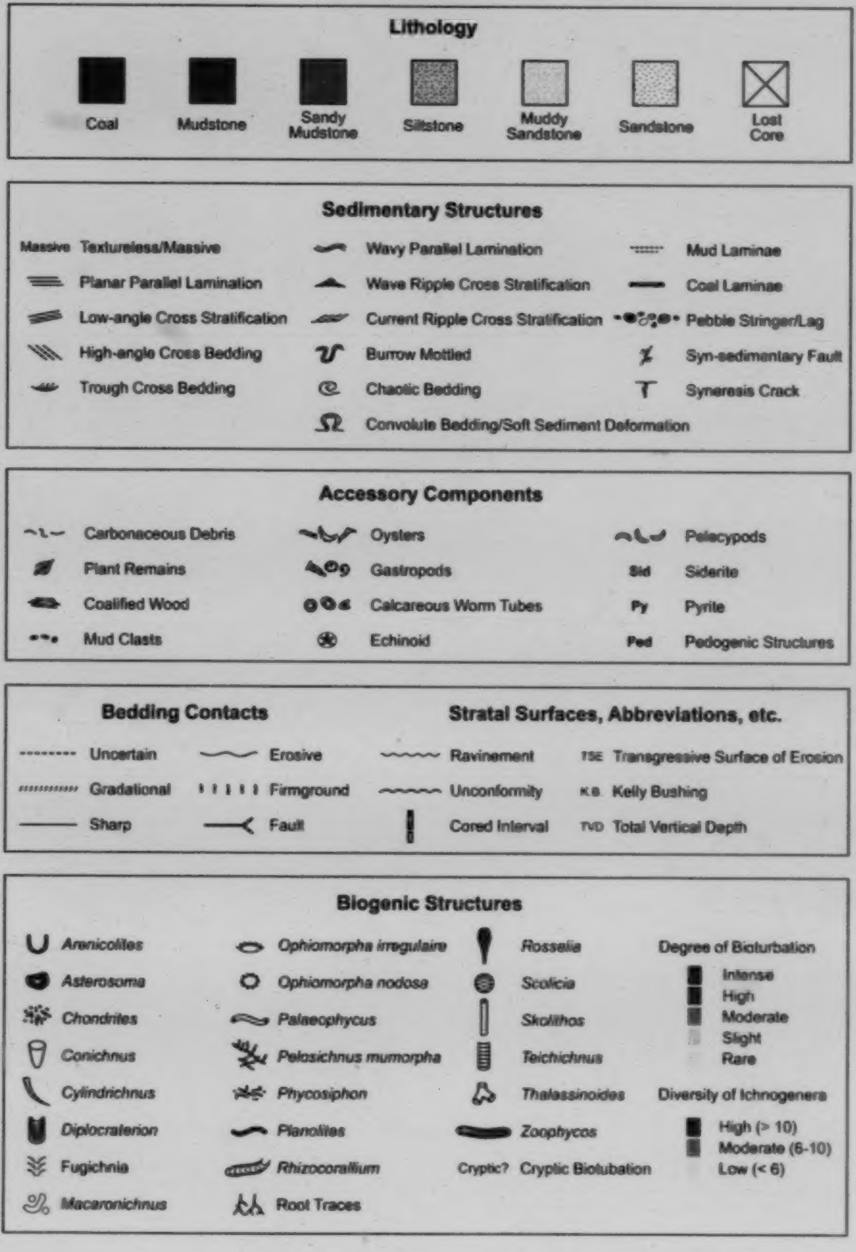
Lithology
Coal
Mudstone
Sandy Mudstone
Siltstone
Muddy Sandstone
Sandstone
Lost Core
Sedimentary Structures
Massive
Textureless/Massive
Planar Parallel Lamination
Low-angle Cross Stratification
High-angle Cross Bedding
Trough Cross Bedding
Wavy Parallel Lamination
Wave Ripple Cross Stratification
Current Ripple Cross Stratification
Burrow Mottled
Chaotic Bedding
Convolute Bedding/Soft Sediment Deformation
Mud Laminae
Coal Laminae
Pebble Stringer/Lag
Syn-sedimentary Fault
Syneresis Crack
Accessory Components
Carbonaceous Debris
Plant Remains
Coalified Wood
Mud Clasts
Oysters
Gastropods
Calcareous Worm Tubes
Echinoid
Pelecypods
Sid
Siderite
Py
Pyrite
Ped
Pedogenic Structures
Bedding Contacts
Uncertain
Gradational
Sharp
Erosive
Firmground
Fault
Stratal Surfaces, Abbreviations, etc.
Ravinement
Unconformity
Cored Interval
TSE
Transgressive Surface of Erosion
K.B.
Kelly Bushing
TVD
Total Vertical Depth
Biogenic Structures
Arenicolites
Asterosoma
Chondrites
Conichnus
Cylindrichnus
Diplocraterion
Fugichnia
Macaronichnus
Ophiomorpha irregulaire
Ophiomorpha nodosa
Palaeophycus
Pelosichnus mumorpha
Phycosiphon
Planolites
Rhizocorallium
Root Traces
Rosselia
Scolicia
Skolithos
Teichichnus
Thalassinoides
Zoophycos
Cryptic?
Cryptic Biotubation
Degree of Bioturbation
Intense
High
Moderate
Slight
Rare
Diversity of Ichnogenera
High (> 10)
Moderate (6-10)
Low (< 6)

Hibernia B-16 3
Cores 1 & 2

Cored Interval:
(Depth from K.B.)
2561.25 - 2589 m

Note: Deviated Well

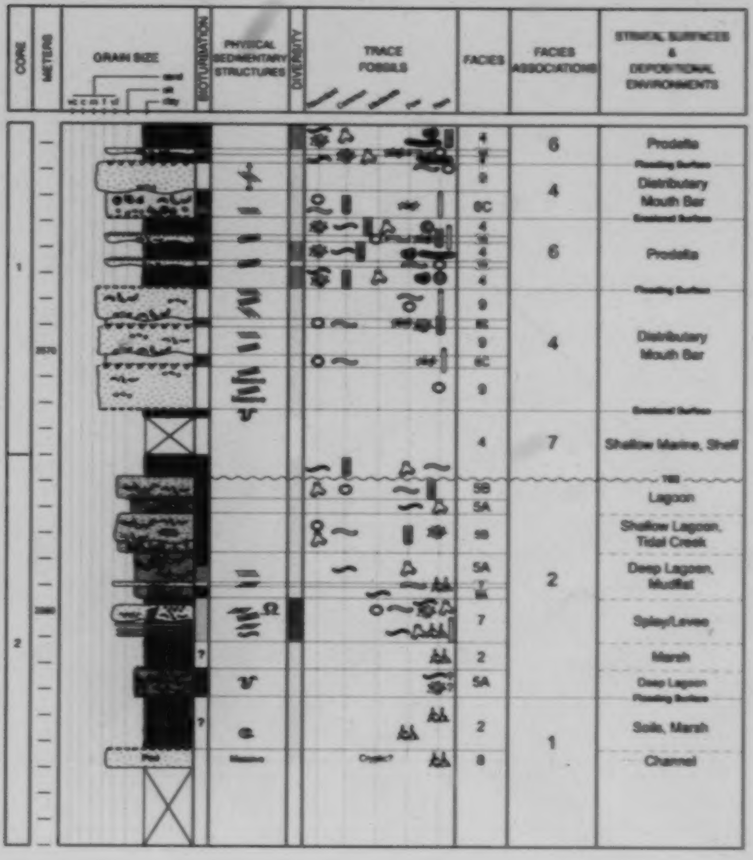
CORE
METERS
GRAIN SIZE
sand
silt
clay
BIOTURBATION
PHYSICAL SEDIMENTARY STRUCTURES
DIVERSITY
TRACE FOSSILS
FACIES
FACIES ASSOCIATIONS
STRATAL SURFACES & DEPOSITIONAL ENVIRONMENTS
1
2
2570
2580
4
9
8C
4
4
4
9
9
8C
9
4
5B
5A
5B
5A
7
2
5A
2
8
6
4
6
4
7
2
1
Prodelta
Flooding Surface
Distributary Mouth Bar
Erosional Surface
Prodelta
Flooding Surface
Distributary Mouth Bar
Erosional Surface
Shallow Marine, Shelf
Lagoon
Shallow Lagoon, Tidal Creek
Deep Lagoon, Mudflat
Splay/Levee
Marsh
Deep Lagoon
Flooding Surface
Soils, Marsh
Channel
?
?

Hibernia B-16 19Z

Core 1

Cored Interval:
(Depth from K.B.)
4080 - 4122.5 m

Note: Deviated Well

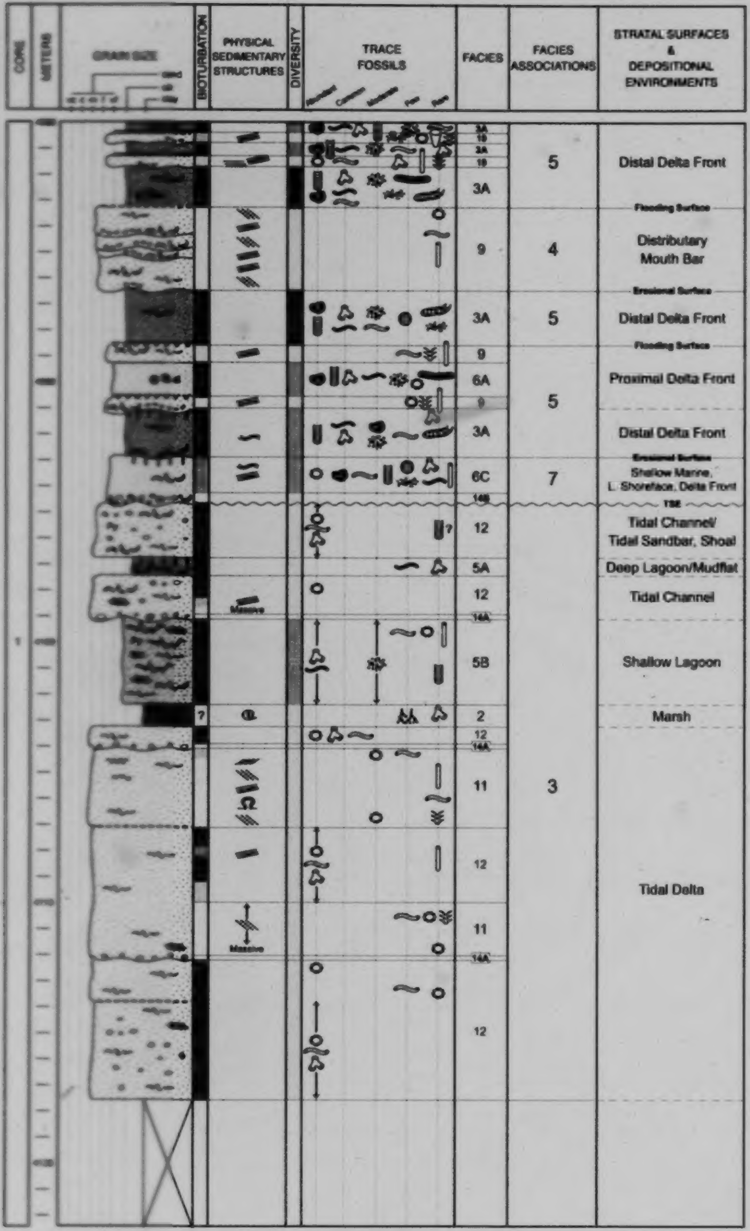
CORE
METERS
GRAIN SIZE
BIOTURBATION
PHYSICAL SEDIMENTARY STRUCTURES
DIVERSITY
TRACE FOSSILS
FACIES
FACIES ASSOCIATIONS
STRATAL SURFACES & DEPOSITIONAL ENVIRONMENTS
3A
5
Distal Delta Front
Flooding Surface
9
4
Distributary Mouth Bar
Erosional Surface
3A
5
Distal Delta Front
Flooding Surface
9
6A
Proximal Delta Front
9
5
3A
Distal Delta Front
Erosional Surface
6C
7
Shallow Marine, L. Shoreface, Delta Front
14B
TSE
12
Tidal Channel/ Tidal Sandbar, Shoal
5A
Deep Lagoon/Mudflat
Massive
12
Tidal Channel
14A
5B
Shallow Lagoon
?
2
Marsh
12
14A
11
3
12
Tidal Delta
Massive
11
14A
12

Hibernia B-16 19Z

Core 2

Cored Interval:
(Depth from K.B.)
4122.5 - 4141.5 m

Note: Deviated Well

Well continued from previous page

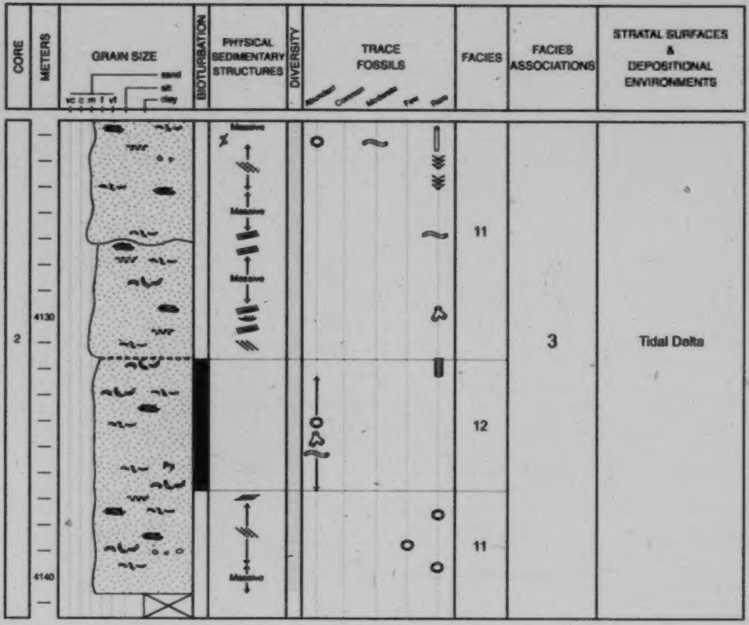
CORE
METERS
GRAIN SIZE
sand
silt
clay
vc c m f vf
BIOTURBATION
PHYSICAL SEDIMENTARY STRUCTURES
DIVERSITY
TRACE FOSSILS
FACIES
FACIES ASSOCIATIONS
STRATAL SURFACES & DEPOSITIONAL ENVIRONMENTS
Massive
Massive
Massive
Massive
4130
4140
2
11
12
11
3
Tidal Delta

Hibernia B-16 20Y

Core 1

Cored Interval:
(Depth from K.B.)
5830 - 5851 m

Note: Deviated Well

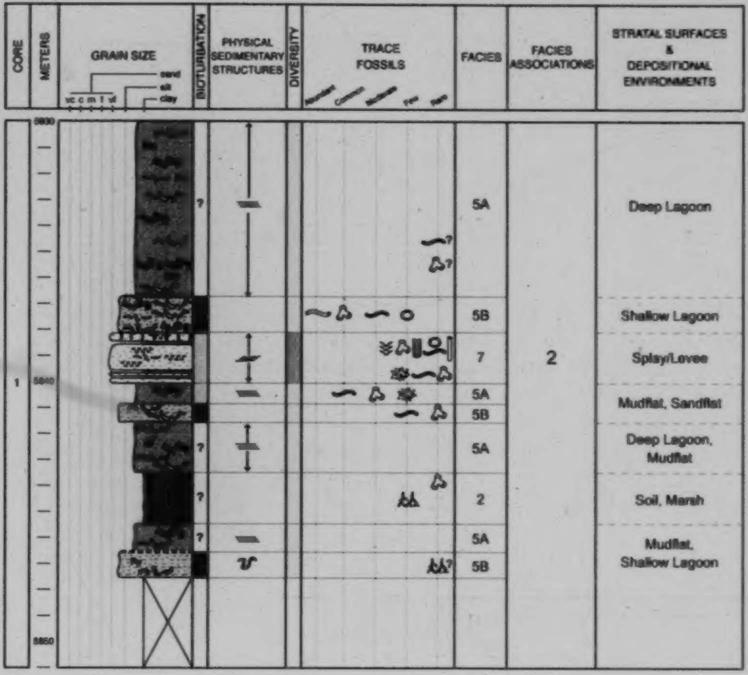
CORE
METERS
GRAIN SIZE
sand
silt
clay
vc c m f vf
BIOTURBATION
PHYSICAL SEDIMENTARY STRUCTURES
DIVERSITY
TRACE FOSSILS
FACIES
FACIES ASSOCIATIONS
STRATAL SURFACES & DEPOSITIONAL ENVIRONMENTS
5830
1
5840
5850
?
5A
5B
7
2
Deep Lagoon
Shallow Lagoon
Splay/Levee
Mudflat, Sandflat
Deep Lagoon, Mudflat
Soil, Marsh
Mudflat, Shallow Lagoon

Hibernia B-16 23

Core 1

Cored Interval:
(Depth from K.B.)
4123 - 4155.1 m

Note: Deviated Well

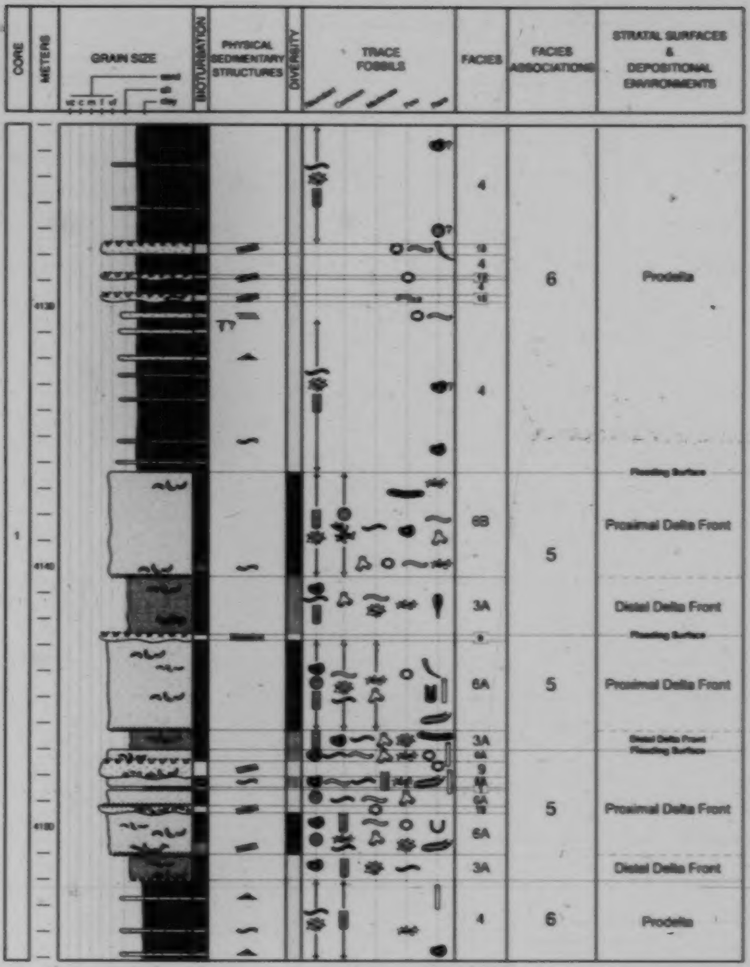
CORE
METERS
GRAIN SIZE
sand
silt
clay
vc c m f vf
BIOTURBATION
PHYSICAL SEDIMENTARY STRUCTURES
DIVERSITY
TRACE FOSSILS
FACIES
FACIES ASSOCIATIONS
STRATAL SURFACES & DEPOSITIONAL ENVIRONMENTS
1
4130
4140
4150
4
4
6B
3A
6A
3A
6A
9
6A
3A
4
6
5
5
5
6
Prodelta
Flooding Surface
Proximal Delta Front
Distal Delta Front
Flooding Surface
Proximal Delta Front
Distal Delta Front
Flooding Surface
Proximal Delta Front
Distal Delta Front
Prodelta

Hibernia B-16 23
Cores 2 & 3

Cored Interval:
(Depth from K.B.)
4237 - 4290.6 m

Note: Deviated Well

Well continued from previous page

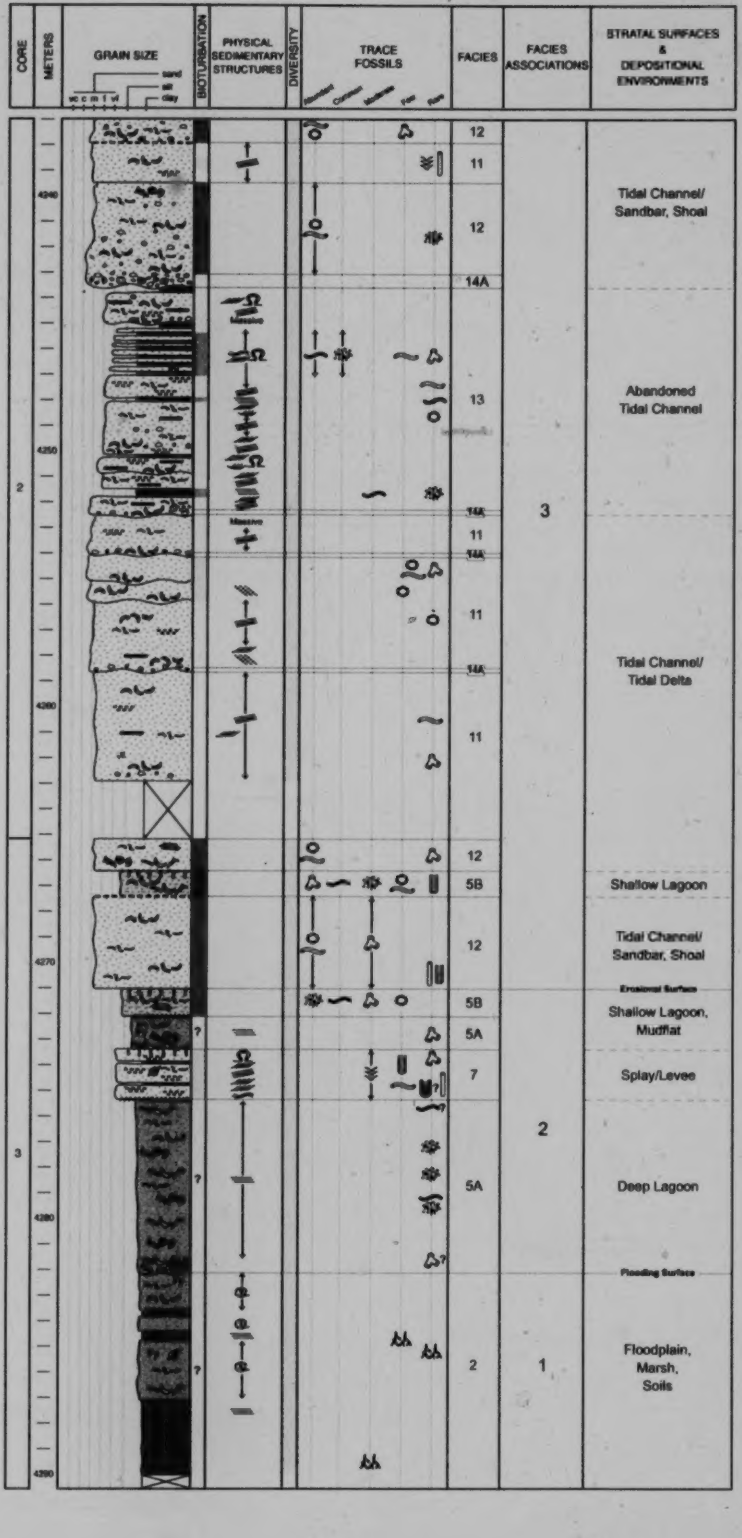
CORE
METERS
GRAIN SIZE
sand
silt
clay
vc c m f vf
BIOTURBATION
PHYSICAL SEDIMENTARY STRUCTURES
DIVERSITY
TRACE FOSSILS
FACIES
FACIES ASSOCIATIONS
STRATAL SURFACES & DEPOSITIONAL ENVIRONMENTS
2
3
4240
4250
4260
4270
4280
4290
Massive
?
12
11
12
14A
13
14A
11
14A
11
14A
11
12
5B
12
5B
5A
7
5A
2
3
2
1
Tidal Channel/ Sandbar, Shoal
Abandoned Tidal Channel
Tidal Channel/ Tidal Delta
Shallow Lagoon
Tidal Channel/ Sandbar, Shoal
Erosional Surface
Shallow Lagoon, Mudflat
Splay/Levee
Deep Lagoon
Flooding Surface
Floodplain, Marsh, Soils

Hibernia B-16 25
Cores 1 & 2

Cored Interval:
(Depth from K.B.)
4199 - 4296 m

Note: Deviated Well

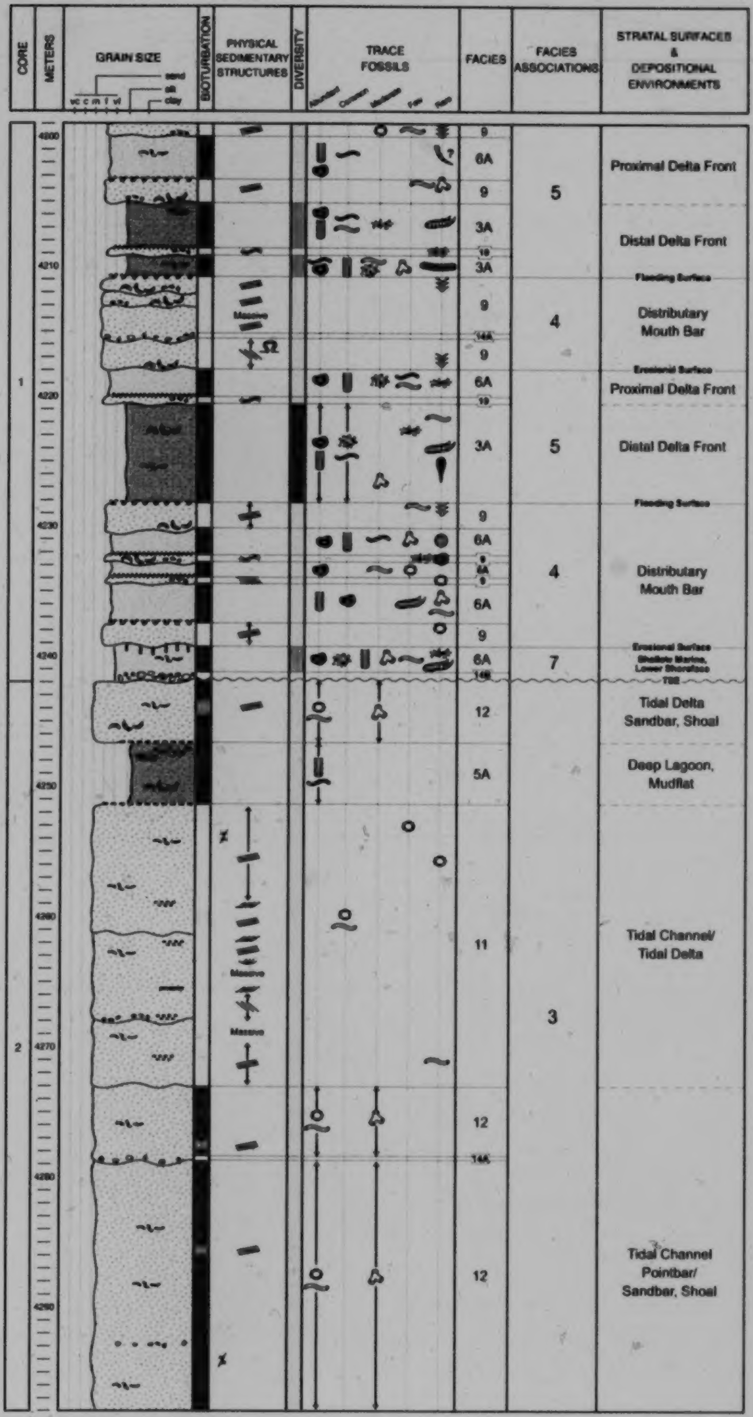
CORE
METERS
GRAIN SIZE
sand
silt
clay
vc c m f vf
BIOTURBATION
PHYSICAL SEDIMENTARY STRUCTURES
DIVERSITY
TRACE FOSSILS
FACIES
FACIES ASSOCIATIONS
STRATAL SURFACES & DEPOSITIONAL ENVIRONMENTS
4200
4210
4220
4230
4240
4250
4260
4270
4280
4290
1
2
Massive
Massive
Massive
9
6A
9
3A
10
3A
9
14A
9
6A
10
3A
9
6A
9
6A
9
6A
9
6A
14B
12
5A
11
12
14A
12
5
4
5
4
7
3
Proximal Delta Front
Distal Delta Front
Flooding Surface
Distributary Mouth Bar
Erosional Surface
Proximal Delta Front
Distal Delta Front
Flooding Surface
Distributary Mouth Bar
Erosional Surface
Shallow Marine, Lower Shoreface
TSE
Tidal Delta Sandbar, Shoal
Deep Lagoon, Mudflat
Tidal Channel/ Tidal Delta
Tidal Channel Pointbar/ Sandbar, Shoal

Hibernia B-27
Cores 1 & 2

Cored Interval:
(Depth from K.B.)
2545.4 - 2581.9 m

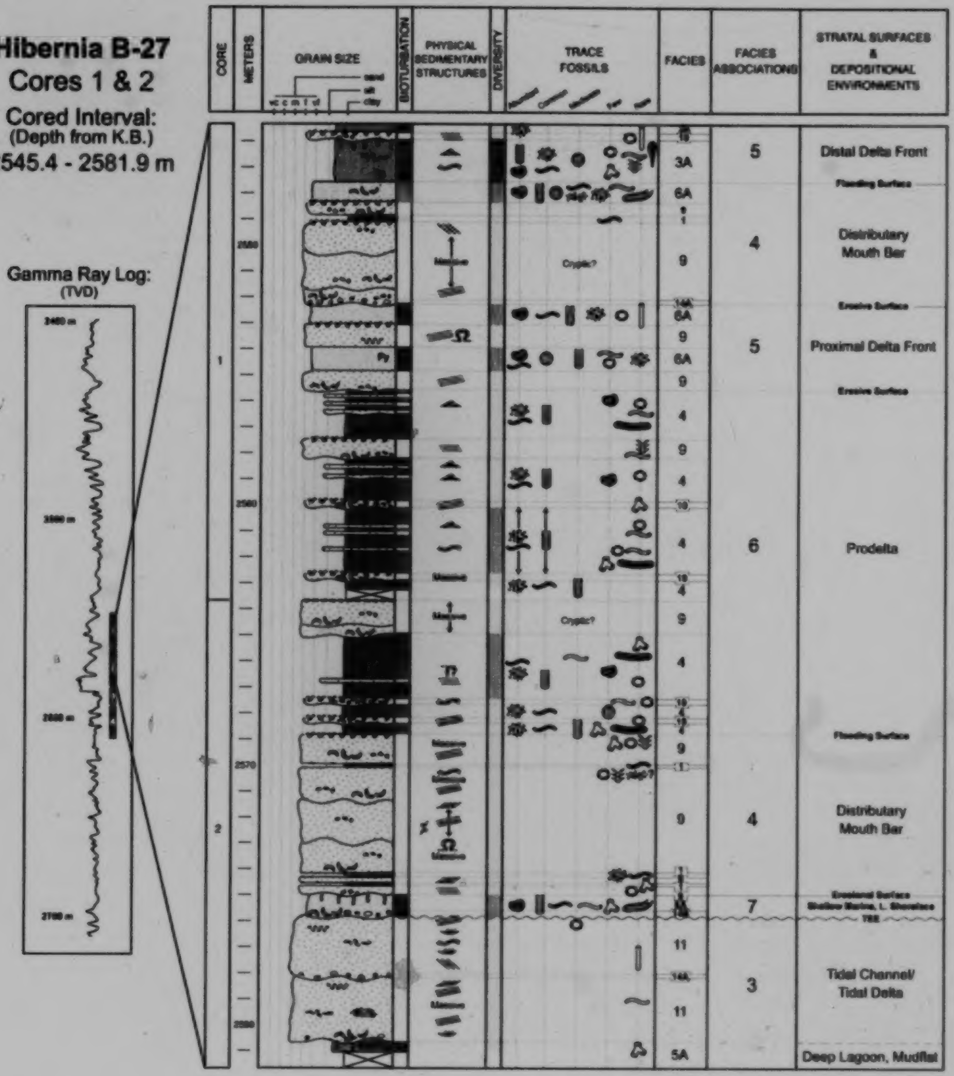

Hibernia B-27

Cores 3 & 4

Cored Interval:
(Depth from K.B.)
2581.9 - 2610 m

Well continued from previous page

Gamma Ray Log:
(TVD)

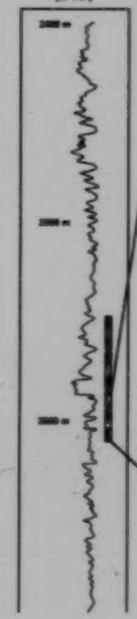

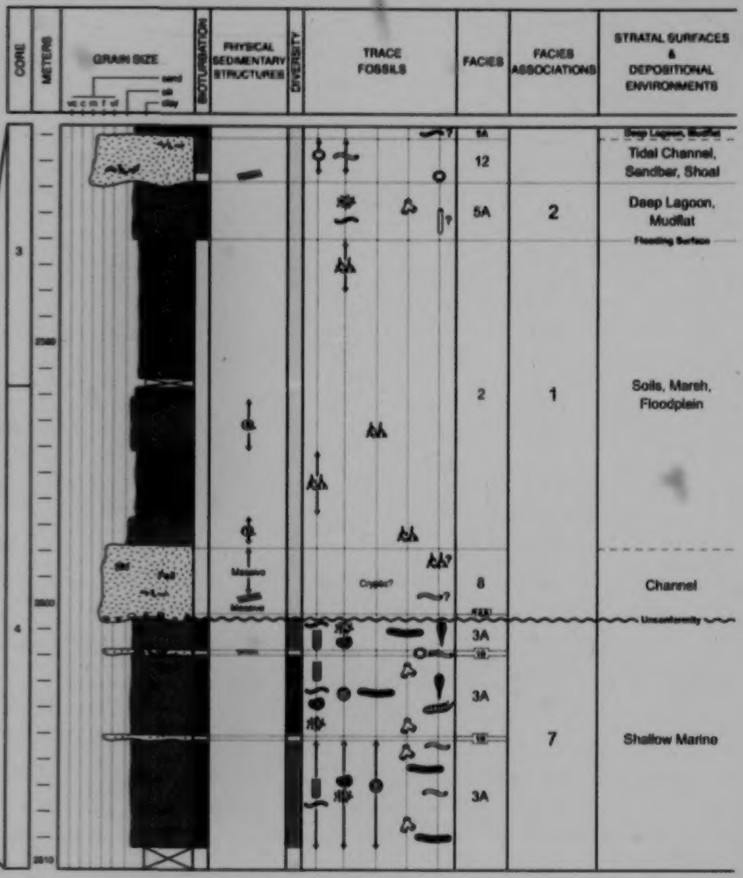

Hibernia B-44

Cores 1 & 2(upper)

Cored Interval:
(Depth from K.B.)
2865 - 2918 m

Note: Deviated Well

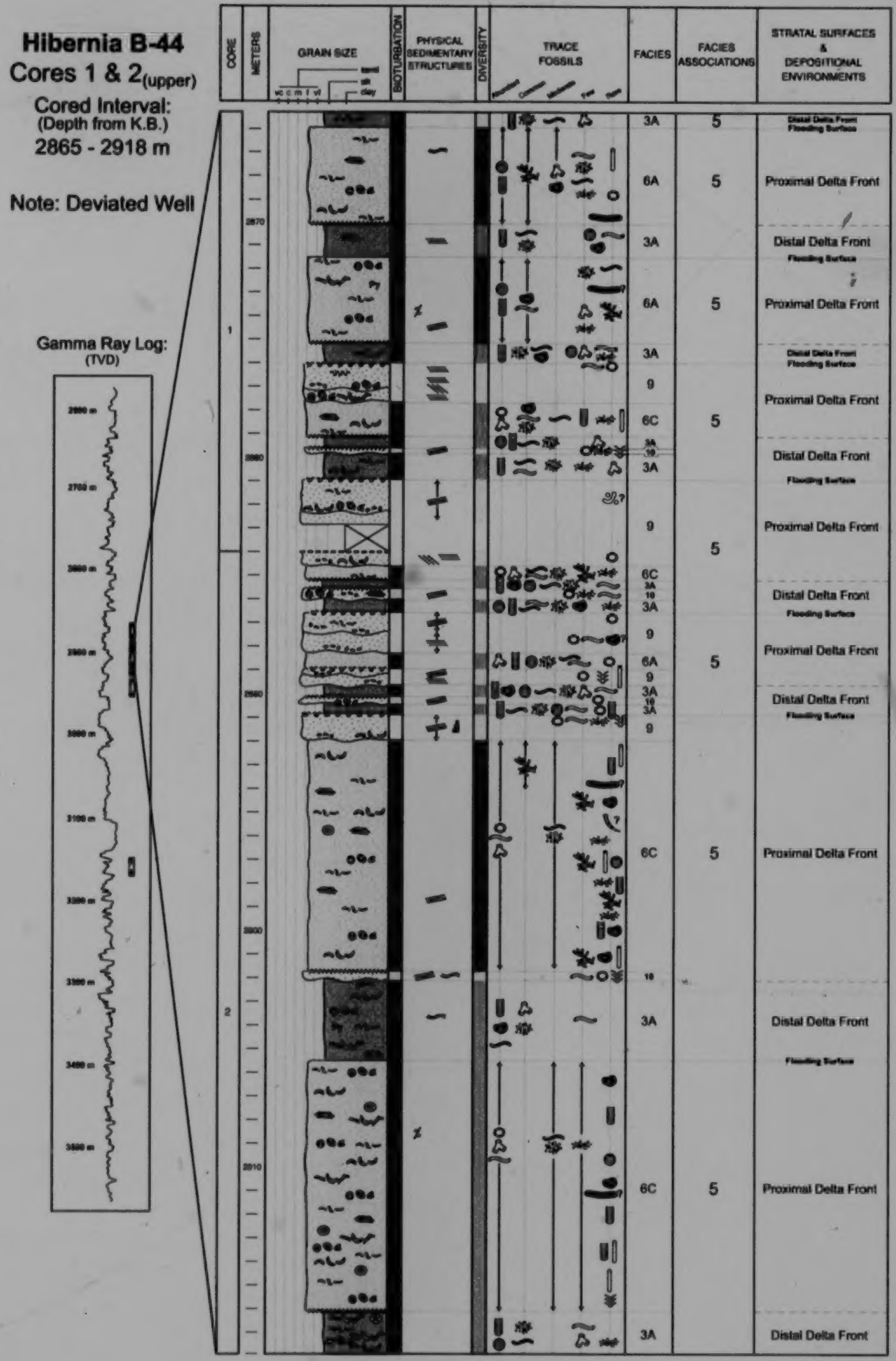

Gamma Ray Log:
(TVD)
2600 m
2700 m
2800 m
2900 m
3000 m
3100 m
3200 m
3300 m
3400 m
3500 m
CORE
METERS
GRAIN SIZE
vc c m f vf
sand
silt
clay
BIOTURBATION
PHYSICAL SEDIMENTARY STRUCTURES
DIVERSITY
TRACE FOSSILS
FACIES
FACIES ASSOCIATIONS
STRATAL SURFACES & DEPOSITIONAL ENVIRONMENTS
1
2
2870
2880
2890
2900
2910
3A
6A
3A
6A
3A
9
6C
3A
10
3A
9
6C
3A
10
3A
9
6A
9
3A
10
3A
9
6C
10
3A
6C
3A
5
Distal Delta Front
Flooding Surface
Proximal Delta Front
Distal Delta Front
Flooding Surface
Proximal Delta Front
Distal Delta Front
Flooding Surface
Proximal Delta Front
Distal Delta Front
Flooding Surface
Proximal Delta Front
Distal Delta Front
Flooding Surface
Proximal Delta Front
Distal Delta Front
Flooding Surface
Proximal Delta Front
Distal Delta Front
Flooding Surface
Proximal Delta Front
Distal Delta Front
Flooding Surface
Proximal Delta Front
Distal Delta Front

Hibernia B-44

Cores $2_{(lower)}$ & 3

Cored Interval:
(Depth from K.B.)
2918 - 2949 m

Core 4

Cored Interval:
(Depth from K.B.)
3145 - 3166 m

Note: Deviated Well

Well continued from previous page

Gamma Ray Log:
(TVD)

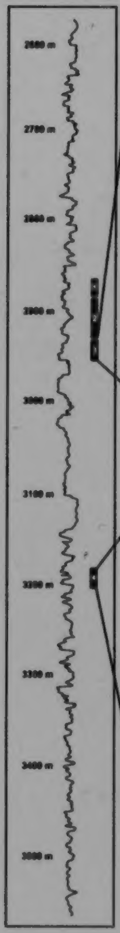

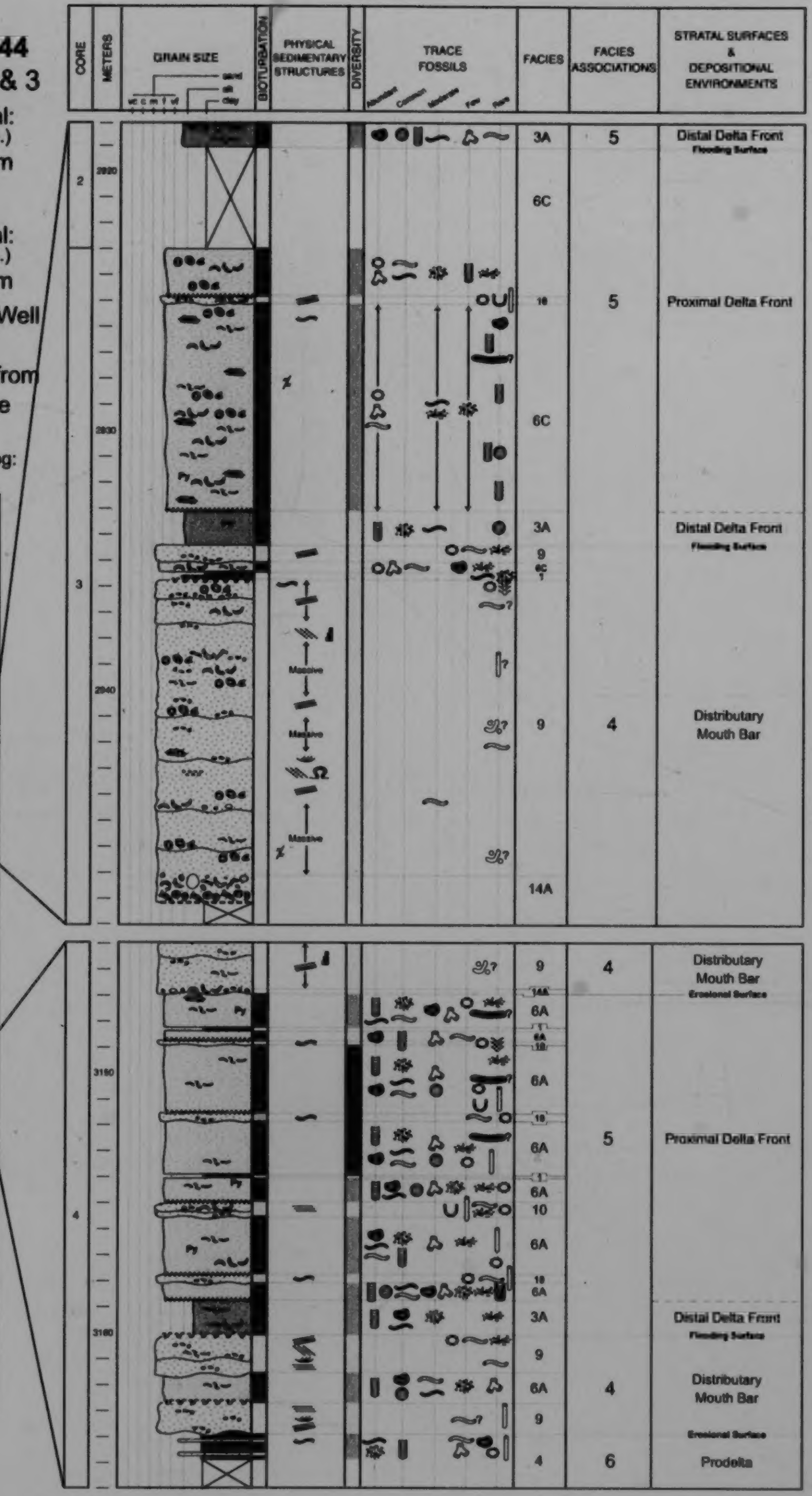
CORE
METERS
GRAIN SIZE
sand
silt
clay
vc c m f vf
BIOTURBATION
PHYSICAL SEDIMENTARY STRUCTURES
DIVERSITY
TRACE FOSSILS
FACIES
FACIES ASSOCIATIONS
STRATAL SURFACES & DEPOSITIONAL ENVIRONMENTS
2
3
4
2920
2930
2940
3150
3160
Massive
Py
3A
6C
6C
3A
9
14A
9
6A
10
4
5
5
4
4
5
4
6
Distal Delta Front
Flooding Surface
Proximal Delta Front
Distal Delta Front
Flooding Surface
Distributary Mouth Bar
Distributary Mouth Bar
Erosional Surface
Proximal Delta Front
Distal Delta Front
Flooding Surface
Distributary Mouth Bar
Erosional Surface
Prodelta

Hibernia C-96
Cores 2 - 4

Cored Interval:
(Depth from K.B.)
2302.5 - 2334.8 m

Gamma Ray Log:
(TVD)

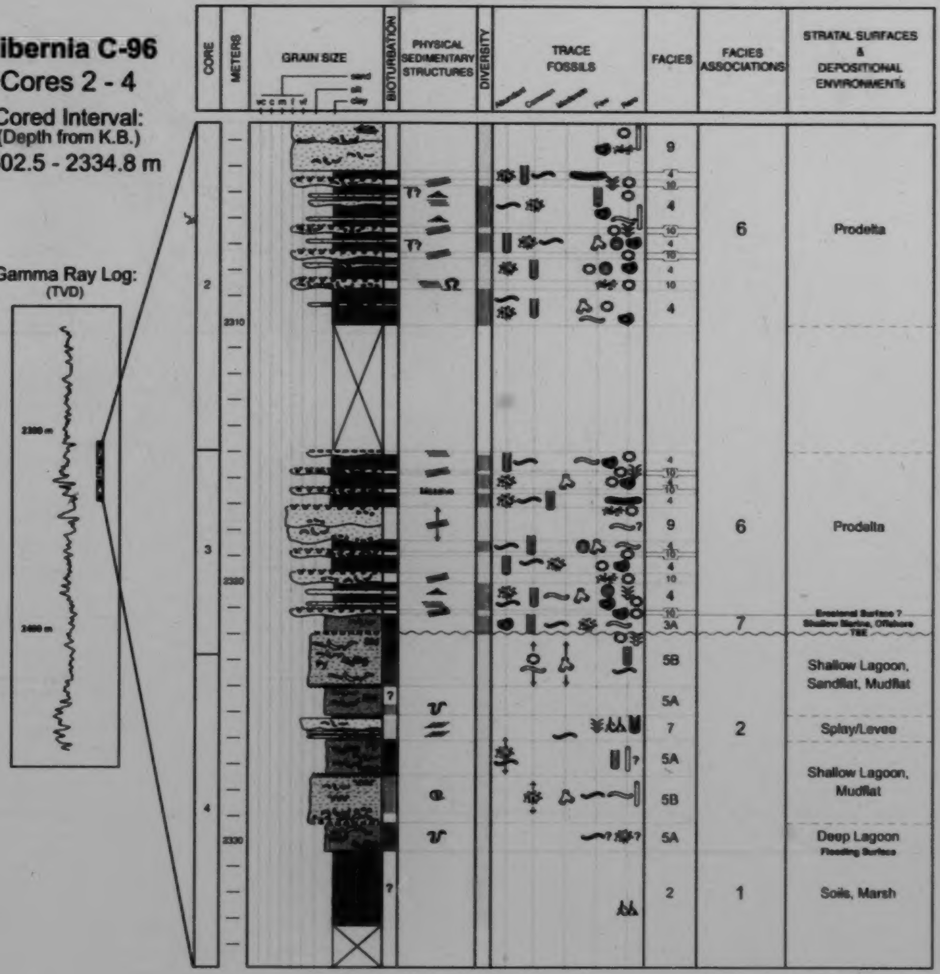
2300 m
2400 m
CORE
METERS
GRAIN SIZE
sand
silt
clay
vc c m f vf
BIOTURBATION
PHYSICAL SEDIMENTARY STRUCTURES
DIVERSITY
TRACE FOSSILS
FACIES
FACIES ASSOCIATIONS
STRATAL SURFACES & DEPOSITIONAL ENVIRONMENTs
2
3
4
2310
2320
2330
Massive
9
4
10
4
10
4
10
4
10
4
4
10
4
10
4
9
4
10
4
10
4
10
3A
5B
5A
7
5A
5B
5A
2
6
6
7
2
1
Prodelta
Prodelta
Erosional Surface ?
Shallow Marine, Offshore
TSE
Shallow Lagoon, Sandflat, Mudflat
Splay/Levee
Shallow Lagoon, Mudflat
Deep Lagoon
Flooding Surface
Soils, Marsh

Hibernia G-55

Core 1

Cored Interval:
(Depth from K.B.)
2443.2 - 2453.9 m

Core 2

Cored Interval:
(Depth from K.B.)
3352.8 - 3371 m

Gamma Ray Log:
(TVD)

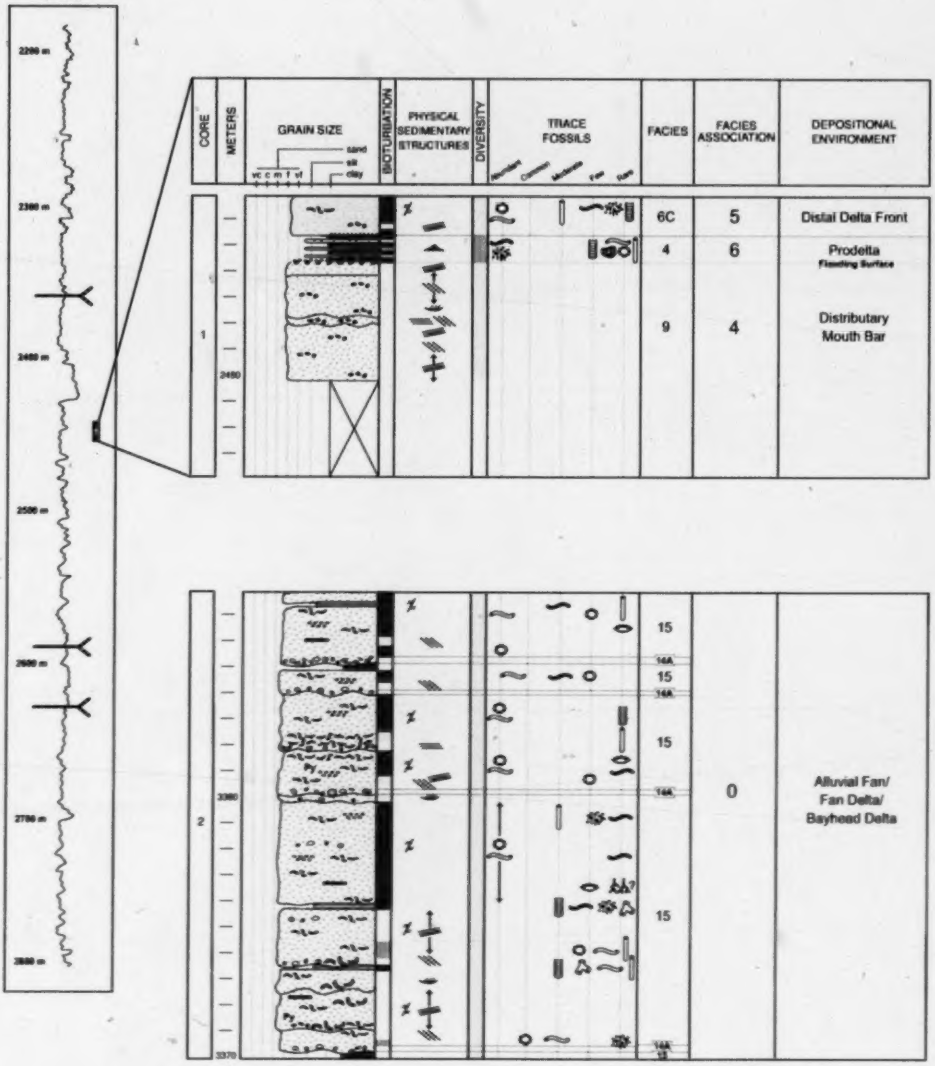
2200 m
2300 m
2400 m
2500 m
2600 m
2700 m
2800 m
CORE
METERS
GRAIN SIZE
sand
silt
clay
vc c m f vf
BIOTURBATION
PHYSICAL SEDIMENTARY STRUCTURES
DIVERSITY
TRACE FOSSILS
FACIES
FACIES ASSOCIATION
DEPOSITIONAL ENVIRONMENT
1
2450
6C
5
Distal Delta Front
4
6
Prodelta
Flooding Surface
9
4
Distributary Mouth Bar
2
3360
3370
15
14A
15
14A
15
14A
15
14A
13
0
Alluvial Fan/
Fan Delta/
Bayhead Delta

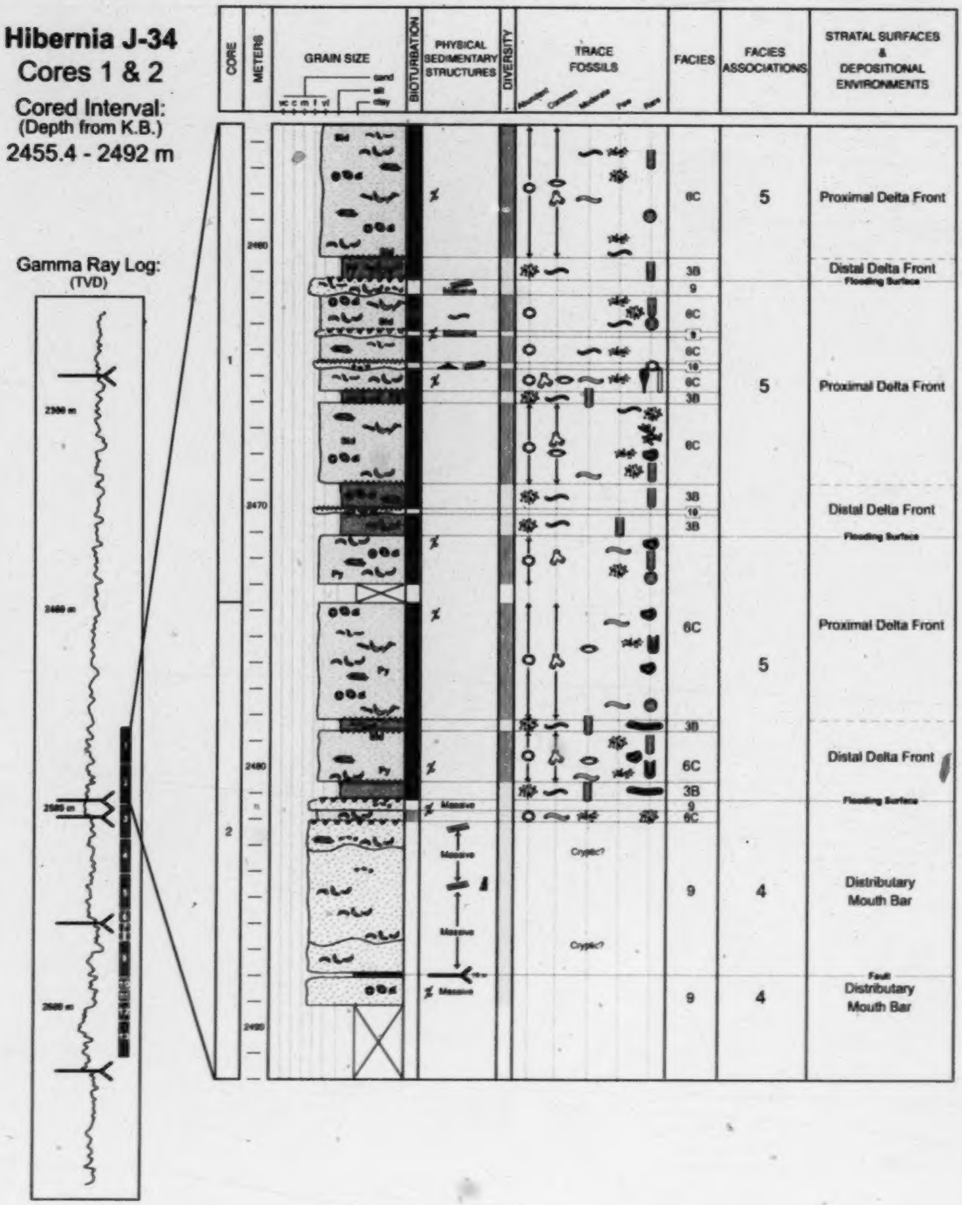
Hibernia J-34
Cores 1 & 2
Cored Interval:
(Depth from K.B.)
2455.4 - 2492 m
Gamma Ray Log:
(TVD)
2380 m
2480 m
2580 m
2680 m
CORE
METERS
GRAIN SIZE
vc c m f vf
sand
silt
clay
BIOTURBATION
PHYSICAL SEDIMENTARY STRUCTURES
DIVERSITY
TRACE FOSSILS
FACIES
FACIES ASSOCIATIONS
STRATAL SURFACES & DEPOSITIONAL ENVIRONMENTS
1
2
2460
2470
2480
2490
Sid
Py
Massive
Cryptic?
Fault
6C
3B
9
10
5
4
Proximal Delta Front
Distal Delta Front
Flooding Surface
Distributary Mouth Bar

Hibernia J-34
Cores 3 & 4

Cored Interval:
(Depth from K.B.)
2492 - 2528.6 m

Well continued from previous page

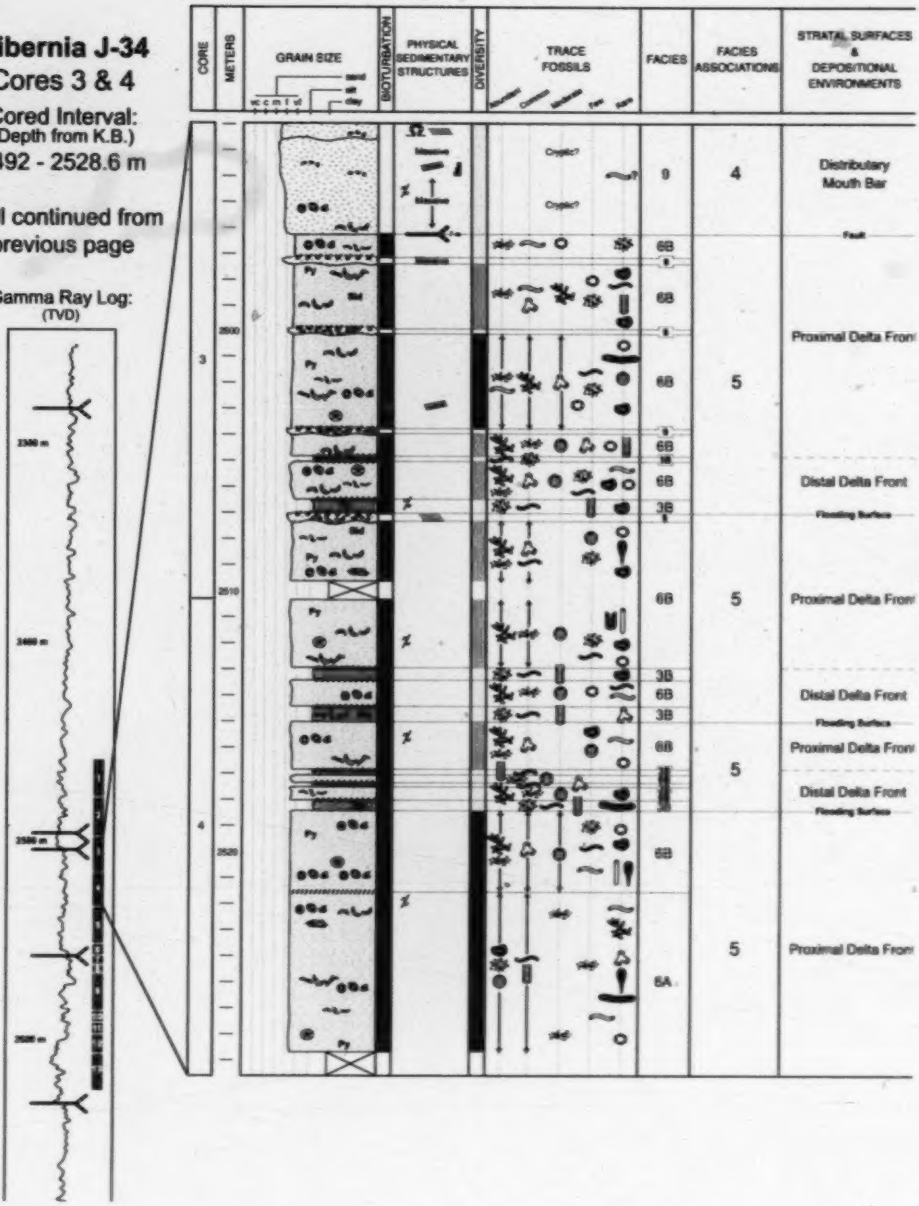
Gamma Ray Log:
(TVD)
CORE
METERS
GRAIN SIZE
vc c m f vf
sand
silt
clay
BIOTURBATION
PHYSICAL SEDIMENTARY STRUCTURES
DIVERSITY
TRACE FOSSILS
FACIES
FACIES ASSOCIATIONS
STRATAL SURFACES & DEPOSITIONAL ENVIRONMENTS
Cryptic?
Massive
Py
Sid
3
4
2500
2510
2520
9
6B
3B
6A
4
5
5
5
5
Distributary Mouth Bar
Fault
Proximal Delta Front
Distal Delta Front
Flooding Surface
Proximal Delta Front
Distal Delta Front
Flooding Surface
Proximal Delta Front
Distal Delta Front
Flooding Surface
Proximal Delta Front

Hibernia J-34

Cores 5 - 9

Cored Interval:
(Depth from K.B.)
2528.6 - 2578.9 m

Well continued from previous two pages

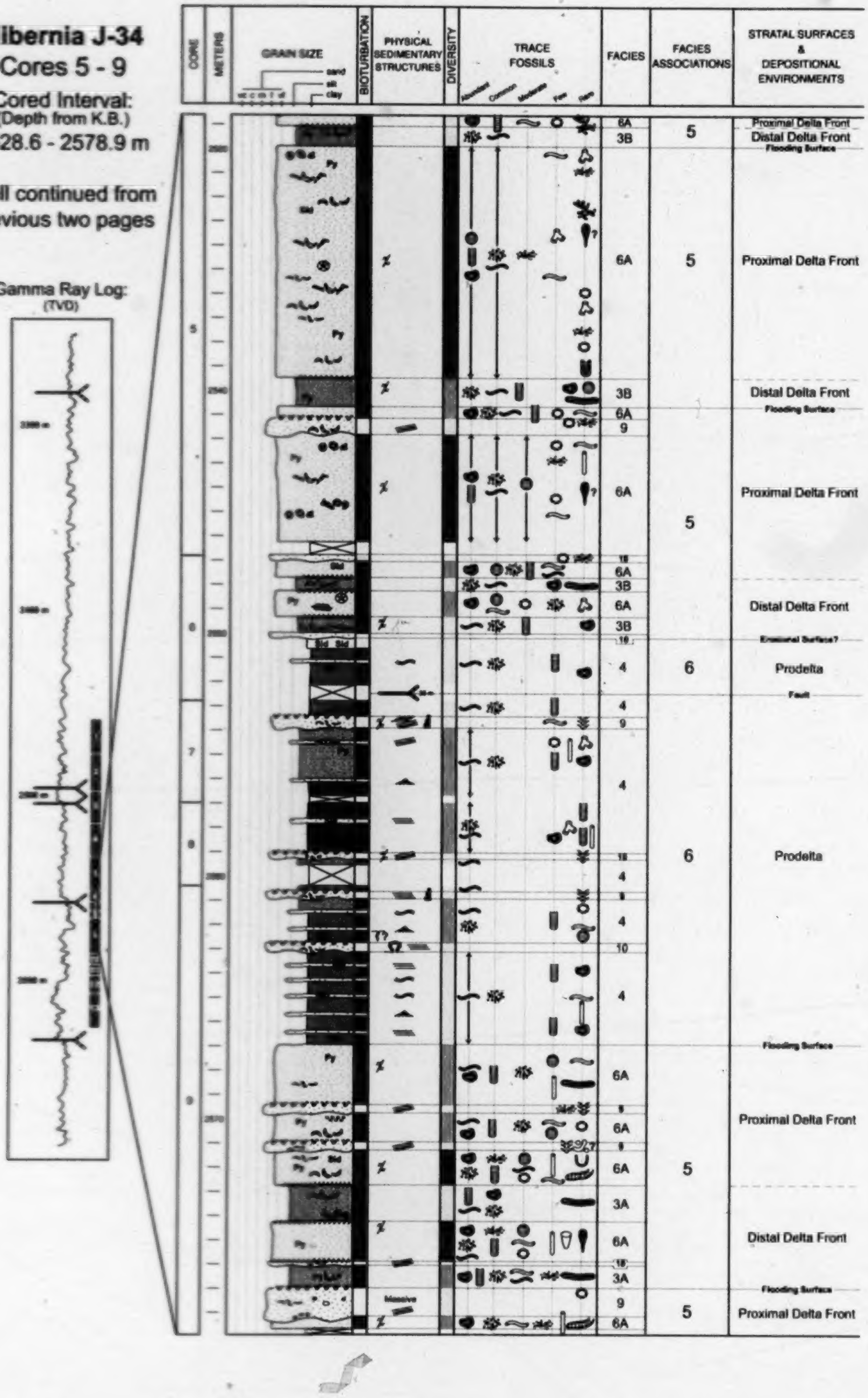
Gamma Ray Log:
(TVD)
CORE
METERS
GRAIN SIZE
sand
silt
clay
BIOTURBATION
PHYSICAL SEDIMENTARY STRUCTURES
DIVERSITY
TRACE FOSSILS
Abundant
Common
Moderate
Few
Rare
FACIES
FACIES ASSOCIATIONS
STRATAL SURFACES & DEPOSITIONAL ENVIRONMENTS
5
6
7
8
9
2530
2540
2550
2560
2570
Py
Sid
Massive
6A
3B
6A
3B
6A
9
6A
6A
3B
6A
3B
4
4
9
4
4
4
10
4
6A
6A
6A
3A
6A
3A
9
6A
5
5
5
6
6
5
5
Proximal Delta Front
Distal Delta Front
Flooding Surface
Proximal Delta Front
Distal Delta Front
Flooding Surface
Proximal Delta Front
Distal Delta Front
Erosional Surface?
Prodelta
Fault
Prodelta
Flooding Surface
Proximal Delta Front
Distal Delta Front
Flooding Surface
Proximal Delta Front

Hibernia J-34

Cores 10 - 13

Cored Interval:
(Depth from K.B.)
2578.9 - 2621.6 m

Well continued from
previous three pages

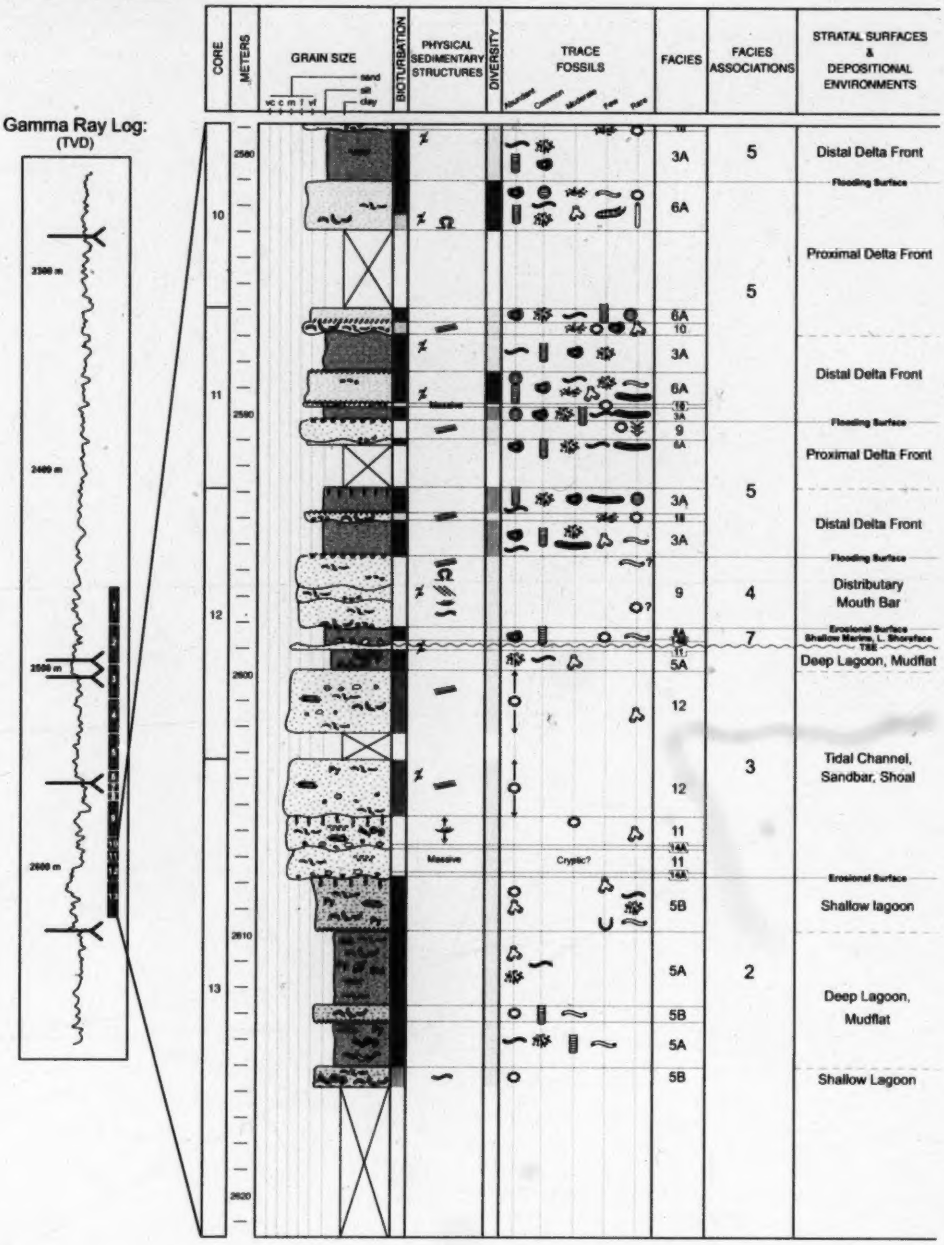
Gamma Ray Log:
(TVD)
2300 m
2400 m
2500 m
2600 m
CORE
METERS
GRAIN SIZE
vc c m f vf
sand
silt
clay
BIOTURBATION
PHYSICAL SEDIMENTARY STRUCTURES
DIVERSITY
TRACE FOSSILS
Abundant
Common
Moderate
Few
Rare
FACIES
FACIES ASSOCIATIONS
STRATAL SURFACES & DEPOSITIONAL ENVIRONMENTS
10
11
12
13
2580
2590
2600
2610
2620
Massive
Cryptic?
3A
6A
6A
10
3A
6A
3A
9
6A
3A
3A
9
11
5A
12
12
11
14A
11
14A
5B
5A
5B
5A
5B
5
5
5
4
7
3
2
Distal Delta Front
Flooding Surface
Proximal Delta Front
Distal Delta Front
Flooding Surface
Proximal Delta Front
Distal Delta Front
Flooding Surface
Distributary Mouth Bar
Erosional Surface
Shallow Marine, L. Shoreface
TSE
Deep Lagoon, Mudflat
Tidal Channel, Sandbar, Shoal
Erosional Surface
Shallow lagoon
Deep Lagoon, Mudflat
Shallow Lagoon

Hibernia K-14

Cores 1 - 3

Cored Interval:
(Depth from K.B.)
2345.1 - 2397.6 m

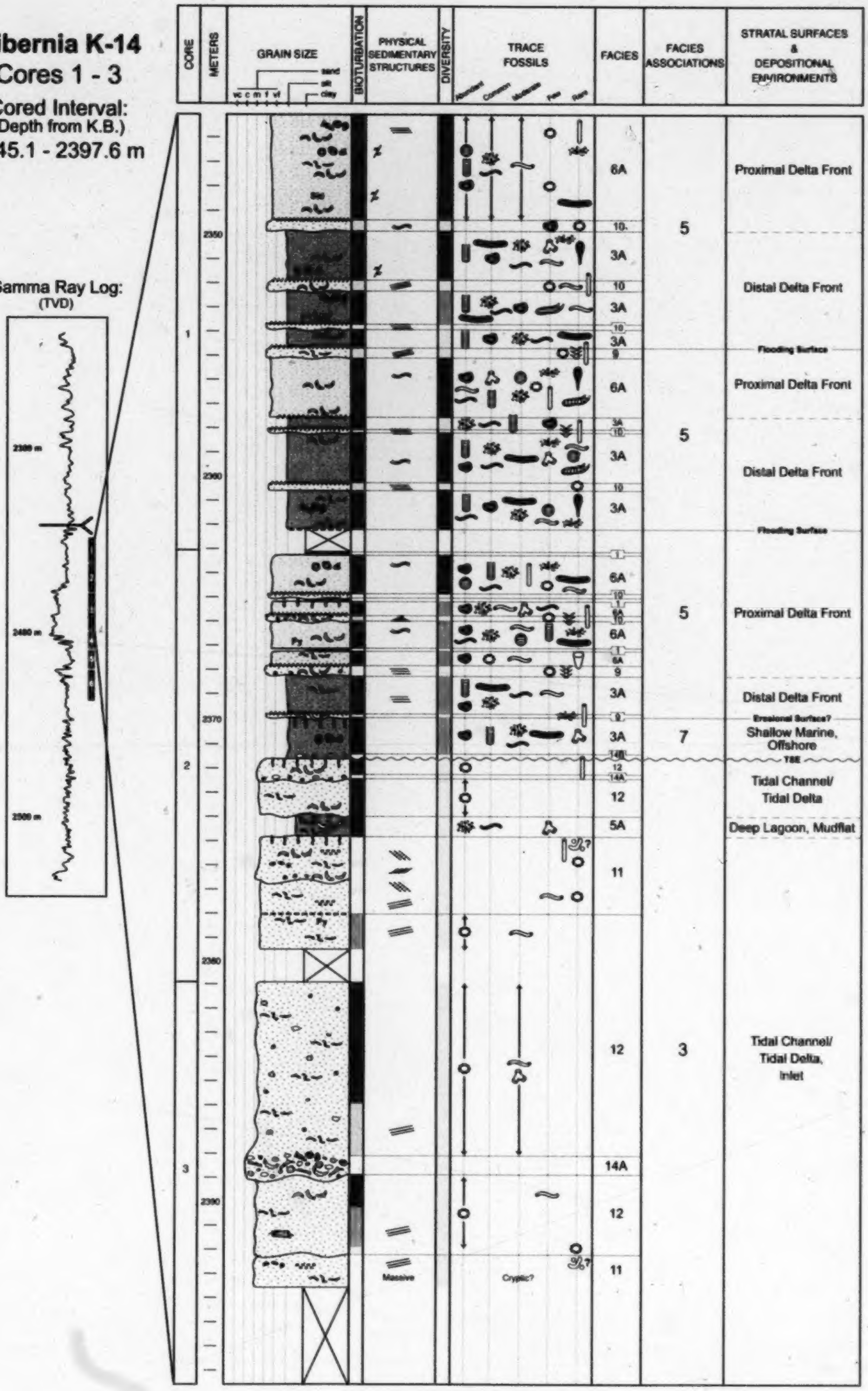
Gamma Ray Log:
(TVD)
2360 m
2400 m
2500 m
CORE
METERS
GRAIN SIZE
sand
silt
clay
vc c m f vf
BIOTURBATION
PHYSICAL SEDIMENTARY STRUCTURES
DIVERSITY
TRACE FOSSILS
Abundant
Common
Moderate
Few
Rare
FACIES
FACIES ASSOCIATIONS
STRATAL SURFACES & DEPOSITIONAL ENVIRONMENTS
1
2
3
2350
2360
2370
2380
2390
Py
6A
10
3A
10
3A
10
3A
9
6A
3A
10
3A
10
3A
1
6A
10
1
6A
10
6A
1
6A
9
3A
9
3A
14B
12
14A
12
5A
11
12
14A
12
11
5
5
5
7
3
Proximal Delta Front
Distal Delta Front
Flooding Surface
Proximal Delta Front
Distal Delta Front
Flooding Surface
Proximal Delta Front
Distal Delta Front
Erosional Surface?
Shallow Marine, Offshore
TSE
Tidal Channel/ Tidal Delta
Deep Lagoon, Mudflat
Tidal Channel/ Tidal Delta, Inlet
Massive
Cryptic?

Hibernia K-14
Cores 4 - 6

Cored Interval:
(Depth from K.B.)
2397.6 - 2440 m

Well continued from previous page

Gamma Ray Log:
(TVD)

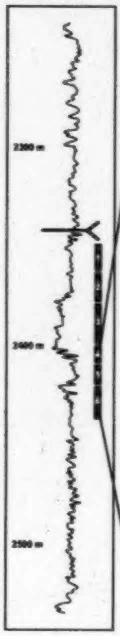

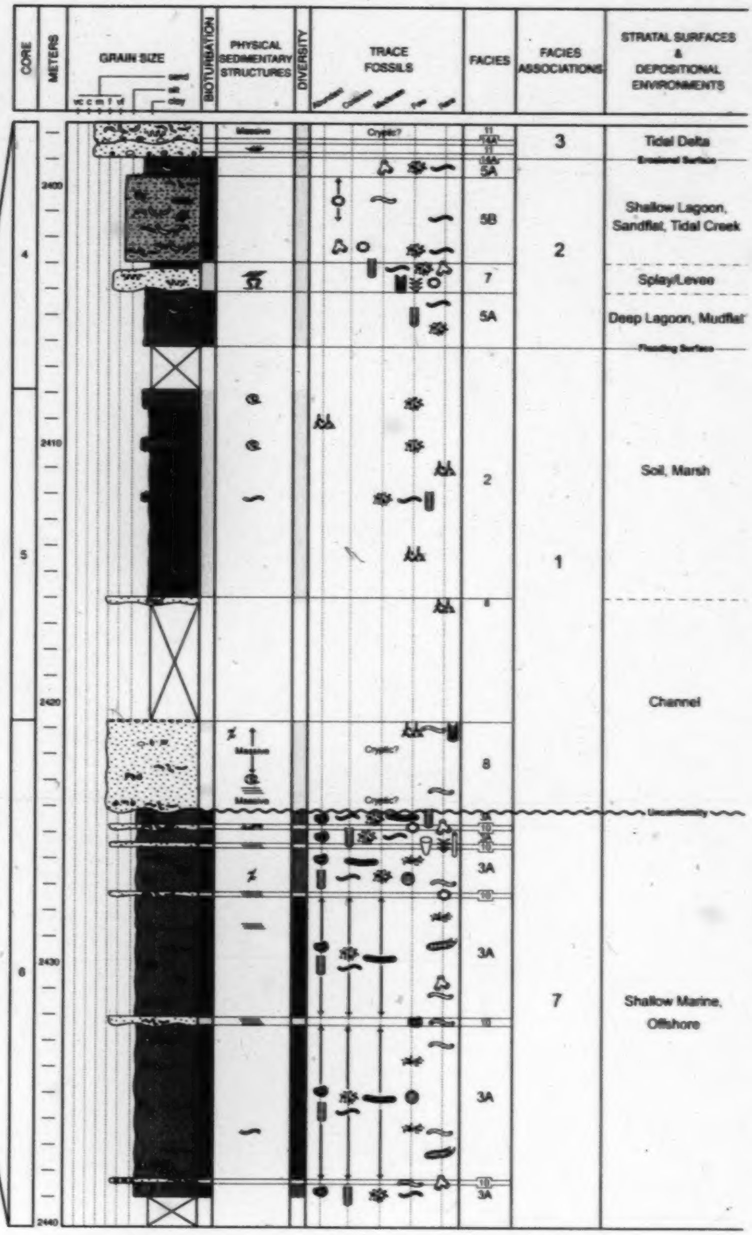
CORE
METERS
GRAIN SIZE
sand
silt
clay
vc c m f vf
BIOTURBATION
PHYSICAL SEDIMENTARY STRUCTURES
DIVERSITY
TRACE FOSSILS
FACIES
FACIES ASSOCIATIONS
STRATAL SURFACES & DEPOSITIONAL ENVIRONMENTS
2400
2410
2420
2430
2440
4
5
6
Massive
Cryptic?
11
5A
5B
7
5A
2
8
3A
10
3
2
1
7
Tidal Delta
Erosional Surface
Shallow Lagoon, Sandflat, Tidal Creek
Splay/Levee
Deep Lagoon, Mudflat
Flooding Surface
Soil, Marsh
Channel
Pbl
Massive
Cryptic?
Unconformity
Shallow Marine, Offshore

Hibernia K-18
Core 1

Cored Interval:
(Depth from K.B.)
2286 - 2304.2 m

Gamma Ray Log:
(TVD)

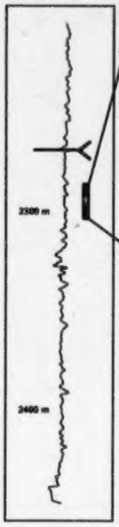

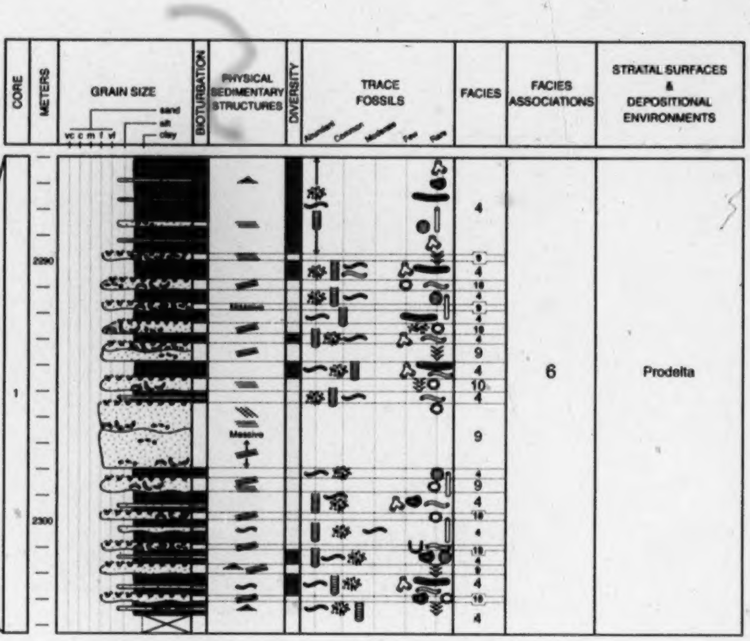
CORE
METERS
GRAIN SIZE
vc c m f vf
sand
silt
clay
BIOTURBATION
PHYSICAL SEDIMENTARY STRUCTURES
DIVERSITY
TRACE FOSSILS
Abundant
Common
Moderate
Few
Rare
FACIES
FACIES ASSOCIATIONS
STRATAL SURFACES & DEPOSITIONAL ENVIRONMENTS
2290
2300
1
Massive
Massive
4
9
10
6
Prodelta

Hibernia O-35

Core 1

Cored Interval:
(Depth from K.B.)
2184 - 2200.3 m

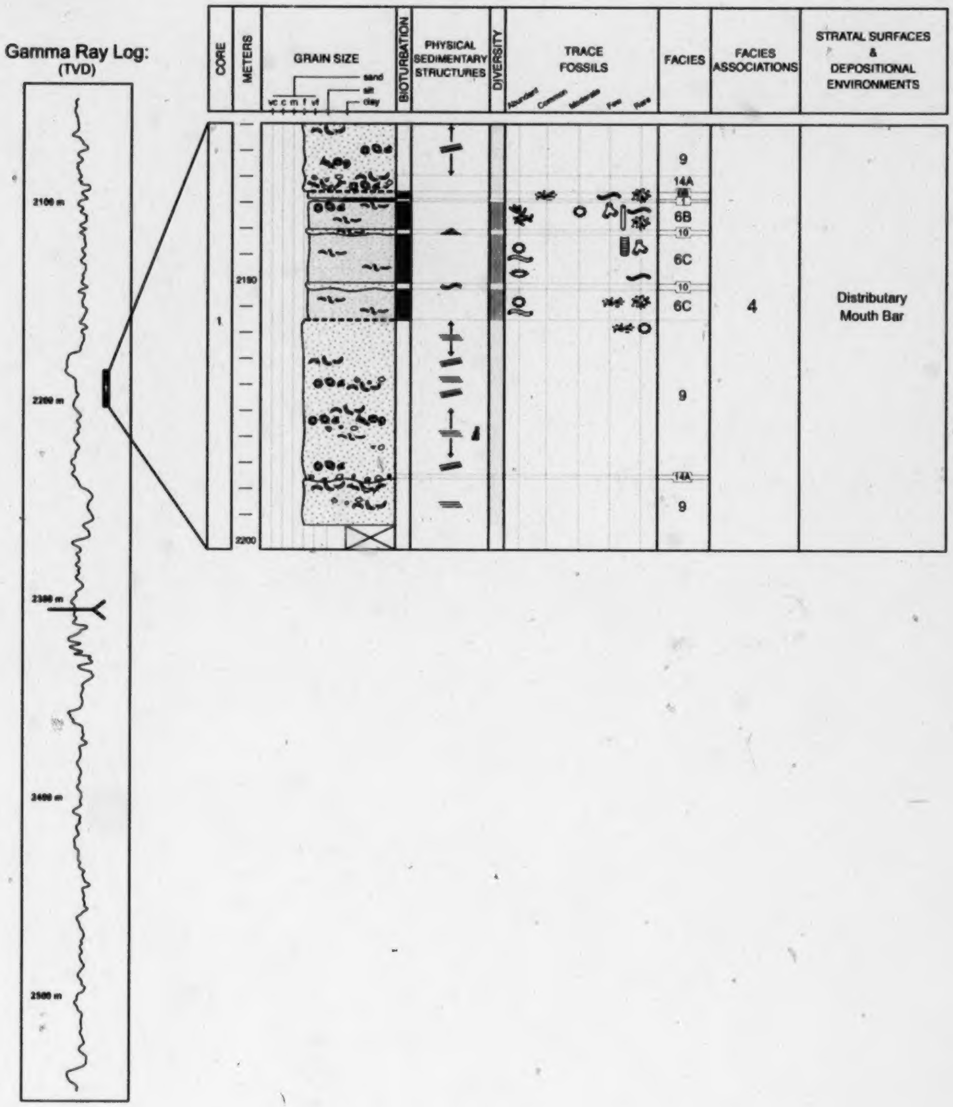
Gamma Ray Log:
(TVD)
2100 m
2200 m
2300 m
2400 m
2500 m
CORE
METERS
GRAIN SIZE
vc c m f vf
sand
silt
clay
BIOTURBATION
PHYSICAL SEDIMENTARY STRUCTURES
DIVERSITY
TRACE FOSSILS
Abundant
Common
Moderate
Few
Rare
FACIES
FACIES ASSOCIATIONS
STRATAL SURFACES & DEPOSITIONAL ENVIRONMENTS
1
2190
2200
9
14A
6B
10
6C
10
6C
9
14A
9
4
Distributary Mouth Bar